# Electron Density-Matching Diamido Ligands to 1st Row Transition Metals: Coordination and Reactivity Trends

**by**

**Tara L. Connors**

B.Sc., Acadia University, 2012

Thesis Submitted in Partial Fulfillment of the
Requirements for the Degree of
Master of Science

in the
Department of Chemistry
Faculty of Science



**SIMON FRASER UNIVERSITY**

**Summer 2016**

# Approval

| | |
|---|---|
| **Name:** | **Tara L. Connors** |
| **Degree:** | **Master of Science (Chemistry)** |
| **Title:** | ***Electron Density-Matching Diamido Ligands to 1$^{st}$ Row Transition Metals: Coordination and Reactivity Trends*** |
| **Examining Committee:** | **Chair:** Hogan Yu<br>Professor |

**Daniel Leznoff**
Senior Supervisor
Professor _____

**Tim Storr**
Supervisor
Associate Professor _____

**Charles Walsby**
Supervisor
Associate Professor _____

**Vance Williams**
Internal Examiner
Associate Professor _____

**Date Defended/Approved:** April 29, 2016

# Abstract

Amido-based ligands can employ a variable R-group which can be used to “tune” the steric and electronic properties of the resulting metal complex, targeting bond activation and catalytic applications. This thesis explored how the chelating diamido ligand $\{(t\text{BuNSiMe}_2)_2\text{O}\}^{2-}$ interacts with the early transition metals scandium(III), titanium(III) and vanadium(III), to discern how the number of *d*-electrons affects the coordination and reactivity of the complexes. The coordination motif is oxidation state-dependent, and structural differences are observed as the number of *d*-electrons changes. Alkylation yielded interesting results: the vanadium complex formed the dinitrogen species $\{[(t\text{BuNSiMe}_2)_2\text{O}]\text{VR}\}_2(\mu\text{-N}_2)$ (R = $\text{CH}_2\text{SiMe}_3$, $\text{CH}_2\text{Ph}$), while scandium produced the expected complex, $\{[t\text{BuNSiMe}_2]_2\text{O}\}\text{ScCH}_2\text{SiMe}_3\bullet\text{THF}$. Concurrently, a diamido ligand containing electron-withdrawing $-\text{CF}_3$ groups, $\{[3,5\text{-}(\text{CF}_3)_2\text{PhNSiMe}_2]_2\text{O}\}^{2-}$, was examined to probe how the altered electronic profile affects the overall coordination and reactivity of later transition metal iron(III) and cobalt(II) complexes. Unusual structural motifs indicated that this ligand warrants additional research.



**Keywords**: Diamido coordination; 1st row transition metal chemistry; coordination chemistry; dinitrogen activation; electronic effects

*To my parents, for their unwavering encouragement;*

*To Graham, for his support and care during this journey of discovery;*

*And to Tucker, for his unconditional love and the joy he brings.*

## Acknowledgements

It can be difficult to find people who will support you and help you, no matter what your goal. In this, I have been incredibly lucky. First and foremost, Prof. Daniel Leznoff has been a fountain of knowledge and experience during my journey at SFU. He has given much of his time to teach me everything I know about air sensitive coordination chemistry, and for that I am very grateful. And more, he has supported and helped me in my desire to forge a link through my personal life and my chemistry training in an attempt to settle onto a career pathway, which I very much appreciate. His openness and thoughtful advice has shaped me into the confident chemist I am today. Thank you, Danny.

I would also like to thank my committee members, Dr. Tim Storr and Dr. Charles Walsby, for taking time from their busy schedules to help guide my chemistry down more successful paths. I defer to your larger experience and knowledge base, and am happy that you were able to share some of it with me. Additionally, I would like to thank my internal examiner, Dr. Vance Williams, for agreeing to judge this work. I would also like to thank Dr. Andrew Lewis for his help and guidance with NMR data, as well as Mr. Paul Mulyk for collecting EA data for my many samples. I would also like to thank Kate Prosser for running ESR samples for me.

Members of the Leznoff group, both past and present deserve a special mention. In particular, I would like to mention Dr. Cassandra Hayes. Thank you for training me in the air sensitive chemistry of the lab, and showing me the ropes. Thank you for being such a wonderful reminder of home. Thank you for being so patient and supportive when I had no idea what I was doing. Thank you for all the wine. I'm sure there was an occasion for all of it. And thank you for all the wonderful memories we've shared, in the lab and out; we'll carry those with us for years to come. I would also like to thank Declan McKearney, for being probably the most dedicated undergrad I could have asked for; your enthusiasm is inspiring. Thank you to Dr. Jeffrey Ovens for teaching me how to run and solve my own air-sensitive crystals on the X-ray diffractometer. Thank you to Didier Savard and Declan McKearney for helping me with my SQuID samples. And thank you

to the rest of the group: Rachel, Wen, John, Ryan, Benson, Matthew, Bryton, Yumeela, Ania, and Debbie, for providing countless diversions and coffee breaks.

There are those who have helped me, not with this degree so much as having brought me to this point and helped to shape me as a person. The first are my parents, and my family. I love you all, and your endless encouragement has taught me that I am my only barrier to success. For you, I push onwards and upwards. Next is Graham, who is a constant reminder of the impact that science has on everyone's lives, all the time. Your enthusiasm astounds and motivates me to keep asking questions. Your support in all that I attempt means the world to me. You make me want to be a better me. Thank you, for everything. Finally, never underestimate the emotional value of a furry friend. Tucker has been a constant source of unrestrained joy in the past three years. Always ready to get outside for some good old-fashioned exercise, but just as ready to curl up and relax, he has brightened every single day that he has been with me. I'll love you, always, Tucker-Duck. Without these connections, I would not be here today, and I would not have made this achievement. It is for everyone I have mentioned that I take pride in this research, and this thesis.

# Table of Contents

# List of Tables

# List of Figures

# List of Schemes

# List of Symbols and Abbreviations

| | |
|---|---|
| $[^{R}NON]^{2-}$ | $\{O[SiMe_2NR]_2\}^{2-}$ |
| ° | Degree |
| $^{1}H$ | Proton |
| Å | Angstrom |
| AF | Antiferromagnetic |
| An | Actinide Metal |
| Anal. | Analysis |
| Calc. | Calculated |
| Cp | Cyclopentadienyl [$-C_5H_5^-$] |
| Cy | Cyclohexyl [$-C_6H_{11}$] |
| D | Dipolar tensor in zero-field splitting |
| DME | Dimethoxyethane |
| E | Main group element |
| EA | Elemental analysis |
| emu | Electromagnetic unit |
| ESR | Electron Spin Resonance |
| $Et_2O$ | Diethyl ether |
| F | Ferromagnetic |
| Fc | Ferrocene |
| FID | Free induction decay |
| g | Gram |
| H | Magnetic field strength |
| *i*Pr | *iso*-Propyl [$-CH(CH_3)_2$] |
| J | Total angular momentum |
| K | Kelvin |
| L | Orbital angular momentum quantum number |
| M | Transition metal |
| M | Magnetisation |
| MAO | Methylaluminoxane |
| Me | Methyl [$-CH_3$] |

| | |
|---|---|
| MHz | MegaHertz |
| mL | Millilitre |
| $m_l$ | Magnetic quantum number |
| mmol | Millimole |
| $m_s$ | Spin magnetic quantum number |
| $M_W$ | Molar mass |
| NMR | Nuclear Magnetic Resonance |
| ORTEP | Oakridge Thermal Ellipsoid Plot |
| Ph | Phenyl [$-C_6H_5$] |
| POV-Ray | Persistance of Vision Raytracer |
| ppm | Parts per million |
| R | General alkyl group |
| RF | Radio frequency |
| s | Singlet (NMR) |
| S | Spin angular momentum quantum number |
| SOC | Spin-orbit coupling |
| SQuID | Superconducting Quantum Interference Device |
| T | Temperature |
| T1 | Spin-lattice relaxation time |
| T2 | Spin-spin relaxation time |
| *t*Bu | *tert*-Butyl [$-C(CH_3)_3$] |
| THF | Tetrahydrofuran |
| $\delta$ | NMR chemical shift |
| $\mu_B$ | Bohr magneton |
| $\mu_{eff}$ | Effective magnetic moment |
| $\mu_{s.o.}$ | Spin-only magnetic moment |
| $\rho$ | Density |
| $X$ | Magnetic susceptibility |

# Chapter 1.

# Introduction

## 1.1. Transition Metal Amido Chemistry

Amido ligands represent a single branch of ancillary ligands studied under the broad umbrella of inorganic coordination chemistry. Monodentate and chelating ancillary ligands have been found to be incredibly useful chemical tools for the promotion of the solubility of transition metal complexes, control over the coordination sphere of a metal complex, as well as offering the ability to target specific steric and/or electronic properties in a metal complex.[1] This is true of amides, as well as more common ancillary ligands, such as phosphines and alkoxides. Like phosphines, amides allow stabilisation of a broad range of oxidation states in metal complexes. Like an alkoxide ligand, they act as negatively-charged σ- and π-donors. However, amides are considered to be much "harder" than their phosphine and alkoxy counterparts, as the electron-density on the nitrogen is much higher than in their "softer" analogues, where the electron-density is substantially more polarizable. Additionally, transition metal amides offer an interesting comparison to the more traditional organometallic complexes, i.e. those containing M – C bonds, particularly Cp-type organometallic chemistry, due to their similarities in synthesis and bonding.[2–5] Bond activation-type experiments suggest that transition metal amides may show an aptitude for similar applications that have yielded positive outcomes with organometallic complexes. For example, various transition metal amido complexes have been shown to act as olefin polymerisation catalysts, as well as initiating a range of bond activations.[6–9] Due to their stabilising effect on a range of oxidation states, amido complexes are able to support reactive intermediates, thus encouraging potentially unusual chemistry. Cummins synthesised the first amido complex Mo{N(*t*Bu)Ar}$_3$ (Ar = 3,5-Me$_2$Ph) which was shown to completely cleave the triple bond of dinitrogen.[10,11] Schrock built upon this chemistry by utilising a molybdenum

triamidoamine species which was able to reduce and cleave dinitrogen at a single molybdenum centre, and with four turnovers at ~66% efficiency.[12–14]

Amide ligands (-$NR_2$) offer this increased stabilisation to metal centres via their steric and electronic flexibility as a function of their variable R-group. With two lone pairs of electrons present on the amide, and an overall negative charge, their σ- and π-donating ability stabilise mid- to high-oxidation state metals (Figure 1.1).[5] Thus, amide ligands are able to act as either 2- or 4-electron donors, depending on the electron-density already present on the metal centre. These ligands have also been shown to support high spin and paramagnetic metal centres.[1,15,16]

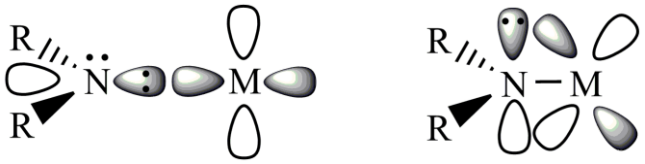


**Figure 1.1. σ- (left) and π-bonding (right) of an amido ligand to a transition metal.**

The first amido-transition metal complex formed was a reaction of titanium tetrachloride with potassium diphenylamide, by Dermer and Fernelius in 1935, who were able to isolate the homoleptic titanium(IV) tetrakis(diphenylamide).[5,17] However, significant growth in the field did not occur until more than 30 years later, when Bradley, Power, and Köhn each contributed to the development of the bis(silylmethyl)amide series, $M[N(SiMe_3)_2]_3$ (M = Sc-$Co^{3+}$).[18–21] The steric bulk of the trimethylsilyl groups prevent coordinative saturation of these metal complexes, resulting in highly reactive species that indicate an aptitude for catalytic applications.[18] Indeed, the cobalt and manganese moieties remain the only published three-coordinate manganese(III) and cobalt(III) complexes; this is likely a result of the steric bulk surrounding the metal preventing coordination of additional ligands or approach of reactive species to the metal centres. Divalent 3-coordinate dimers of manganese, iron, and cobalt have also been synthesised by Power, taking the form $[M\{N(SiMe_3)_2\}_2]_2$ (M = Mn, Fe, Co).[22,23] In addition, Power showed that a sufficiently sterically inhibiting amido ligand can yield a 2-coordinate divalent metal complex, with the formation of $M[N(SiMePh_2)_2]_2$ (M = Fe, Co).[24]

Due to the structure and bonding of an amide ligand (-$NR_2$), one of the R-groups may be substituted by a linking backbone to form an overall chelating diamido ligand, further stabilising the resulting metal complex via the chelate effect.[7,25–28] Many chelating amides also feature a neutral donor in the backbone, which may also bind to the metal centre if it is sufficiently electron-poor (Figure 1.2). Building off the backbone further allows expansion into polydentate amido ligands, for example the tripodal (triamido)amine, $\{[Me_3SiNCH_2CH_2]_3N\}^{3-}$.[29] In addition to chelation, a diamido ligand may also bridge between metal centres, although this option is much less common.[30] In a multi-dentate amido ligand there is an additional R-group on the amide that can be used to "tune" the ligand properties by varying the steric and electronic properties of the R-group. For example, a methyl group on the amide would allow very different binding abilities on a metal complex than a bulky mesityl group, as a result of the altered steric constraints.[6] This ligand "tuning" via the amido R-group is a particular focus in this research, targeting preferential binding to either early or late transition metals.

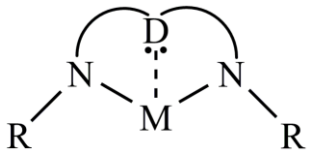


**Figure 1.2. Diamido ligand featuring a neutral donor bound to a metal.**

In addition to Cummins' amido molybdenum complex that splits dinitrogen, and Power's extremely bulky low-coordinate amido transition metal complexes, amido complexes have also shown an aptitude towards olefin polymerisation and hydroamination reactions. Bochmann produced two chelating diamido zirconium complexes that were activated using methylaluminoxane to give high molecular weight polyethylene with moderate activity levels.[7] Hydroamination reactions form nitrogen heterocycles selectively using metal-based catalysts, most typically of either transition metals or lanthanides. Bis-amido titanium and zirconium catalysts have been found to yield positive results in hydroamination reactions of organic substrates.[31,32] Research into transition metal amides have found their applications to be as wide and variable as their structures may be, thus encouraging further development into these fascinating compounds.

## 1.2. Early Transition Metal Diamido Chemistry

### 1.2.1. Characteristics and Complex Formation of Early Transition Metal Amides

Early transition metals represent the left-most section of the transition block of the periodic table, covering groups III, IV, and V in particular. Sometimes group VI is included as well, as it shares similarities with the previous groups. These early metals are characterised by few electrons in the outermost *d*-orbitals, resulting in larger radii as the outer *d*-orbitals expand, and subsequent low ionization potentials, and high valence states.[33]

As discussed in the previous section, amides are pervasive in modern coordination chemistry. Their ability to act as either 2- or 4-electron donors make them ideal for coordination to the electron-poor early transition metals, which act as π-acceptors into vacant *d*-orbitals.[5] It has been observed that the M – N bond distances are generally shorter than the predicted σ-bond length with the early metals, and this has been interpreted as evidence for amido π-bonding to the metal centre.[6] Due to the ideal relationship between electron-rich amide and electron-poor metal, there has been copious research of these ligand frameworks with the early transition metals.[6] Although monodentate amido complexes have been well-covered,[6] the majority of the research predominantly features multi-dentate amido ligands, as they offer further stabilisation via the chelate effect, in addition to the ability to use the ideal R-group for the desired properties.[15] Most amido R-groups studied consist of electron-rich alkyl or aryl groups, such as -*t*Bu, -Ph, -2,4,6-$Me_3$Ph, -3,5-*i*$Pr_2$Ph, as well as the alkyl-analogue, -$SiMe_3$. There are relatively few examples of amido substituents containing electron-poor moieties such as fluorinated groups. Schrock has published several examples of tripodal triamidoamine complexes with pentafluorophenyl substituents bound to the amides,[34–36] although these represent the majority of the literature on these electron-deficient amido R-groups. Typical structural motifs containing diamido ligands with the early transition metals, particularly of the 3*d* metals, will be discussed in the remainder of this section, as well as common reactivity pathways that have been found to occur.

Early transition metal amides have been synthesised with a broad range of coordination numbers and oxidation states, and comprise the majority of known metal amides.[6] Particularly for the early transition metals, which only have partially filled valence orbitals, the M – N amide distance is typically shorter than the sum of the covalent radii of M and N, which is suggestive of some π-bonding between the relevant atoms. Group III organometallic chemistry has recently received substantial attention, as their high Lewis acidity from empty *d*-orbitals and large atomic radii can yield unique reactivity patterns but also generate synthetic challenges. The acidity enables weak Lewis bases, such as THF, to ligate with the metal complex, which may interfere with the target synthesis; it also increases the tendency of the metal complexes to retain salts generated as by-products of the synthetic process, which can severely inhibit further reactivity of the complex.[37] These characteristics also encourage the resulting complexes to form dimeric structures, particularly if solvent molecules are not ligated. On the other hand, metallocene and amido-based group IV ($d^0$) chemistry has been extensively researched as these complexes have been shown to perform well as catalysts in olefin polymerisation (see Section 1.2.2).[38] Diamido ligands in particular have the ability to provide sufficient steric bulk to direct substrates to the active site of the complex. The group IV metals have illustrated their ability to react with a variety of substrates, including olefins, acetylenes, nitriles, isonitriles, dihydrogen gas, and even the C-H bonds of ligands. Groups V and VI amido-based complexes have witnessed significant growth as the presence of vanadium and molybdenum in the nitrogenase enzymes have been discovered, leading to developments in synthetic dinitrogen activation and cleavage with these metal complexes.[10,14,39] The desire to catalytically perform the reduction of the dinitrogen molecule to ammonia at ambient conditions is highly sought-after, as the currently used Haber-Bosch process has very large energy requirements.[40]

Research into complexes of the group III metals scandium and yttrium is desirable due to its relationship to group IV metals.[41] By studying the group III analogues to known group IV complexes, it was theorised that the higher Lewis acidity of the more electron-poor group III metals would encourage greater reactivity in bond-activation processes.

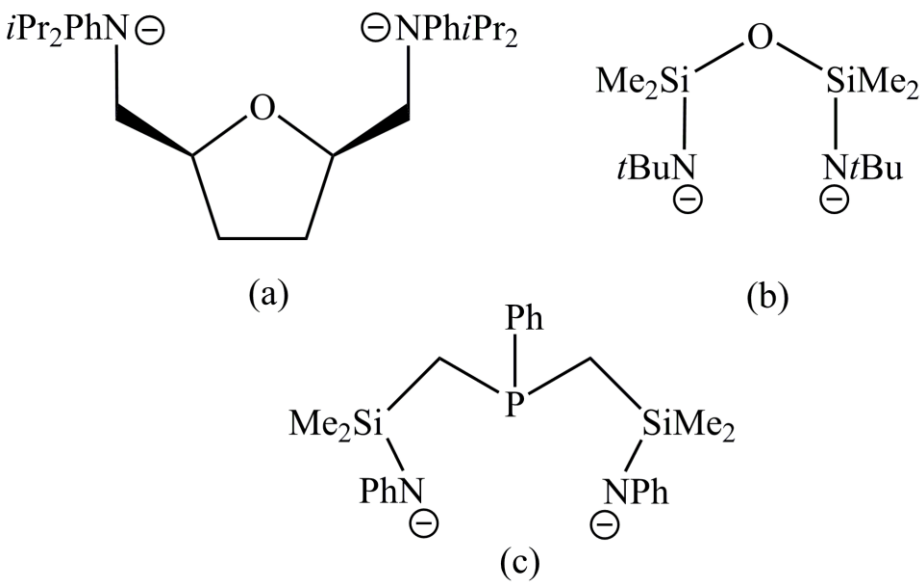


**Figure 1.3. Diamido ligands known to complex with yttrium(III) ($d^0$). (a) $[^{THF}BDPP]^{2-}$; (b) $[^{tBu}NON]^{2-}$; (c) $[^{PhPh}NPN]^{2-}$.**

Yttrium(III) ($d^0$) has been examined by several researchers under the umbrella of diamido coordination chemistry, forming complexes with each of the diamido ligands shown in Figure 1.3. Fryzuk et. al. attempted to produce the hydrido derivative of $[^{PhPh}NPN]YCl•THF$ through addition of $LiAlH_4$, and found that it instead transferred the ligand from the yttrium to the aluminum, forming a dinuclear aluminate.[42] This characteristic was exploited by Leznoff et. al. using an yttrium complex containing two equivalents of ligand to a single metal. They found that addition of the bis-complex $\{Y[^{tBu}NON]_2\}Li•THF$ to $CrCl_3•3THF$ afforded the otherwise difficult-to-obtain $\{[^{tBu}NON]CrCl\}_2$ complex in addition to the "regular" yttrium complex, $[^{tBu}NON]YCl•THF$.[43] Despite the development of these yttrium(III) diamido complexes, there has been comparatively little in regards to scandium diamides.[15] There are several known polydentate ligands that incorporate diamido groups to scandium(III), $d^0$ (Figure 1.4), including variations of triamidoamine ligands, tetradentate diamido-diamine ligands, as well as tridentate diamidoamine ligands.[44] The diamido-diamine ligands (Figure 1.4b) were developed to allow for further functionalisation at the metal, as triamidoamine ligands (Figure 1.4a) prevent this by fully charge-balancing the cationic nature of the metal. Indeed, this functionalisation was well-explored, as derivatives of this complex were synthesised with an alkyl, benzamidinate, as well as primary and secondary amide ligands via halide metathesis reactions.[44] The diamidoamine scandium complex (Figure

1.4c) has also been functionalised to an organometallic compound, although isolation difficulties have limited the usefulness of this particular complex.[44]

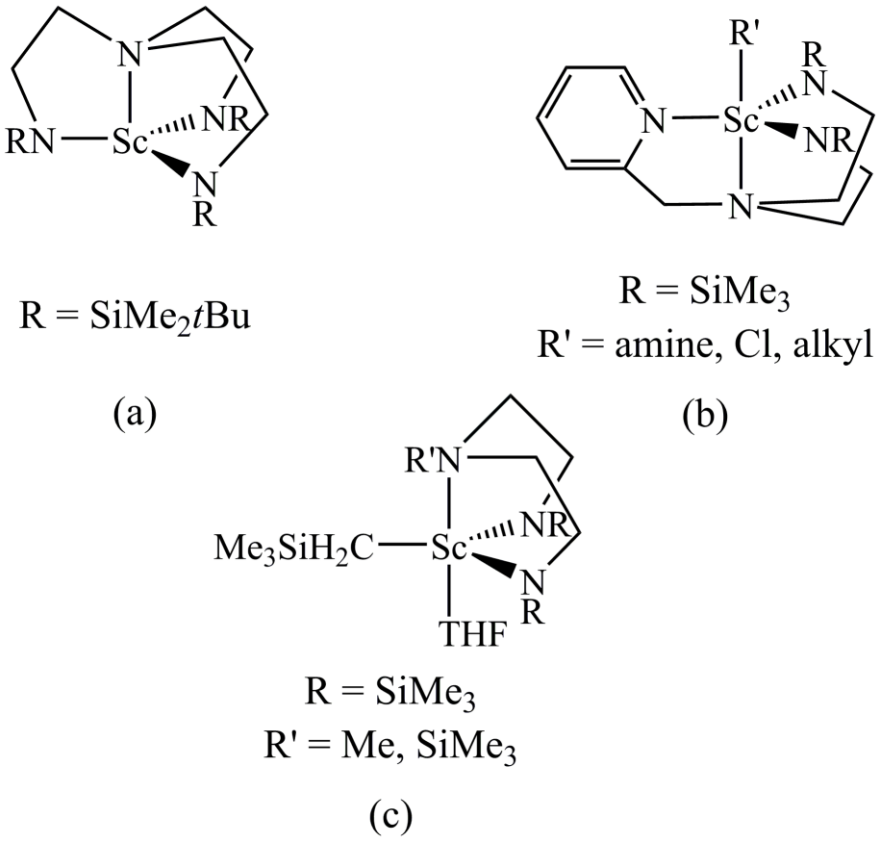


**Figure 1.4. Diamido-donor complexes of scandium. (a) triamidoamine; (b) diamidodiamine; (c) diamidoamine.**

As previously discussed, Dermer and Fernelius discovered the first transition metal amide, a titanium(IV) ($d^0$) complex.[17] Since then, there have been many more titanium(IV) amides reported.[6] However, to this day there is only one known paramagnetic diamido donor titanium(III) ($d^1$) system: [$^{SiMe_3}$NNN]TiX (X = Cl, H, $CH(SiMe_3)_2$) (Figure 1.5).[15,45] The X = halide and hydride versions both appear as dimers, while for X = alkyl, the complex is a 4-coordinate monomer. The halide-containing dimer, {[$^{SiMe_3}$NNN]TiCl}$_2$, was found to be an antiferromagnetically coupled complex with a solution magnetic moment of 1.65 $\mu_B$. It was proposed that the bulkiness of the alkyl promotes the room-temperature stability of this compound, as reactions with less bulky alkyls were unsuccessful.[45]

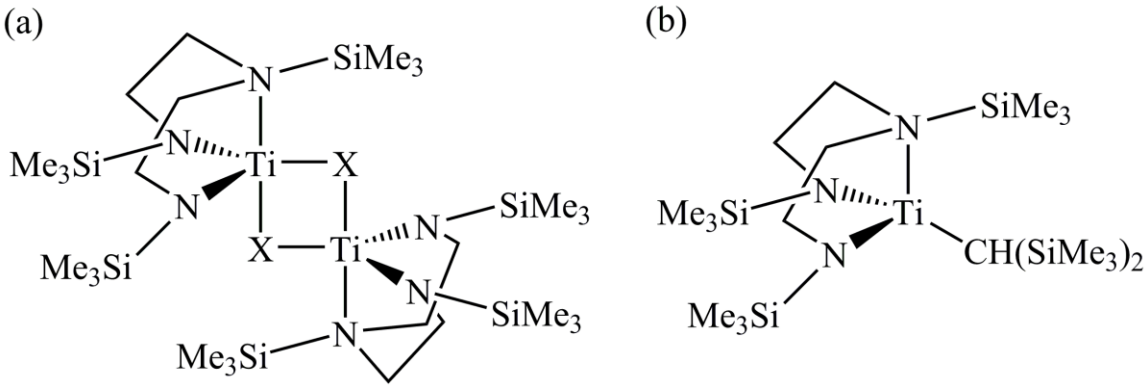


**Figure 1.5. Single literature example of a titanium diamido-donor complex: (a) dimer, X = Cl, H; (b) alkyl monomer.[45]**

There are comparatively many more diamido vanadium complexes known in the literature. This is primarily due to the discovery of vanadium inclusion in the nitrogenase enzyme when molybdenum is absent from the system, which prompted research into synthetic vanadium dinitrogen fixation abilities.[39] The vanadium analogue to the diamido titanium complex discussed above was prepared by Cloke and co-workers, including the chloride-bridged dimer, the hydrido-bridged dimer, and the related diamidotitanium alkyl monomer.[46] However, addition of the reducing agent $KC_8$ to $\{[^{SiMe_3}NNN]V(\mu\text{-}Cl)\}_2$ under an atmosphere of dinitrogen saw the incorporation of $N_2$ into the complex and further bond cleavage. Fryzuk synthesised a structurally similar vanadium complex with a $[^{CyPh}NPN]^{2-}$ ligand, forming a chloride-bridged vanadium(III) ($d^2$) dimer.[47] Attempts to reduce this complex with $KC_8$ unfortunately yielded no isolable products.

Related to amido ligands are amidinates, or monoanionic bidentate amido-amine ligands where the two chelating nitrogen atoms share a delocalised double bond. They also feature a variable R-group as in standard amido-based ligands, and so are very useful for the tuning of particular steric and electronic properties in a metal complex. Gambarotta et. al. have reported a number of vanadium(II) ($d^3$) and vanadium(III) ($d^2$) complexes coordinated with either two or three chelating amidinate ligands.[48] Through modification of steric hindrance as controlled by R-groups present on the nitrogen atoms, they found that this steric hindrance determined whether a complex was stable as a dimer or a monomer (Figure 1.6). They also prepared a dinitrogen species from a vanadium amidinate complex. From the same group, a series of vanadium(III)

monoamides were also synthesised, featuring both halide-bridged and amido-bridged dimers; one of the mononuclear complexes, $[(Me_3Si)_2N]_2VCl•THF$, also formed a rare metal-borohydride complex when $NaBH_4$ was added, $[(Me_3Si)_2N]_2V(BH_4)•THF$.[49]

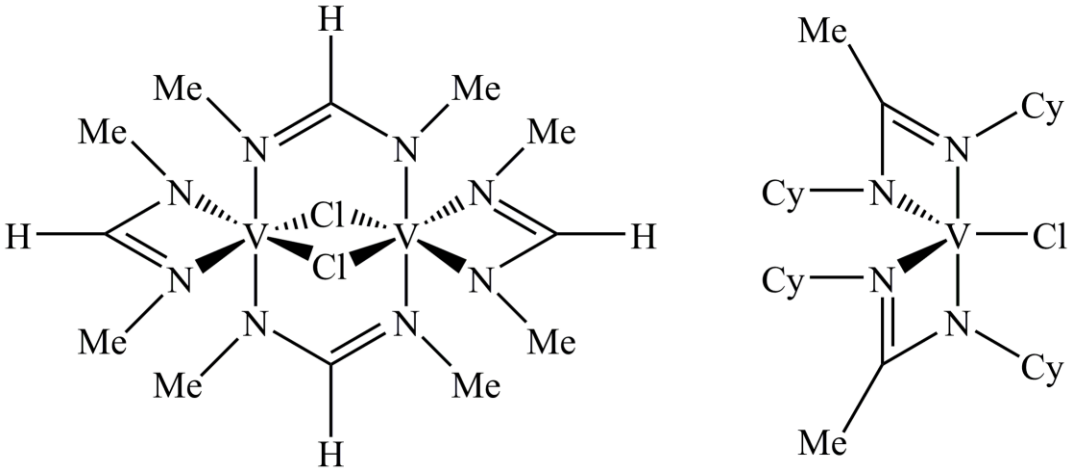

**Figure 1.6. Gambarotta's vanadium(III) amidinate complexes.**

Schrock has synthesised a tripodal triamidoamine vanadium(III) ($d^2$) complex of an interesting nature, $[(C_6F_5NCH_2CH_2)_3N]V$.[50] Instead of a regular alkyl or aryl R-group on the amide, he has used a pentafluorophenyl group, which would pull electron density away from the amido-metal bond. It is speculated that the altered electronics surrounding the metal affect the metal's ability to bind other donating ligands into its open coordination site. While it was found to bond with THF as well as an oxide, a ligand which bonds primarily through π back-bonding such as CO and $N_2$ had no reaction with the complex.

## 1.2.2. Reactivity of Early Transition Metal Amides

Bradley compared the chemistry of transition metal alkylamido complexes to that of complexes with metal-carbon bonds in regards to the synthesis, bonding, as well as general reactivity.[5] Indeed, it appears that such traditional organometallic-type chemistry goes hand-in-hand with metal-amido complexes. Recently, research utilising diamidoamine-based complexes has expanded towards the development of non-metallocene based olefin polymerisation catalysts.[6] Those complexes containing $d^0$ early transition metals have shown particular promise as catalyst precursors.[42] In addition,

amido-based complexes have shown aptitude for dinitrogen activation, as catalysts in hydroamination reactions, as well as in other bond activation reactions.[6] The inert nature of amido ligands once they are attached to a metal, combined with the control over the steric and electronic contribution to the overall complex as a result of the variable R-group make this type of ligand suitable for many organometallic-type applications.

### *Olefin Polymerisation*

Amido ligands have been studied extensively in recent years as an alternative to the ubiquitous cyclopentadienyl (Cp) ligand, which has led to development of amido-based complexes as catalysts for olefin polymerisation. Moving toward amido-based catalysts, Bercaw introduced a scandium (Group III) complex containing a chelating Cp ligand with a pendant amide group in 1990 (Figure 1.7a).[6,41,51] Supposedly a result of the constrained character of the ligand, the complex performed moderately well as a catalyst for facile olefin insertion and β-H and β-alkyl elimination.[51] It was then found that a ligand backbone of $SiMe_2$ yielded highly active catalysts, while larger backbones resulted in lower activities.[51–56] Piers later began developing scandium complexes using the monoanionic *β*-diketiminate ligand (Figure 1.7b), from which they were able to form a cationic complex with addition of $B(C_6F_5)_3$ that promoted the activity of ethylene polymerisation.[57]

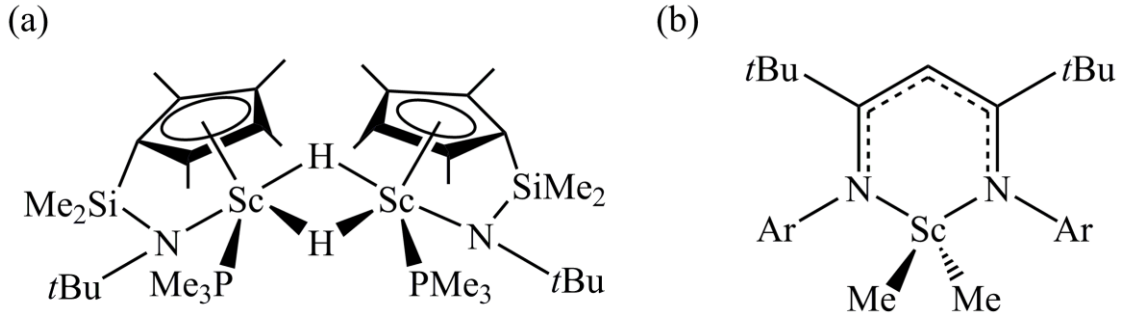


**Figure 1.7. (a) Bercaw's scandium complex featuring a $Cp^-$ ligand with a pendant chelating amide; (b) Piers' scandium *β*-diketiminate complex (Ar = 2,6-*i*$Pr_2$Ph).**

Moving to group IV metals, these are known to produce reasonably effective catalysts, particularly as metallocenes.[52] Based on Ziegler's $TiCl_4$-$AlClEt_2$ catalyst, titanocene dichloride activated with $AlClEt_2$ was also found to be a moderately active catalyst for the polymerisation of ethylene. Using the superior activator MAO

(methylaluminoxane), $ZrCl_2Cp_2$ was found to have the ability to polymerise propene, although the ratio of MAO required is very large in order to reach high activities. The discovery of these two structurally basic pre-catalysts prompted much research into the various permutations of these metal complexes to be examined as potential improvements on the originals.

From the success of the basic metal halide and Cp-based catalysts, researchers eventually progressed to studying the catalytic properties of pure amido-based complexes. Tinkler proposed that because the electron-deficient $d^0$ metals perform best as catalysts, the weaker donating ability of amides versus cyclopentadienyl ligands would result in more active catalysts.[58] Indeed, titanium and zirconium complexes were both found to perform well as amido-based alkene polymerisation catalysts, both as neutral and cationic species.[7,26,58–62] Diamides appear to be the most prevalent,[26,58,59,62] although a diamidoamine ligand gives moderate activity as an ethylene polymerisation catalyst in a cationic zirconium complex.[60] McConville developed bulky diamido dialkyl titanium(IV) complexes which exhibited high activity towards the polymerisation of 1-hexene when in the presence of a Lewis acid cocatalyst.[63] In addition, a zirconium bis(amide) system featuring a cyclometallated $–N(SiMe_3)_2$ ligand and a cationic metal centre has shown moderate polymerisation activity for ethylene.[61] A dialkyl-diamidosilylether zirconium complex (Figure 1.8b) showed comparatively little ability compared to a related bis-diamido zirconium complex, which was activated with MAO by removal of one of the diamido groups.[7] Overall, the mid-90's witnessed significant growth in this area with reports of a number of primarily Zr(IV) and Ti(IV) amido complexes displaying alkene polymerisation abilities (Figure 1.8).[7,9,25–28,38,64–68]

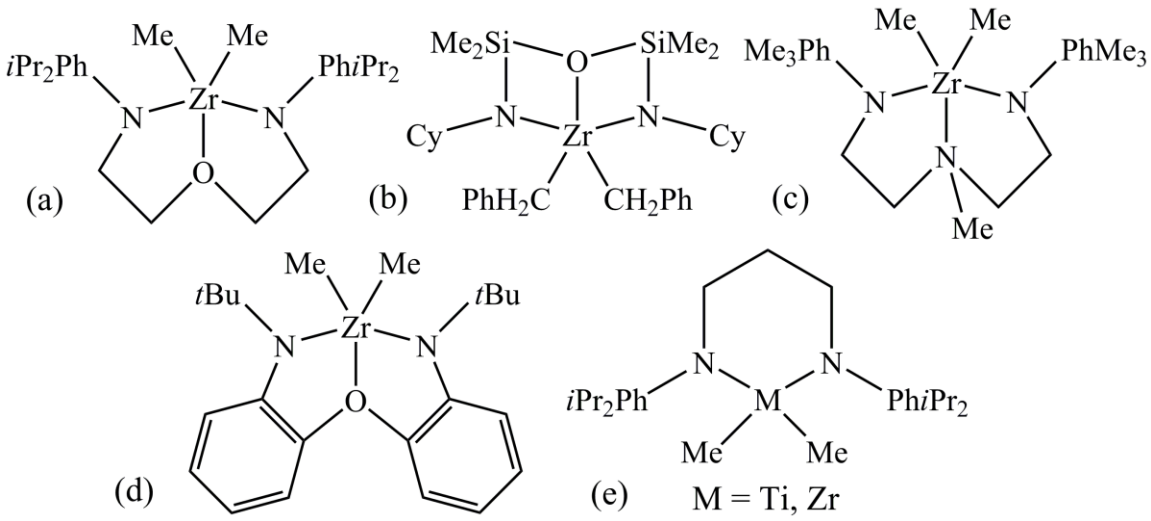


**Figure 1.8. Alkene polymerisation catalysts of zirconium and titanium diamido complexes.**

### *Dinitrogen Fixation*

Early transition metals in high oxidation states are known to have high enough reduction potentials such that they are able to induce dinitrogen bond cleavage.[39,69] However, amido ligands act as ancillary ligands, resisting further functionalisation from added reagents to the amido-metal complexes; this makes early transition metal amido-based complexes ideal for exploring dinitrogen activation chemistry.[70] Research involving the synthesis of vanadium dinitrogen complexes increased with the discovery of its presence of a vanadium centre in one of the subtypes of the nitrogenase enzyme, although its role in the enzyme is unclear.[71–73] Indeed, many vanadium complexes, both amido-based and not, have been shown to activate dinitrogen.[39,74–80] Few of these are currently able to cleave it.[74,77,79,80]

Titanium has also been shown to activate dinitrogen, although this primarily appears to occur from titanocene reagents.[81–83] However, Gambarotta set the stage for the related amido chemistry in 1991, when he published a mixed valent titanium(I)/titanium(II) dinitrogen amido complex, $\{[(Me_3Si)_2N]TiCl(TMEDA)\}_2(\mu\text{-}N_2)$.[84] Since then, Fryzuk has also published an interesting diamido titanium(III) complex using his $^{R}[NPN]^{2-}$ (R = Ph) ligand, which cleaves the added dinitrogen to form $\{[N(PN)N]Ti\}_2$, where each added nitrogen forms a double-bonded P – N unit that bridges between the titanium centres (Figure 1.9).[85] While dinitrogen activation is not a common reaction with

scandium, Evans was able to produce a side-on bound dinitrogen between two scandocene-type complexes through a multi-step process (see Section 2.2.3 for further discussion).[86]

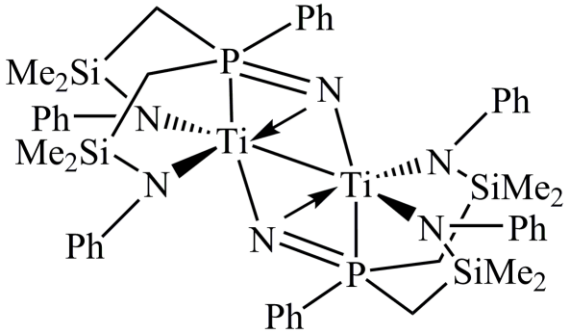


**Figure 1.9. Unusual cleavage product of a titanium(III) dinitrogen complex.**

In addition to the chloro, hydrido, and alkyl moieties of [$^{SiMe_3}$NNN]VX, Cloke was also able to form a dinitrogen dimer, featuring an end-on bridge.[79] Fryzuk has developed a series of vanadium diamidophosphine chloride-bridged dimers, and showed that minor steric changes can prevent the formation of a dinitrogen moiety.[47] According to Keppert, the chemistry of niobium(III) and tantalum(III) little resembles the chemistry of vanadium(III).[33] In the realm of amido chemistry, however, these elements are often explored together. For example, Fryzuk has successfully synthesised $^{R'R''}$[NPN]$^{2-}$ complexes with vanadium, niobium, as well as tantalum. As previously discussed, the vanadium complex did not activate dinitrogen;[47] the tantalum complex, however, produced an interesting dinitrogen compound that was bound both side-on and end-on simultaneously.[87] The niobium complex was successively formed, although it was reportedly highly unstable.[47] More recently, Sita has developed a $\eta^5$-cyclopentadienyl/$\eta^2$-amidinate ligand that is capable of supporting the majority of metals in groups IV through VI, and these complexes have been shown to activate dinitrogen.[88] From here, he has been able to explore how dinitrogen coordination changes solely based on the metal, as the ligand always remains the same.

### *Hydroamination*

Hydroamination is a very desirable process for organic chemists, as it offers an inexpensive and direct method of forming otherwise synthetically-demanding amines, imines, and enamines.[32] The hydroamination process involves the use of either alkenes

or alkynes and an amine, and a catalyst to direct the reaction.[89] The two groups may be combined intramolecularly to form heterocycles, or from separate starting materials reacting intermolecularly. The mechanism of addition of the amine across the unsaturated bond follows either a Markovnikov or anti-Markovnikov pathway, and may result in either R or S configurations.

The first catalyst to initiate this reaction was a metallocene based lanthanide catalyst, made with both lanthanum and lutetium, in 1989.[90] More than a decade later the first amido-based complex was synthesised that also successfully catalysed this reaction.[91] Scott et. al. first attempted to use yttrium coordinated with a biaryl diamine ligand and a monoamide, along with two THF adducts (Figure 1.10a); the lanthanum and samarium analogues were subsequently synthesised. While the rate of hydroamination was substantially faster with the yttrium moiety, the enantiomeric excess was significantly reduced when testing the lanthanide species. It was also found that the yttrium species containing silylamides required higher conversion temperatures and twice the time to achieve the same quantity of conversion as the yttrium species containing alkylamides instead.

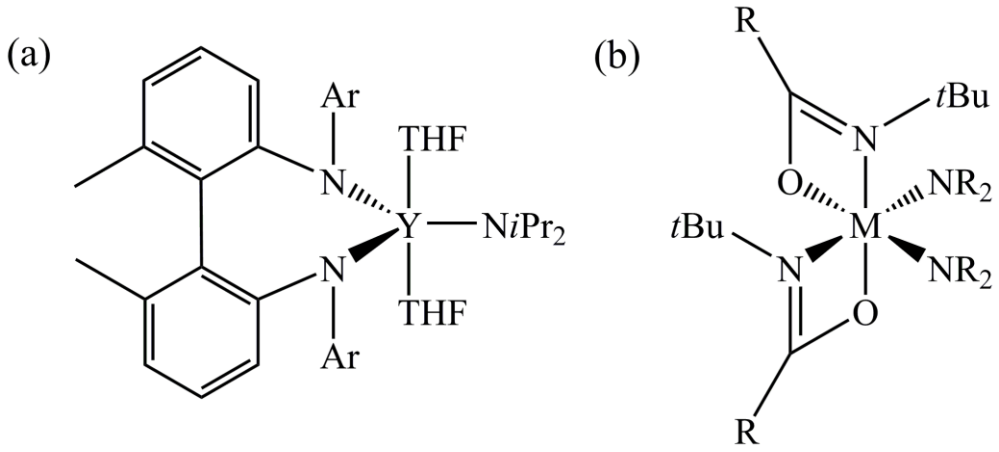


**Figure 1.10. Hydroamination catalysts. (a) Scott's amido lanthanide catalysts; (b) Schafer's amidinate amido transition metal catalysts.**
(a) Where Ar = 3,5-di-*t*Bu, 2-ethyl, 2-Cy, 2-Me-5-*t*Bu. (b) M = Ti, Zr; R = Me, Et.

Titanium and zirconium complexes have performed well as catalysts for the hydroamination of primary amines with alkynes. Schafer showed that complexes of diamido amidate titanium and zirconium (Figure 1.10b) are tunable, *via* the R-groups

present on the ligands, and were able to catalyse the hydroamination reaction both intramolecularly and intermolecularly, using alkynes and primary amine groups.[92] Alternatively, Gade has developed titanium imido complexes that are able to perform hydroamination reactions of terminal alkynes with anti-Markovnikov regioselectivity.[93] Richeson is also using titanium imido complexes to synthesise biologically-relevant guanidines via hydroamination reactions.[94] This research indicates the relevance of early transition metal amides to developing new and dynamic catalysts for otherwise difficult syntheses.

## 1.3. Late Transition Metal Diamido Chemistry

### 1.3.1. Structure and Bonding of Late Transition Metal Amido-based Complexes

There are considerably fewer known metal amide complexes with the late transition metals as opposed to the earlier metals. The attributed rationale for this is due to the σ- and π-donor mismatch of the amide moiety with the more electron-rich metal centres.[6] Despite this, however, there is a growing interest in late transition metals with amido ligands in the field of catalysis; again, this is likely because of the similarity in properties of the amide complexes to traditional Cp-type organometallic complexes. In addition, iron and cobalt are desirable metals in catalysis, due to their wide availability, low toxicity and cost, and their success in previously employed catalysts.[95–97]

There are numerous monodentate amide complexes known with each 1$^{st}$-row transition metal in various oxidation states (except for zinc), the most prominent of which is the series featuring the bis(trimethylsilyl)amides (discussed in section 1.1).[6,18,20,22,98] Many of the 2$^{nd}$ and 3$^{rd}$ row metals have also been examined, particularly those metals predominant in industrial catalysis, such as ruthenium, rhodium, palladium, and platinum, as well as iridium, silver, and gold.

In the mid-1980's, Power examined low-coordinate chromium, manganese, iron, cobalt and nickel amido complexes.[23,24,99–102] After the synthesis of manganese(II) and cobalt(II) tris-amido complexes with the –N(SiMe$_3$)$_2$ ligand,[23] it was postulated that a

bulkier amido group could result in a two-coordinate system. Thus, Power was able to form two-coordinate, monomeric iron(II) and cobalt(II) complexes featuring two bis(diphenylmethylsilyl)amido groups, which were able to encapsulate the metal centre and prevent dimerisation (Figure 1.11a).[24] In addition, he also synthesised diphenylamido complexes of nickel(II) and cobalt(II) (Figure 1.11b).[100] They each formed dimers containing two bridging and two terminal amido groups. The nickel(II) complex also formed a three-coordinate tris-amido anionic complex, which also featured a lithium counter-ion.

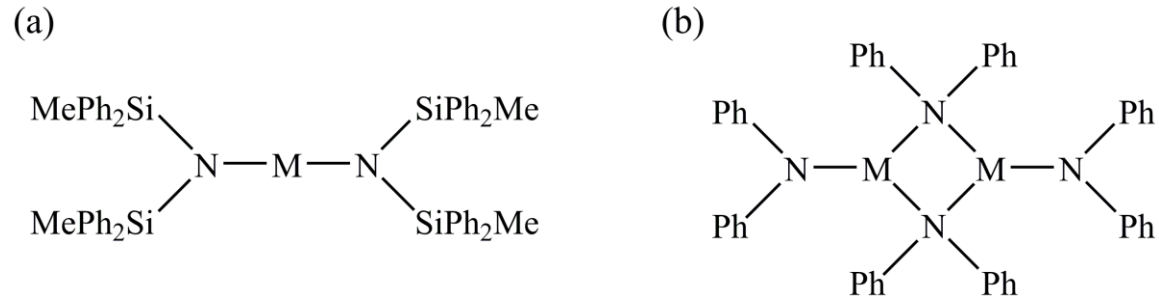


**Figure 1.11. Sterically hindered amide complexes of the late 1st row transition metals. (a) M = Fe(II), Co(II); (b) M = Co(II), Ni(II).**

In the early 1990's, Bergman synthesised a ruthenium amido complex.[103] In their synthesis, they began with the ethylene containing complex, $(PMe_3)_4Ru(C_2H_4)$, and added aniline. Heating overnight resulted in the clean formation of the amidoaryl product, $(PMe_3)_4Ru(H)(NHPh)$. More recently, Bergman expanded his research into parent amido complexes of other late transition metals in addition to ruthenium.[104] First developing the complexes *trans*-$[Ru(dmpe)_2(H)(NH_2)]$ (dmpe = 1,2-bis(dimethyl-phosphino)ethane) and $Cp^*Ir(PMe_3)(Ph)(NH_2)$ from the corresponding metal chlorides and a $NaNH_2/NH_3$ mixture,[105] they were then able to make the synthetic leap to the rare iron parent-amido compound, $Fe(dmpe)_2(H)(NH_2)$,[106] as well as *cis*-$[Ru(PMe_3)_4(H)(NH_2)]$.[107]

There are also a number of amido-bridged dimers containing the heavier transition metals.[108–116] Tilley and Matsuzaka have independently synthesised the same complex motif with ruthenium(II), and iridium(II/III), respectively, utilising the sterically uninhibited amide –NHPh, in the formation of $[Cp^*M(\mu\text{-NHPh})]_2$.[113,114] Additionally, Matsuzaka developed a rhodium(III) analogue, although one of the bridging amido

groups was replaced with a bridging bromide, and a bromide counterion to balance charge.[108] Boncella was able to form the amido-bridged dimer $[PdR(PMe_3)(\mu\text{-}NHPh)]_2$, where R = Ph, Me, as well as some related palladium(II) monomers.[109] Furthermore, Heck, Roundhill, and Woollins were each able to synthesise complexes of platinum(II) and platinum(IV), each featuring bridging parent amido ligands.[112,115,116]

Interestingly, there have been cluster compounds of silver(I) and gold(I) published with amide ligands as well. In 1996, Lappert developed the macrocycle $[Ag\{N(SiMe_3)_2\}]_4$, which features alternating Ag-N atoms (Figure 1.12).[110] A few years later, Rees published the gold(I) analogue of Lappert's silver compound, which exhibits the same structural motif.[111] It should be noted that further reactivity of these monodentate amide complexes result in loss of the amide group.

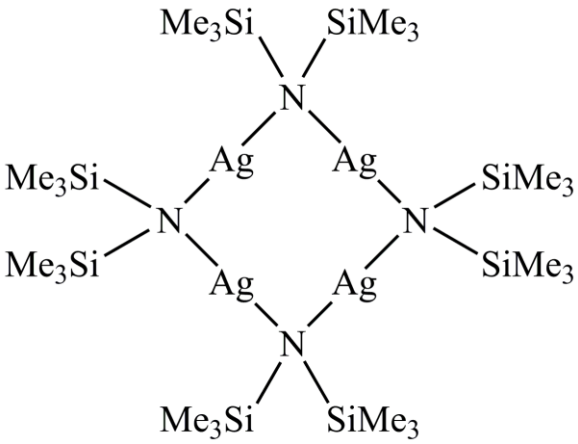


**Figure 1.12. Lappert's macrocyclic silver amide complex.**

Fryzuk developed complexes containing a $[PNP]^-$ ligand, 1,3-bis[(diphenyl-phosphino)methyl]tetramethyldisilazane, with many of the preferred metals for catalysis – nickel, palladium, platinum, rhodium, and iridium (Figure 1.13).[117–122] Many of these form 4-coordinate species containing the tridentate (diphosphino)amido ligand and a halide, which allows for additional reactivity. These complexes are unique in that they are formed with soft metals and use a ligand that combines soft phosphines and a hard amide donor, which traditionally would not form a bond with these metals. By connecting the hard and soft ligand donors together in a chelating ligand, the amide's enforced proximity to the metal centre encouraged metal-amide bond formation.

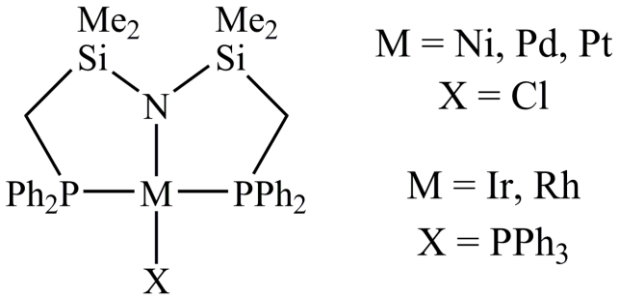


**Figure 1.13. Fryzuk's [PNP]MX complexes with late transition metals.**

In addition to amido ligands for the synthesis of metal complexes, nitrogen donor atoms can be used in alternate binding motifs; these amine/imine motifs are reported in numerous publications. As an example, Kempe has recently synthesised additional first row transition metal complexes with the aminopyridinato ligand; this ligand had already been studied extensively in the past, and represents a synthetically important and flexible class of amido ligand.[38,123,124] In Kempe's research, formation of mononuclear complexes of scandium(III), iron(III), manganese(II), iron(II), and cobalt(II) was explored with either two or three of these aminopyridinato ligands bound (Figure 1.14).[125] Whereas an amido ligand forms a sigma bond with a cationic metal complex through donation of an additional lone pair on the nitrogen, an amine can only π-donate its lone pair to the metal complex. Since amides are primarily bound to a metal through a σ-bond and donate their negative charge to the metal centre, thus charge-balancing the complex, they typically exhibit shorter bond distances than their amine counterparts which are neutral species sharing their lone-pair's electron density with a metal.

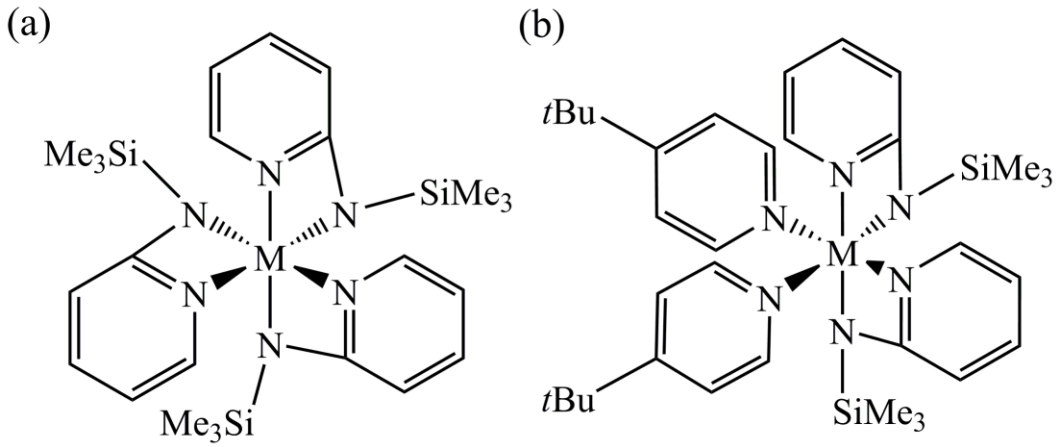


**Figure 1.14. Kempe's amidopyridinate complexes with late 1st row transition metals. (a) M = Sc(III), Fe(III); (b) M = Mn(II), Fe(II), Co(II).**

The Leznoff group has focused on developing research on diamidoether ligands with late 1st row transition metals in the past; of particular note are chromium, iron, and cobalt complexes. In each case, the M(II) diamido dimer formed an amido-bridged structure, where each ligand featured a terminal amido group and a bridging amido group between two metal centres (Figure 1.15).[126–128] In addition, Roesky reported the related Mn(II) complex with the same diamido ligand, which exhibited the same binding properties.[129] The related M(III) complexes have also been explored with this diamido ligand family, forming instead halide-bridged dimers. These are known with iron and chromium; the cobalt(III) complex synthesis has been unsuccessful through various methods thus far.[43,130]

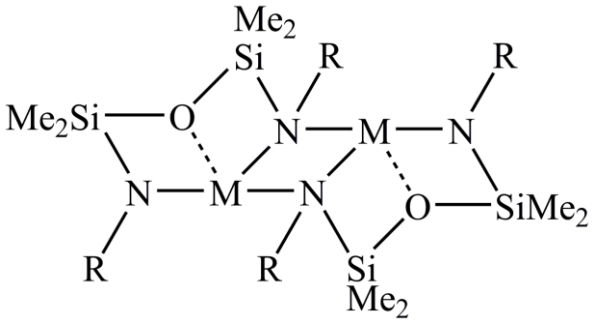


**Figure 1.15. Diamido metal(II) complex developed within the Leznoff group.**

The major drawback of the M(II) diamido complexes is the lack of halide ligands, which typically represent potentially reactive sites for further applications, most notably towards catalysis. Leznoff has discovered that by adding two equivalents of metal (iron, cobalt) to one diamido ligand, a multinuclear complex can be formed via a bridging diamido ligand and terminal halides off each metal (Figure 1.16).[16] These halides can indeed be activated, as the Co(II) moiety was alkylated, forming a dinuclear high-spin Co(II) dialkyl complex.

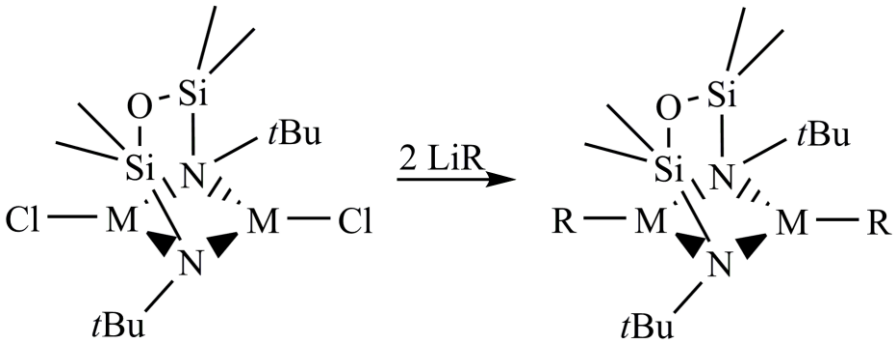


**Figure 1.16. Multinuclear diamido-bridging complex from the Leznoff group, where M = Fe(II), Co(II).**

Central to all of these complexes is the challenge of actually bonding the amido group to the transition metal. Since the late transition metals are considered "soft" Lewis acids, and amides are hard Lewis bases, the mismatch presents a synthetic challenge, which can be overcome using several techniques. As has been illustrated above with Fryzuk and Kempe's work, using a chelating ligand which also contains softer donors (such as Fryzuk's [PNP] ligand) can force the hard amide to bond with the metal. Another method makes use of an yttrium complex which acts as a ligand transfer agent.[43] Addition of the bis(diamido)silylether yttrium(III) complex, {Y[$^{t\text{Bu}}$NON]$_2$}Li•THF, to $FeCl_3$ resulted in one of the ligands transferring to the iron centre, forming the halide-bridged dimer {[$^{t\text{Bu}}$NON]FeCl}$_2$. A third method reduces the high electron rich character of the bonding amide group by using an electron-withdrawing R-group, facilitating the ligand to bind to later electron-rich transition metals. Schrock has reported tripodal triamidoamine complexes with fluorinated R-groups,[131] the putative complexes with more electron-rich R-groups may otherwise have failed to form, although this approach has not been used by any other research group. Such complexes containing this unusual amido-ligand electronic profile would be expected to produce interesting chemistry. This will be an approach explored in this thesis.

### 1.3.2. Notable Reactivity Experiments of Late Transition Metal Amides

Some of these late transition metal amide complexes were found to have unusual reactivity. Fryzuk alkylated the complex Ir($CH_3$)$PPh_2$[PNP] with methyl iodide in an unexpected manner.[122] Instead of replacing a ligand or simply adding to the iridium

centre, the methyl bound to the phosphide ligand while the iodide bound to the metal, forming $Ir(CH_3)I(PPh_2Me)$[PNP]. With the nickel and palladium complexes, MCl[PNP], Fryzuk found that Grignard-type metathesis reactions would produce the alkylated complex, MR[PNP], with a variety of RMgX Grignard substrates (R = Me, $CH_2CH=CH_2$, $CH=CH_2$, Ph).[118] The requirement was only that there were no *β*-hydrogen atoms present on the Grignard R-group. Alkyllithium reagents were able to produce the same products, but in a substantially lower yield.[118]

In 1987, Bryndza and Bercaw reported a ruthenium amide, $Cp^*(PMe_3)_2RuNPh_2$.[132] While they were not able to form any other ruthenium amides, they did discover that addition of CO did not affect the $Ru\text{-}NPh_2$ moiety, and instead replaced a phosphine group. In a related field, Kozak has recently developed a series of amine-bis(phenolate) iron(III) complexes, which show an aptitude for C-C cross coupling reactions of Grignard reagents with alkyl halides.[133–135] This particular application may in future translate to amide-based iron complexes.

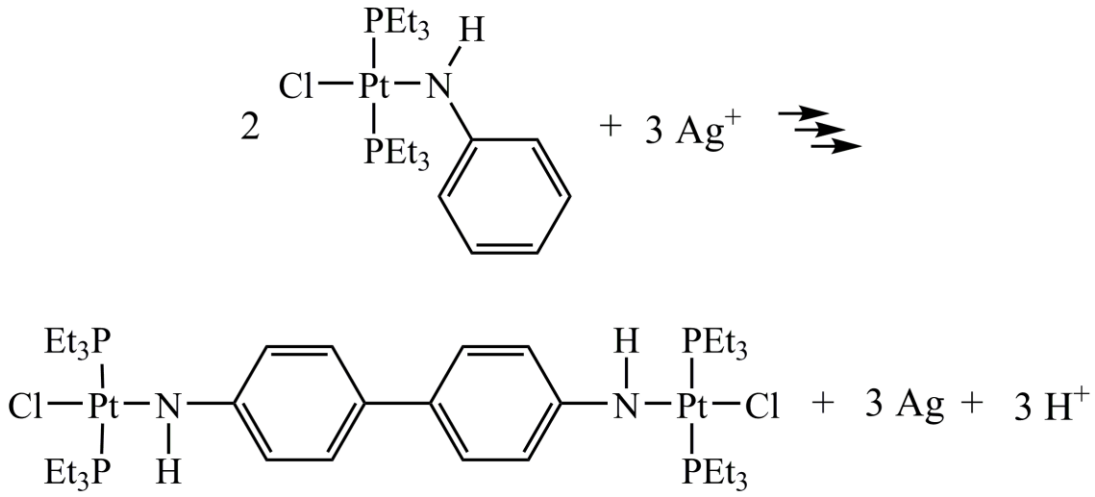

**Scheme 1.1. Platinum amide dimerisation via oxidation with $AgPF_6$.**

In terms of heavy metal amide complexes, a focus on platinum led to some unexpected results. Alcock was able to oxidatively dimerise a platinum complex, $(PEt_3)_2PtCl(NHPh)$, at the *para* position of the amido phenyl, via the addition of $AgPF_6$, and formed a dicationic product and metallic silver (Scheme 1.1).[136,137] Bryndza and Tam were likewise able to synthesise a series of Pt(II) amides of the general form (DPPE)PtR(amido), where DPPE = 1,2-bis(diphenylphosphino)ethane, R = Me, Ph,

$CH_2Ph$, amido = NMePh, $N(CH_2Ph)H$, $NMe_2$.[138] In the case of R = Me, each of the amido complexes, when reacted with CO, formed a M-N insertion product, (DPPE)PtMe[C(O)amido]. These insertion products are similar to the products of CO insertion of M-O (alkoxide) bonds; their findings indicate that the M-N bond is somewhat weaker than the related M-O bond, indicative of an aptitude towards catalytic applications. Trogler found that the platinum complex $(PEt_3)_2PtH(NHPh)$, could regioselectively insert acrylonitrile into the Pt-N bond via a 1,2-insertion, forming a hydrido alkyl platinum(II) species (Scheme 1.2). [139]

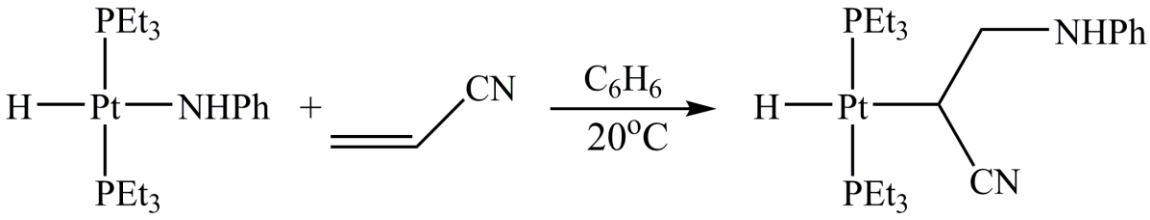


**Scheme 1.2. 1,2-insertion of acrylonitrile into platinum(II) hydridoamido complex.**

Kempe developed a series of lanthanide bis(aminopyridinato) -ate complexes which were able to act as ligand transfer agents towards late transition metals.[140] With these transfer agents, the synthesised nickel and platinum aminopyridinato complexes were reported (Figure 1.17). Additionally, the ligands each chelated to the metal in a tetradentate fashion, and were of the form bis(aminopyridinato)siloxyether. The nickel complex, when activated with $EtAlCl_2$ (Al/Ni = 150) at room temperature was able to oligomerise ethylene.[123]

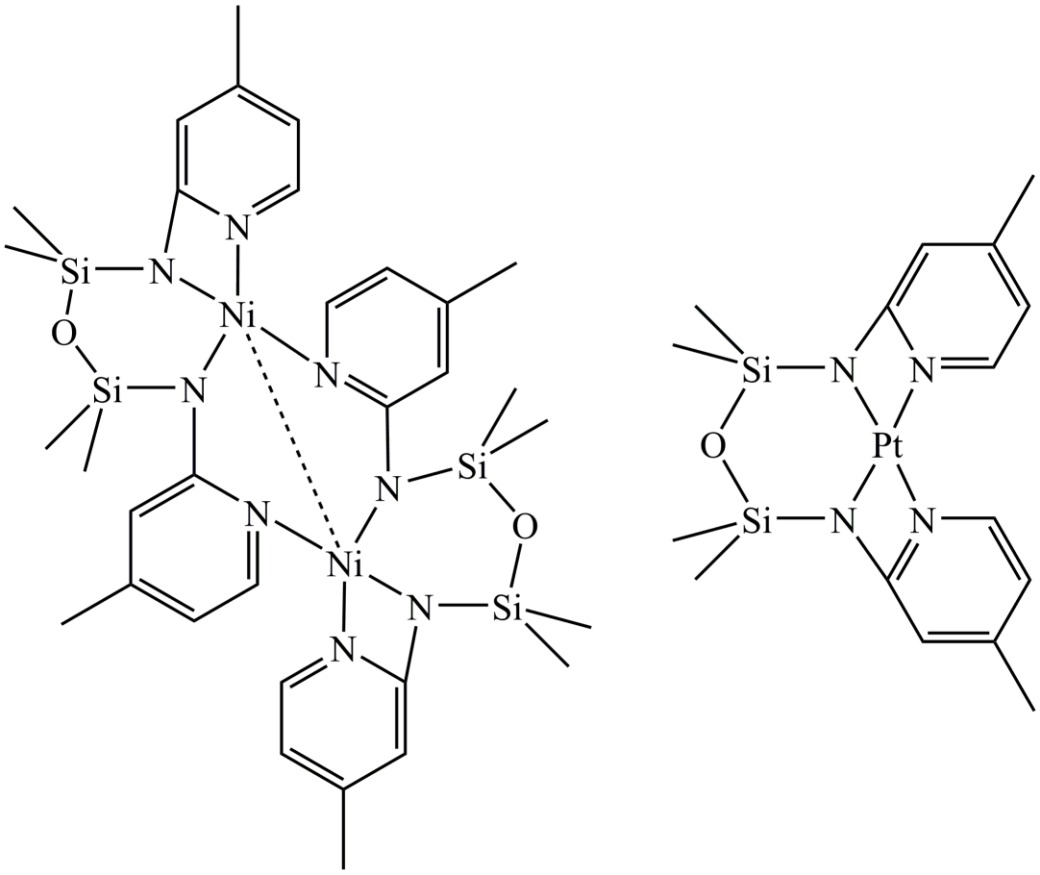


**Figure 1.17. Kempe's nickel and platinum aminopyridinato complexes.**

## 1.4. Research Direction

### 1.4.1. Diamido Silylether Ligand Design and Synthesis

The diamido ligands employed within the Leznoff group feature a silylether backbone that can participate in neutral metal bonding during the formation of metal complexes. Of the form $[^{R}NON]^{2-}$, these ligands exhibit greater stability than their monoamide counterparts as a result of the chelate effect. The silylether backbone provides a certain amount of flexibility in complex formation, as the oxygen can be pulled in toward the metal centre, or repelled by excessive electron density.

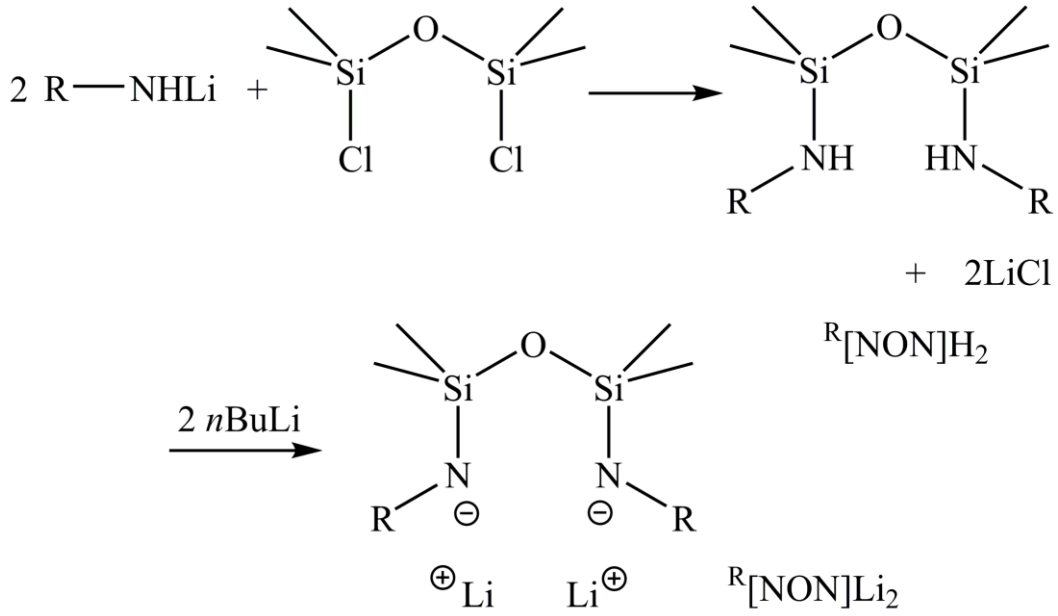


**Scheme 1.3. General synthesis of $[^{R}NON]^{2-}$ ligands.**

Synthesis of these ligands is relatively straightforward (Scheme 1.3).[130] Monolithiation of a primary alkyl or aryl amine produces a lithiated amide that can then be added to a solution of dichlorotetramethyldisiloxane, $(ClSiMe_2)_2O$, at 0 °C, with two equivalents of amide to one $(ClSiMe_2)_2O$. This salt metathesis reaction results in the formation of the protonated ligand, $(RHNSiMe_2)_2O$, and produces lithium chloride as a by-product. In the case of R = *t*Bu or propyl (i.e., alkyl groups), the amine does not have to be lithiated initially, and four equivalents of amine can be added directly to the siloxane backbone. The basicity of the amine facilitates the reaction directly, producing HCl, which the third and fourth equivalents neutralise by formation of the *t*Butyl-ammonium chloride salt.

Typical amines that have been used in the Leznoff group include $tBuNH_2$, 2,4,6-$Me_3PhNH_2$, 2,6-$iPr_2PhNH_2$, and 3,5-$(CF_3)_2PhNH_2$.[130] The variety of possible amines used to make the $^{R}[NON]^{2-}$ amido ligand is indicative of many possible complexes that can be formed, each with its own attributes. The choice of amine allows control over the desired steric and electronic properties of the resulting ligand, to aid in targeting a metal complex with particular properties. For example, the $^{t\text{Bu}}[NON]^{2-}$ ligand results in siginificant steric bulk immediately surrounding the metal in a complex, while the $^{3,5\text{-}(CF_3)_2Ph}[NON]^{2-}$ ligand offers a more electron-poor amide, which may influence how it bonds to metals.[130]

## 1.4.2. Synthetic Methodology

The $[^{R}NON]^{2-}$ ligand system contains a relatively weak Si-N bond, which, due to the oxophilicity of silicon, makes these ligands moisture sensitive. Therefore, throughout this thesis, all synthetic and characterization manipulations used standard inert-atmosphere techniques; most notably, this includes the use of a Schlenk line, as well as a glovebox with a nitrogen atmosphere. All solvents were dried using reflux systems with sodium metal, and benzophenone as an indicator (with the exception of hexanes, which does not use benzophenone).

In this research project, deprotonation of the $[^{R}NON]H_2$ ligands with two equivalents of *n*BuLi to form the dilithium salt (Scheme 1.3) was followed by the addition of a metal halide. These reactions usually involved the use of polar solvents, such as tetrahydrofuran (THF) or dimethoxyethane (DME), for increased solubility of the starting materials. The metal halides may also exist as solvent adducts; those employed typically contain three equivalents of THF that increase the solubility of the metal halide in that solvent. These reactions used salt metathesis as a driving force, as the favourable salt formation facilitates the desired reaction between ligand and metal (Scheme 1.4). A simple filtration in a relatively non-polar solvent, such as toluene or hexanes, removed the LiCl salt and was usually sufficient for purification of the resulting metal complex.

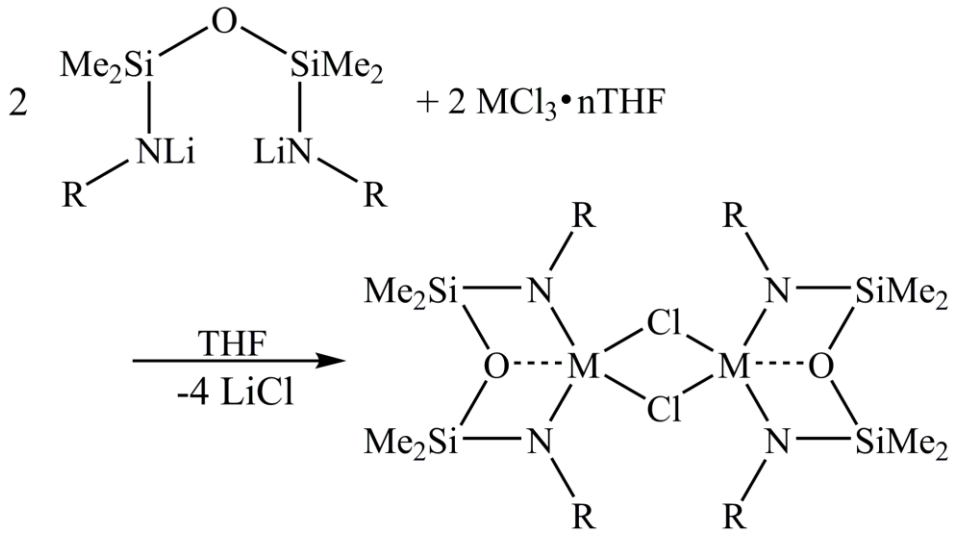


**Scheme 1.4. General metal coordination complex formation using the diamido ligands, $[^{R}NON]^{2-}$.**

These coordination complexes then served as starting materials for a wide range of reactions, including halide-for-alkyl substitution, hydride addition, reduction or oxidation reactions, to name but a few.

### 1.4.3. Properties of $[^{R}NON]^{2-}$ Metal Complexes

The majority of diamido complexes synthesised in the Leznoff group utilise the $[^{tBu}NON]^{2-}$ ligand. With work done by Bochmann, Roesky, and Leznoff, this ligand has appeared in conjunction with many transition metals[7,16,43,129] – primarily with the 1st row transition metals, actinides,[141] as well as some main group elements.[129] These complexes adopt a variety of conformations in response to the charge on the metal as well as steric bulk (Figure 1.18). For example, the transition metal complexes where the metal is in the +3 oxidation state consistently form a dihalide-bridged dimer, whereas the +2 oxidation state metal complexes form an amido-bridged dimer. In the case of Bochmann's Zr(IV) complex, two ligands simply bind to one metal centre.[7] The actinides, U(IV) and Th(IV), although they have an expanded coordination sphere compared to their transition metal counterparts, only bind one ligand and retain two chlorides in these $[^{tBu}NON]^{2-}$ complexes.[141] The main group complexes ($Ge^{2+}$, $Sn^{2+}$, $Te^{2-}$) are different again, preferring to bind only a ligand, leaving free a lone pair of electrons for additional reactivity.[129]

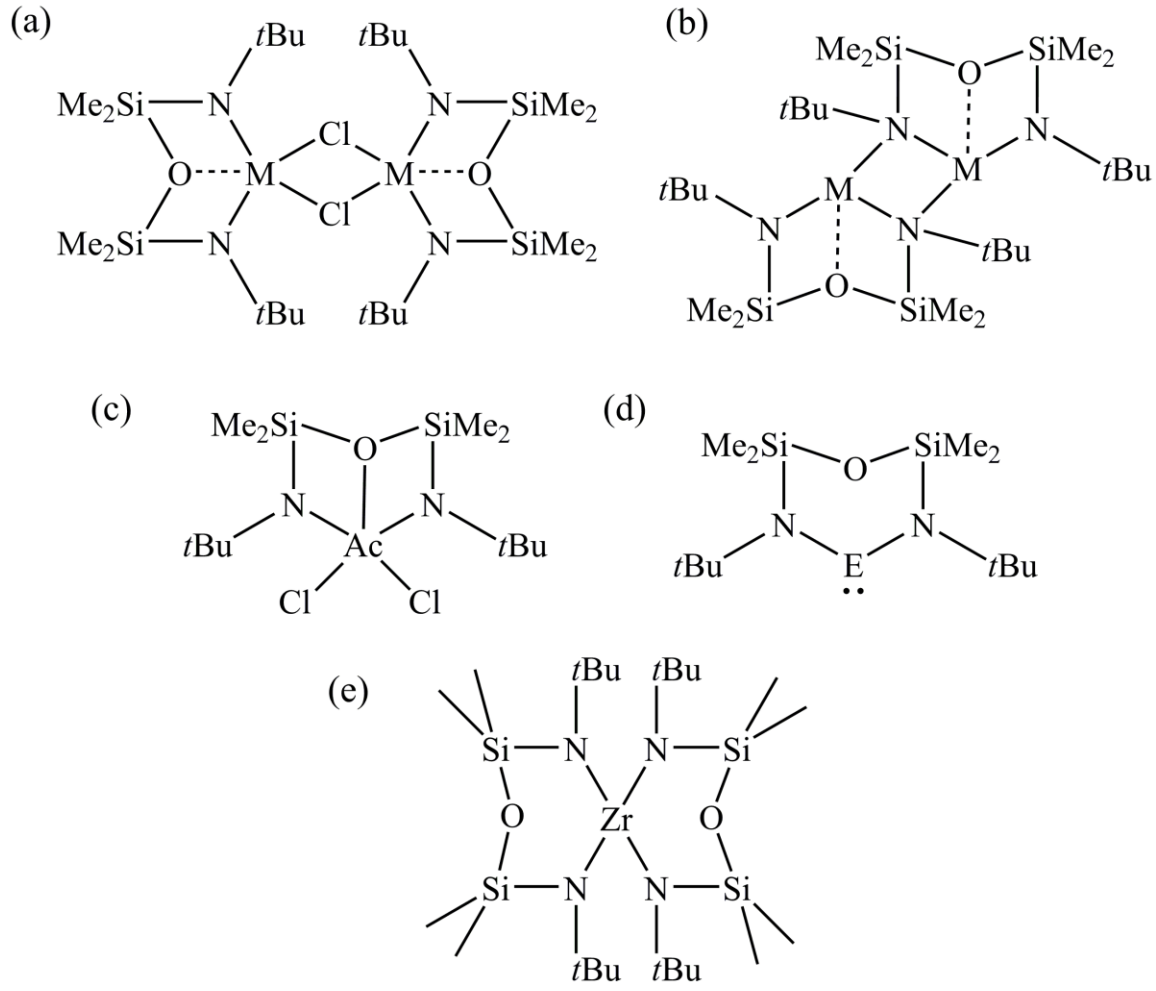


**Figure 1.18. General complexation motifs of [$^{tBu}$NON]$^{2-}$ with (a) $M^{3+}$ = Y, Cr, Fe; (b) $M^{2+}$ = Cr, Mn, Fe,Co; (c) $Ac^{4+}$ = U, Th; (d) $E^{2+}$ = Ge,Sn; $E^{4+}$ = Te; (e) $Zr^{4+}$.**

Switching the R-group from *t*Bu to 2,4,6-Me$_3$Ph, [$^{Me_3Ph}$NON]$^{2-}$ complexes have shown to be versatile in conjunction with the actinides, which are electronically similar to the early transition metals. While thorium(IV) ($d^0f^0$) has been shown to form an "ate"-complex dimer containing this ligand in THF, it is also able to form a bis-diamido thorium(IV) complex free of solvent and salt when the reaction is performed in a non-coordinating solvent.[142] This particular ligand, when complexed to cobalt(II), yields the familiar amido-bridged dimer, as seen with the [$^{tBu}$NON]$^{2-}$ ligand and +2 oxidation state metals.[126] When complexed with iron(III), an unexpected "ate"-type complex is formed, which exhibits Li-aryl interactions.[143] This structure is also retained in the related

[$^{i}Pr_2^{Ph}$NON]$^{2-}$ complex. The iron congener also exhibits the unique magnetic property of spin-admixture.[144]

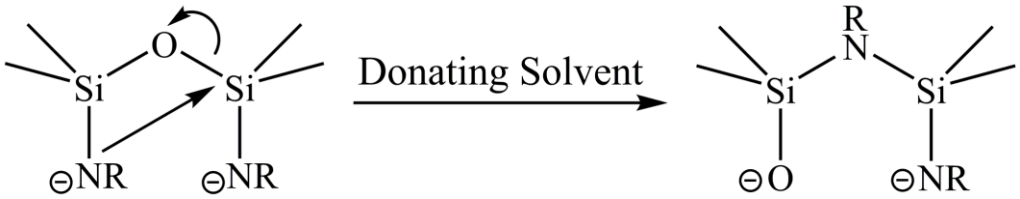


**Scheme 1.5. Retro-Brook rearrangement of [$^{Ar}$NON]$^{2-}$ ligands.**

The aryl diamido silylether ligands (Ar = $Me_3Ph$, $iPr_2Ph$) do exhibit one interesting trait, which makes them very useful to synthetic organometallic chemists. When the diamido ligands are lithiated in a polar aprotic solvent such as THF, a 1,3-silyl retro-Brook rearrangement occurs. This rearrangement is proposed to be facilitated by ion-pair separation, where the solvent's oxygen-donor prevents close association of lithium counter-cations, and the resulting more basic amido anion nucleophilically attacks the silyl moiety bound to the other amide group.[128] This weakens the silyl-ether bond, and the breakage of this bond results in a rearranged mixed amino/amido/siloxo ligand (Scheme 1.5). Mixed-donor ligands are very rare and usually require several steps to synthesise; however, these ligands are able to rearrange over several hours at room temperature during the lithiation step. These have been utilised as ligands on chromium(II), and they form an oxo-bridged dimer where the amide bonds to the metal only in the terminal position.[128] When the amido R = $iPr_2Ph$, the *ipso*-C of the aryl group in the metal complex interacts in a rare $\eta^2$-fashion with the chromium centre.

## 1.4.4. Research Hypothesis

As discussed above, [$^{t}$BuNON]$^{2-}$ has been used in conjunction with a number of transition metals, particularly within the 1$^{st}$ row. However, the early 1$^{st}$ row transition metals have been largely ignored. While [$^{t}$BuNON]$^{2-}$ complexes of yttrium and zirconium exist, the early 1$^{st}$ row complexes remain unknown. Therefore, it would be prudent to develop these complexes and to study their reactive properties in an effort to develop a trend across the entire 1$^{st}$ row. Since many of the metal complexes currently reported are in the +3 oxidation state, and this is a stable state for the early transition metals, the

synthesis of [$^{t\text{Bu}}$NON]-$M^{3+}$ halides were targeted in this thesis. Structural differences and reactive behaviour between the resulting complexes can be attributed to the changing number of *d*-electrons on the metal. Thus, the following experiments aim to discern how the metal *d*-electrons affect the structure and reactivity of the [$^{t\text{Bu}}$NON]$^{2-}$ metal complexes, specifically scandium ($d^0$), titanium ($d^1$), and vanadium ($d^2$).

Unlike [$^{t\text{Bu}}$NON]$^{2-}$, the [$^{(CF_3)_2\text{Ph}}$NON]$^{2-}$ ligand has not been examined in conjunction with any metals. As the only diamido silylether ligand in the series that has been developed with a substantially electron-withdrawing amido R-group, this ligand presents a unique opportunity to investigate the effect of altered ligand electronics on the resulting diamidometal complexes.[130] While both alkyl and aryl amido R-groups have been used to synthesise various complexes by the Leznoff group,[16,43,126,128,130,143] allowing control over the steric properties of the ligand, the change in electronic properties of the base ligand has not yet been explored. Therefore, the second project in this thesis examined how a change in ligand electronics affected the structure and reactivity of the resulting metal complexes. Comparison between these new complexes and previously published related aryl-amido ligands will help to determine the role of electron-donating ability in a diamido-based metal complex.

## 1.5. Characterisation of Paramagnetic Coordination Complexes

There are several standard techniques used to definitively characterise organometallic complexes; x-ray diffraction and nuclear magnetic resonance (NMR) spectroscopy are the most often employed. Other methods typically used are elemental analysis (EA), infrared (IR) spectroscopy, and mass spectrometry (MS). To characterise the compounds in this thesis there are two factors that must be considered: (a) the air sensitivity of the compounds, and (b) the presence of paramagnetic metals. The air sensitivity limits the use of certain techniques; for example, MS and IR spectroscopy cannot easily be used without the introduction of oxygen or water molecules to the sample, and so it was not used in this research. The paramagnetism of the complexes introduced interesting characteristics which required additional consideration, in particular with NMR spectroscopy.

### 1.5.1. Nuclear Magnetic Resonance Spectroscopy Techniques

The presence of unpaired electrons in an NMR sample often gives a spectrum that can be difficult to interpret. When all electrons are paired (i.e. in a diamagnetic complex), the $^{1}$H NMR spectrum will show resonances for each proton in the compound as clearly defined, sharp peaks that generally appear between 0 and 10 ppm. Protons that are related by symmetry will absorb at the same frequency, so that the integration of a peak corresponds with the number of protons it represents.

Unpaired electrons present in the sample interact with the nuclear spin of the protons during the experiment by polarising the nuclear spin density, giving a spectrum which may manifest as broadened peaks and highly shifted resonances that lack coupling information.[145] Figure 1.19 gives an example of this effect, showing the $^{1}$H NMR spectrum of a diamagnetic ligand, and again when it is bound to a paramagnetic metal centre. Protons that are structurally closer to the atom containing the unpaired electron(s) usually display these paramagnetic effects more dramatically than those which are more distant. Interaction with the unpaired electron(s) can be described via two methods: the first, the Fermi contact shift, is a through-bond effect; the second, called the pseudo-contact shift, is a through-space effect.[146] Thus, the shifting and broadening of the signals corresponding to a particular proton environment can be predicted, although determining the factors affecting the proton's signal usually require complex calculations.[147] The peaks may be shifted up to +/- 200 ppm, or broadened until they disappear into the baseline completely, as a result of the unpaired electron(s). The degree of broadening of the signals which should be observed in the spectrum is dependent on the effect of the unpaired electron(s) on the T2 nuclear spin relaxation. When a magnetic field is applied to a sample containing NMR-active nuclei, a Boltzmann distribution of spin states is achieved; a radio frequency (RF) pulse at the resonance frequency alters the spin population ratio, and the excess nuclei are excited into the upper spin state.[148] As these excited nuclei relax back to their ground state, a free induction decay (FID) signal is measured. However, the interaction of the nuclear spin with the unpaired electron(s) as mediated by the dipolar coupling greatly increases the T2 transverse relaxation rate, resulting in a faster-than-normal relaxation of the nuclear spins.[146] Despite the FID measurement occuring directly after the RF-pulse which results

in a measurable signal, the resonance signals may relax too quickly to be observed, resulting in either severely broadened peaks, or no visible peaks at all. To account for the faster relaxation rates and subsequent broadened signals, a typical paramagnetic $^{1}$H NMR experiment will use a much larger number of total scans than its diamagnetic counterpart in order to maximise the signal-to-noise ratio.

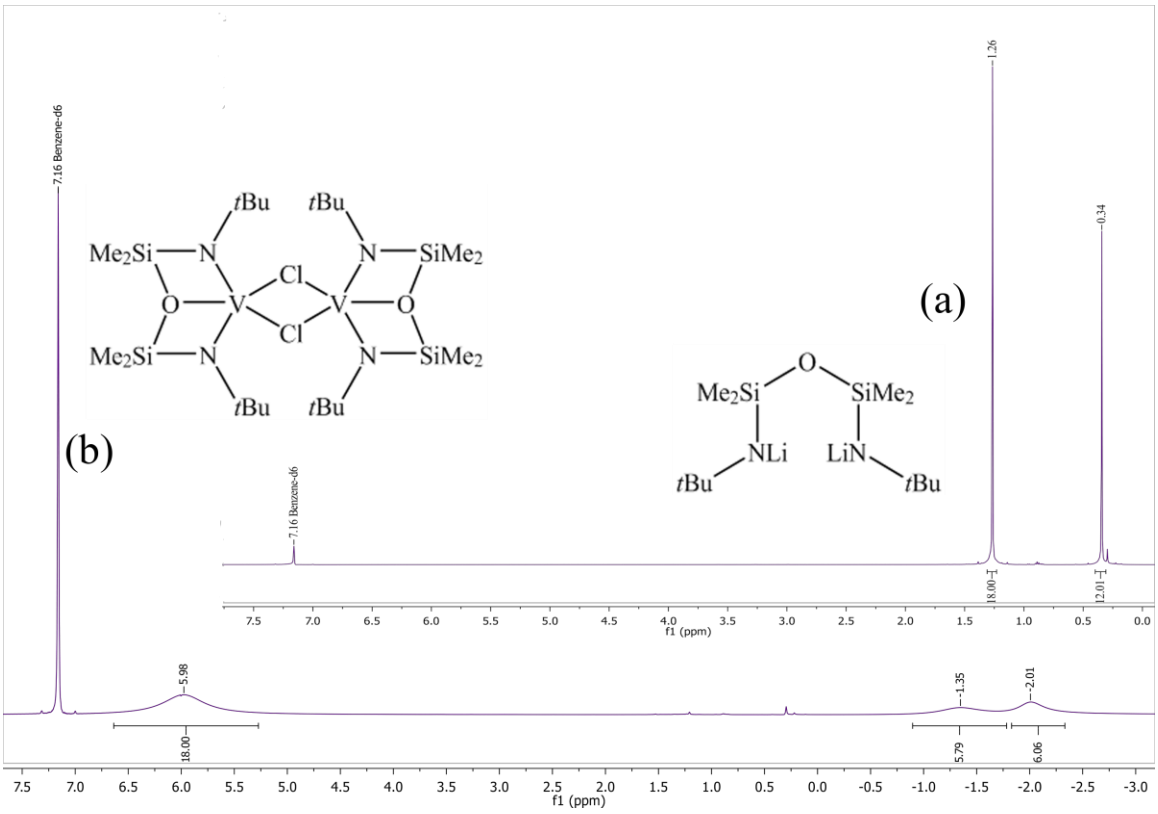


**Figure 1.19. Effect of a paramagnetic centre on the $^{1}$H NMR spectrum. (a) [$^{t\mathrm{Bu}}$NON]Li$_2$ ligand, diamagnetic; (b) {[$^{t\mathrm{Bu}}$NON]VCl}$_2$ (V$^{3+}$, *d*$^2$), paramagnetic.**

Signal integrations can be difficult to interpret, depending on the signal to noise ratio, signal overlap, as well as experimental conditions.[146] Provided the peak remains relatively sharp in the $^{1}$H NMR spectrum, and has well-defined tails, the integrations may be collected using crude numerical integration. With severely broadened peaks, the tails become unclear, and so can be more difficult to define the actual integral region. Here it is more accurate to use a Gaussian fit to the curve to determine the actual integration. Therefore, assigning a paramagnetic $^{1}$H NMR spectrum does become more difficult, but is still often achievable. The most important and useful step is to verify that the correct

number of signals are present compared to what would be expected, as the chemical shifts of the peaks are less indicative of a proton's chemical environment. Integrations are the next most helpful tool in assigning a paramagnetic $^{1}$H NMR spectrum.

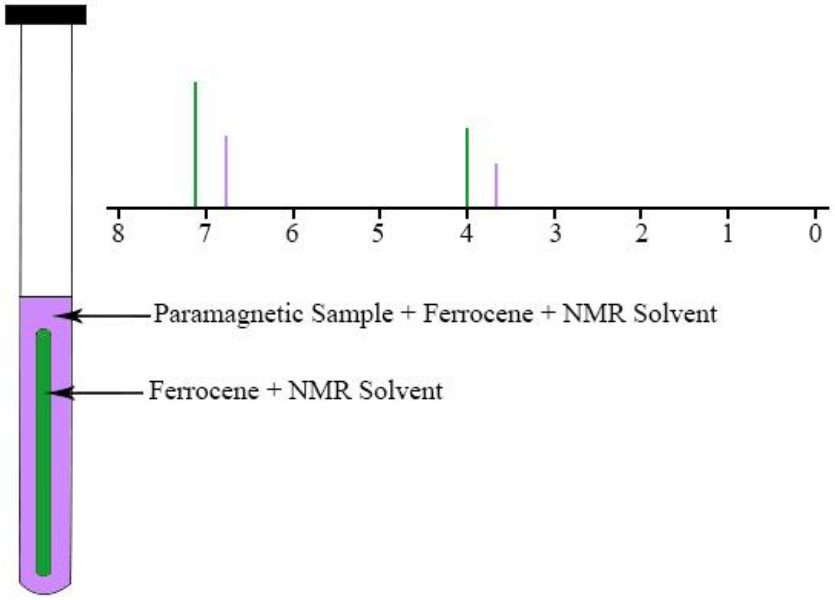


**Figure 1.20. Evans' Method NMR experiment set-up and identification. Represented peaks for each sample are for ferrocene (~4 ppm) and the NMR solvent (~7 ppm).**

In addition to the basic paramagnetic $^{1}$H NMR spectrum, there is also a technique that allows the estimation of the magnetic moment of the sample through a simple NMR experiment. This is known as the Evans' Method NMR experiment.[149] In this experiment, a sealed capillary tube containing the NMR solvent of choice plus a small amount of ferrocene is added to the NMR tube (Figure 1.20). In this case, the ferrocene acts as an internal standard. In the rest of the tube, a known mass of sample is dissolved in a known volume of the chosen NMR solvent, and provided it is inert, a small amount of ferrocene is also added to this sample. Once the tube is appropriately sealed, a $^{1}$H NMR experiment is run. The resulting spectrum should show two sets of peaks. The first set is of the ferrocene; the ferrocene in the sealed capillary tube will appear in its normal position of ~4.0 ppm (depending on the NMR solvent, usually $d_6$-benzene or $d_8$-toluene), as it does not interact with the paramagnetic material. However, the ferrocene added to the bulk sample will be affected by the paramagnetic centre, and thus will display a shifted signal. The same shifting will occur between the NMR solvent signal

that is in the sealed capillary versus that in the bulk sample. The difference between these two sets should be the same value (thus it is possible to do this technique without the addition of ferrocene to the bulk sample). The peak shift value, plus the mass and volume information can then be input into Equation 1.1 for the determination of the mass susceptibility of the sample.[149] The last two terms in Equation 1.1 may be ignored for the purposes of this technique, as the mass susceptibility of the solvent, $\chi_o$, is negligible since it is diamagnetic.[150] From the mass susceptibility, the solution effective magnetic moment, and subsequently the number of unpaired electrons in the complex, may be calculated. This can then give information regarding oxidation state and geometry of the complex. This will be discussed in more detail in Section 1.5.3.

$$X_g = \frac{-3\Delta f}{4\pi f m} + X_o + \frac{[X_o(d_o - d_s)]}{m} \qquad (1.1)$$

$X_g$ = mass susceptibility; $\Delta f$ = signal shift (Hz); $f$ = spectrometer frequency for nucleus (Hz); $m$ = mass of substance in 1 mL of solution; $\chi_o$ = mass susceptibility of the solvent; $d_o$ = density of the solvent; $d_s$ = density of solution.

## 1.5.2. Single Crystal X-Ray Diffraction

X-ray diffraction allows the determination of atomic coordinates in a single crystal unit cell, which results in the identification of the molecular structure. While this is a powerful and definitive tool used in coordination and organometallic chemistry, the information is typically supported by the $^1$H NMR spectrum obtained, as well as any other characterisation methods used. However, where NMR spectra are based on samples in solution, x-ray diffraction data defines the solid structure of a molecule, and provides information on crystal packing as well.

While the instrumental details and theoretical background are beyond the scope of this thesis,[151] the importance of this technique to the research presented here is undeniable. Knowledge of the atomic coordinates in a structure translates to connectivity information, as well as bond distances and angles between atoms.[145] This is relevant for determining the presence of metal-metal bonds, or various intermolecular interactions. By comparison with existing related structures, the strength of an interaction may be estimated, which may lead toward educated guesses on further reactivity – often an important piece of information in organometallic chemistry.

### 1.5.3. Magnetic Properties and SQuID Magnetometry

There are two methods used to collect the magnetic data in this thesis; the first, the Evans' method NMR experiment has already been discussed in section 1.5.1, and provides the magnetic moment data of the sample in solution.[149] While this technique potentially introduces a large amount of error in quantity measurement of the sample, it does provide a good approximation for the room temperature magnetic moment, and may additionally be used for variable temperature data collection, provided the sample remains solubilised. It also provides insight into the sample's structure in the solution state. The second method uses a Superconducting Quantum Interference Device (SQuID) to measure the solid state magnetic data across a large range of temperatures, from 300 K down to 1.8 K. The value of this method is to determine whether the unpaired electron(s) in the complex in the solid-state behave according to the Curie law when placed in a magnetic field, or if there is coupling between unpaired electrons, or even if there are long-range ordering effects. This instrument provides the data for the determination of essentially any magnetic property that may be present. Other techniques that are able to provide bulk magnetic data in the solid state, such as the Gouy method, were not used in this thesis.

The SQuID magnetometer measures an electromagnetic unit (emu) value that corresponds to the total magnetisation (M) of the sample, in relation to the temperature of the sample. As a paramagnetic sample gets colder, the paramagnetic behavior typically becomes more pronounced, as thermal motion decreases. Total magnetisation (M) over the applied magnetic field (H), may be related to the susceptibility. The mass magnetic susceptibility, $X_g$, is calculated as the magnetisation divided by the applied external magnetic field. The molar susceptibility may be calculated from the mass susceptibility by multiplication by the molecular weight. Therefore, the molar susceptibility may be calculated as per Equation 1.2 from the magnetisation by multiplying the molecular weight, and dividing by the applied magnetic field expressed in Gauss, H. Corrections for the magnetisation imparted by the sample holder and the sample mass are taken into account here as well, and this is reflected in Equation 1.2.

$$X_m = \frac{[(M_{total} - M_{holder}) * M_W]}{H * mass} \qquad (1.2)$$

The molar susceptibility consists of the susceptibility contributions of all of the paired (diamagnetic) electrons, as well as the unpaired electron(s). The diamagnetic contributions are small in comparison to the paramagnetic contribution, although they must be corrected for in order to calculate an accurate effective magnetic moment. The diamagnetic contributions can be estimated empirically by using Pascal's constants,[152] and are simply the sum of all the diamagnetic susceptibilities imparted from the atoms' paired electrons present in the sample, and in their bonds. Equation 1.3 illustrates the calculation of the paramagnetic molar susceptibility. From this value, the effective magnetic moment may be calculated (Equation 1.4), which has the units of Bohr magneton ($\mu_B$). The effective magnetic moment acts as a scale for the number of unpaired electrons, and can be related by the total spin quantum number, S. This interpretation assumes that there is no contribution from orbital angular momentum. Given a spin-only magnetic moment (calculated using Equation 1.5), the number of unpaired electrons yield standard values for the magnetic moment, which are summarised in Table 1.1. Variable temperature magnetic data collected via the SQuID magnetometer are usually plotted in two ways; the first is the magnetic moment vs. temperature, which can be correlated to the effective number of unpaired electrons in the sample over a range of temperatures and readily illustrates non-Curie Law effects; the other is X vs. T, which effectively illustrates antiferromagnetic coupling between unpaired electrons and long-range intra- and intermolecular ordering effects.

$$X_{para} = X_m - X_{dia} \qquad (1.3)$$

$$\mu_{eff} = 2.282\sqrt{X_{para}T} \qquad (1.4)$$

**Table 1.1. Spin-only values of effective magnetic moment correlated to the number of unpaired electrons.**

| # Unpaired Electrons | S | $\mu_{s.o.}$ ($\mu_B$) |
|---|---|---|
| 1 | 1/2 | 1.73 |
| 2 | 1 | 2.83 |
| 3 | 3/2 | 3.87 |
| 4 | 2 | 4.90 |
| 5 | 5/2 | 5.92 |

While a diamagnetic sample is repelled from a magnetic field, paramagnetism is defined as a sample's overall attraction towards a magnetic field, as the unpaired electron's spin (S) and orbital (L) angular momentum interact with the field. In a particular sample containing significant effects from both the spin angular momentum and the orbital angular momentum, the calculation for the effective magnetic moment, $\mu_{eff}$, becomes more complicated. Depending on the geometry around the metal from which the unpaired electron(s) originates, and therefore the crystal field splitting of the *d*-orbitals, the orbital angular momentum contribution may be "quenched" if the unpaired electron(s) are unable to move between degenerate and symmetric orbitals on the metal, leaving only the spin angular momentum to contribute to the overall magnetic moment. Thus, the spin-only formula (Equation 1.5; results in the right column of Table 1.1) is obtained, where S is the number of unpaired electrons divided by two. Typically, the first row transition series has small orbital contributions, and so the spin-only formula is usually sufficient for describing the magnetic moment with reasonable accuracy.

$$\mu_{s.o.} = 2\sqrt{S(S+1)} \qquad (1.5)$$

The Curie law states that the magnetic susceptibility (X) of a paramagnetic material is inversely proportional to temperature, and they are related by the Curie constant.[153] While many materials do not follow this Law, those that do – termed Curie law materials - result in temperature independent effective magnetic moments. For many mononuclear, spin-only compounds, the Curie Law is obeyed.. Systems which contain any spin-orbit coupling (SOC), however, display temperature-dependent magnetisation which generally result in an overall reduction in magnetic moment at lower temperatures. Spin-orbit coupling results in the coupling of the spin angular momentum and the orbital angular momentum, to give total angular momentum described by quantum number J.

At low temperatures, a second-order effect is commonly noted in both temperature-dependent and –independent magnetic data. A sudden drop in $\mu_{eff}$ below ~10 K is typically attributed to zero-field splitting. Zero-field splitting occurs in systems with S > ½; the degeneracy of the ground state can be removed through dipolar interactions and SOC (Figure 1.21).[154] The difference between the resulting separated states, then, is quantified as the dipolar tensor (D), and can be obtained through fitting a

mathematical model to the magnetic data. Often, low crystal field symmetry has been found to give large zero-field splitting effects. The $E_n$ transitions refer to the energy difference between the possible energy states that result from the interaction of the unpaired electron spin moment with the applied magnetic field.

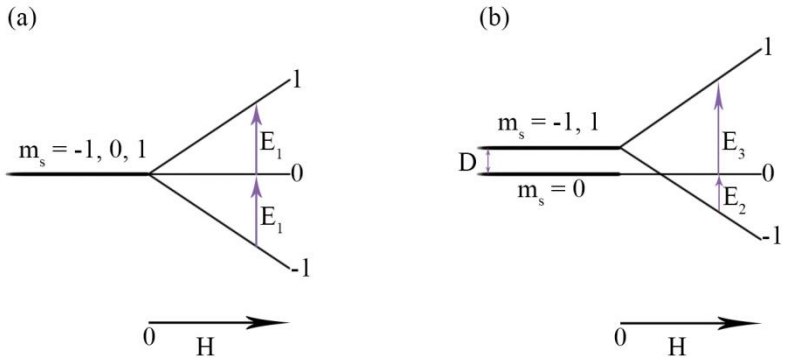


**Figure 1.21. Zero-field splitting removes the degeneracy of the energy transitions when a magnetic field is introduced. (a) no zero field splitting; (b) zero-field splitting observed, with D > 0.**

The unpaired electrons of two or more paramagnetic metal centres in a multi-nuclear complex may also magnetically couple. There are two primary means by which the unpaired electrons may interact, either by direct metal-metal orbital overlap, or through the ligands, called superexchange, as it is an indirect process.[155] Following either of these conditions, the unpaired electrons may couple; there are two common coupling motifs. If the spin of the two unpaired electrons align antiparallel to each other, then this is termed antiferromagnetic coupling, and the overall magnetic moment will be smaller than predicted by the spin-only formula, as the electrons' magnetic moment is reduced by the antiparallel alignment of spins. If they align parallel, then this is called ferromagnetic coupling, and the overall magnetic moment will be larger than predicted by the spin-only formula, as the ground-state S-value of the complex increases. Antiferromagnetic coupling is more commonly observed than ferromagnetic coupling. The coupling effects are easily interpreted from a plot of magnetic moment versus temperature (Figure 1.22).

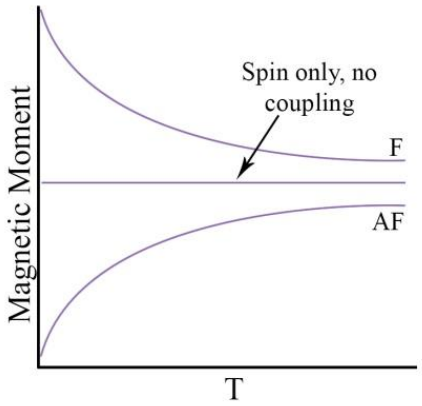


**Figure 1.22. Effect of magnetic coupling on the magnetic moment versus temperature.**

### 1.5.4. Other Characterisation Techniques

Various other supportive techniques may be employed in the characterisation of air-sensitive and paramagnetic coordination complexes. Rather than using mass spectrometry (MS) which determines structure based on molecular fragments, the more traditional technique of CHN elemental analysis (EA) was utilised in this research, which instead analyses a small sample in a sealed metal holder for carbon, hydrogen, and nitrogen content by combustion analysis, giving percentages of these elements as a function of total content. This technique works well, as it also gives information on the purity of the sample; higher than expected carbon and hydrogen percentages may indicate the presence of residual solvent, while overall lower than expected values may indicate the presence of remaining salt.

Another technique that may be utilised in the characterisation of paramagnetic complexes is electron spin resonance (ESR) spectroscopy. ESR measures the energy difference between the two states that result from the interaction of the unpaired electron spin moment with the magnetic field; this energy difference is typically in the microwave range.[156] ESR provides information on the interaction of the unpaired electron(s) with the surrounding nuclei, which therefore gives an indication of its environment within the molecule. For example, in the case of organic radicals, ESR is useful for determining if the radical is localised on a single atom, or delocalised across the molecule. However,

metals which contain more than one unpaired electron may experience ESR silence as a result of Kramer's rule.[154] A system that contains an even number of unpaired electrons may not have $m_J$ degeneracy at its lowest energy level (called a Kramer's doublet); the presence of only singlet levels may manifest as large anisotropic zero-field splitting (Figure 1.21) with large enough energies that the transition cannot be observed in the microwave region.

The common example used to illustrate this effect is of the $V^{3+}$ ion, which has a $3d^2$ electron configuration, and an ESR silent spectrum. In this case, the observed splitting of 8 $cm^{-1}$ is greater than $h\nu$ for the instrument's microwave frequencies. If, however, the energy of the zero-field splitting is less than that of the ESR's microwave frequencies, it should be possible to obtain a spectrum from the sample. A higher magnetic field may also enable the successful observation of the energy transitions. An emerging technology, high-frequency high-field ESR (HFESR) has more recently allowed studies on such metal complexes, as the high frequency makes it possible to probe systems with high zero-field splitting.[157] However, the large expense of these HFESR instruments means they are not readily accessible.

# Chapter 2.

# Early Transition Metal Diamido Silylether Complexes and their Reactivity

## 2.1. Introduction

First-row transition metals have been relatively well explored in conjunction with various diamido-donor ligands.[15,16,43,129] Of particular note in this section of work is the role of $[^{t\text{Bu}}\text{NON}]^{2-}$ with the first-row metals. Complexes are known with each of the late transition metals, however, the early first row has remained untouched in terms of this ligand framework. Complexes of yttrium(III) and zirconium(IV) have been published,[7,43] so there is precedent for expanding the chemistry of this ligand into the early first row transition metals.

Herein is described the synthesis and characterisation of the diamido-donor halide-bridged complexes of scandium, titanium and vanadium, all in the +3 oxidation state. Scandium is considered a rare earth metal, and in the +3 oxidation state is diamagnetic, $d^0$. Scandium amides have been well explored in the literature, along with their alkylated counterparts.[44,47,158–166] While complexes of diamagnetic Ti(IV) have been shown to exhibit excellent polymerisation properties – some catalysts were able to achieve greater than 1000 g $mmol^{-1}$ $h^{-1}$ $bar^{-1}$ of 1-hexene polymer – the chemistry of Ti(III) has not been as fully explored.[166] This is primarily because Ti(III) is paramagnetic, with a $d^1$ orbital configuration. Due to the additional care which must be taken in characterisation of paramagnetic complexes, as discussed in Chapter 1, it is unsurprising that titanium(III) has been much less explored than its diamagnetic counterpart, Ti(IV). However, presence of an unpaired electron also opens new avenues for reactivity that may not have been applicable to a diamagnetic complex. Vanadium(III)

($d^2$) has been relatively well-explored in the literature, owing to its tendency to form dinitrogen complexes relatively easily.[39,74]

The synthesis of these related complexes allowed additional comparison of structural features with their late metal counterparts, as well as providing further reactivity studies, which allowed a trend to be elucidated across the first row as a function of metal *d*-electron configuration. The synthesis and characterisation of the three primary complexes is first described, before moving into a discussion of the reactivity of each complex in turn. In the case of the paramagnetic titanium and vanadium complexes, the magnetic properties are also studied.

## 2.2. Results & Discussion

In this chapter, the metal complexes discussed are formed from addition of one equivalent of $Li_2\{(t\text{BuNSiMe}_2)_2\text{O}\}$, abbreviated $Li_2[^{t\text{Bu}}\text{NON}]$, to one equivalent of $MCl_3$ (Scheme 2.1). In the case of titanium and vanadium, the metal halide exists as a THF adduct, which promotes solubility in that solvent. LiCl is formed as a by-product from the salt metathesis reaction, which must be filtered from the desired product, a dichloride-bridged dimer of the general form $\{[^{t\text{Bu}}\text{NON}]\text{MCl}\}_2$. Further details of these complexes will be discussed in the following section.

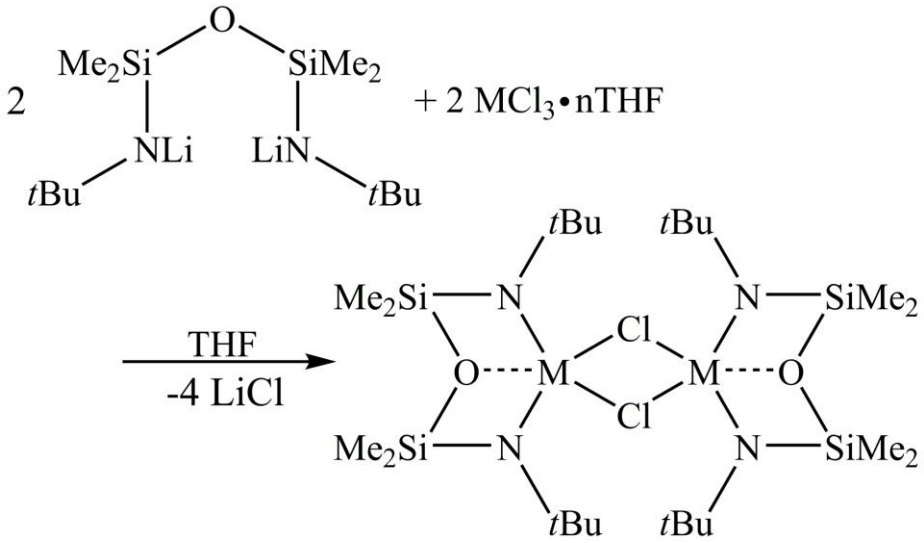


**Scheme 2.1. Synthesis of $\{[^{t\text{Bu}}\text{NON}]\text{ScCl•THF}\}_2$ (n=0), $\{[^{t\text{Bu}}\text{NON}]\text{TiCl}\}_2$ (n=3), and $\{[^{t\text{Bu}}\text{NON}]\text{VCl}\}_2$ (n=3); complexes 1-3, respectively.**

### 2.2.1. MCl[$^{tBu}$NON] Complexes: Synthesis & Characterisation

The addition of $Li_2[^{tBu}NON]$ to $ScCl_3$ in a solution of THF results in the toluene-soluble colourless solid, $\{[^{tBu}NON]ScCl(THF)\}_2$ (**1**) in high yield (92%) and purity. X-ray quality crystals grown by slow evaporation of a toluene solution revealed a dichloride-bridged dimer with a chelating diamido ligand capping each scandium ion, which additionally retain a THF ligand each (Figure 2.1). The scandium atoms in **1** are each found to have a distorted octahedral geometry.

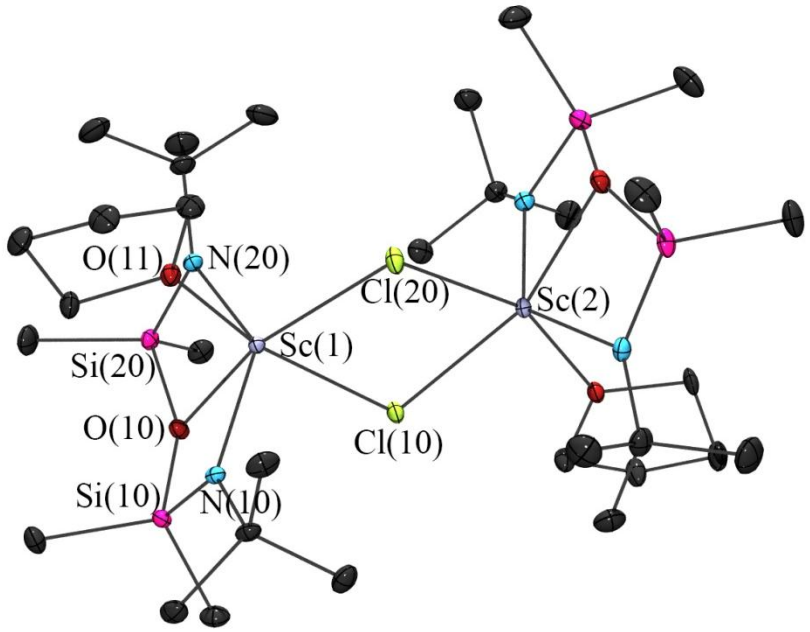


**Figure 2.1. X-Ray crystal structure of $\{[^{tBu}NON]ScCl(THF)\}_2$ (1).**

**Table 2.1. Selected interatomic distances (Å) and angles (°) for {[$^{t\text{Bu}}$NON]ScCl(THF)}$_2$ (1).**

| Bond Lengths | | Bond Angles | |
|---|---|---|---|
| Sc(1)-Sc(2) | 3.9879(6) | Cl(10)-Sc(1)-Cl(20) | 77.55(2) |
| Sc(1)-Cl(10) | 2.5264(6) | Cl(20)-Sc(2)-Cl(10) | 77.44(2) |
| Sc(1)-Cl(20) | 2.6241(7) | Cl(10)-Sc(1)-N(10) | 93.88(6) |
| Sc(1)-N(10) | 2.108(2) | Cl(10)-Sc(1)-N(11) | 104.07(6) |
| Sc(1)-N(11) | 2.102(2) | Cl(20)-Sc(1)-N(10) | 118.83(6) |
| Sc(1)-O(10) | 2.305(2) | Cl(20)-Sc(1)-N(11) | 109.58(6) |
| Sc(1)-O(11) | 2.245(2) | Cl(10)-Sc(1)-O(10) | 82.76(5) |
| Si(10)-O(10) | 1.660(2) | Cl(10)-Sc(1)-O(11) | 158.31(5) |
| Si(11)-O(10) | 1.662(2) | Cl(20)-Sc(1)-O(10) | 159.24(5) |
| Si(10)-N(10) | 1.695(2) | Cl(20)-Sc(1)-O(11) | 82.42(5) |
| Si(11)-N(11) | 1.700(2) | O(10)-Sc(1)-N(10) | 68.72(7) |
| | | O(10)-Sc(1)-N(11) | 68.84(7) |
| | | O(11)-Sc(1)-N(10) | 88.47(7) |
| | | O(11)-Sc(1)-N(11) | 90.38(7) |
| | | N(10)-Sc(1)-N(11) | 130.93(8) |
| | | Si(10)-O(10)-Si(11) | 155.9(1) |

The Sc-Cl bonds in **1** are not equal (Table 2.1); the Sc(1) – Cl(20) distance is 2.6241(7) Å, while the Sc(1) – Cl(10) distance is only 2.5264(6) Å. While the latter is within the ionic radius of 2.56 Å, the former lies outside of these bounds.[167] This suggests that the crystal packing favours the dimerisation, although it would be reasonable to suspect that in a non-crystalline form, complex **1** exists as a monomer. Luo reported a {CpSc(THF)$_2$}$_2$($\mu$-Cl)$_2$ dimer complex containing Sc – Cl bond lengths of 2.5502(14) & 2.5283(15) Å, corroborating long Sc – Cl distances in sterically constrained chloride-bridged scandium dimers.[162] In comparison, Piers' structure of the β-diketiminato-containing complex, [ArNC(*t*Bu)CHC(*t*Bu)NAr]Sc(NH*t*Bu)Cl (Ar = 2,6-$^{i}$Pr$_2$-C$_6$CH$_3$), features a terminal chloride, with a Sc-Cl distance of 2.125(2) Å;[158] however, the simple amide ScCl$_2$[N(SiMe$_3$)$_2$](THF)$_2$ showcases distances of 2.379(1) Å and 2.398(1) Å.[165] These drastically different values between complexes illustrates the large variation possible in Sc-Cl interatomic distances.

While there are no other known scandium complexes with the [$^{R}$NON]$^{2-}$ ligands, the Sc – N amido bond distances in **1** of 2.108(2) Å and 2.102(2) Å are on par with Piers'

[ArNC(*t*Bu)CHC(*t*Bu)NAr]Sc(NH*t*Bu)Cl (Ar = 2,6-$^{i}Pr_2$-$C_6CH_3$), which have 2.125(2) and 2.115(2) Å Sc – N distances for the diamido ligand.[158] Dehnicke's $ScCl_2[N(SiMe_3)_2](THF)_2$ has a Sc-N distance of 2.039(2) Å, although this difference may be attributed to a monoamide versus a chelating diamide binding with scandium.[165]

There is also a bond formed between the scandium metal and the neutral silylether in complex **1**, with a Sc – O bond distance of 2.305(2) Å. The hemilabile nature of the M – O silylether bond is often observed in $[^{R}NON]^{2-}$ metal complexes, particularly in the electron-rich late metal complexes.[143] Although all of the complexes described here feature this M – O bond, it is only formed when the metal centre requires additional electron-density, which defines the silylether's hemilability.[168] In addition to the neutral backbone binding to the scandium atom, however, the metal has also captured a THF as a neutral ligand. This is likely due to the high Lewis acidity of the metal. The bond distance of 2.245(2) Å is again longer than in Dehnicke's $ScCl_2[N(SiMe_3)_2](THF)_2$, which has Sc-O(THF) bond distances of 2.176(2) Å and 2.175(2) Å.[165] Although each of these listed interatomic distances lie outside the covalent radius of 2.11 Å for Sc – O bonds,[167] these bonds can be more accurately described as dative bonds to the metal centre, i.e., donation of a lone-pair of electron density from the ligand to an empty orbital on the metal, rather than a covalent sharing of electron density from each atom.

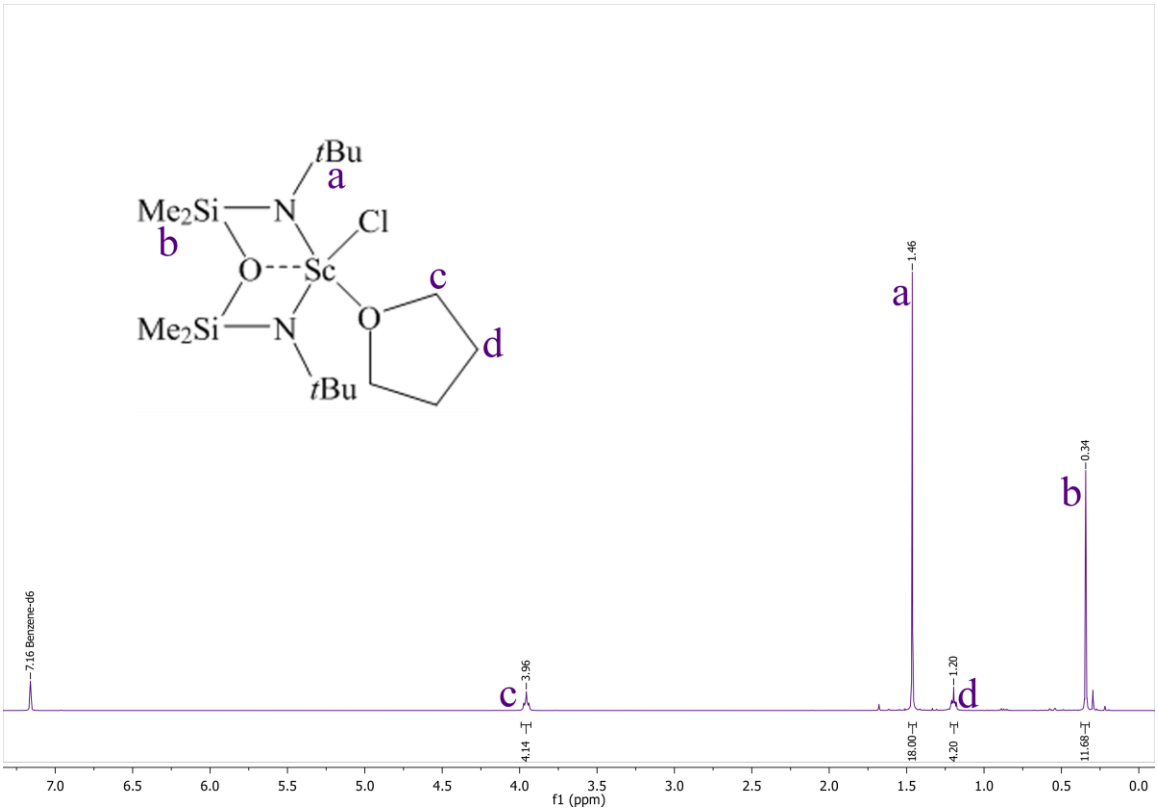


**Figure 2.2. $^{1}$H NMR spectrum of {[$^{tBu}$NON]ScCl•THF}$_2$ (1) in $d_6$-benzene.**

In the $^{1}$H NMR spectrum of **1** (Figure 2.2), there are four peaks visible. At 1.46 ppm, and integrating to 18H, is the peak that corresponds to the *t*butyl protons. The peak at 0.34 ppm that integrates to 12H is assigned to equivalent dimethylsilyl groups on the backbone of the ligand. These two peaks are shifted from where they appear in the free lithiated ligand, thereby indicating that the ligand is bound to the metal. The additional two multiplet peaks, appearing at 1.20 ppm and 3.96 ppm, and each integrating to 4H indicate the presence of one bound THF adduct per monomer. The overall number of peaks present in this spectrum suggests that the complex exists as a monomer in solution, and the long Sc – Cl dimer distance in the solid state structure would seem to support this theory. However, it is possible that there could be an equilibrium between monomer and dimer states, and a variable-temperature NMR experiment could help to discern which state is more prevalent in the room temperature solution sample.

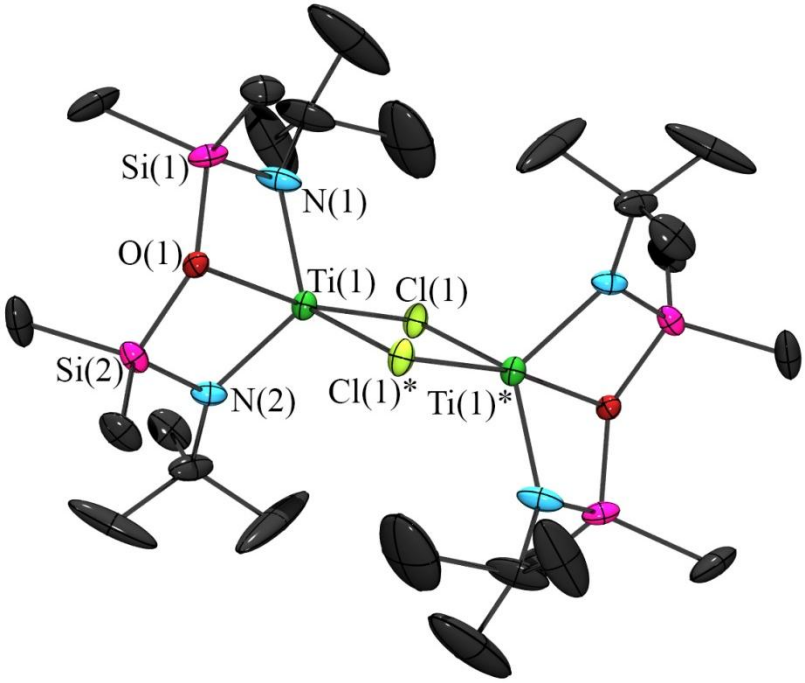


**Figure 2.3. X-Ray crystal structure of {[$^{tBu}$NON]TiCl}$_2$ (2).**

**Table 2.2. Selected interatomic distances (Å) and angles (°) for {[$^{tBu}$NON]TiCl}$_2$ (2).**

| Bond Lengths | | Bond Angles | |
|---|---|---|---|
| Ti(1) – Ti(1)* | 3.3033(7) | Cl(1) – Ti(1) – Cl(1)* | 91.39(6) – 94.73(6) |
| Ti(1) – Cl(1) | 2.410(1) – 2.416(2) | Cl(1) – Ti(1) – N(1) | 105.84(8) – 122.00(8) |
| Ti(1) – Cl(1)* | 2.426(2) – 2.460(2) | Cl(1) – Ti(1) – N(2) | 105.26(9) – 121.39(9) |
| Ti(1) – N(1) | 1.950(2) | Cl(1)* – Ti(1) – N(1) | 98.32(8) – 113.49(8) |
| Ti(1) – N(2) | 1.962(3) | Cl(1)* – Ti(1) – N(2) | 97.66(9) – 113.61(9) |
| Ti(1) – O(1) | 2.240(2) | O(1) – Ti(1) – Cl(1) | 88.53(6) – 88.56(6) |
| O(1) – Si(1) | 1.672(2) | O(1) – Ti(1) – Cl(1)* | 170.68(6) – 171.74(6) |
| O(1) – Si(2) | 1.669(2) | O(1) – Ti(1) – N(1) | 73.78(8) |
| Si(1) – N(1) | 1.720(2) | O(1) – Ti(1) – N(2) | 73.23(9) |
| Si(2) – N(2) | 1.708(3) | N(1) – Ti(1) – N(2) | 120.3(1) |
| | | Si(1) – O(1) – Si(2) | 139.4(1) |

In contrast to the reaction to produce the scandium-containing **1**, the reactions of [$^{tBu}$NON]Li$_2$ with MCl$_3$•3THF (where M = Ti, V) resulted in much lower yields of {[$^{tBu}$NON]TiCl}$_2$ (**2**) and {[$^{tBu}$NON]VCl}$_2$ (**3**) (<50%), accompanied by unknown by-products in addition to the expected LiCl. In contrast to **1**, products **2** and **3** are soluble in

hexanes; slow evaporation of a concentrated solution produced X-ray quality crystals (Figures 2.3 & 2.4). However, while crystals of **2** could be obtained from the Ti-based reaction, the bulk of the crude product remained impure, despite many attempts at chemical purification. The impure state of this product implies that further characterisation and reactivity studies in the solution state based on this material are inconclusive at best. On the other hand, complex **3**, while obtained in a relatively low yield, could be purified much more readily. The low isolated yield may be attributable to slow decomposition of the product over time, as the product does appear to have a limited shelf-life of about a month once synthesised.

The single-crystal data shows that titanium (**2**) and vanadium (**3**) complexes are isostructural, featuring a tridentate [$^{R}$NON] ligand donor that interacts with the metal centre as with **1**; two bridging chlorides are also present, although there is no THF ligand retained. The unit cells for complexes **2** and **3** are different. Complex **2** contains only one monomer within each unit cell, while complex **3** contains two separate monomers. For complex **3**, the molecules' other halves are completed by the similar metal centre in the adjacent unit cells; i.e. V(1) in cell one dimerises with V(1) of cell two, while the V(2) centres do likewise. This means that the resulting bond lengths between the two crystallographically unique dimers are slightly different, although quite similar in all aspects. Thus, only the data for one of the dimers has been related in Table 2.3. The data for complex **2** showed a large amount of disorder in the *t*Butyl carbons, as well as the bridging chloride (Table 2.2). In each case, the disorder was dealt with by splitting the electron-density of each atom into two, and altering the occupancy for each set to 50%. Thus, there are two populations of electron density for each *t*Butyl carbon and the chloride, although only one population is shown in Figure 2.3.

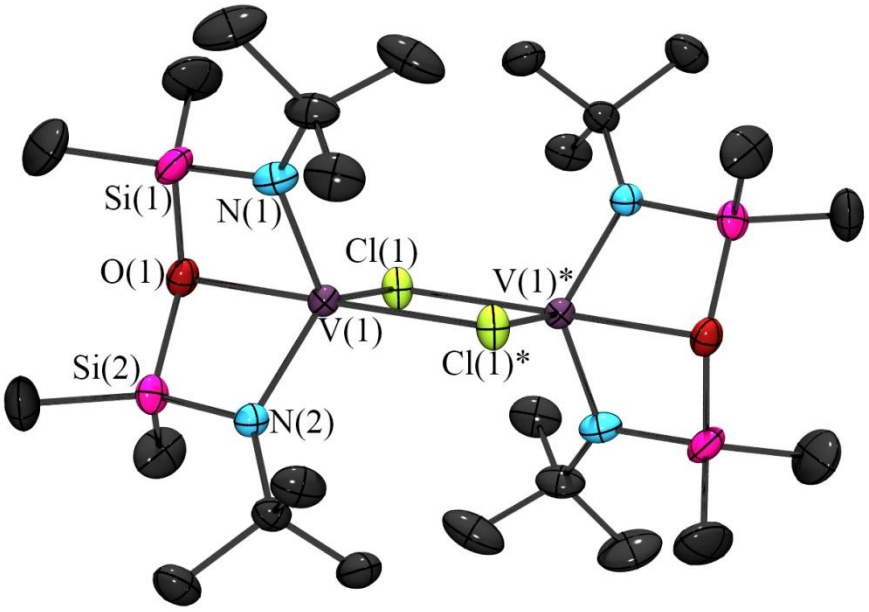


**Figure 2.4. X-ray crystal structure of {[$^{tBu}$NON]VCl}$_2$ (3) .**

**Table 2.3. Selected interatomic distances (Å) and angles (°) for {[$^{tBu}$NON]VCl}$_2$ (3).**

| Bond Lengths | | Bond Angles | |
|---|---|---|---|
| V(1) – V(1)* | 3.5100(8) | Cl(1) – V(1) – Cl(1)* | 86.29(3) |
| V(1) – Cl(1) | 2.386(1) | Cl(1) – V(1) – N(1) | 117.79(9) |
| V(1) – Cl(1)* | 2.4242(8) | Cl(1) – V(1) – N(2) | 117.88(7) |
| V(1) – N(1) | 1.922(2) | Cl(1)* – V(1) – N(1) | 105.87(9) |
| V(1) – N(2) | 1.905(3) | Cl(1)* – V(1) – N(2) | 105.75(7) |
| V(1) – O(1) | 2.168(2) | O(1) – V(1) – Cl(1) | 89.85(6) |
| O(1) – Si(1) | 1.684(2) | O(1) – V(1) – Cl(1)* | 176.13(6) |
| O(1) – Si(2) | 1.682(3) | O(1) – V(1) – N(1) | 76.1(1) |
| Si(1) – N(1) | 1.712(2) | O(1) – V(1) – N(2) | 75.94(9) |
| Si(2) – N(2) | 1.716(2) | N(1) – V(1) – N(2) | 116.5(1) |
| | | Si(1) – O(1) – Si(2) | 138.5(1) |

Analysis of the N – M – N and Cl – M – Cl bond angles with respect to the M – O bond defines whether the metals reside in a distorted trigonal bipyramidal geometry, or a square pyramidal geometry. This is known as the τ-value, and uses a simple calculation (Equation 2.1), where, if the result is close to 0, then the geometry is defined as square pyramidal; however, if the result is closer to 1, then it is trigonal bipyramidal.[169] If the calculated τ-value is close to 0.5, this indicates a high degree of distortion. In this

calculation, there are two angles that must be considered, which are representative of the swing between the two geometries. In a five-coordinate system with square pyramidal geometry, one ligand will occupy the apical position, while the other ligands form a square base; the angles across these "base pair" ligands will each be 180° in a perfect square pyramid. However, in a trigonal pyramidal geometry, one base pair will be 180° where the other is 120° to accommodate the apical ligand, forming a trigonal shape. The angles of these two base pairs are the α and β angles used in the calculation. These base pair ligand angles are used to determine the actual geometry of a metal-centre in a structure, and to quantifiably measure its distortion from the ideal geometry. Thus, complex **2** was found to have a τ-value between 0.42 and 0.47, indicative of a highly distorted square pyramidal geometry – the range is again the result of the disordered chloride. Complex **3** was discovered to have a τ-value of 0.50, indicating that this structure is perfectly balanced between the two possible 5-coordinate geometries. This calculation provides an easy method to quantifiably determine the geometry around a 5-coordinate metal centre, for which there exists a continuum of possible geometries.

$$\tau = \frac{\alpha - \beta}{60} \qquad (2.1)$$

α = angle 1 and β = angle 2

The dimerisation resulting from bridging chlorides is a common structural motif in titanium and vanadium amido chemistry.[45,47,49] Overall shorter M – Cl bond distances (2.386(1) Å [**3**] – 2.460(2) Å [**2**]) suggest that the halides are held more tightly than in **1**. Fryzuk's ([$^{CyPh}$NPN]VCl)$_2$ dimer exhibits similar V - Cl bond lengths to that of **3**, at 2.3632(4) Å and 2.4913(4) Å, suggesting that this is a relatively common value for bridging V – Cl bonds.[47] The V – N amido bonds in **3** are slightly shorter, however, it is still within the expected range. Stephan's β-diketimidate titanium complex validates reasonable bond distances for the Ti – Cl (2.2997(13) Å) and Ti – N amido bonds (2.086(2) Å and 2.088(3) Å), as they are quite close to those of complex **2**.[170]

The M – O bond to the silylether is the longest in the scandium complex (2.305(2) Å), and the shortest for the vanadium complex (2.168(2) Å). This may be a result of steric constraint, since the scandium contains that extra THF ligand, or

alternatively, may be based on the decreasing ionic radii progressing through the series ($Sc^{3+}$ = 0.745 Å, $Ti^{3+}$ = 0.670 Å, $V^{3+}$ = 0.640 Å).[167] Although the change in ionic radii is not quite as large as the change in bond lengths, the ionic radii likely play a significant role.

As the data shows, there are distinct similarities between complexes **1**, **2**, and **3**. As the metals are all present in the +3 oxidation state, the structures each exhibit the dihalide-bridged dimer that has been found in the previous literature complexes. Of the three other known $\{[^{tBu}NON]MCl\}_2$ (M = Cr, Fe, and Y with an additional THF) complexes, the M – Cl bond length also varies significantly, ranging between 2.30 Å and 2.70 Å.[43,144] Although the scandium complex has retained a THF ligand due to the metal's high oxophilicity and Lewis acidity, the titanium and vanadium complexes are isostructural. The yttrium dimer similarly features an additional THF, and so it is unsurprising that its smaller group III congener does the same. The metal – amide bond lengths appear to be within normal ranges; however, it should be noted that in both the scandium and yttrium complexes they are significantly longer than all of the other complexes, coming in at around 2.1 – 2.3 Å, whereas the group IV and V complexes M – N bonds are each around 1.9 Å. This may be due to steric constraints introduced by the remaining THF adduct, forcing the amido ligand further from the metal centre, or simply a result of the larger ionic radii of those two metals in comparison to the titanium and vanadium. This is mirrored by the longer metal – silylether interaction as well, and is again corroborated with the previously published complexes.[43,144] Each of these structures display an interaction between the metal and the silylether backbone, and have developed a trend (Table 2.4), whereby the scandium and yttrium have the longest distances, and then the distance decreases across the row from titanium to chromium. This is likely due to the ionic radii of the metals, which is supported by the larger Y-O distance ($Y^{3+}$ = 0.900 Å) of 2.435(13) Å than the 2.305(2) Å Sc-O distance. The $Mn^{3+}$ complex is not known, but in the reported $[NON]Fe^{3+}$ complex the Fe-O distance has increased significantly to 2.597(4) Å compared to the early transition metal analogues; this is likely the turning point where additional electron density is not required by the metal centre, and so the silylether is not required to donate electron density. Thus, it appears that the number of *d*-electrons on the metal do play a role in the structure and bonding of each of these complexes. Of particular note are solvent adduct formation and hemilabile silylether

donation, which may be a function of the changing ionic radii of the metals involved – a direct result of the changing number of *d*-electrons.

**Table 2.4. Interatomic distances (Å) between the metal centres and the silylether backbone of {[$^{t\text{Bu}}$NON]MCl}$_n$ (n = 1,2) complexes.**

| | | | |
|---|---|---|---|
| Sc-O<br>2.305(2)<br>Y-O<br>2.435(13) | Ti-O<br>2.240(2) | V-O<br>2.168(2) | Cr-O<br>2.147(5) |

## *$^1$H NMR and Magnetic Properties of Paramagnetic Complexes 2 and 3*

It should be noted that the diamido titanium(III) complex (**2**) has many challenges associated with its synthesis. Because of its low yield and purification challenges, only a very small quantity of crystallised complex **2** was able to be obtained for characterisation and further studies. Thus the results presented herein are limited, particularly as solution studies would be expected to be affected by any residual impurities present. We believe that the low yield and large amount of impurities are a result of impure and/or unstable starting material, $TiCl_3$•3THF, which in future should be made fresh in-house.

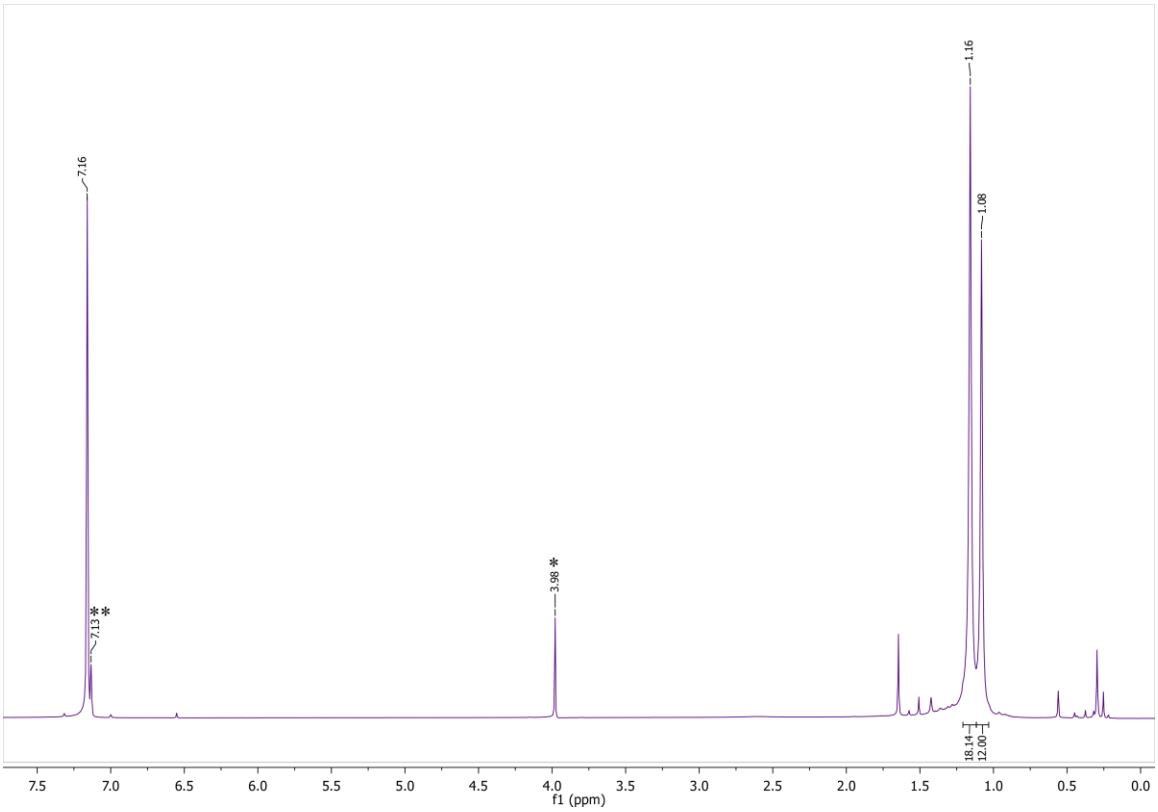


**Figure 2.5. $^{1}$H NMR spectrum of {[$^{t\text{Bu}}$NON]TiCl}$_2$ (2) in $d_6$-benzene.**
* = Ferrocene signal for Evans method experiment (internal capillary). No ferrocene in main sample.
** = $d_6$-Benzene signal from internal sample.

The $^{1}$H NMR spectrum of **2** (Figure 2.5) shows two peaks that appear to be relatively sharp, which is unexpected considering Ti(III)'s $d^1$ paramagnetism. Titanium(III) has been shown to be a fast-relaxing centre, often producing enough nuclear line broadening that $^{1}$H NMR signals are lost completely.[146] The *t*Butyl signal appears at 1.16 ppm and integrates to 18H, while the silylmethyl peak appears at 1.08 ppm, corresponding to the expected 12H, and this is substantially different from free ligand – protonated or lithiated – which appears around 0.19 ppm (12H, $SiMe_2$) and 1.19 ppm (18H, *t*Bu). However, the sharpness of these signals suggest that they correspond to a diamagnetic complex – perhaps [$^{t\text{Bu}}$NON]$TiCl_2$ or {[$^{t\text{Bu}}$NON]TiO}$_2$ – and are inconsistent with typical NMR data for Ti(III) complexes. An ESR experiment from the crystalline sample showed a singlet for the unpaired electron on the Ti(III) centre, although a smaller additional signal indicated additional coupling of the unpaired electron, potentially to the adjacent nitrogen nuclei (Figure A1).

In addition, the structure of this complex in solution does remain unclear – fluxional behaviour in the solution state may allow complex **2** to adopt a variety of conformations which can produce a spectrum with this signal pattern, either as a monomer or as a dimer. Indeed, a good experiment to determine whether complex **2** exists as a mononuclear or dinuclear complex is variable-temperature (VT) NMR. Magnetic analysis gives an indication of any magnetic interactions between the metal centres, thereby providing evidence for dimerised complexes. Solution magnetic moment data was obtained via an Evans' method study.[149] For complex **2**, the calculated magnetic moment ($\mu_{eff}$) was found to be approximately 1.0 $\mu_B$ per titanium, which is substantially smaller than the calculated value of approximately 1.73 $\mu_B$ for a non-coupled $d^1$ spin-only unpaired electron on the metal centre. This could suggest an antiferromagnetic interaction between two metal centres, which would diminish the overall magnetic moment, although diamagnetic impurities would affect this value as well, particularly if they are present in significant amounts. A VT Evans' method NMR experiment could provide further information regarding the predominant solution structure of this complex. However, in any case, the inherent impurities in the sample of complex **2**, despite using hand-picked crystals to obtain this NMR data, make the results of this experiment questionable at best, considering the monomer-dimer equilibria possible in the solution state. Further reactivity studies based on this complex – while attempted in some cases - are also difficult to assess as a result of the impurity of the material.

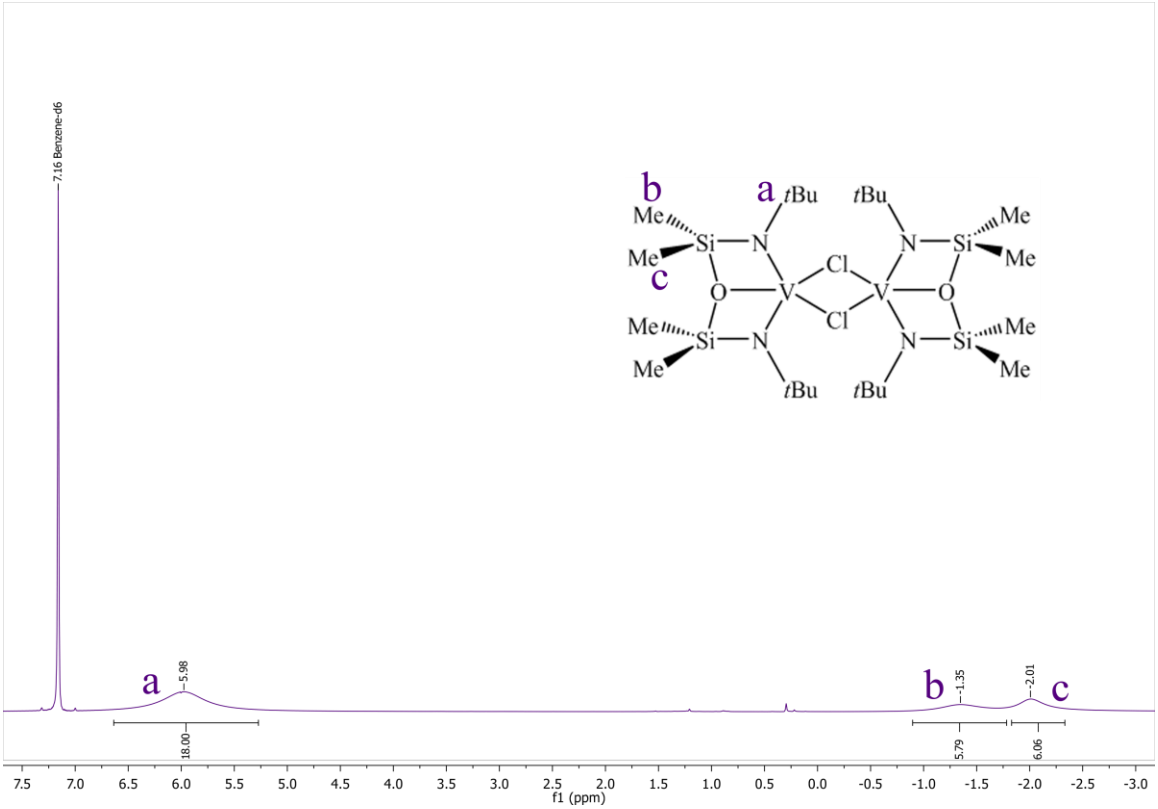


**Figure 2.6. $^{1}$H NMR spectrum of {[$^{tBu}$NON]VCl}$_2$ (3) in $d_6$-benzene.**

The $^{1}$H NMR spectrum of **3** (Figure 2.6) shows a paramagnetic species, as the three peaks are shifted from their implicit diamagnetic positions, and clearly broadened. The signal at approximately 6.0 ppm corresponds to the 18H's of the *t*Butyl groups. The silylmethyl signal is split into two peaks that each integrate to 6H, appearing at -1.4 ppm and -2.0 ppm. The split is an indication that the dimer is maintained in the solution state, where the equivalency of the silylmethyl signals is broken into two halves. This can be rationalised by labelling one methyl on each silyl group as in the "up" position, while the other methyl on each silyl group is in the "down" position. Each of the "up" methyl protons are exchangeable by symmetry with each other, but not with the "down" methyl protons, and vice versa; this results in two signals of equivalent integrations for the silylmethyl protons. However, to confirm this rationale, a VT-NMR experiment would be useful.

To determine the fundamental magnetic properties of a paramagnetic complex, two routes may be taken – a solid state sample anaylsis via SQuID magnetometry which

gives variable temperature data, or a solution sample analysis using the Evans' method NMR technique at room temperature. While Evans' method is typically only performed at room temperature, it is also possible to also do a variable-temperature experiment, providing further information about how the unpaired electron affects the shifted internal standard signals. It should be noted that since the Evans' method data is collected in solution state, monomer-dimer equilibria in the sample can have a large effect on the magnetic moment.

Similar to complex **2**, an Evans' method $^{1}$H NMR measurement for complex **3** revealed a solution magnetic moment of approximately 2.2 $\mu_B$ per vanadium centre. This value is smaller than the expected value of 2.83 $\mu_B$ for a non-coupled $d^2$ vanadium(III) centre, and is suggestive of antiferromagnetic coupling between two metal centres. The experimental value obtained has some systematic error, as the calculation of the magnetic moment relies on the accurate knowledge of the concentration of sample in solution, and due to the milligram quantities this introduces a large amount of weighing error. This does provide evidence suggesting that the complex remains dimerised in the solution state, for if it were to break apart upon dissolution, any coupling between metal centres would be expected to disappear. A VT Evans' method NMR experiment could provide further information assuming that the complex remains soluble at all temperatures. To obtain more specific details of the magnetic interaction between the metal centres, a solid state sample was prepared and analysed using a SQuID magnetometer (Figure 2.7). At 300 K, the effective magnetic moment approaches 2.5 $\mu_B$ per metal centre, although the graph indicates that $\mu_{eff}$ may continue to increase slightly at warmer temperatures. The initial lower-than-expected moment suggests the presence of spin-orbit coupling, and a steady decline with lower temperatures is indicative of antiferromagnetic coupling between the metal centres. We attempted to model the $X_m$ vs. T data using an equation that describes the interaction between a symmetric homonuclear dimer for an S = 1 system, with an additional molecular field approximation term to empirically account for any low temperature effects.[171] However, while the model appeared to fit the data well above 50K, the estimated g (1.57), J (-2.32), and J' (-285.5) values were found to be inconsistent with the fundamental assumptions of the model; which is to say that the J' value should be a correction term for J, and so should be at least 10x smaller than the J value. All other attempts to fit the data to a model were

unsuccessful, and this is likely due to the combination of small spin-orbit coupling (SOC), weak antiferromagnetic interactions, as well as zero-field splitting effects, which is observed as the sudden drop in magnetic moment below 10 K. There is no maximum observed in the $X_m$ vs. T data, suggesting that any coupling present is weak.

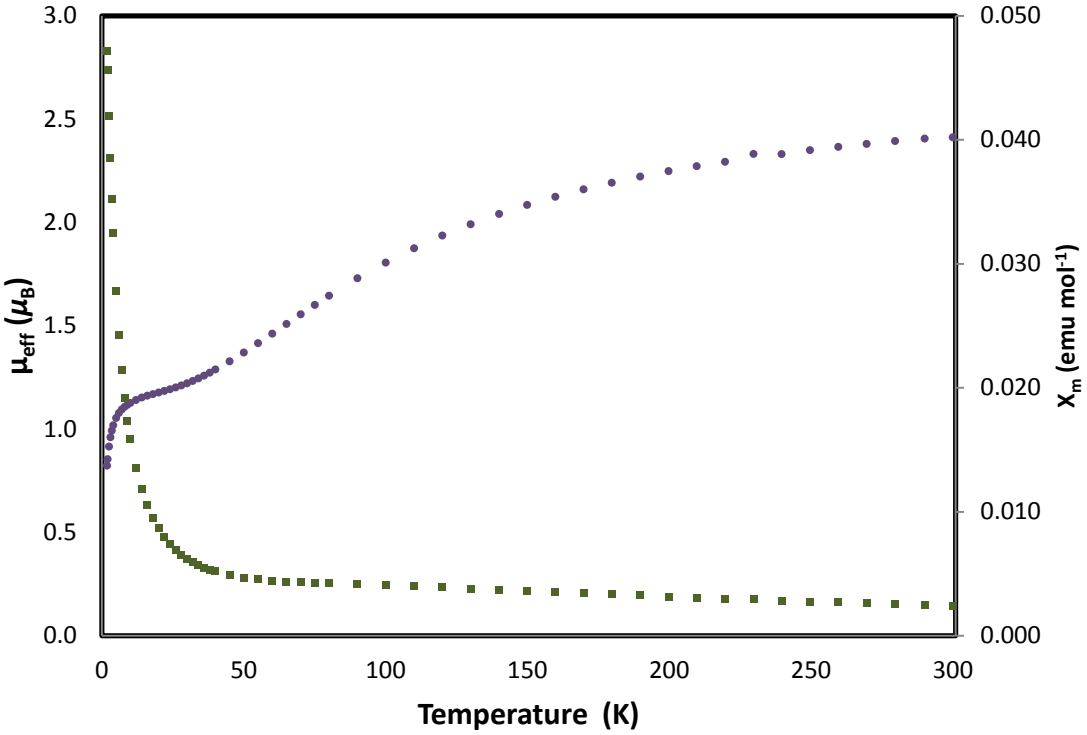


**Figure 2.7. Plot of effective magnetic moment data from 1.8 - 300 K for {[$^{t\text{Bu}}$NON]VCl}$_2$ (3) per vanadium centre.**

Purple circles = $\mu_{eff}$ values; green squares = $X_m$ values.

To our knowledge, there has not been a solid state, variable temperature magnetism study completed on any literature complexes containing vanadium(III) dimers. However, there have been a number of room temperature magnetic moment determinations on vanadium chloride-bridged dimers, as well as hydride-bridged dimers. Cloke has published a chloride-bridged diamidoamine vanadium(III) dimer which exhibits a solution magnetic moment of 2.78 $\mu_B$ per monomer, and thus the two metal centres do not appear to interact with each other.[46] The related hydride-bridged structure, however, shows a reduced room temperature magnetic moment of 1.76 $\mu_B$ per vanadium. Since no oxidation of the metal occurred, the reduction of $\mu_{eff}$ must be attributed to substantial antiferromagnetic coupling between the metals. Gambarotta also synthesised a

vanadium(III) dimer, $[(Cy_2N)_2VCl]_2$ (Cy = cyclohexyl), which had a reduced magnetic moment of 1.79 $\mu_B$ per monomer at room temperature in the solid state; this also indicated antiferromagnetic coupling.[49] So it seems that the vanadium centres may be weakly coupled at room temperature, although without other reported variable temperature data to compare with, it is difficult to pinpoint whether complex **3**'s magnetic properties are similar to its related congeners.

### 2.2.2. Alkylation Reactions of Diamidoether Scandium, Titanium, and Vanadium Halide complexes

After the successful synthesis of complexes **1**-**3**, we considered that the alkylation of each may provide insight into the differences and similarities of the chemistry as a function of changing the number of *d*-electrons. The alkylating reagent $LiCH_2SiMe_3$, which is commonly used for these types of reactions, was chosen to target prototypical trimethylsilylmethyl complexes in order to provide suitable literature comparisons.

#### *Scandium*

The alkylation reaction of complex **1** was performed by addition of one equivalent of $LiCH_2SiMe_3$ to a toluene solution of **1**, which through salt metathesis formed complex **1a**, $[^{tBu}NON]ScCH_2SiMe_3$•THF in 92% yield, after isolation and purification from the LiCl byproduct. X-ray quality crystals were formed from slow evaporation of a concentrated hexanes solution (Figure 2.8). The reaction resulted in removal of chloride and replacement with the alkyl, thereby breaking the dimer. In spite of this change, the THF still remained bound, indicating that the scandium still exhibits high oxophilicity, particularly as the neutral silylether remains bound as well. Overall, the resulting scandium centre has a distorted 5-coordinate square pyramidal geometry with a $\tau$-value of 0.29, with the alkyl carbon in the apical position.[169]

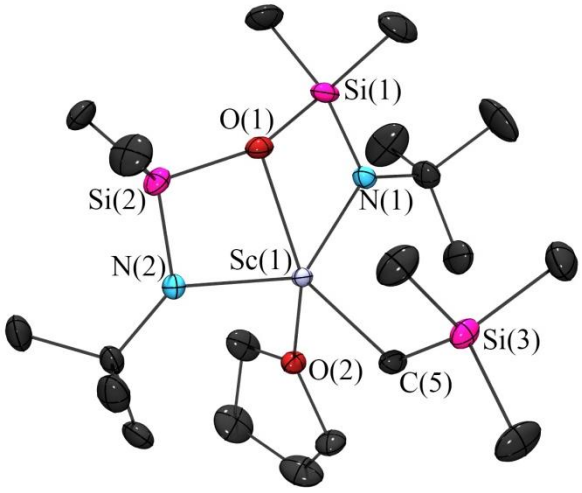


**Figure 2.8. X-Ray crystal structure of [$^{tBu}$NON]ScCH$_2$SiMe$_3$•THF (1a).**

**Table 2.5. Selected interatomic distances (Å) and angles (°) for [$^{tBu}$NON]ScCH$_2$SiMe$_3$•THF (1a).**

| Bond Lengths | | Bond Angles | |
|---|---|---|---|
| Sc(1) – N(1) | 2.113(2) | N(1) – Sc(1) – N(2) | 130.61(7) |
| Sc(1) – N(2) | 2.108(2) | O(1) – Sc(1) – N(1) | 69.50(6) |
| Sc(1) – O(1) | 2.282(2) | O(1) – Sc(1) – N(2) | 69.45(6) |
| Sc(1) – C(5) | 2.222(2) | O(2) – Sc(1) – N(1) | 99.40(6) |
| Sc(1) – O(2) | 2.172(2) | O(2) – Sc(1) – N(2) | 100.93(6) |
| O(1) – Si(1) | 1.672(2) | O(1) – Sc(1) – C(5) | 117.79(6) |
| O(1) – Si(2) | 1.665(2) | O(2) – Sc(1) – C(5) | 94.27(6) |
| Si(1) – N(1) | 1.696(2) | N(1) – Sc(1) – C(5) | 110.52(7) |
| Si(2) – N(2) | 1.698(2) | N(2) – Sc(1) – C(5) | 112.23(7) |
| C(5) – Si(3) | 1.830(2) | Si(1) – O(1) – Si(2) | 149.5(1) |
| | | Sc(1) – C(5) – Si(3) | 127.7(1) |

In comparison to **1**, the Sc – N distances are relatively unchanged, and so are still comparable to literature values for typical Sc – N bonds (Table 2.5).[158,165] The Sc – O bond to the backbone has lengthened slightly in **1a**, while the THF donor bond to scandium is significantly shorter. This push-pull effect of the bond distances may be an effect of steric strain introduced by the bulky alkyl. The Sc – N bond distances of 2.108(2) Å and 2.113(2) Å are longer than the 2.039(2) Å in Dehnicke's $ScCl_2[N(SiMe_3)_2](THF)_2$, although this may also be a result of steric constraint from the diamido ligand versus Dehnicke's monoamide.[165] However, when compared to Piers' β-

diketiminato scandium structure, the bond lengths appear to be typical for a diamido ligand.[158] A methyl-derived version of Piers' scandium complex with a Sc – C distance of 2.212(2) Å revealed that the Sc-C distance of 2.222(2) Å in **1a** is unremarkable. In addition, Piers' dialkyl scandium β-diketiminato complexes have Sc – C distances of 2.1954(14) Å and 2.2446(13) Å when the alkyls are $–CH_2SiMe_3$ groups, and 2.210(9) Å and 2.245(9) Å when the alkyls are $–CH_3$ groups; these distances are comparable to that in **1a**.[172]

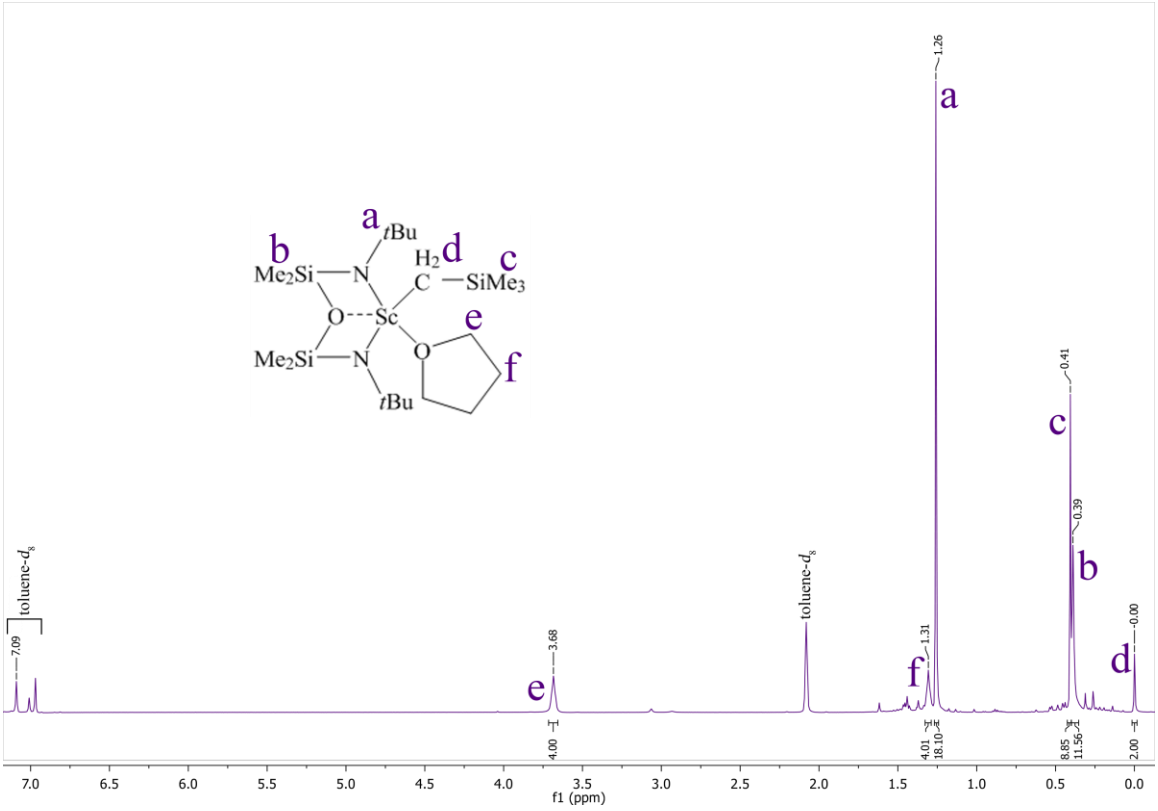


**Figure 2.9. $^1$H NMR spectrum of [$^{tBu}$NON]ScCH$_2$SiMe$_3$•THF (1a) in $d_8$-toluene.**

The $^1$H NMR spectrum of the alkylated scandium complex, **1a** (Figure 2.9), shows that the *t*Butyl peaks have shifted from 1.39 ppm in **1** to 1.26 ppm in **1a**, while the dimethylsilyl peaks have shifted from 0.30 ppm to 0.39 ppm. The THF-assigned peaks are still visible, although they now appear at 1.31 ppm and 3.68 ppm. In addition to these, there are two new peaks. One appears at 0.00 ppm with an integration of 2H; this is assigned to the $CH_2$ moiety of the alkyl that is bound to the scandium centre. The second is at 0.41 ppm with an integration of 9H, which corresponds to the trimethylsilyl protons of the alkyl.

Formation of the diamidoscandium alkyl complex **1a** opens up new potential reactivity pathways that rely on the presence of a M – C bond, including ethylene polymerisation, as there are several literature complexes that show such proficiency (see section 1.2.5).[41,160,161,166,173]

### *Titanium*

The alkylation product of **2** was sought to determine whether it would behave more closely to the scandium (**1**) or vanadium (**3**) complexes. However, due to the purification issues regarding complex **2**, only a small-scale reaction of crystalline complex **2** with $LiCH_2SiMe_3$ was attempted, and milligram quantities of orange crystals were isolated. However, the crystals did not confirm similarity to either complexes **1** or **3**.

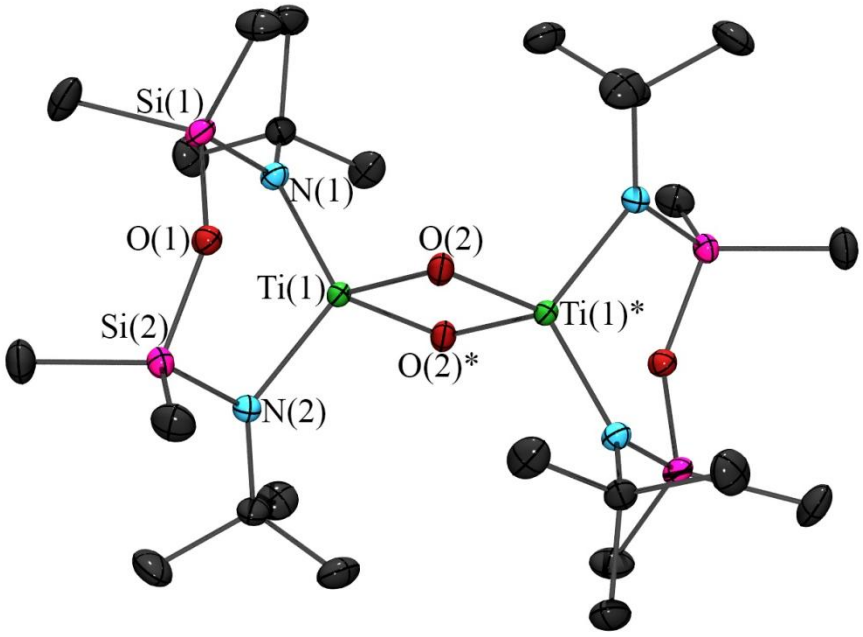


**Figure 2.10. X-Ray crystal structure of {[$^{tBu}$NON]Ti(OH)}$_2$ (2a).**

**Table 2.6. Selected interatomic distances (Å) and angles (°) for {[$^{t\text{Bu}}$NON]Ti(OH)}$_2$ (2a).**

| Bond Lengths | | Bond Angles | |
|---|---|---|---|
| Ti(1) – Ti(1)* | 2.7529(2) | O(2) – Ti(1) – O(2)* | 84.05(3) |
| Ti(1) – O(1) | 2.3601(7) | N(1) – Ti(1) – N(2) | 114.31(3) |
| Ti(1) – O(2) | 1.9159(6) | O(2) – Ti(1) – N(1) | 109.19(3) |
| Ti(1) – O(2)* | 1.7882(7) | O(2) – Ti(1) – N(2) | 113.87(3) |
| Ti(1) – N(1) | 1.9427(8) | O(2)* – Ti(1) – N(1) | 116.02(3) |
| Ti(1) – N(2) | 1.9508(5) | O(2)* – Ti(1) – N(2) | 115.59(3) |

As Figure 2.10 depicts, the alkylation of complex **2** did not occur as predicted. A diamdiotitanium dimer with two bridging hydroxides was isolated (**2a**), with Ti – O distances of 1.7882(7) – 1.9159(6) Å (Table 2.6), consistent with Ti-OH distances (typical Ti-oxo, Ti=O, distances are much shorter at approximately 1.6 Å).[174] The distance between the silylether group and the titanium centre has increased from 2.244(3) Å to 2.3601(7) Å; this is now too long for a bond between them. However, the Ti – N distances have remained essentially unchanged at 1.9427(8)/1.9508(5) Å. Titanium(III), being relatively electron-poor, is quite oxophilic, and several complexes are known to have titanium hydroxide bonds.[174–176] The presence of these hydroxides is likely due to impure titanium starting material rather than hydrolysis during the reaction and further illustrates that the diamido-titanium complex **2** could not be utilised in its present state for exploring further reactivity.

### *Vanadium*

As for complexes **1** and **2**, reaction of complex **3** with $LiCH_2SiMe_3$, targeting the analogous vanadium alkyl was attempted. In this case, the alkylation reaction of **3** generated an alkylated product, but also one that included activated dinitrogen. To further validate this result, a second alkylation reaction was performed, this time using the reagent $KCH_2Ph$. The ensuing product was comparable: dinitrogen activation was observed with the addition of both $LiCH_2SiMe_3$ (**3a**) and $KCH_2Ph$ (**3b**) to the initial halide-bridged complex, **3** (Figure 2.11). Complexes **3a** and **3b** were fully characterised, producing clean $^1$H NMR spectra, and orange-brown crystals suitable for X-ray crystallography. In addition, the elemental analysis further supports the presence of bound dinitrogen in these species. Vanadium amido complexes have been known to

activate and bond dinitrogen;[39,74] however, for this reaction to occur simultaneously with the alkylation is rare.

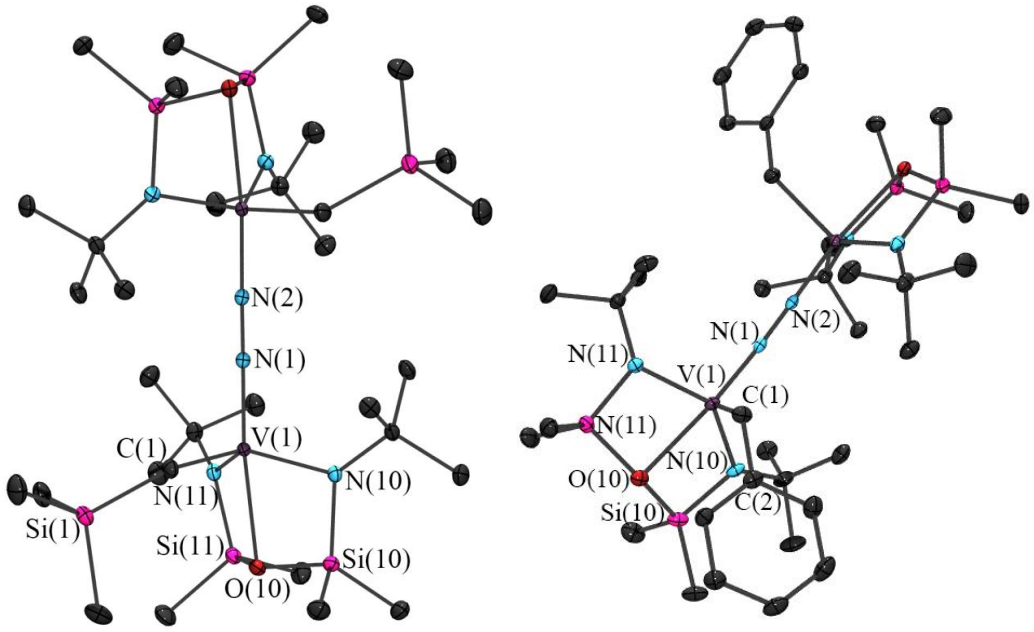


**Figure 2.11. X-ray single crystal structures of {[$^{tBu}$NON]VR}$_2$($\mu$-N$_2$), where R = $CH_2SiMe_3$ (3a), $CH_2Ph$ (3b).**

**Table 2.7. Selected interatomic distances (Å) and angles (°) for {[$^{t\text{Bu}}$NON]VR}$_2$-($\mu$-N$_2$), where R = $CH_2SiMe_3$ (3a), $CH_2Ph$ (3b).**

| Bond Lengths | -$CH_2SiMe_3$ Alkyl Complex (3a) | -$CH_2Ph$ Alkyl Complex (3b) |
|---|---|---|
| N(1) – N(2) | 1.238(2) | 1.236(3) |
| V(1) – N(1) | 1.744(1) | 1.742(2) |
| V(1) – N(10) | 1.911(2) | 1.904(2) |
| V(1) – N(11) | 1.908(2) | 1.904(2) |
| V(1) – O(10) | 2.340(1) | 2.317(2) |
| V(1) – C(1) | 2.098(2) | 2.128(3) |
| C(1) – R* | 1.859(3) | 1.489(4) |
| **Bond Angles** | | |
| V(1) – N(1) – N(2) | 173.9(2) | 176.3(2) |
| N(1) – V(1) – O(10) | 173.93(7) | 172.07(9) |
| N(1) – V(1) – N(10) | 103.43(8) | 102.76(9) |
| N(1) – V(1) – N(11) | 108.04(8) | 107.1(1) |
| N(10) – V(1) – N(11) | 121.47(8) | 127.33(9) |
| O(10) – V(1) – N(10) | 71.74(7) | 72.38(8) |
| O(10) – V(1) – N(11) | 72.40(7) | 72.29(8) |
| O(10) – V(1) – C(1) | 88.88(7) | 90.56(9) |
| C(1) – V(1) – N(1) | 96.28(8) | 97.0(1) |
| C(1) – V(1) – N(10) | 109.13(8) | 107.5(1) |
| C(1) – V(1) – N(11) | 114.76(8) | 110.6(1) |
| V(1) – C(1) – R* | 127.0(1) | 118.2(2) |

*R = Si(1) in **3a**, C(2) in **3b**.

The diamido vanadium complexes **3a** and **3b** are each dimers joined together through an end-on bound dinitrogen species, in addition to each metal centre binding an alkyl group from the salt metathesis reaction. The vanadium centres therefore remain in a distorted trigonal bipyramidal geometry for both **3a** and **3b**, with $\tau$-values of 0.874 and 0.746, respectively, indicating that **3b** is more distorted than **3a**. The alkyl group is bent at a V(1)-C(1)-R* angle of 127° (**3a**) and 118° (**3b**), away from the dimer's core axis (Table 2.7). The N – N distances of 1.238(2) and 1.236(3) Å, and the V – N distances of 1.744(1) and 1.742(2) Å in **3a** and **3b** are typical for end-on dinitrogen bound vanadium complexes, and suggests that the dinitrogen unit has been di-reduced to $[N{=}N]^{2-}$.[75–78] For comparison, V – N distances of 1.7248(18) Å in the $[(Me_3CCH_2)_3V]_2(\mu\text{-}N_2)$ complex prepared by Teuben et al, 1.761(6)/1.773(6) Å in the {[$\eta^5$-($C_5H_4CH_2CH_2NMe_2$)]-

V(PhCCPh)(PMe$_3$)}$_2$($\mu$-N$_2$) complex prepared by Liu et al, and 1.772(3) Å in the [V(OR)$_3$]$_2$($\mu$-N$_2$) (R = *t*Bu$_2$(Me)CO$^-$) system prepared by Nocera et al have been reported.[75,76,78] Free dinitrogen has a N-N distance of 1.098 Å, and so the lengthening of this bond to 1.238(2) Å in **3a** and 1.236(3) Å in **3b** is indicative of a two-electron reduction.[39] Gambarotta has developed a triamido vanadium complex – also beginning with V(III) – which forms an end-on bound dinitrogen bridging two monomers, and exhibits a N-N bond length of 1.257(6) Å and a V – N bond length of 1.707(3) Å.[177] He has also synthesised an amidinate complex with V(II), which, upon heating promotes the loss of THF and the activation of dinitrogen; this is also bound end-on and the elucidated N-N bond length was 1.235(6) Å.[48] These related examples confirm the nature of complex **3**'s N-N bond length, and the rationale of a di-reduced moiety. The V – N (amide) bond lengths are relatively unchanged from **3**, although in both cases the V – O bond length has increased, from 2.164(3)/2.166(3) Å in **3**, to 2.340(1) Å (**3a**) and 2.317(2) Å (**3b**). This is likely a result of increased steric hindrance as introduced by the adjoined alkyl group.

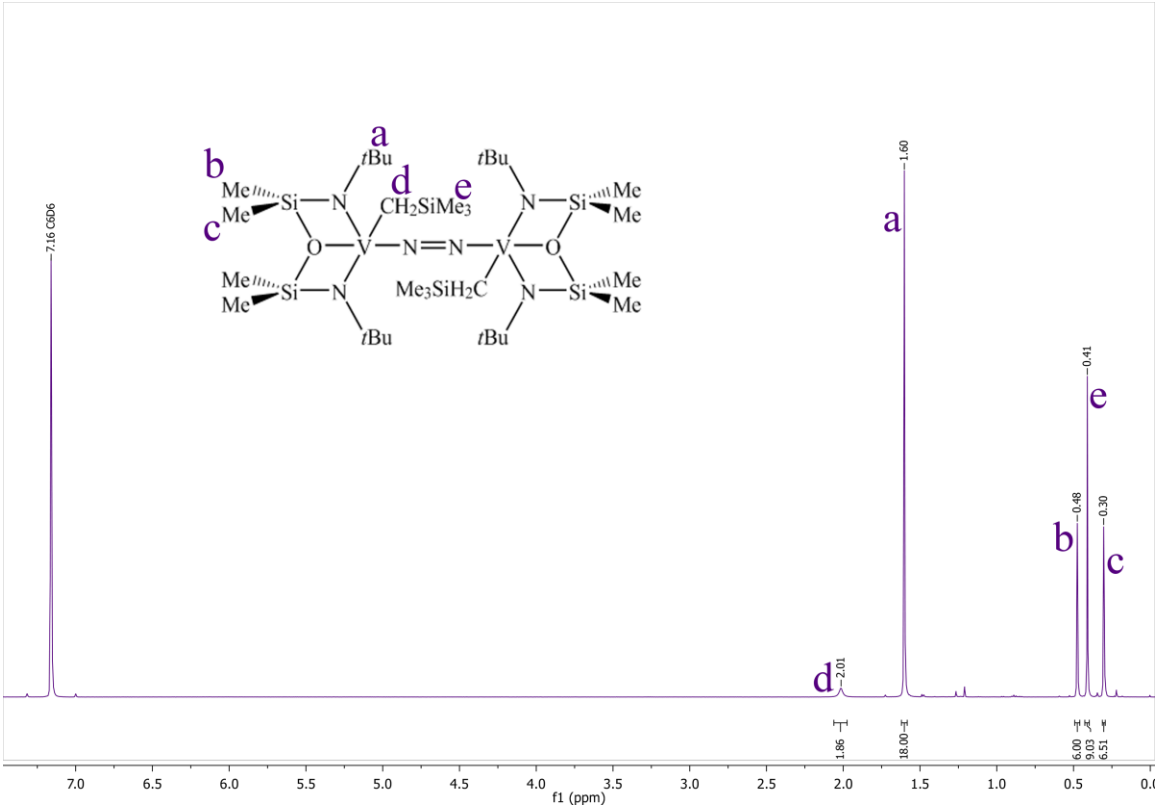


**Figure 2.12. $^1$H NMR spectrum of {[$^{t\text{Bu}}$NON]VCH$_2$SiMe$_3$}$_2$($\mu$-N$_2$) (3a) in $d_6$-benzene.**

For **3a**, the $^{1}$H NMR spectrum shows the five expected peaks for the diamido alkyl complex (Figure 2.12). More surprising, however, is the change to a completely diamagnetic spectrum. The *t*Butyl moiety produces a sharp signal at 1.60 ppm that integrates to 18H. The silylmethyl peaks remain as two singlets, appearing at 0.30 ppm and 0.48 ppm, corresponding to 6H each. In addition to these, a singlet at 0.41 ppm, integrating to 9H, indicates the trisilylmethyl group of the alkyl, while the $CH_2$ moiety of the alkyl has a signal at 2.01 ppm. This is a rather deshielded signal, considering it is bound directly to the $SiMe_3$ moiety, which usually produces signals in the 0-1 ppm range. In addition to this unexpected shift, the peak's slightly broadened nature suggests that perhaps the vanadium centre's paramagnetism has some impact on the closest protons.

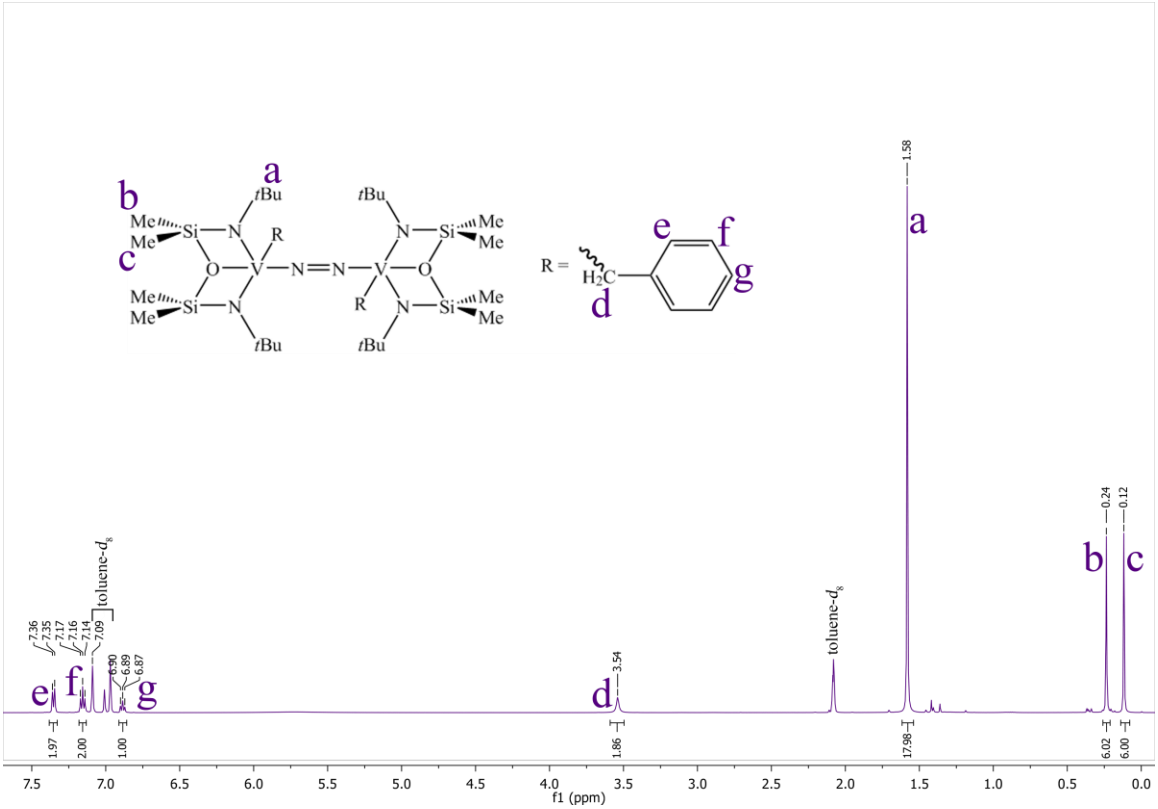


**Figure 2.13. $^{1}$H NMR spectrum of {[$^{t\mathrm{Bu}}$NON]VCH$_2$Ph}$_2$($\mu$-N$_2$) (3b) in $d_6$-benzene.**

The $^{1}$H NMR spectrum for **3b** (Figure 2.13) is similar to that of **3a**. The *t*Butyl peak, integrating to 18H, appears at 1.58 ppm, while the two silylmethyl ligand backbone peaks, each integrating to 6H, appear at 0.12 and 0.24 ppm. The three clean muliplets appearing at 6.89, 7.16, and 7.35 ppm (1H, 2H, and 2H, respectively) represent the

aromatic protons of the benzyl alkyl. The benzyl $CH_2$ moiety that binds to the vanadium centre appears at 3.54 ppm (2H), and is again slightly broadened.

Assuming, based on the x-ray data, that if the dinitrogen species has been di-reduced to form $[N=N]^{2-}$, then this would require each vanadium centre to be mono-oxidised to $V^{4+}$, $d^1$. Solution magnetic studies indicate that **3a** has a room temperature magnetic moment of 1.5 $\mu_B$ per vanadium centre, which is consistent with the vanadium oxidation state assignment. Although the spin-only moment for one unpaired electron is calculated as 1.73 $\mu_B$, the presence of spin-orbit coupling within the vanadium(IV) centre would be expected to lower this value slightly, the observed 1.5 $\mu_B$ is reasonable.[155] In order to probe any potential magnetic coupling through the dinitrogen bridge, solid state magnetic data for **3a** was collected using a powder sample which was determined to be pure by $^1$H NMR spectroscopy and EA.

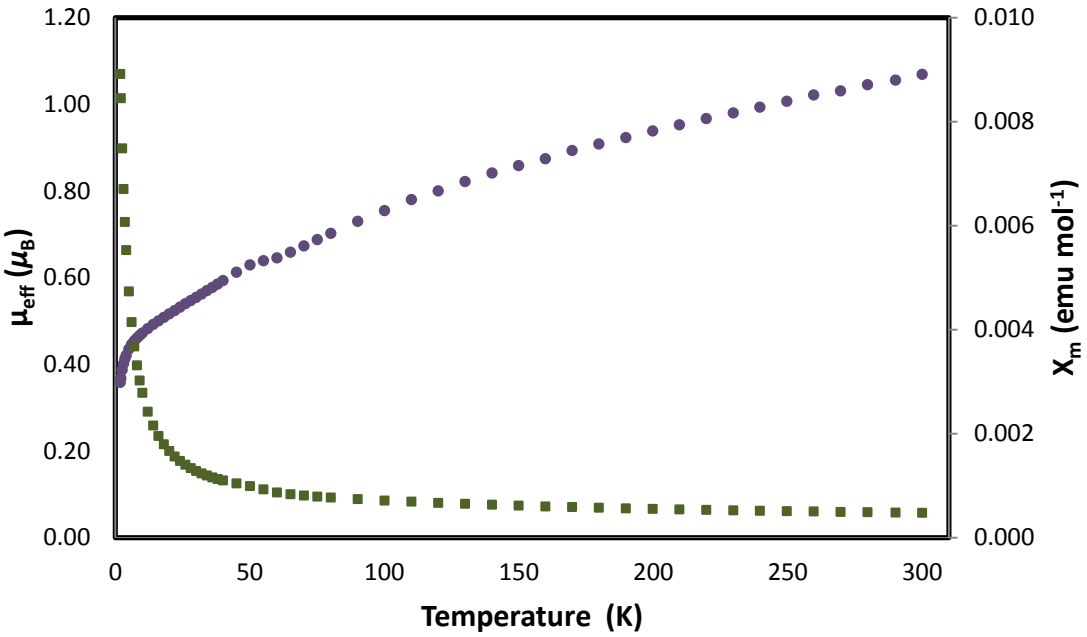


**Figure 2.14. Plot of effective magnetic moment data from 1.8 - 300 K for {[$^{tBu}$NON]VCH$_2$SiMe$_3$}$_2$($\mu$-N$_2$) (3a) per vanadium centre.**

Purple circles = $\mu_{eff}$ data; green squares = $X_m$ data.

While the plot of the effective magnetic moment ($\mu_{eff}$) vs. temperature (Figure 2.14) generally follows the expected shape, it does not appear to flatten out upon approaching room temperature (300 K), the highest temperature collected. Although the

SQuID magnetometer is capable of reaching up to 400 K, concerns regarding sample decomposition above room temperature limited the collection of magnetic susceptibility data above 300 K. The data does, however, reach a reasonable $\mu_{eff}$ of 1.07 $\mu_B$ per vanadium centre. This is lower than in the solution state, suggesting that there are other effects lowering the magnetic moment. Alternatively, perhaps a higher temperature must be reached in order to attain the maximum magnetic moment for this complex. Other effects that may be lowering the magnetic moment include orbital contributions resulting from the trigonal bipyramidal geometry around the vanadium centre. In addition to that, there may also be antiferromagnetic coupling, resulting in an overall diminished magnetic moment, which may vary depending on the strength of the coupling. This coupling was attempted to be modelled with a Bleaney-Bowers equation, although the data could not be met with a reasonable fit. This is likely due, again, to small spin-orbit coupling effects, weak antiferromagnetic coupling, as well as zero-field splitting effects, all occurring simultaneously. There is no observable maximum in the $X_m$ vs. T data, indicating no long-range ordering. Unfortunately, we are unable to compare this data with other vanadium dinitrogen complexes, as the literature does not report the details of the magnetic properties of these types of complexes. While the magnetic data was not collected for complex **3b**, it would be expected that it would exhibit similar data as in **3a**, due to the structural similarities between the two, particularly in bond lengths and angles between the vanadium centres through the dinitrogen.

The formation of the dinitrogen complexes **3a** and **3b** each occur cleanly, and relatively quickly, each producing brown-red powders. Unlike the alkylation of the scandium complex, **1**, complex **3** does not have an additional THF present. It is conceivable that when the dimer breaks and the alkyl binds to each vanadium monomer, there is an open coordination site that is also sterically well-shielded, which is ideal for a dinitrogen molecule to bind in an end-on fashion, and linking the monomers back together.[78,178] It is well-known that the early transition metals are reducing enough to bind the generally inert dinitrogen molecule, so it is expected that the formation of a vanadium dinitrogen dimer may form if the conditions are just right. Typically, however, dinitrogen complexes form through reduction reactions using $KC_8$, and not through a simple alkylation reaction.[39,69] However, the alkylation reaction yields a more electron-rich vanadium centre than the original halide-containing complex, and the additional

reducing power this provides may help to drive the activation of the dinitrogen molecule. For example, the case of the related vanadium tris(amide) complex $[R_2N]_3V(THF)$ (R = *i*Pr, Cy), a stable compound reported by Gambarotta et al which was crystallized from toluene, is instructive..[178] When the THF was removed through heating and dissolution into a concentrated solution of hexanes, crystals were examined and found to contain a dinitrogen moiety, $[(R_2N)_3V]_2(\mu\text{-}N_2)$ (R = *i*Pr, Cy). Gambarotta cites thermal instability as the cause of this reaction, as the related complex, where R = Ph, does not activate dinitrogen upon undergoing solvent replacement. Additionally, Mindiola and colleagues reported a vanadium alkylidene complex that rearranged into a vinylimide and subsequently was reduced and bound a dinitrogen molecule.[179]

Overall, each alkylation reaction with the diamido scandium, titanium, and vanadium complexes produced a different result. The scandium complex (**1**) simply resulted in a monomeric alkyl complex through a straightforward halide-for-alkyl metathesis reaction. The reactions of complex **3** had an open site available and sufficient reducing power to activate a dinitrogen molecule, thereby forming a new type of dimer from complex **3**, and forming two new dinitrogen-containing vanadium species, complexes **3a** and **3b**. Alkylation of the diamido titanium complex **2** was meant to indicate whether its behaviour would be more similar to either complex **1** or **3**; however, likely due to impure $TiCl_3$•3THF, a hydroxide-bridged diamidotitanium(III) dimer (**2a**) was instead isolated.

## 2.2.3. Reduction Reactions

### *Reduction of Scandium Complexes*

The diamido scandium(III) complexes **1** and **1a** contain $d^0$ metal centres. In addition to being diamagnetic, this also presents an opportunity: addition of a reducing agent, such as $KC_8$, could facilitate otherwise difficult-to-access chemistry. In this instance, as formal reduction of the metal centre is highly unlikely, the resulting reduced complex may instead activate dinitrogen. There is only one known scandium dinitrogen complex, published by Evans in 2010.[86] In this previous work, using a multi-step procedure, working through the chloride-containing complex, the conversion to an allylic form, followed by abstraction of the allyl using a tetraphenylborate salt, this dinitrogen

complex was finally formed through reduction via $KC_8$ with a short reaction time in THF solvent. The resulting complex illustrated a side-on bound dinitrogen between scandocene centres: $[(C_5Me_4H)_2Sc]_2(\mu\text{-}\eta^2\text{:}\eta^2\text{-}N_2)$. The N-N bond distance was consistent with mono-reduced dinitrogen, $(N{=}N)^{2-}$, and the side-on bridging motif reflects the dinitrogen bonding trends of the larger lanthanides. It should also be noted that this reported dinitrogen complex is a highly coloured species, as compared to that of **1** and **1a**. Also of note, Fryzuk published several zirconium(IV) (also $d^0$) dinitrogen complexes, featuring both side-on and end-on dinitrogen moieties, using $KC_8$ to reduce atmospheric dinitrogen.[180,181] Chirik also synthesised a side-on bound dinitrogen zirconium dimer, through addition of a lithium alkyl reagent.[182] These findings further support the possibility of forming a dinitrogen-containing complex from **1** or **1a**.

In a preliminary effort to test this particular reactivity avenue, the reaction of **1** with $KC_8$ was carried out. Although crystallisation of the resulting product has been elusive, a relatively clean, symmetric, and considerably changed $^1$H NMR spectrum indicates that a clean reaction appears to have occurred. Some smaller singlets at 0.18 ppm and 1.19 ppm that have an integration ratio of 2:3 protons, respectively are consistent with free ligand, and the singlet at 0.26 ppm corresponds with silicone grease in the $d_8$-toluene solvent.[183] The peaks appearing between 2.5 and 4.0 ppm are likely some decomposition product; the range of these unknown peaks suggest protons that are bound to or near to nitrogen or oxygen, which may indicate ligand fragmentation. The solvent used in this reaction was toluene, which would not be expected to fragment easily. The remaining signals representing what is likely the product (Figure 2.15) consist of the peaks at 0.76 and 0.79 ppm (each integrating to 6H), and another singlet at 1.28 ppm (18H). Elemental analysis data indicated from a low %N content that $N_2$ had likely not been incorporated into the solid analysed (unidentified) product(s).

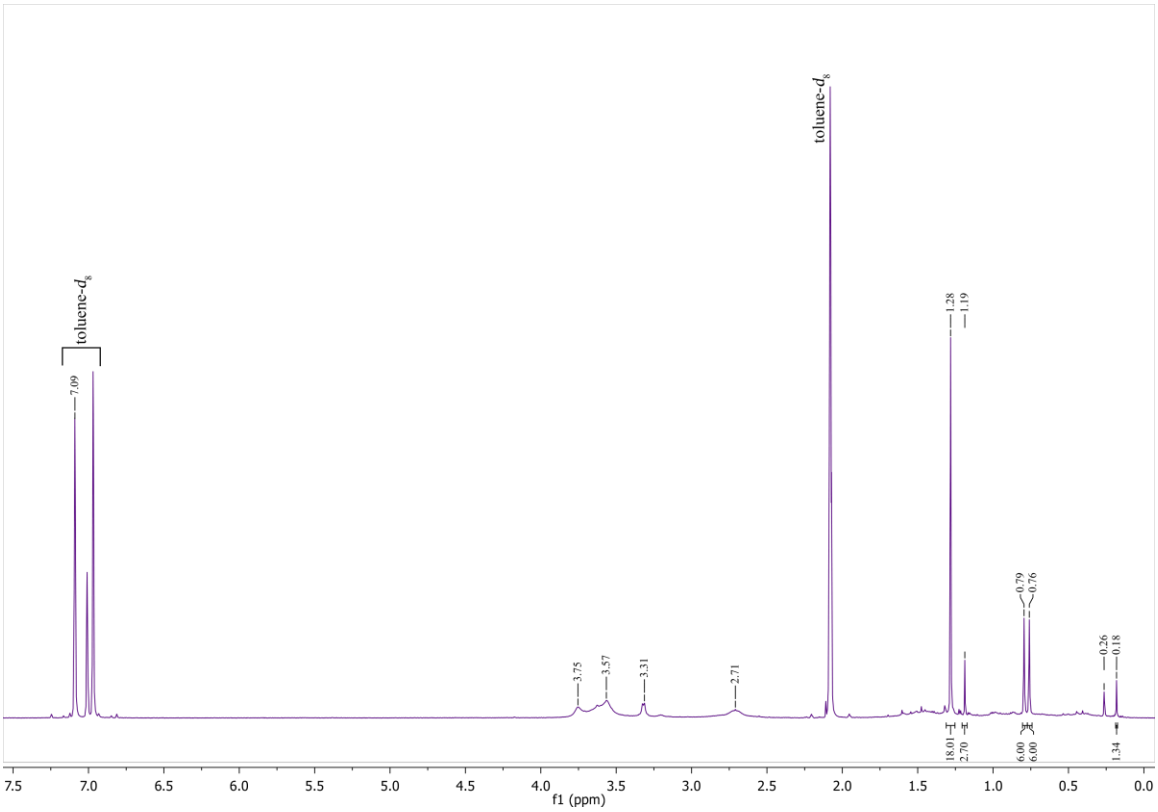


**Figure 2.15. $^1$H NMR spectrum of reaction of {[$^{tBu}$NON]ScCl•THF}$_2$ (1) with $KC_8$ in *$d_8$*-toluene.**

Further research on this reaction may entail closer adherence to Evans' procedure for the synthesis of his dinitrogen scandocene dimer.[86] The diamidoscandium alkyl complex **1a** is already available. If **1a** could then undergo alkyl abstraction, as illustrated in other reactivity systems, then perhaps the addition of $KC_8$ would yield a more obvious dinitrogen product. Tris(perfluorophenyl)boron is an appropriate choice of reagent for alkyl abstractions, and an initial attempt to proceed down this synthetic route should be approached using an NMR tube experiment in future.

### *Reduction Attempts of Vanadium Complexes*

The literature has shown that other vanadium(III) dihalide-bridged dimers, upon addition of yielded $N_2$-coordination to the metal and reduction of the dinitrogen moiety.[79,80] The bond distances of the V-N and N-N bonds in **3a** are indicative of a 2-electron reduction of the dinitrogen species. This means that two additional 2-electron reductions are required to break the N-N bond completely. The most direct method to

attempt that reduction is through the addition of a strong reducing agent, such as $KC_8$. Two possible pathways were considered here: in the first, it may be possible to produce dinitrogen activation without the alkylation product; and in the second, addition of 1 equivalent of $KC_8$ to **3a** may reduce the N-N bond to at least a single bond. The final goal is to reduce N-N moiety such that the bond is completely broken.

Unfortunately, preliminary reactions of both **3** and **3a** with 1 equivalent of $KC_8$ were deemed unsuccessful, as the $^1$H NMR spectra produced in both cases were indicative of significant decomposition (Figures A2 and A3, for complexes **3** and **3a**, respectively).

## 2.2.4. Attempts at Hydride Complex Formation

### *$KEt_3BH$ with Scandium Complexes*

Scandium is known to form hydride complexes; the mono-cyclopentadienyl scandium hydride dimers are particularly well-known, and so it was logical to examine if the diamido containing-complexes **1** or **1a** could be converted to scandium hydrides.[53,173,184–187] Fryzuk recently published an interesting example – a ferrocene-linked bis(phosphinoamide) mononuclear scandium complex, which was shown to dimerise with a dihydrido bridge after addition of $H_2$ gas.[188] Preliminary attempts of $H_{2(g)}$ addition to complex **1a** did not yield an isolable product.

Although there are several routes one can take, $MEt_3BH$ (M = Li, Na, K) are common hydride transfer reagents for the formation of metal hydride complexes. By addition of these reagents to **1**, production of the scandium hydride could be anticipated. Addition of the borohydride to **1a**, however, may also produce a hydride, but it could alternatively remove the alkyl as alkane, which would result in an open reaction site for further reactivity.

Upon attempting the borohydride-reagent additions to **1** and **1a**, the products displayed highly impure $^1$H NMR spectra. Crystals obtained from the reaction with **1a** were determined to be potassium tetraethylborate. Thus, preliminary successes in creating a scandium hydride were elusive. Further research into synthesising

diamidoscandium hydride complexes should likely involve a re-evaluation of the hydride-producing reagents available, particularly as they relate to the previously published complexes.

### *Hydride Addition to Vanadium Complexes*

It is known that early transition metals favourably react with electron-rich σ-donors; for example, there are many known early transition metals bound to halides, as well as with amido ligands.[1,6] Hydrides also fall into this category, and as discussed, scandium in particular readily forms hydrido complexes.[189] Presumably vanadium(III) has more electron density than its scandium(III) counterpart, as organometallic-type vanadium hydrides are sparse in the literature. An example published by Cloke and colleagues in 1999, however, gives some hope for this reaction. In developing a set of scandium, titanium, and vanadium diamidoamine complexes, Cloke was able to synthesise the hydrido-containing version of each metal complex as well.[46] Cloke presented the initial complex as the dichloride-bridged dimer $\{[N\{N''\}_2]VCl\}_2$, (where $[N\{N''\}_2]$ = $\{[(Me_3Si)N\{CH_2CH_2N(SiMe_3)\}_2]$) which when reduced using $KC_8$ under $H_{2(g)}$, formed the dihydrido-bridged dimer, $\{[N\{N''\}_2]V\}_2(\mu\text{-}H)_2$. In addition, alkylation of the initial chloride-containing vanadium complex saw the formation of a mononuclear vanadium alkyl complex, $[N\{N''\}_2]VCH(SiMe_3)_2$, which also formed the same hydrido-bridged dimer when placed in an atmosphere of $H_{2(g)}$. These results are not only encouraging, but they are also closely related complexes to **3**, **3a**, and **3b**. Thus, it was decided to pursue the reaction of both complexes **3** and **3a** with $KEt_3BH$, another common hydride transfer reagent, in an effort to complete preliminary reactivity studies.

The reaction of **3** with $KEt_3BH$ resulted in a $^1H$ NMR spectrum that does not resemble that of the starting material (Figure A4). Also with no indication of any remaining ligand, this spectrum suggests complete decomposition of the starting material.

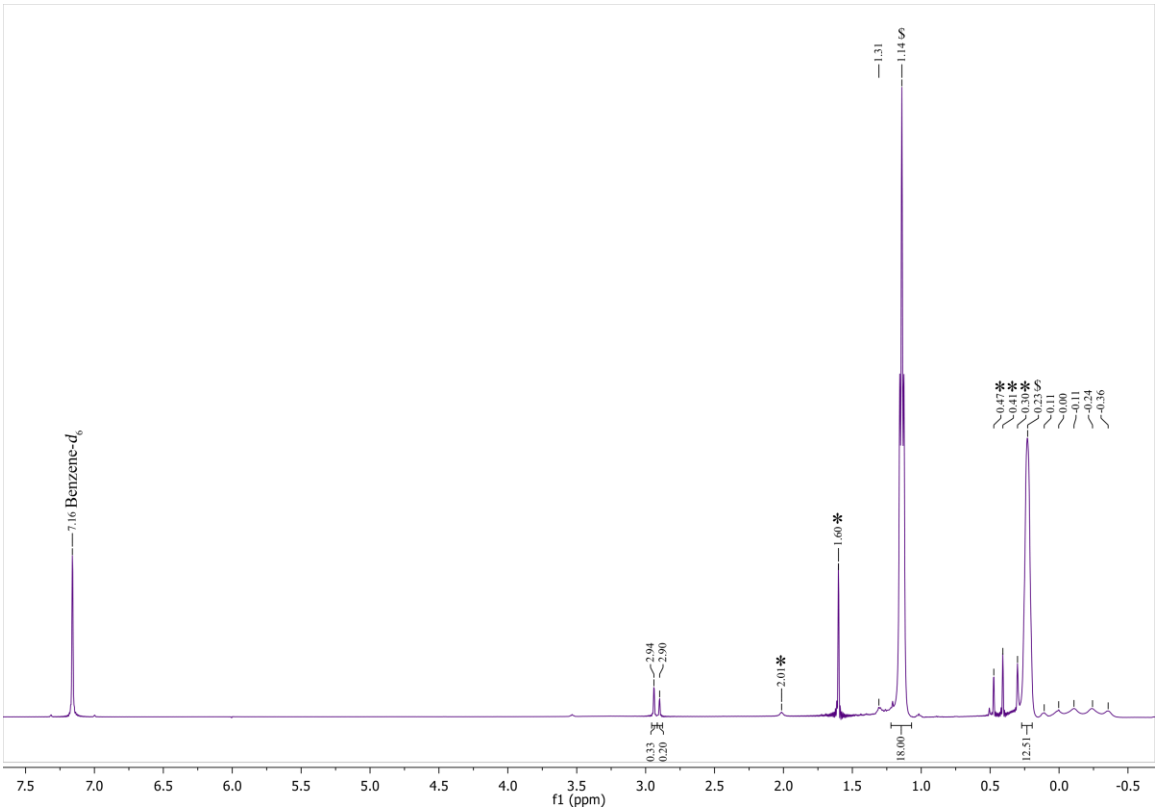


**Figure 2.16. $^{1}$H NMR spectrum of reaction of {[$^{tBu}$NON]VCH$_2$SiMe$_3$}$_2$($\mu$-N$_2$) (3a) with KEt$_3$BH in $d_6$-benzene.**

* = free ligand; $ = major product ligand signals.

The same reaction of KEt$_3$BH with **3a** gives much more promising results. All of the peaks for the starting material are still present in the $^{1}$H NMR spectrum (Figure 2.16), appearing at 0.30 ppm, 0.41 ppm, 0.47 ppm, 1.60 ppm, and 2.01 ppm; however, these signals appear as a minor product here. The major product gives only two peaks, in an 2:3 integration ratio, suggesting that the ligand is intact, although in a new environment, as the peaks are at different shifts than any of the complex's precursors. There are an additional two small peaks at 2.90 and 2.94 ppm, which may belong to a minor product that could also be the source of a quintet of peaks of equal intensity between -0.4 and 0.1 ppm. While the origin is unknown, we could speculate that it is a result of remaining alkylated BEt$_3$ ($^{10}$B, 19.9%, I = 3; $^{11}$B, 80.1%, I = 3/2), particularly since the alkyl moiety on the starting **3a** seems to have been removed in the product. Given these potentially encouraging results, it would be wise to revisit hydride addition, perhaps following Cloke's method more closely, particularly the reaction of **3** with the addition of H$_{2(g)}$.[46]

### 2.2.5. Attempts at Ethylene Polymerisation by the Scandium Complexes

There has been some reference in the literature of scandium's ability as an alkene polymerisation catalyst.[41,51,53,190–193] Bercaw's group, in particular, worked primarily with derivatives of linked permethylscandocene complexes as Ziegler-Natta catalysts of α-olefins, forming isobutene from propene, as well as showing ethylene insertion, oligomerisation, and polymerisation.[41,190,191] The group III catalysts are generally based on the successful catalyst design of group IV complexes, although in the case of scandium congeners, the resulting polymerisation activity is typically quite low.[166] With this in mind, it was determined that it would be worth testing if **1a** can perform as a traditional ethylene polymerisation catalyst.

As a precursor to the polymerisation reactions, the addition of 1 equivalent of the catalyst activator $B(C_6F_5)_3$ to **1a** was done as an overnight reaction in toluene (in the absence of ethylene). Crystallisation attempts were unsuccessful, and the $^1$H NMR spectrum shows several more peaks than expected. It would be predicted that the boron reagent would abstract the alkyl from the complex, forming a cationic scandium complex, counterbalanced by the now-alkylated anionic borate. The resulting $^1$H NMR spectrum (Figure A5) would be expected to show the same quantity of signals and the same integrations as that of the starting alkyl complex, although the signals would likely be shifted from their original positions. Instead, many additional and significant signals appear in the product spectrum, and are unable to be assigned to the expected product. The starting material does not appear to remain. A $^{19}$F NMR spectrum, had it been collected, would have given an indication of whether the alkyl had indeed formed a bond with the boron centre, as the environment surrounding the perfluorophenyl groups would have changed. An NMR tube experiment to track the progress of the reaction would be worth pursuing in the future.

Nevertheless, two experiments were targeted: **1a** in 5 mL of toluene, and **1a** plus 1 eq. $B(C_6F_5)_3$ in 5 mL of toluene, under ethylene. Each reaction flask was purged of nitrogen before steady addition of ethylene gas. One atmosphere of gas was flowed over each reaction mixture for 15 minutes, before lowering the pressure and leaving the reaction overnight, for approximately 18 hours in total under a steady stream of ethylene

gas. At the end of this reaction time, each flask was evacuated, removing any unreacted gas as well as solvent. At this point, the flasks qualitatively differed: the flask without activator appeared as simply recovered starting material. The flask containing **1a** and the activator, however, also appeared to have a small amount of solid product in addition to the other species. Workup of this reaction used acidified methanol, which is a standard reagent for processing of metal-catalysed alkene polymerisation reactions, facilitating the cleavage of the metal catalyst from the polymer chain and subsequent dissolution of the metal complex for removal from the polymer.[63] Only a small amount of polymer was obtained, so it was concluded that complex **1a** is a poor ethylene catalyst, and analysis of the polymer was not pursued any further as such.

## 2.3. Conclusion & Future Work

In this research, seven new early transition metal complexes featuring a diamidoether ligand of the framework $[^{t\text{Bu}}\text{NON}]^{2-}$, have been synthesised and characterised. Three of these are new diamidoether transition metal halide complexes of the general form $\{[^{t\text{Bu}}\text{NON}]\text{MCl}\}_2$ (**1**-**3**), appearing as halide-bridged dimers in the solid state. The exchangeable halides gave way to the formation of three new alkyls (**1a**, **3a**, & **3b**), two of which contained activated di-reduced dinitrogen.

However, preliminary reactivity studies of complexes **1**-**3** were either inconclusive, or unsuccessful. While the alkylation of the diamido scandium complex (**1**) was successful, producing **1a**, attempts to reduce it with $KC_8$ to form a hydrido complex, or polymerise ethylene with **1a** were each challenging. While the reaction with $KEt_3BH$ clearly did not work, the ethylene and $KC_8$ reactions are less clear-cut. The reaction with ethylene may well have produced a small amount of polyethylene, but due to the small quantity the catalyst is inherently poor. Also, McConville suggested that perhaps toluene is a poor solvent choice for polymerisation reactions as it may competitively bind to the catalyst active site, and so the reaction may in fact perform better, and produce more polymer, if done in benzene instead.[26,63,194] In addition, the $KC_8$ reaction with **1** had a $^1$H NMR that suggested a relatively clean reaction occurred. However, the determination of that product was elusive, as no x-ray quality crystals could be grown. Therefore, future work for the reduction of **1** involves following Evans' published procedure, who was able

to produce the only known scandium dinitrogen complex.[86] Further research on these scandium complexes should attempt to answer the following questions: does the scandium form a hydrido complex if a different hydride-containing reagent is used? Will further purification of the product of the $KC_8$ reaction result in an easier-to-interpret elemental analysis and $^1H$ NMR? Will increased catalyst loading increase the amount of polyethylene produced to an identifiable level?

Limited research was completed in regards to the titanium complex **2**. Although the purity of the $TiCl_3$•3THF starting material was checked by $^1H$ NMR as well as EA, the synthesis of **2** consistently gave highly impure, difficult-to-isolate product, thus making further reactions difficult to perform. Therefore, the best way to move forward with these complexes is likely to synthesise the starting material in-house, rather than trusting a commercial source.[195] It would be desirable, with a larger quantity of pure complex **2**, to test its ability as a polymerisation catalyst in particular. In addition to furthering the reactivity studies on this complex, it would also be desirable to examine the magnetic properties in more detail, to determine if the same trends are present as with the vanadium counterpart.

The diamido vanadium complex (**3**) has been the most interesting of this series, as the alkylation reactions additionally produced vanadium dinitrogen species. More importantly, this is a consistent motif, as the same system was generated with two different alkyls (-$CH_2SiMe_3$, **3a**; -$CH_2Ph$, **3b**). Unfortunately, further reduction with $KC_8$ was unsuccessful in weakening the N-N double bond further. In addition, potentially positive results in the hydride addition reactions were ultimately inconclusive. Perhaps more ideal results could be obtained using an alternate hydride source or hydrogen gas as a reagent.

Despite the negative results of the preliminary reactivity experiments, the goal of forming the diamido complexes with the early 1$^{st}$ row transition metals has been met. The scandium clearly behaves differently from the vanadium in that it retains a THF adduct, and forms a mononuclear scandium alkyl compound. The vanadium, in contrast, binds atmospheric dinitrogen upon alkylation. Disappointingly, this research did not discover which complex the alkylated titanium complex would resemble, as there have

been previous complex motifs published that alternately suggest titanium(III) behaves more like either scandium(III) or vanadium(III).

In comparison to previously known complexes containing the [$^{t\text{Bu}}$NON]$^{2-}$ ligand, the structural features are mostly typical. In terms of other +3 metals, only iron and chromium are known, for the first row of transition metals.[16,43,130] They also form halide-bridged dimers, with no additional solvent adducts, very much like complexes **2** and **3**. Alternatively, the +2 metal complexes are quite well known, with chromium, manganese, iron, cobalt, nickel, and copper all having amido-bridged structures, with no remaining halides.[126,128–130] Therefore, it can be said that the structural features of complexes **1**-**3** are typical for the 1$^{st}$ row transition metals in the +3 oxidation state. As the reactivity studies still need further development, trends cannot yet be established.

## 2.4. Experimental

### 2.4.1. General Procedures, Materials, and Instrumentation

All procedures and techniques were carried out under an inert atmosphere of nitrogen, either in conjunction with an Mbraun Labmaster 130 glovebox, or using standard Schlenk vacuum-line techniques. All glassware was dried in an oven at 160°C overnight before use. All solvents, including tetrahydrofuran (THF), dimethoxyethane (DME), toluene, and diethylether, were dried over sodium wire with a benzophenone indicator under a nitrogen atmosphere before use. Hexanes was dried in the same manner, although did not include the benzophenone indicator. Deuterated NMR solvents were freeze-pump-thawed three times, and refluxed over sodium before vacuum transfer into a dry bomb for storage under nitrogen. The ligand [$^{t\text{Bu}}$NON]$Li_2$ was prepared by the published literature procedure.[130] All other reagents were obtained by commercial sources, and were employed as is.

NMR spectra were recorded at 294 K, unless otherwise stated, on either a 400 MHz Bruker Avance III spectrometer, a 500 MHz Bruker Avance III spectrometer, or a 600 MHz Bruker Avance II spectrometer with a 5 mm QNP cryoprobe. All $^1$H NMR shifts are reported in ppm relative to the impurity of the internal solvent; specifically, benzene-

$d_6$ at δ = 7.16 and toluene-$d_8$ at δ = 2.08, 6.97, 7.01, and 7.09.[142] Elemental analyses of C, H, and N were performed at Simon Fraser University by Mr. Paul Mulyk, using a Carlo EA 1110 CHN elemental analyzer. Variable temperature magnetic susceptibility measurements over the temperature range of 1.8 – 300 K were collected using solid samples at fields of both 10 000 G and 15 000 G on a Quantum Design (MPMS-XL7) SQuID magnetometer equipped with an Evercool closed-cycle helium compression system. Samples were prepared in low-background polycarbonate gelcaps housed in straws, and the samples were run by Didier Savard and Declan McKearney. The resulting data was corrected for the diamagnetism of the constituent atoms using Pascal's constants.[152] The Evans' method was used to collect room temperature magnetic susceptibilities in solution.[149]

## 2.4.2. Synthesis of Sc[$^{tBu}$NON]Cl•THF (1)

[$^{tBu}$NON]$Li_2$ (0.355 g, 1.23 mmol) dissolved in THF (15 mL), was added dropwise to a solution of $ScCl_3$ (0.186 g, 1.23 mmol) in THF (75 mL), and stirred at room temperature over 72 hours. The solvent was removed under reduced pressure and the product was subsequently filtered through celite in toluene. The solvent was again removed under reduced pressure, revealing a colourless powder of [$^{tBu}$NON]ScCl•THF (0.482 g, 91.8%). Anal. Calcd. for $C_{32}H_{76}N_4Cl_2Sc_2O_4Si_4$: C, 45.00; H, 8.97; N, 6.56. Found: C, 44.97; H, 8.87; N, 6.46. $^1$H NMR (benzene-$d_6$, 500 MHz, 298 K): δ 0.34 (s, 12H, Si(C$H_3$)$_2$), 1.20 (m, 4H, O(CH$_2$C$H_2$)$_2$, THF), 1.46 (s, 18H, (C$H_3$)$_3$C), 3.96 (m, 4H, O(C$H_2$CH$_2$)$_2$, THF). $^{13}$C{$^1$H} NMR (toluene-$d_8$, 125.7 MHz, 298 K): δ 6.56 (Si($C$H$_3$)$_2$), 25.67 (C($C$H$_3$)$_3$), 36.49 (O(CH$_2$$C$H$_2$)$_2$, 52.58 ($C$(CH$_3$)$_3$), THF), 71.97 (O($C$H$_2$CH$_2$)$_2$, THF). X-ray quality crystals were obtained through slow evaporation of a concentrated toluene solution at room temperature.

## 2.4.3. Synthesis of Sc[$^{tBu}$NON]$CH_2SiMe_3$•THF (1a)

$LiCH_2SiMe_3$ (0.105 g, 1.12 mmol) dissolved in toluene (20 mL), was added dropwise to a solution of [$^{tBu}$NON]ScCl•THF in toluene (60 mL), and stirred at room temperature over 72 hours. The solvent was removed *in vacuo*, and the product was filtered through celite in hexanes. The solvent was again removed, resulting in a

colourless powder of [$^{t\text{Bu}}$NON]Sc$CH_2SiMe_3$•THF (0.458 g, 91.5%). Anal. Calcd. for $C_{20}H_{49}N_2O_2ScSi_3$: C, 50.17; H, 10.31; N, 5.85. Found: C, 49.47; H, 10.36; N, 6.02. Some THF lost upon vacuum treatment for elemental analysis. Calculated values for 0.8 THF equivalents per molecule: C, 49.66; H, 10.29; N, 6.03. $^1$H NMR (toluene-$d_8$, 500 MHz, 298 K): δ 0.00 (s, 2H, Sc-C$H_2$-Si$(CH_3)_3$), 0.39 (s, 12H, Si(C$H_3$)$_2$), 0.41 (s, 9H, $ScCH_2$Si(C$H_3$)$_3$), 1.26 (s, 18H, C(C$H_3$)$_3$), 1.31 (m, 4H, O($CH_2$C$H_2$)$_2$, THF), 3.68 (m, 4H, O(C$H_2CH_2$)$_2$, THF). $^{13}$C{$^1$H} NMR (toluene-$d_8$, 150.9 MHz, 298 K): δ 4.45 (Si($CH_3$)$_2$), 6.48 ($CH_2$Si$(CH_3)_3$), 24.97 ($CH_2$Si($CH_3$)$_3$), 36.25 (C($CH_3$)$_3$), 38.17 (O($CH_2CH_2$)$_2$, THF), 52.26 ($C(CH_3)_3$), 70.70 (O($CH_2CH_2$)$_2$, THF). X-ray quality crystals were obtained through slow evaporation of a concentrated hexanes solution at room temperature.

## 2.4.4. Synthesis of Ti[$^{t\text{Bu}}$NON]Cl (2)

[$^{t\text{Bu}}$NON]$Li_2$ (0.100 g, 0.35 mmol) was dissolved in THF (5 mL), and added dropwise to a solution of $TiCl_3$•3THF (0.129 g, 0.35 mmol) in THF (10 mL). The resulting solution was stirred at room temperature over 72 hours. The solvent was then removed under reduced pressure, and the product was filtered through celite in hexanes. Removal of the hexanes yielded a dark green powder (0.105 g, impure). X-ray quality crystals were obtained through slow evaporation of a concentrated hexanes solution at room temperature. Attempts to purify this product from residual ligand in a viable manner have been unsuccessful. Anal. Calcd. for $C_{24}H_{60}N_4Cl_2O_2Si_4Ti_2$: C, 40.27; H, 8.45; N, 7.83. Found: C, 40.30; H, 8.46; N, 7.86. $^1$H NMR (benzene-$d_6$, 500 MHz, 298 K): δ 1.08 (s, 12H, Si(C$H_3$)$_2$), 1.16 (s, 18H, C(C$H_3$)$_3$). $\mu_{eff}$ (293 K, benzene-$d_6$) = 1.0 $\mu_B$. Addition of one equivalent of $LiCH_2SiMe_3$ to a small amount of this crude product followed by recrystallization yielded several crystals of **2a**.

## 2.4.5. Synthesis of V[$^{t\text{Bu}}$NON]Cl (3)

[$^{t\text{Bu}}$NON]$Li_2$ (1.553 g, 5.38 mmol) was dissolved in THF (20 mL), and added dropwise to a solution of $VCl_3$•3THF (2.012 g, 5.38 mmol) in THF (80 mL). The resulting solution was stirred at room temperature over 72 hours. The solvent was then removed under reduced pressure, and the product was filtered through celite in hexanes. Removal of the hexanes yielded a dark blue-green mixture, which was then washed with

cold pentane to obtain the pure blue powder, [$^{t\text{Bu}}$NON]VCl (0.900 g, 46.4%). Anal. Calcd. for $C_{24}H_{60}N_4Cl_2O_2Si_4V_2$: C, 39.93; H, 8.38; N, 7.76. Found: C, 40.08; H, 8.45; N, 7.63. $^1$H NMR (benzene-$d_6$, 500 MHz, 298 K): δ -2.01 (br, 6H, Si(C$H_3$)$_2$), -1.35 (br, 6H, Si(C$H_3$)$_2$), 5.98 (br, 18H, C(C$H_3$)$_3$). $\mu_{eff}$ (293 K, benzene-$d_6$) = 2.2 $\mu_B$. X-ray quality crystals were obtained through slow evaporation of a concentrated hexanes solution at room temperature.

## 2.4.6. Synthesis of {[$^{t\text{Bu}}$NON]VCH$_2$SiMe$_3$}$_2$($\mu$-N$_2$) (3a)

Two equivalents of LiCH$_2$SiMe$_3$ (0.030 g, 0.320 mmol) dissolved in hexanes (5 mL), was added dropwise to a solution of {[$^{t\text{Bu}}$NON]VCl}$_2$ (0.116 g, 0.160 mmol) in hexanes (10 mL). The solution was stirred at room temperature over 48 hours, and the solvent was then removed *in vacuo*. The product was filtered through celite in hexanes. Removal of the hexanes yielded a brown-red powder, {[$^{t\text{Bu}}$NON]VCH$_2$SiMe$_3$}$_2$($\mu$-N$_2$) (0.114 g, 83.4%). Anal. Calcd. for $C_{32}H_{82}N_6O_2Si_6V_2$: C, 45.04; H, 9.68; N, 9.85. Found: C, 45.04; H, 9.64; N, 9.74. $^1$H NMR (benzene-$d_6$, 500 MHz, 298 K): δ 0.30 (s, 6H, Si(C$H_3$)$_2$), 0.41 (s, 9H, VCH$_2$Si(C$H_3$)$_3$), 0.48 (s, 6H, Si(C$H_3$)$_2$), 1.60 (s, 18H, C(C$H_3$)$_3$), 2.02 (s, 2H, VC$H_2$Si(CH$_3$)$_3$). $\mu_{eff}$ (293 K, benzene-$d_6$) = 1.5 $\mu_B$. X-ray quality crystals were obtained through slow evaporation of a concentrated hexanes solution at room temperature.

## 2.4.7. Synthesis of {[$^{t\text{Bu}}$NON]VCH$_2$Ph}$_2$($\mu$-N$_2$) (3b)

Two equivalents of KCH$_2$Ph (0.039 g, 0.295 mmol) dissolved in THF (5 mL), was added dropwise to a solution of {[$^{t\text{Bu}}$NON]VCl}$_2$ (0.107 g, 0.148 mmol) in THF (10 mL). The solution was stirred at room temperature over 24 hours, and the solvent was then removed *in vacuo*. The product was filtered through celite in toluene. Removal of the toluene yielded a brown powder, {[$^{t\text{Bu}}$NON]VCH$_2$Ph}$_2$($\mu$-N$_2$) (0.112 g, 87.8%). Anal. Calcd. for $C_{38}H_{74}N_6O_2Si_4V_2$: C, 52.99; H, 8.66; N, 9.76. Found: C, 52.93; H, 8.73; N, 9.58. $^1$H NMR (toluene-$d_8$, 500 MHz, 298 K): δ 0.12 (s, 6H, Si(C$H_3$)$_2$), 0.24 (s, 6H, Si(C$H_3$)$_2$), 1.58 (s, 18H, C(C$H_3$)$_3$), 3.54, (s, 2H, VC$H_2$Ph), 6.89 (t, 1H, N-Ar-*para*), 7.16 (t, 2H, N-Ar-*meta*), 7.35 (d, 2H, N-Ar-*ortho*). X-ray quality crystals were obtained through slow evaporation of a concentrated hexanes solution at room temperature.

### 2.4.8. General Reduction Reaction by $KC_8$

To a 10 mL solution of [$^{t\text{Bu}}$NON]ScCl•THF (0.047 g, 0.141 mmol) in toluene, one equivalent of $KC_8$ (0.018 g, 0.141 mmol) was added. The reaction was allowed to stir overnight, then was filtered through celite to remove any unreacted $KC_8$. From the filtered solution, the solvent was removed to yield a sightly yellow powder (0.0178 g).

### 2.4.9. General Hydride Addition Reaction by $KEt_3BH$

To a 15 mL solution of {[$^{t\text{Bu}}$NON]$VCH_2SiMe_3$]$_2$($\mu$-$N_2$) (0.050 g, 0.121 mmol) in THF, two equivalents of a 1.0 M solution of $KEt_3BH$ (0.242 mL, 0.242 mmol) was added via syringe. The reaction was stirred overnight, and the solvent was removed under reduced pressure. The solid obtained was filtered through celite in hexanes, and the solvent was removed under reduced pressure. Two products were evident: a dark brown powder and a tan coloured powder, with a total mass of 0.054 g.

### 2.4.10. General Ethylene Polymerisation Reaction

[$^{t\text{Bu}}$NON]$ScCH_2SiMe_3$•THF (0.025 g, 0.053 mmol) and $B(C_6F_5)_3$ (0.027 g, 0.053 mmol) was added to a round bottom flask under inert atmosphere with 5 mL of toluene. The round bottom flask was connected to a Schlenk line, and the flask was freeze-pump-thawed three times to evacuate the headspace. 1 atm of ethylene gas was actively bubbled over the flask's contents for 15 minutes, then the pressure was reduced and bubbled overnight. After the ethylene gas was disconnected, the solvent was removed from the flask, and only powder appeared to remain. In open atmosphere, the contents were filtered with a 10% HCl solution in methanol through a Buchner funnel. There was no isolable precipitate, and therefore no polymer obtained.

### 2.4.11. X-Ray Crystallography

Crystallographic data for all structures are collected in Tables A1, A2, and A3 (Appendix A). Each crystal was coated in paratone oil and mounted onto a MiTeGen Micro Mount and transferred to the cold stream at 150 K on the X-Ray diffractometer. Crystal descriptions are as follows: complex **1** is a colourless block with dimensions

0.119 x 0.283 x 0.343 $mm^3$; complex **1a** is a colourless block with dimensions 0.25 x 0.15 x 0.30 $mm^3$; complex **2** is a green block with dimensions 0.139 x 0.274 x 0.665 $mm^3$; complex **2a** is an orange block with dimensions 0.246 x 0.315 x 0.487 $mm^3$; complex **3** is a red plate with dimensions 0.25 x 0.25 x 0.10 $mm^3$; complex **3a** is a red-brown block with dimensions 0.128 x 0.188 x 0.380 $mm^3$; and complex **3b** is a red-brown block with dimensions 0.114 x 0.214 x 0.226 $mm^3$.

All data was collected on a Bruker SMART instrument equipped with an APEX II CCD area detector fixed at a distance of 5 cm from the crystal, and a Triumph monochromated Mo Kα fine focus sealed tube (λ = 0.71073 nm) operated at 1.5 kW (50 kV, 30 mA) and filtered with a graphite monochromator. The temperature was regulated using an Oxford Cryosystems Cryostream set at 150 K.

All structures were solved using direct methods (SIR 92) and refind by least-squares procedures using CRYSTALS.[196] Hydrogen atoms on carbon atoms were included at geometrically idealised positions (C – H bond distance of 0.95 Å) and were not refined. The isotropic thermal parameters of the hydrogen atoms were fixed at 1.2 times that of the preceding carbon atom. The plots for the crystal structures were generated using ORTEP-3 for windows (v. 1.08)[197] and rendered using POV-Ray (v. 3.6.1).[198] Unless otherwise indicated, thermal ellipsoids are shown at the 30% probability level and hydrogen atoms are omitted for clarity.

Complexes **1**, **1a**, **2a**, **3a**, and **3b** presented no issues, and so all atomic coordinates and anisotropic displacement parameters for all non-hydrogen atoms were refined. Complex **2** was found to contain disordered *t*Bu-N groups as well as the bridging Cl; these groups were treated accordingly, and all other non-hydrogen atomic parameters were refined as normal. Complex **3** was found to have one disordered *t*Bu-N group, which was treated accordingly, and all other non-hydrogen atomic parameters were refined as normal.

# Chapter 3.

# Late Transition Metal Complexes Containing an Electron-Withdrawing Diamido Ligand

## 3.1. Introduction

Iron and cobalt have been studied extensively with the $[^{R}NON]^{2-}$ (R = *t*Bu, $Me_3Ph$, *i*$Pr_2Ph$) ligand systems developed in the Leznoff group. The first to be reported, $\{FeCl[^{tBu}NON]\}_2$, featured the halide-bridged structure that is common from this ligand system and metals of the +3 oxidation state.[130,144] The iron(III) centres exhibited a spin-admixture, a magnetic property that results in mixing of energy levels of the S = 5/2 high spin state and the S = 3/2 state, yielding magnetic moments between these two extremes. When R = 2,4,6-$Me_3Ph$ or 2,6-*i*$Pr_2Ph$, the structure shifts to accommodate the inclusion of an additional LiX (X = Cl, Br) per iron, fitting in the middle of the dimer, which are stabilised via rare Li-π interactions with the aryl rings on the amido groups (Figure 3.1); the bulkiness of these aryl groups force the orientation of the rings in this structure.[130,143] A result of the large separation between the iron(III) centres, the magnetic data for these systems shows each iron as a high spin, $d^5$, temperature independent, and uncoupled metal centre. There also exists the salt-free iron(III) diamido complexes, of the form $\{[^{Me_3Ph}NON]FeX\}_2$ (X = Br, I) (Figure 3.2).[127] In the iodide version each iron centre features a terminal diamido ligand and bridging halides between the iron atoms, as is expected. However, the bromide version shows each halide bridging the metal centres *as do each diamido ligand*. This difference in structure was attributed to the atomic radii difference between the two halides. The cobalt(II) complex with $[^{R}NON]^{2-}$ (R = *t*Bu, $Me_3Ph$) exhibits the standard amido-bridged dimer.[130] Thus far, no cobalt(III) complexes have been developed with this diamido ligand system.

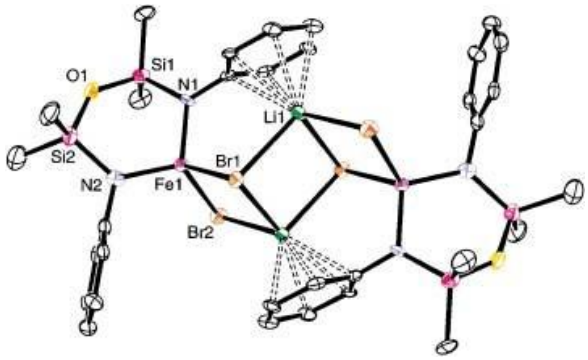


**Figure 3.1. Structure of $\{FeX_2Li[^{R}NON]\}_2$ (when R = 2,4,6-$Me_3Ph$, and X = Br; when R = 2,6-$^{i}Pr_2Ph$, and X = Cl).**
Reproduced from *Chem. Eur. J.*, **2003**, *9*, 4757-4763.

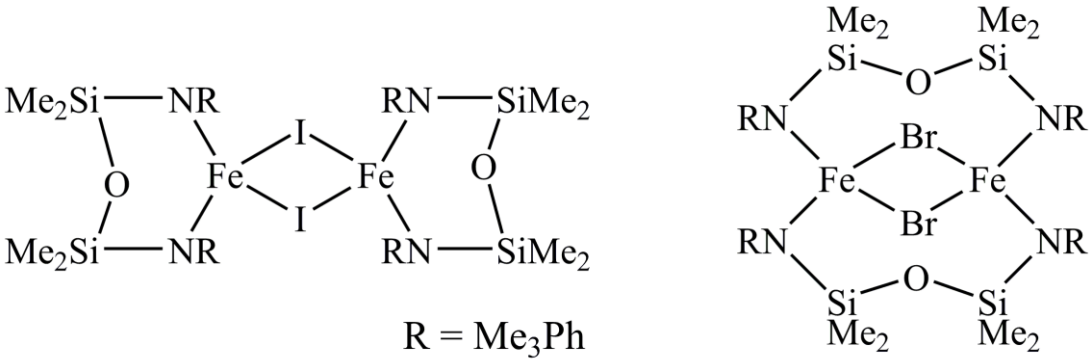


**Figure 3.2. Geometric alterations based upon change in halide present in salt-free $\{[^{Me_3Ph}NON]FeX\}_2$ (X = Br, I) complexes.**

The drawback of the M(II) complexes is that they lack substitutable halide ligands as reactive sites, forming the amido-bridged structures discussed in Chapter 1 (see Figure 1.15). Thus, amido/halide complexes were developed by addition of 2 equivalents of $MX_2$ to one $[^{t\text{Bu}}NON]^{2-}$.[16] Through this route, $\{MX_2[^{t\text{Bu}}NON]\}_n$ (M = Fe, Co; X = Cl, Br; n = 1,2, oligomer) complexes were able to be formed (Figure 3.3). Indeed, attempts to alkylate the cobalt(II) complex resulted in the terminal halides being replaced by $-CH_2SiMe_3$, while the cobalt(II) centres displayed antiferromagnetic coupling. These alkyl-substituted diamido complexes should show interesting organometallic reactivity.

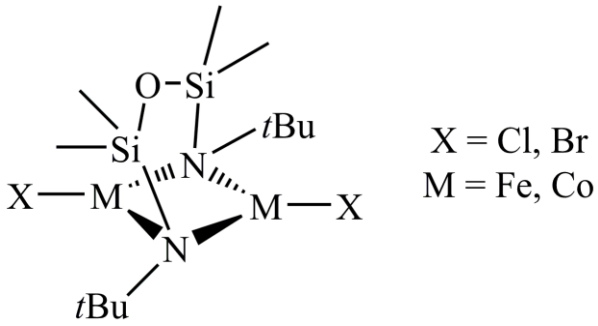


**Figure 3.3. $[^{tBu}NON]M_2X_2$ complex obtained from 2:1 metal:ligand reaction.**

This chapter focuses on using primarily iron(III) and cobalt(II), as well as some work with chromium(II), alongside the more electron-withdrawing ligand, $[^{(CF_3)_2Ph}NON]^{2-}$ ligand. The R-groups typically incorporated into the $[NON]^{2-}$ framework on the amide to date include electron-donating alkyl or aryl groups. In this case, however, the $CF_3$ groups on the phenyl rings draw electron density away from the amide, likely resulting in very different properties compared to its electron-rich counterparts. However, the only previous attempt at forming a complex with this ligand was a reaction with iron(III), which instead formed a reduced iron(II) 1-dimensional chain of $[FeBr_2(THF)_2]_n$.[143] With the limited exploration regarding this ligand, this chapter seeks to form metal complexes utilising this electron-withdrawing diamido ligand with the 1st row transition metals - specifically the late transition metals iron, and cobalt (and some preliminary work with chromium) - and to analyse the structural and reactivity properties in comparison to the related complexes containing the more electron-donating diamido systems.

## 3.2. Results & Discussion

### 3.2.1. Synthesis & characterisation of iron(III) and cobalt(II) coordination complexes

The metal halides $FeCl_3$ and $CoCl_2$ were each added to one equivalent of the dilithiated ligand, in dimethoxyethane (DME). Filtration of the product mixtures in toluene removed the LiCl by-product, revealing the respective products in relatively high yield and purity. X-ray quality crystals were grown via slow evaporation of a concentrated

solution of toluene. Fe[$^{3,5\text{-}(CF_3)_2Ph}$NON]Cl•LiCl•2DME (**4**) was isolated as reddish-brown crystals, while Li{[$^{3,5\text{-}(CF_3)_2Ph}$NON]$_2$Co$_2$Cl}•2DME (**5**) formed as vibrant green crystals.

### *Iron*

The x-ray crystal structure of Fe[$^{3,5\text{-}(CF_3)_2Ph}$NON]Cl•LiCl•2DME (**4**) revealed a monomeric metal centre with one ligand bound in a bidentate fashion (Figure 3.4). Additionally, the iron centre was bound to two chlorides; the more weakly-held chloride maintained close association with the remaining lithium ion, which was supported by two DME molecules. While this complex exists as a mononuclear structure, the more strongly bound chloride is oriented towards the lithium/DME adduct in the adjacent molecule; this ensures that the iron atoms in each molecule are well separated. In summation, the product was found to be a four-coordinate tetrahedral iron(III) "-ate" complex. Use of DME as a solvent commonly creates reaction products which contain solvent-supported salt adducts, due to the solvent's tendency to chelate to lithium ions and preventing the salt from being fully removed upon filtration. Attempts to form a salt-free product by synthesis using THF or diethyl ether solvents were likely successful, as indicated by clean $^1$H NMR spectra, although single-crystals for X-ray crystallographic analysis were not able to be grown from either of these solvents. Thus, the structure of the salt-free complex remains unknown.

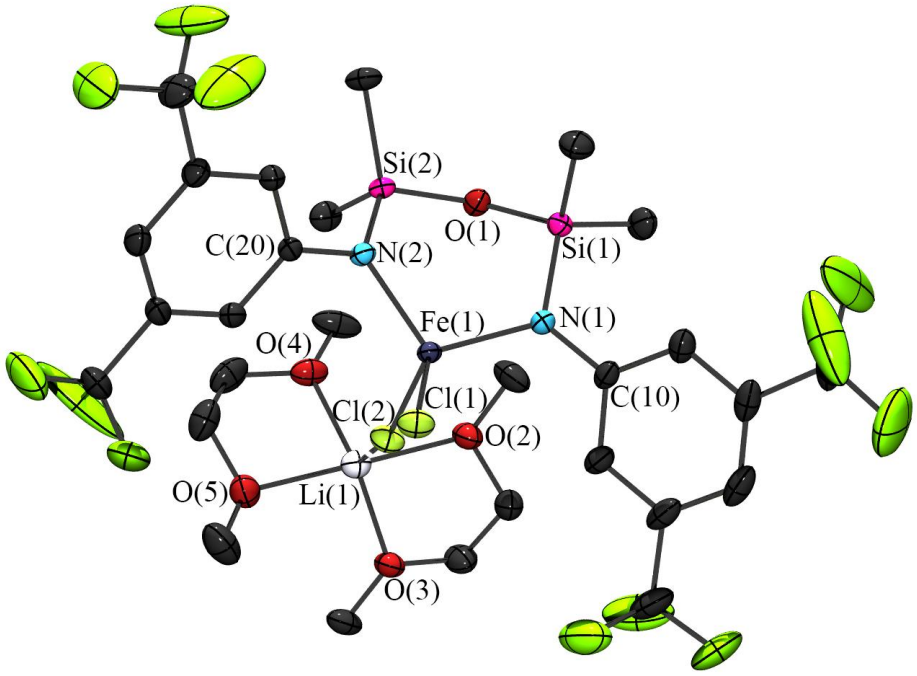


**Figure 3.4. X-ray crystal structure of Fe[$^{3,5\text{-}(CF_3)_2Ph}$NON]Cl•LiCl•2DME (4).**

**Table 3.1. Selected interatomic distances (Å) and angles (°) for Fe[$^{3,5\text{-}(CF_3)_2Ph}$NON]Cl•LiCl•2DME (4).**

| Bond Distances | | | |
|---|---|---|---|
| Fe(1) – Cl(1) | 2.2131(6) | Si(2) – N(2) | 1.743(2) |
| Fe(1) – Cl(2) | 2.2704(7) | N(1) – C(10) | 1.406(3) |
| Fe(1) – O(1) | 3.109(2) | N(2) – C(20) | 1.394(2) |
| Fe(1) – N(1) | 1.928(2) | Cl(2) – Li(1) | 2.650(6) |
| Fe(1) – N(2) | 1.925(1) | Li(1) – O(2) | 1.952(5) |
| O(1) – Si(1) | 1.640(1) | Li(1) – O(3) | 2.049(5) |
| O(1) – Si(2) | 1.641(1) | Li(1) – O(4) | 2.071(5) |
| Si(1) – N(1) | 1.740(2) | Li(1) – O(5) | 1.987(6) |
| **Bond Angles** | | | |
| Cl(1) – Fe(1) – Cl(2) | 104.58(2) | Cl(2) – Fe(1) – N(1) | 110.98(5) |
| N(1) – Fe(1) – N(2) | 109.01(7) | Cl(2) – Fe(1) – N(2) | 111.72(5) |
| Cl(1) – Fe(1) – N(1) | 111.24(5) | Fe(1) – N(1) – C(10) | 119.6(1) |
| Cl(1) – Fe(1) – N(2) | 109.26(5) | Fe(1) – N(2) – C(20) | 120.8(1) |
| Fe(1) – Cl(2) – Li(1) | 149.7(1) | Si(1) – O(1) – Si(2) | 135.6(1) |

The iron centre of complex **4** is slightly distorted from a pure tetrahedral geometry; while the Cl(1) – Fe(1) – Cl(2) angle is exactly 104.58(2)°, the N(1) – Fe(1) – N(2) angle is larger, at 109.01(7)° (Table 3.1). This distortion is likely caused by the chelating nature of the ligand; steric strain would dictate the angle at which the amides bind to the iron centre. The iron-amide bonds (1.928(2)/1.925(1) Å) are slightly longer than those exhibited in related complexes; $\{FeBr_2Li[^{Me_3Ph}NON]\}_2$ has Fe – N distances of 1.877(5) Å and 1.905(4) Å,[143] while $\{FeCl[^{tBu}NON]\}_2$ possesses Fe – N distances of 1.887(5)/1.894(4) Å.[144] The salt-free analogue containing the mesityl groups on the ligand, $\{FeBr[^{Me_3Ph}NON]\}_2$, exhibits slightly shorter Fe – N bond lengths, at 1.864(8) Å and 1.880(7) Å.[127] These are still within a comparably similar range to that of complex **4**. This slight lengthening exhibited by complex **4** may be a result of the electron-withdrawing nature of the $CF_3$ groups, drawing some of the electron density away from the amides, thereby weakening its bonding ability to the iron centre. However, this can be considered a small effect. The Fe(1) – O(1) distance of 3.109(2) Å precludes any bond formed between them, as $\{FeCl[^{tBu}NON]\}_2$ exhibits a Fe – O bond at a distance of 2.597(4) Å. The Fe(1) – Cl(1) (terminal) distance of 2.2131(6) Å is quite short in comparison to the bridging chlorides of $\{FeCl[^{tBu}NON]\}_2$ (2.3181(19) Å and 2.4652(17) Å). This is likely because the chloride is terminal, and its electrons are not being shared by multiple metals. In contrast to this, the Fe(1) – Cl(2) (bridging) is longer, at 2.2704(7) Å. While still not as long as in $\{FeCl[^{tBu}NON]\}_2$, this is indicative of a stronger bond with the iron centre than with the lithium, to which the chloride also maintains an interaction, particularly since the Cl(2) – Li(1) bond is considerably longer at 2.650(6) Å. Complex **4** is structurally different from the previous iterations of iron(III) $[^{R}NON]^{2-}$ complexes. Since the steric constraints of the $[^{(CF_3)_2Ph}NON]^{2-}$ ligand are relatively similar to those of $[^{Me_3Ph}NON]^{2-}$, it must be supposed that the altered structure is most probably a result of the substantial electron-withdrawing effect of the ligand. No Li-π interactions appear to have developed based on the orientation of the aryl rings in relation to the lithium ion; this is likely a result of the aryl rings supporting less electron density as it is pulled towards the $-CF_3$ groups.

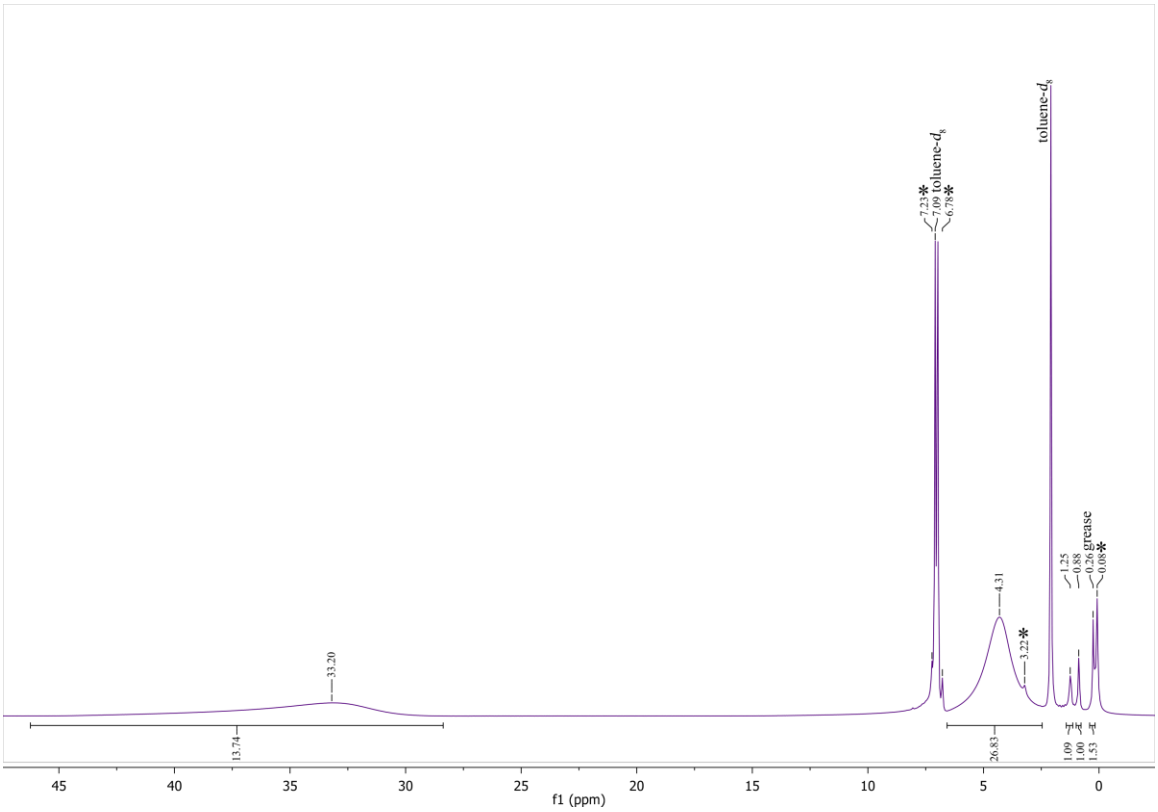


**Figure 3.5. $^{1}$H NMR spectrum of Fe[$^{3,5\text{-}(CF_3)_2Ph}$NON]Cl•LiCl•2DME (4) in $d_8$-toluene.**
* = signals which correspond to protonated ligand

The $^{1}$H NMR spectrum obtained for complex **4** (Figure 3.5) is consistent with an iron(III) paramagnetic complex spectrum. Including the DME adducts, and working from the solid state structure, there would be five predicted signals, in a 12:12:8:4:2 ratio. The two broadened signals at 4.31 and 33.20 ppm integrate in a 2:1 ratio, respectively. Due to this unexpected ratio, and the lack of additional broadened signals, this spectrum cannot be assigned with any confidence. There is, however, a small quantity of residual protonated ligand is detected, corresponding with peaks at 0.08 ($SiMe_2$), 3.22 (RNH), 6.78 (*ortho*-H) and 7.23 (*para*-H) ppm (shown by * in Figure 3.5).

While $^{19}$F NMR spectra were collected for all products utilising the [$^{3,5\text{-}(CF_3)_2Ph}$NON]$^{2-}$ ligand, only two representative spectra are illustrated in Appendix A, for complex **4** (Figure A6) and complex **5** (see below, Figure A7). This ligand was difficult to purify, and this is evident in the $^{19}$F NMR spectra. Where only a single signal should be predicted for many of these complexes, multiple are found. In addition, adding this ligand

to paramagnetic metal centres produces an uncertainty in what is displayed in the $^{19}F$ NMR spectra. It is possible that peaks attributable to the compound are not observed, and only diamagnetic impurities are found in the spectra. Therefore, while $^{19}F$ NMR is typically very helpful in the characterisation of fluorine-containing compounds, it has been found to be of limited use in this thesis.

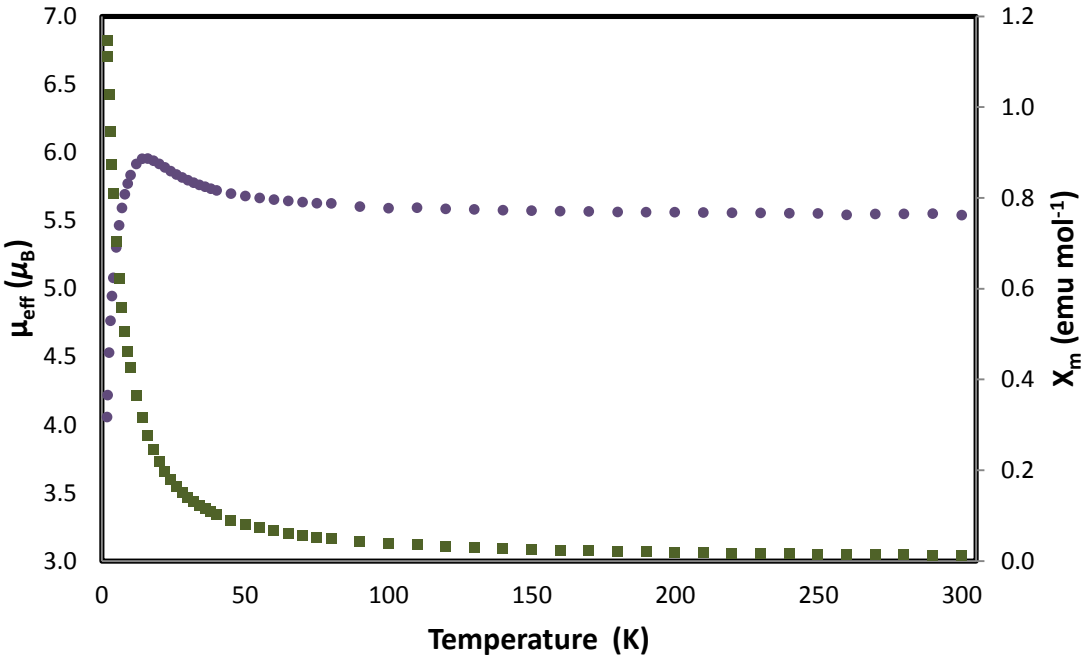


**Figure 3.6. Plot of effective magnetic moment data from 1.8 - 300 K for Fe[$^{3,5-(CF_3)_2Ph}$NON]Cl•LiCl•2DME (4).**

The spin-only magnetic moment for a high-spin tetrahedral iron(III) complex (S = 5/2) is 5.92 $\mu_B$. A solution magnetic moment of 5.5 $\mu_B$ was calculated at room temperature for complex **4**. While this value is slightly lower than that of the spin-only value, this could be explained by a small diamagnetic impurity in the sample, such as any free ligand present. Since we predict iron(III) to have 5 unpaired electrons in a high-spin tetrahedral configuration, and there are 5 *d*-orbitals, it is expected that there is no orbital angular momentum contribution present, and therefore there should not be any spin-orbit coupling; thus a value close to the spin-only moment is observed. In solid state, the data for complex **4** primarily echoes the solution magnetic data (Figure 3.6). With a temperature independent (Curie law) moment from room temperature until approximately 50 K, the magnetic moment is stable at about 5.6 $\mu_B$. While this is a

marginally lower value than the expected spin-only value for an S = 5/2 system, it is still within reasonable bounds, and the lowered value can again likely be attributed to any small diamagnetic impurity that may be present, such as remaining ligand. The source of the increase at ~20 K is unknown, and would normally be associated with coupling between metal centres; however, as complex **4** is a monomer in the solid state, this rationale is unlikely. It may be possible that at very low temperatures the complex undergoes a structural change, the most likely of which would be to become 5-coordinate through the initiation of a Fe – O bond from the ligand. Low-temperature increases in the magnetic moment such as this have been attributed to structural phase transitions in other transition metal amido complexes in the literature.[199] The drop-off below 20 K to 4.06 $\mu_B$ is likely due to zero-field splitting, which has been noted in previous iron(III) magnetic data of related diamido complexes.[143,144,171]

The previously reported iron diamido complexes have displayed interesting properties. The spin admixture exhibited by the iron(III) dimer when R = *t*Bu is a rare magnetic effect induced by the presence of a five-coordinate centre, and is not observed in the related R = $Me_3Ph$, *i*$Pr_2Ph$ congeners which have four-coordinate, tetrahedral centres as in complex **4**. A structural shift towards accommodating the inclusion of an additional lithium halide salt per iron is found for R = $Me_3Ph$, *i*$Pr_2Ph$-based iron systems; the salt forms a bridge that connects the two halves of the dimer, and is stabilised via rare Li-π interactions with the aryl rings on either diamido ligand (Figure 3.1), and the metal centres are then found to be magnetically uncoupled due to the large separation between them.[130,143] Complex **4** does not exhibit any of this odd structural or magnetic behaviour, and as a mononuclear structure, the magnetic properties behave as a temperature-independent iron(III) system down to approximately 20 K.

### *Cobalt*

The X-ray crystal structure for Li{[$^{3,5\text{-}(CF_3)_2Ph}$NON]$_2$$Co_2Cl$}•2DME (**5**) revealed a structure very different from those previously discussed. A result of the +2 oxidation state of the metal, this complex exists as a dimer featuring amido-bridged cobalt centres, reminiscent of the amido-bridged dimers that were found for [$^R$NON]$^{2-}$ complexes with iron, chromium, and cobalt previously (Figure 1.15 - from Chapter 1).[16,126,128] Therefore, there are a total of two cobalt atoms, and two diamido ligands (Figure 3.7), although they

are arranged in a highly asymmetric manner. Each ligand interacts with the metal centres in a unique bonding motif; in the first diamido ligand, each amide bonds to both cobalt atoms, while in the second diamido ligand, each amide only bonds to one metal centre. Thus, each cobalt atom features three total bonds to amides. Each cobalt centre here appears unique, as one gains its fourth coordination point via the siloxyether ligand backbone, while the second instead retains a chloride ligand. Inclusion of a potential metal-metal bond between the cobalt atoms would bring the geometry surrounding each metal centre to five-coordinate capped tetrahedral, although it is unclear if such a Co – Co bond actually exists in this complex (see below). Both cobalt atoms remain in the +2 oxidation state, and the whole complex is charge balanced by a $Li^+$ counterion, which forms an interaction with the chloride ligand. In addition to this, there are two DME molecules present in the unit cell, clustering around the lithium ion (simplified to show only the DME oxygen atoms in the figure below).

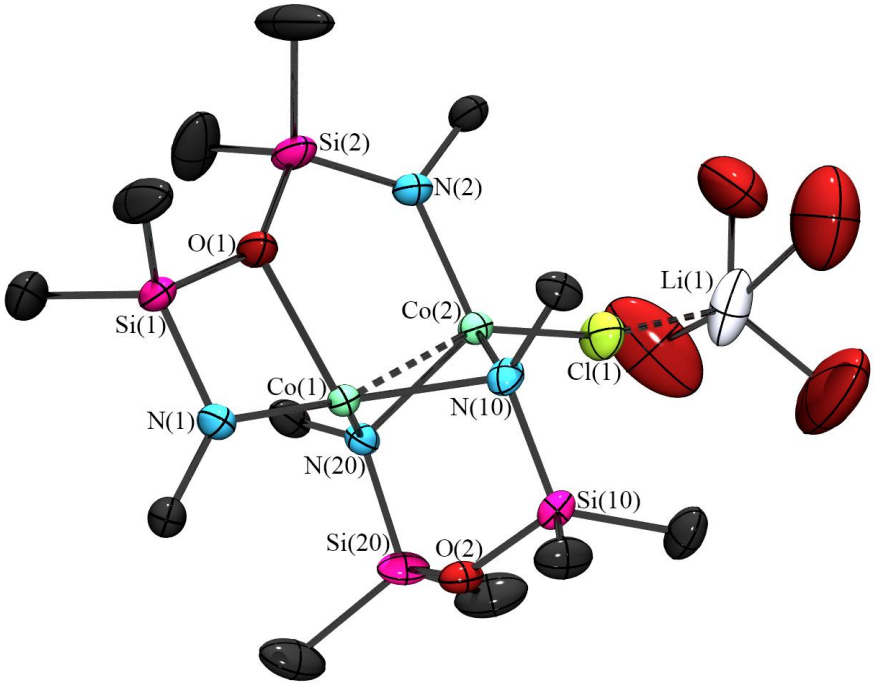


**Figure 3.7. X-ray crystal structure of Li{[$^{3,5\text{-}(CF_3)_2Ph}$NON]$_2$Co$_2$Cl}•2DME (5).**
The $(CF_3)_2$Ph groups have been simplified to Me for clarity, and the DME molecules have been simplified to show the position of the oxygen atoms only.

**Table 3.2. Selected interatomic distances (Å) and angles (°) for Li{[$^{3,5-(CF_3)_2Ph}$NON]$_2$Co$_2$Cl}•2DME (5).**

| | | | |
|---|---|---|---|
| **Bond Distances** | | | |
| Co(1) – Co(2) | 2.590(2) | O(1) – Si(1) | 1.670(5) |
| Co(1) – O(1) | 2.164(5) | O(1) – Si(2) | 1.676(5) |
| Co(2) – O(2) | 3.433(5) | N(10) – Si(10) | 1.758(5) |
| Co(2) – Cl(1) | 2.258(2) | N(20) – Si(20) | 1.760(5) |
| Co(1) – N(1) | 1.932(5) | O(2) – Si(10) | 1.643(4) |
| Co(1) – N(10) | 2.034(5) | O(2) – Si(20) | 1.643(5) |
| Co(1) – N(20) | 2.021(5) | Cl(1) – Li(1) | 2.55(2) |
| Co(2) – N(2) | 1.971(6) | Li(1) – O(5) | 1.95(2) |
| Co(2) – N(10) | 2.089(5) | Li(1) – O(6) | 1.92(2) |
| Co(2) – N(20) | 2.067(5) | Li(1) – O(7) | 2.17(2) |
| N(1) – Si(1) | 1.715(6) | Li(1) – O(8) | 1.84(2) |
| N(2) – Si(2) | 1.693(5) | | |
| **Bond Angles** | | | |
| Co(2) – Co(1) – O(1) | 89.6(1) | Co(1) – Co(2) – Cl(1) | 156.28(8) |
| Co(2) – Co(1) – N(1) | 164.3(2) | Co(1) – Co(2) – N(2) | 92.5(2) |
| N(1) – Co(1) – O(1) | 75.0(2) | Co(1) – Co(2) – N(10) | 50.1(1) |
| N(10) – Co(1) – N(20) | 92.3(2) | Co(1) – Co(2) – N(20) | 49.9(1) |
| N(1) – Co(1) – N(10) | 136.3(2) | N(10) – Co(2) – N(20) | 89.5(2) |
| N(1) – Co(1) – N(20) | 129.2(2) | N(2) – Co(2) – N(10) | 108.7(2) |
| O(1) – Co(1) – N(10) | 111.6(2) | N(2) – Co(2) – N(20) | 109.9(2) |
| O(1) – Co(1) – N(20) | 104.0(2) | N(2) – Co(2) – Cl(1) | 111.2(2) |
| Co(2) – Co(1) – N(10) | 52.0(1) | Cl(1) – Co(2) – N(10) | 118.5(1) |
| Co(2) – Co(1) – N(20) | 51.5(1) | Cl(1) – Co(2) – N(20) | 117.1(1) |
| Si(1) – O(1) – Si(2) | 145.0(3) | Co(2) – Cl(1) – Li(1) | 168.3(4) |
| Co(1) – O(1) – Si(1) | 91.4(2) | Cl(1) – Li(1) – O(5) | 119.4(9) |
| Co(1) – O(1) – Si(2) | 123.2(3) | Cl(1) – Li(1) – O(6) | 97.1(8) |
| Si(10) – O(2) – Si(20) | 136.4(3) | Cl(1) – Li(1) – O(7) | 92.8(7) |
| | | Cl(1) – Li(1) – O(8) | 116.4(9) |

The Co(1) – Co(2) distance of 2.590(2) Å in complex **5** (Table 3.2) is similar to the Co – Co bond in the related {[$^{t\text{Bu}}$NON]Co}$_2$ complex, which has a distance of 2.5682(13) Å.[130] However, this should be considered much too long to be a real Co-Co bond.[167] Presuming this, the geometry about the cobalt(II) centres would instead be that

of a distorted tetrahedron. The two diamido ligands are relatively planar and are roughly oriented perpendicular to each other, and each contributes an amide that bridges the cobalt centres. In the first ligand, N(1) is singly bound to Co(1) (1.932(5) Å), and N(2) is singly bound to Co(2) (1.971(6) Å); the diamido-silylether ligand frame is overall planar. These bond lengths are typical of Co – N bonds, as compared with $\{[^{tBu}NON]Co\}_2$, which possesses 1.906(3) Å (terminal) and 2.029(3)/2.051(4) Å (bridging) metal-amide bond lengths.[130] For the second ligand, both N(10) and N(20) bind to both Co(1) and Co(2), bridging between them. The bonds between Co(1) and N(10) and N(20) are typical of Co – N bridging bond lengths, at 2.021(5)/2.034(5) Å; however, the Co(2) bonds to N(10) and N(20) are a bit longer at 2.067(5)/2.089(5) Å. This is indicative of a weaker overall bond to Co(2), likely a result of steric strain from the bulky R-groups on the amido ligands. Additionally, Co(1) also forms a bond with the neutral backbone donor (2.164(5) Å), while Co(2) instead retains a chloride (2.258(2) Å). As $\{[^{tBu}NON]Co\}_2$ features a weak Co-O interaction at 2.448(4) Å, this 2.164(5) Å bond length signifies a much stronger interaction.[130] The halide-containing version of $\{[^{tBu}NON]Co\}_2$, $\{Co_2Cl_2[^{tBu}NON]\text{-}(LiCl)\bullet 2THF\}_2$, synthesised by using 2 equivalents of metal to 1 ligand, confirms that the Co-Cl bond length in complex **5** (2.258(2) Å) is within normal bounds.[16] There is likely not a true bond between the $Cl^-$ and $Li^+$ ions, as the 2.55 Å distance is longer than the combined ionic radii of 2.40 Å, as described by Shannon.[167] While complex **5** is highly asymmetric about the metal centres, each cobalt atom maintains four definite bonds, and the geometry about the metal centres appears quite close to a tetrahedron.

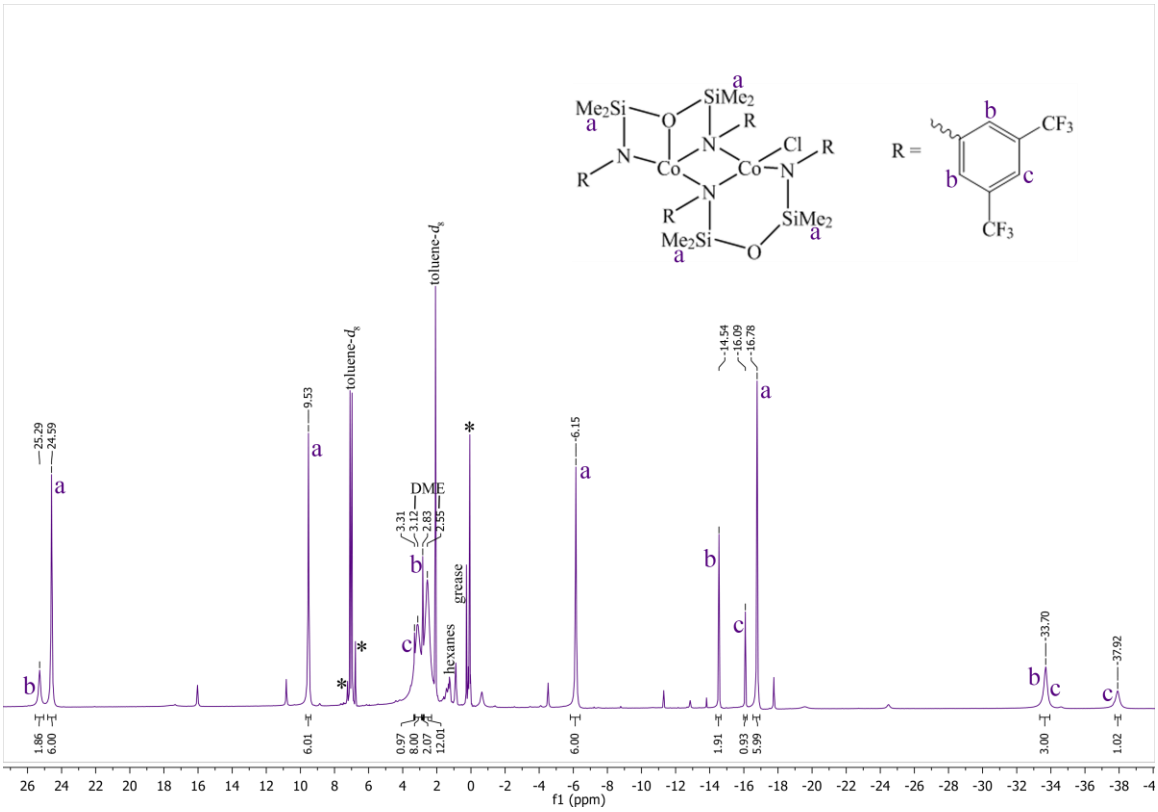


**Figure 3.8. $^{1}$H NMR spectrum of Li{[$^{3,5\text{-}(CF_3)_2Ph}$NON]$_2$Co$_2$Cl}•2DME (5) in $d_8$-toluene.**
General peak assignments for $^{1}$H environments; * = remaining free ligand.

The $^{1}$H NMR spectrum of complex **5** was collected from crystalline sample. The asymmetric nature of the structure, however, yields many visible peaks in the $^{1}$H NMR spectrum. In Figure 3.8, the peak-picked signals were those determined to belong to the major product in the sample, although the presence of multiple smaller signals is indicative of at least one minor product as well. This minor product may simply be a different solvent adduct, or a salt-free form of the complex which was determined via x-ray crystallography in the solid state. The high-spin cobalt(II) centres, in their roughly tetrahedral environments, introduce 3 unpaired electrons each, which affects the shifting of the peaks quite dramatically, resulting in a spectrum containing signals from -38 ppm to 26 ppm. However, cobalt(II) typically produces spectra which are highly shifted, but also remain quite sharp.[16] Thus, the integrations are still quite useful in the assignment of this spectrum.

Due to the large quantity of signals, it is likely that the asymmetric solid state structure is at least somewhat maintained in solution; the major product has certainly not shifted to form the more symmetric amido-bridged structure, or many fewer signals would be observed. In order to clarify the peak assignments this complex was also synthesised in THF and diethyl ether. The appropriate $^{1}$H NMR spectra for the reactions in THF (Figure A8) and diethyl ether (Figure A9) can be found in Appendix A. As both DME and THF are known to form adducts to metal complexes, and ether typically does not, it was reasoned that comparison between the $^{1}$H NMR spectra of each of the three product analogues would help to identify the common peaks between them, and any differences would either be a result of solvent adducts, or perhaps a minor related product. Indeed, this method worked well, although only the representative DME adduct $^{1}$H NMR spectrum is shown in Figure 3.8. Crystals could not be obtained of the complexes from these other solvents, although the similarities in the $^{1}$H NMR spectra suggest that the complex is in fact produced in the alternate solvents.

A result of the asymmetry of the structure, it was expected that each ligand group would be inequivalent. This means that in the solid state, it was expected that there should be a total of 14 observable proton environment signals, including those of the DME adducts. In this spectrum (Figure 3.8), there was determined to be 13 relevant signals. The “relevant” signals were determined through comparative analysis between the three different $^{1}$H NMR spectra. The remaining unassigned signals can be attributed to solvents or a minor product that exists across all three versions of this complex. Since it was expected that each silylmethyl group would be inequivalent, there were four peaks integrating to 6 H’s; these appear at 24.6, 9.5, -6.2, and -16.8 ppm. All other protons in the complex are part of the phenyl groups; these are the *ortho*- and *para*- protons. It was expected that each phenyl group would also be inequivalent to all others, and so we would predict there to be four signals integrating to 2 H’s (the *ortho*-protons), and four integrating to 1 H (the *para*-protons) each. This was, for the most part, found to be accurate. Three *ortho*-H peaks were found at 25.3, 2.8, and -14.5 ppm, and three *para*-H peaks were found at 3.3, -16.1, and -37.9 ppm. However, in each of the three spectra compared, there consistently appeared a slightly broadened peak at about -33.7 that integrated to 3 H’s. The persistence of this signal in each spectrum suggested that it is relevant to the complex, and so it is proposed that this peak at -33.7 ppm represents a

coincidental overlap of peaks for both the *ortho*-H's and the *para*-H - and explains the reason for observing one less signal than what was predicted. Finally, the two broad peaks appearing at 2.5 and 3.1 ppm integrate to 12H and 8H respectively, which corresponds to two environmentally-equivalent DME adducts, and these signals only appear in the NMR spectrum corresponding to the reaction in DME solvent.

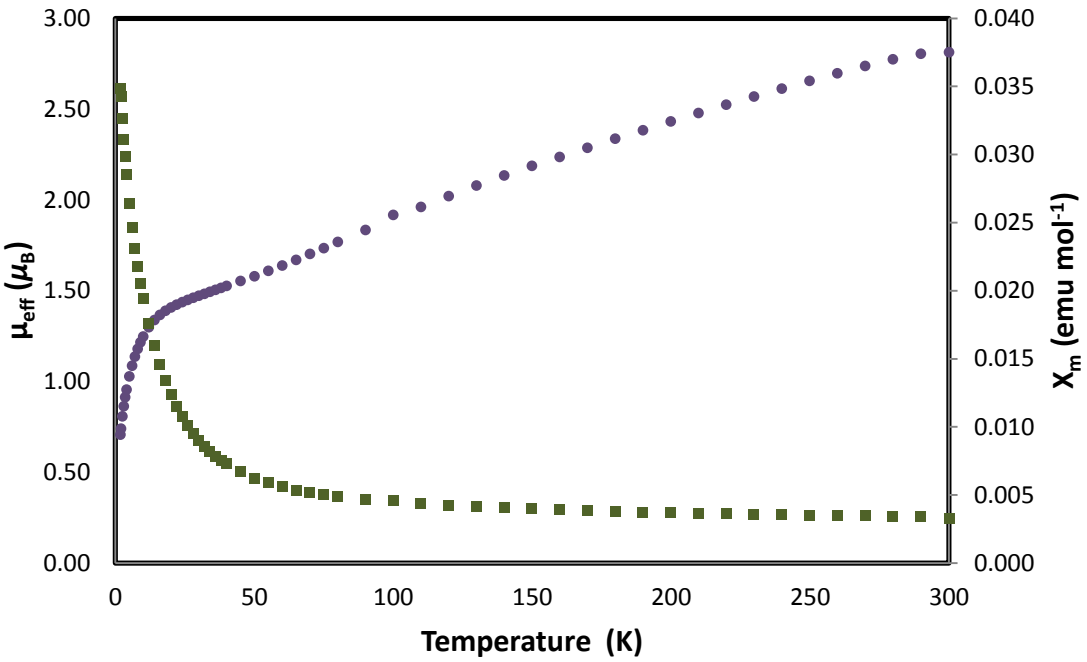


**Figure 3.9. Plot of effective magnetic moment data per metal centre from 1.8 - 300 K for Li{[$^{3,5\text{-}(CF_3)_2Ph}$NON]$_2$Co$_2$Cl}•2DME (5).**

In a tetrahedral geometry, it would be expected that each cobalt(II), $d^7$, centre would exhibit 3 unpaired electrons (S = 3/2, $\mu_{eff}$ = 3.87 $\mu_B$ for a spin-only system), with only one option for the electrons to fill the *d*-orbitals. In solution, however, the room temperature magnetic moment of complex **5** was calculated to be 2.7 $\mu_B$ per metal centre, which roughly corresponds to two unpaired electrons for each cobalt atom. Additionally, the room temperature magnetic moment in the solid state was 2.81 $\mu_B$ per metal centre (Figure 3.9), although the plot appears to still have an increasing magnetic moment as it approaches 300 K, which suggests that the magnetic moment would continue to approach the spin-only value if the temperature was increased further. The reduction from the ideal spin-only value is likely a result of orbital overlap between the metal centres or antiferromagnetic coupling, diminishing the observed effective magnetic

moment. Given the long Co – Co bond distance in the crystal structure, it is more likely that antiferromagnetic coupling through the bridging amido ligands is partly responsible for the drop in magnetic moment with decreasing temperature; however, no observed maximum in the X vs. T data indicates that any coupling present is relatively weak. No modelling was explored since this highly temperature dependent data includes both antiferromagnetic interactions (J) and significant orbital contributions (lambda), along with zero-field splitting (D) below 20 K, a well-documented phenomenon in Co(II) complexes.[200] Since all three of these phenomena likely have similar energies (given the absence of a maximum in X vs. T), modelling of three parameters (J, lambda and D) would yield highly correlated results of little interpretive value.

Previously published structures of cobalt(II) diamido dimers have been reported by the Leznoff group.[130] Taking the form $\{[^{R}NON]Co\}_2$ (R = *t*Bu, 2,4,6-$Me_3Ph$), these complexes are amido-bridged dimers, however, they contain no pendant halides, and both cobalt centres feature a weak bond to the ether backbone.[130] In all, these cobalt complexes are considerably more symmetric than complex **5**, and this is likely attributable to the altered electronics of the ligand. When R = *t*Bu, there is strong antiferromagnetic coupling between the cobalt(II) centres, and a room temperature magnetic moment of 1.84 $\mu_B$ per cobalt(II) centre. The coupling is weaker when R = $Me_3Ph$, which manifests as an effective magnetic moment closer to that of the spin-only value (3.1 $\mu_B$ at 300 K). Complex **5** (2.81 $\mu_B$) exhibits significantly weaker coupling than the R = *t*Bu moiety, although it is still considerably stronger than in the R = $Me_3Ph$ congener. This cannot be explained by the Co – Co bond distances, as **5** exhibits the longest bond length of the three (2.590(2) Å); while it is similar to the R = *t*Bu complex (2.5682(13) Å), it is significantly longer than the R = $Me_3Ph$ complex (2.468(3) Å), and so this seems to suggest that amide-mediated antiferromagnetic coupling is the primary mechanism for the reduction in magnetic moment.[126]

A couple of related cobalt tetramers have also been previously synthesised and may offer further insight into the magnetic trends of complex **5**. $\{Co_2Br_2[^{tBu}NON]\}_2$ was made from two equivalents of $CoBr_2$ to one equivalent of ligand, and the corresponding reaction with $CoCl_2$ produced the "-ate" complex $\{Co_2Cl_2[^{tBu}NON](LiCl)\bullet 2THF\}_2$.[16,201] The room temperature effective magnetic moments of these two complexes (1.84 $\mu_B$ and

2.23 $\mu_B$ respectively) provide further insight into related cobalt complexes and their magnetic properties and together suggest that complex **5** experiences considerably less orbital overlap and/or coupling behaviour between metal centres than its various related congeners, as the room temperature magnetc moment in the solid state is the least reduced from the spin-only value for each metal centre. However, the significant reduction in effective magnetic moment at room temperature from the spin-only value of 3.87 $\mu_B$ still indicates a substantial effect.

### 3.2.2. Attempts toward the synthesis of iron(II) and chromium(II) diamido coordination complexes

Complexes of iron(II) and chromium(II) with the electron-rich $[^{R}NON]^{2-}$ ligands have been previously synthesised in the Leznoff group, forming dimers that feature terminal and bridging amido groups (Figure 3.10).[127] The iron(II) complex made from $FeCl_2$ with the $[^{t\text{Bu}}NON]^{2-}$ ligand exhibits bonding of the neutral donor backbone, while the $[^{Me_3Ph}NON]^{2-}$ does not. In the $[^{Me_3Ph}NON]^{2-}$-containing complex, the iron centres are in a distorted trigonal geometry, bonding only the terminal and bridging amido ligands.

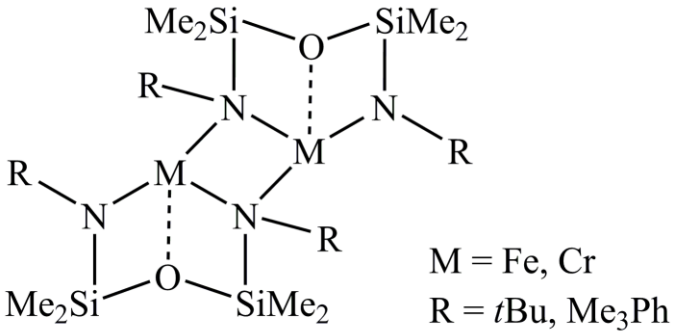


**Figure 3.10. Amido-bridged $M^{2+}$ complex bonding motif.**

A chromium(II) complex was formed from $CrCl_2$ and $[^{Me_3Ph}NON]^{2-}$, and possesses the expected amido-bridged dimer motif, as well as bonding of the neutral donor.[128] Additionally, a short Cr – Cr bond distance (2.384(2) Å) suggests that there is a metal-metal bond present in the complex as well. The chromium(III) $[^{t\text{Bu}}NON]^{2-}$ complex has also been synthesised, but an yttrium complex was required to successfully transfer the ligand to the $CrCl_3$ starting material.[43]

As previously discussed, the $[^{Me_3Ph}NON]^{2-}$ ligand offers a good comparison to the $[^{(CF_3)_2Ph}NON]^{2-}$ ligand, as the steric constraints will be similar, although the aryl R-group is less electron-withdrawing than the bis-$CF_3$-containing version. The best comparison ligand would incorporate the 3,5-$Me_2$Ph R-group, although no diamido complexes using this ligand have been previously prepared in the Leznoff group. The formation of the iron(II) and chromium(II) complexes with the $[^{(CF_3)_2Ph}NON]^{2-}$ ligand was sought in this research, for comparison with the reported $[^{Me_3Ph}NON]^{2-}$-containing complexes.

To one equivalent of $MCl_2$ (M = Fe, Cr) in THF, $Li_2[^{(CF_3)_2Ph}NON]$ was added dropwise, and the resulting solution was allowed to stir overnight. Filtration in toluene to remove the byproduct LiCl, isolated the product. In each case, a gummy brown solid was formed. Unfortunately, in the course of these reactions, crystals were not able to be grown. Thus, identification of the products is based solely on $^1$H NMR interpretation and elemental analysis.

In the case of the iron(II) reaction product, the CHN elemental analysis matched the expected values relatively closely, provided an additional THF molecule is added to the molecular formula for the %CHN calculation. However, the $^1$H NMR spectrum featured several broadened and shifted peaks, resulting in an unassignable spectrum (Figure A10). Attempts to wash the product to obtain a powder continued to yield a product that was no more solid than before. It was determined that the product could not easily be identified, as CHN analysis is of limited use with no other useful data to corroborate. Mossbauer techniques may have been useful in determining the oxidation state of the iron metal, as would ESR spectroscopy. Similarly, the chromium(II) reaction initially appeared to be promising, as the CHN elemental analysis was nearly consistent with a formulation of $[^{(CF_3)_2Ph}NON]Cr(LiCl)\bullet 2THF$. However, the $^1$H NMR did not show any identifiable signals (Figure A11), perhaps due to extreme paramagnetic broadening, and further attempts to isolate a purified product proved unsuccessful. Future attempts towards the formation of these desired products may utilise alternate solvents, particularly with DME as complexes **4** and **5** both crystallised well from this solvent. X-ray quality crystals are desirable for these products as they will give a better picture of bonding and potential reactivity available.

### 3.2.3. Attempts toward the formation of iron(III) and cobalt(II) alkyl complexes

Amido cobalt(II) alkyl complexes have been generated previously in the Leznoff group, while iron(III) alkyls have remained thus far elusive. $LiCH_2SiMe_3$ was used in a metathesis reaction to replace the chlorides on $Co_2Cl_2[^{tBu}NON]$, forming the dialkyl $Co_2(CH_2SiMe_3)_2[^{tBu}NON]$ with high-spin, S = 3/2 metal centres.[16] The related iron(II) amido/alkyl complexes have also been synthesised.[201] In contrast, attempts to alkylate iron(III) amido complexes resulted in reduction to the dimeric iron(II) complex which has no metathesisable halides in its amido-bridged structure.[143] Although not desirable, this reduction may also be a potential pathway in other related iron(III) diamido systems.

To prepare for the possibility that addition of an alkylating agent may cause the iron(III) to be reduced, two equivalents of $LiCH_2SiMe_3$ were added to a toluene solution of complex **4**, one for each halide bound to the iron centre. It was supposed that should only one halide be replaced by the alkyl group, the unreacted equivalent of $LiCH_2SiMe_3$ could be easily removed from the product. Crystals of the resulting brown solid were not able to be produced. Addition of one equivalent of alkylating agent was not attempted, although it may prove an interesting proof of concept in future work. The $^1$H NMR spectrum (Figure A12), however, is completely changed from the starting material, although it remains uninterpretable. There are several sharp peaks from solvent impurities. In addition, there are several broadened signals between 15 and 40 ppm. It is encouraging to note that these signals are most likely indicative of persistent iron(III), since iron(II) usually produces relatively sharp signals in $^1$H NMR spectra.[146] In addition, an elemental analysis was not able to be obtained, as the product was too oily to prepare the sample; this would suggest the presence of impurities as pure metal complexes are typically solid. Without a crystal structure, this product could not be characterised. However, because the spectrum is very different from the starting material, it is indicative that a reaction occurred.

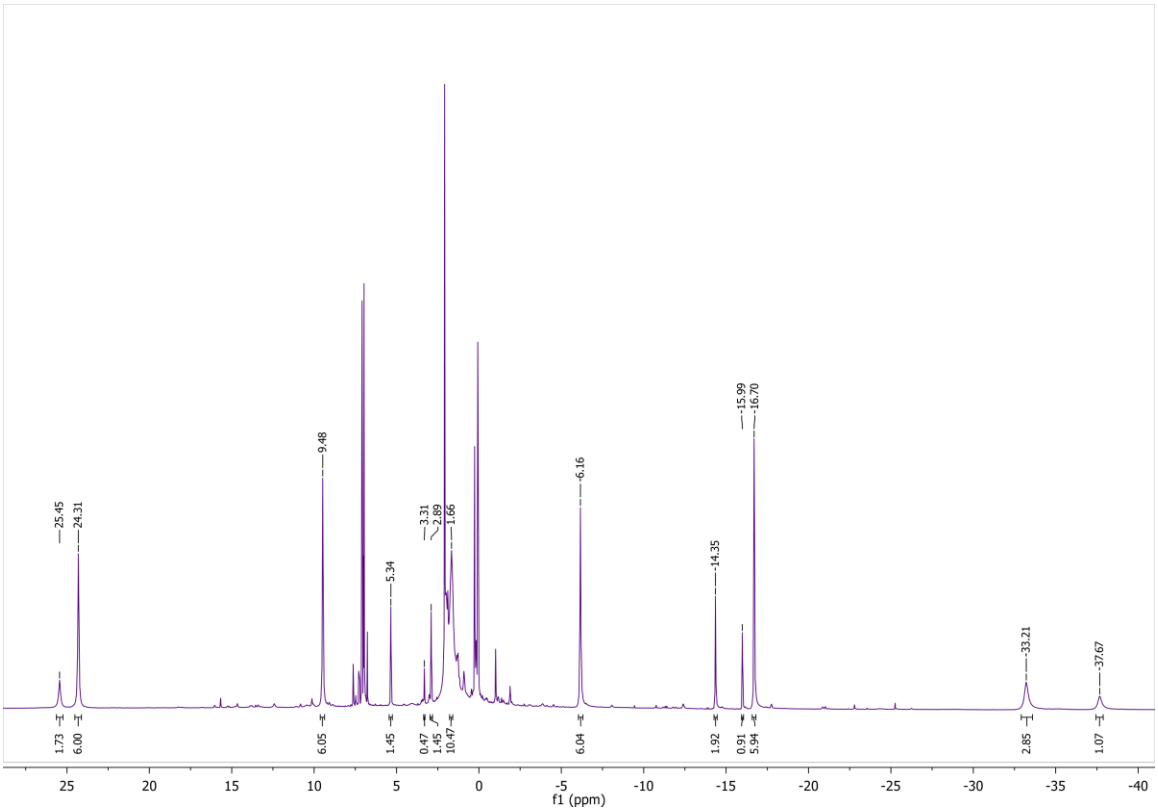


**Figure 3.11. $^{1}$H NMR spectrum of the alkylation product of Li{[$^{3,5-(CF_3)_2Ph}$NON]$_2$Co$_2$Cl}•2DME (5) in *d*$^8$-toluene.**

The cobalt(II) complex **5** also features a potential reactive halide that may be replaced by an alkyl. To a DME solution of complex **5**, one equivalent of $LiCH_2SiMe_3$ was added. Crystals of the green complex were unable to be grown, although the product exhibited greater solubility in toluene than its precursor. The $^{1}$H NMR spectrum (Figure 3.12) was very similar to complex **5**, although all the signals are shifted very slightly from the starting material. For a product that has only added the alkyl, and has otherwise remained unchanged, it would be expected that there should be 14 signals, disregarding the presence of DME adducts; therefore, 12 signals for the original complex, plus 2 for the added alkyl. A total of 13 signals were found, with the same overlap by integration of one of the signals that was found in complex **5**. In addition to the expected signals, two peaks appearing at 5.34 ppm and 1.66 ppm roughly conform to the requisite integrations of the alkyl, 2H and 9H respectively. They are also slightly broadened, which is suggestive of close proximity to a paramagnetic cobalt centre. Lastly, the peaks that were attributed to the DME adducts have disappeared. The

elemental analysis most closely matched the proposed product with remaining two DME adducts, indicating that there are remaining impurities. However, without a crystal structure, the definitive confirmation of the synthesis of a cobalt(II) alkyl product remains elusive. It is possible that an alternative alkylating agent, such as $KCH_2Ph$ or MeLi, would produce a more easily isolable alkyl product.

## 3.3. Conclusion

In this chapter, iron and cobalt chemistry was explored with the electron-withdrawing diamido ligand $[^{3,5\text{-}(CF_3)_2Ph}NON]^{2-}$, producing the complexes $Fe[^{3,5\text{-}(CF_3)_2Ph}NON]Cl{\bullet}LiCl{\bullet}2DME$ (**4**) and $Li\{[^{3,5\text{-}(CF_3)_2Ph}NON]_2Co_2Cl\}{\bullet}2DME$ (**5**), which are different from other diamido complexes previously obtained in the Leznoff group.[43,127,130,143] Attempts to add the $[^{3,5\text{-}(CF_3)_2Ph}NON]^{2-}$ ligand to the early transition metal halides of $Sc^{3+}$, $Ti^{3+}$, $V^{3+}$, and $Cr^{2+}$ failed, and may be indicative of a change in the electronics of the ligand resulting in altered binding affinities. Some of these reactions failed, while others resulted in multiple products that could not be characterised. Since the early transition metals are electron-poor, they would ideally bond with an electron-rich, donating ligand. Typically amido ligands are the ideal candidates for this. However, the 3,5-$(CF_3)_2Ph$ groups in this diamido ligand are more electron-withdrawing than the other aryl R-groups used previously, and these R-groups would predictably pull electron density away from the amide, resulting in a much more weakly donating diamido ligand that may not provide sufficient electronic stability for early transition metals. However, given the right combination of conditions (starting reagents, solvents, temperature, etc.), these complexes may still be able to form.

On the other hand, the more electron-rich iron(III) and cobalt(II) centres are a good match for the more electron-poor amides. While the iron(III) complex (**4**) was a mononuclear –"ate" complex, the cobalt(II) complex (**5**) exhibited an asymmetric amido-bridged structure. Neither of these complexes conform to the standard structure exhibited by the same diamido complexes featuring the more standard R-groups on the amides (i.e., R = *t*Bu, $Me_3Ph$, $iPr_2Ph$). Therefore, some simple reactions were also examined in an effort to probe the similarities between complexes **4** and **5** and their

more standard counterparts. These reactivity studies were generally inconclusive, although some evidence indicated potentially favourable reactions. Specifically, the $^{1}$H NMR spectra for the alkylation product of complex **5** indicated that the reaction was successful. However, purification attempts were unsuccessful, and thus further attempts to form a cobalt alkyl complex may focus on an alternative alkylating agent or a different solvent. It would also be interesting to show that addition of one equivalent of alkylating agent to the iron(III) complex **4** reduces it to the iron(II) complex, which is also desired as it has thus far failed to be synthesised. Further attempts to make the iron(II) complex may also be attempted in the traditional manner, perhaps by using an alternative solvent, as DME so far appears to produce more positive results with this ligand system than THF.

Previous work has shown that the structures of the diamido metal complexes are directly affected by the metal's oxidation state. Metals of the +2 oxidation state form amido-bridged dimers, whereas in the +3 oxidation state they instead form halide-bridged dimers. In the case of iron, addition of $I_2$ to $\{Fe[^{Me_3Ph}NON]\}_2$ resulted in the formation of the oxidised $\{FeI[^{Me_3Ph}NON]\}_2$, the related halide-bridged structure.[127] However, the oxidation of cobalt(II) to cobalt(III) complexes has been unsuccessful with this ligand system. Preliminary results of the addition of $I_2$ to complex **5** did not produce concrete evidence towards the formation of a halide-bridged structure. A change in colour, and a $^{1}$H NMR spectrum with considerably more symmetry indicates a positive reaction, although the nature of the product is unclear (Figure A13). Further work into this and related oxidation reactions may provide very interesting results.

The similarity of **4** to Kozak's iron(III) amine-bis(phenolate) complexes suggests that **4** may also be a candidate as a catalyst in Grignard C-C cross-coupling reactions that could be pursued in future. A comparison can be drawn between **4**'s ability to catalyse the coupling of *o*-tolylmagnesium bromide with bromocyclohexane and Kozak's 97% yield using his (amine)bis(phenolato)iron(acac) complex with these reactants.[202]

While the chemistry involving the 1$^{st}$ row transition metals and the $[^{3,5\text{-}(CF_3)_2Ph}NON]^{2-}$ ligand still has substantial scope for exploration, the synthesis and preliminary reactivity studies of the iron(III) (**4**) and cobalt(II) (**5**) complexes have been

an intriguing glimpse into the coming chemistry of this unique diamido ligand. As the steric effects of these diamido ligands have been more fully explored, it will be interesting to examine how the more electron-poor amide affects the reactions in which it undergoes with various metal halides, the resulting structures of the metal complexes and their subsequent reactivity. Already a preference for later transition metals has emerged, and unique complex structures also complement the altered electronics.

## 3.4. Experimental

### 3.4.1. General Procedures, Materials, and Instrumentation

All procedures and techniques were carried out as reported in Section 2.4.1. The ligand [$^{(CF_3)_2Ph}$NON]$Li_2$ was prepared by the published literature procedure.[130]

### 3.4.2. Synthesis of Fe[$^{(CF_3)_2Ph}$NON]Cl•LiCl•2DME (4)

[$^{(CF_3)_2Ph}$NON]$Li_2$ (0.100 g, 0.166 mmol) was dissolved in DME (5 mL), and added dropwise to a solution of $FeCl_3$ (0.027 g, 0.166 mmol) in DME (10 mL). The resulting solution was stirred at room temperature over 48 hours. The solvent was removed *in vacuo*, and then filtered through celite in toluene. Removal of toluene under reduced pressure yielded a purple-red powder of [$^{(CF_3)_2Ph}$NON]FeCl•LiCl•2DME (**4**) (0.123 g, 82.3%). X-ray quality crystals were obtained through slow evaporation of a concentrated toluene solution at room temperature. Anal. Calcd. for $C_{28}H_{38}N_2Cl_2F_{12}FeLiO_5Si_2$: C, 37.35; H, 4.25; N, 3.11. Found: C, 37.44; H, 4.27; N, 3.50. $^1$H NMR (toluene-$d_8$, 500 MHz, 298 K): δ 0.08 (s, Si(C$H_3$)$_2$), 0.26 (s, Si(C$H_3$)$_2$), 0.88 (s, (C$H_3$-O-CH$_2$)$_2$), DME), 1.25 (s, (CH$_3$-O-C$H_2$)$_2$), DME), 4.27 (s, (CF$_3$)$_2$Ph-*para*), 32.88 (s, (CF$_3$)$_2$Ph-*ortho*) ppm. $\mu_{eff}$ (293 K, toluene-$d_8$) = 5.45 $\mu_B$.

### 3.4.3. Synthesis of Li{$Co_2$[$^{(CF_3)_2Ph}$NON]$_2$Cl}•2DME (5)

[$^{(CF_3)_2Ph}$NON]$Li_2$ (0.100 g, 0.166 mmol) was dissolved in DME (5 mL), and added dropwise to a solution of $CoCl_2$ (0.022 g, 0.166 mmol) in DME (10 mL). The resulting

solution was stirred at room temperature over 48 hours. The solvent was removed under reduced pressure, and then filtered through celite in toluene. Removal of the toluene yielded a dark green powder of Li{$Co_2Cl[^{(CF_3)_2Ph}NON]_2$}•2DME (**5**) (0.079 g, 62.8%). X-ray quality crystals obtained through slow evaporation of a concentrated toluene solution at room temperature. Anal. Calcd. for $C_{48}H_{56}N_4ClCo_2F_{24}LiO_6Si_4$: C, 38.09; H, 3.73; N, 3.70. Found: C, 38.20; H, 3.77; N, 4.20. $^1$H NMR (toluene-$d_8$, 500 MHz, 298 K): δ -37.92 (s, 1H, $(CF_3)_2$Ph-*para*), -33.70 (s, 3H, $(CF_3)_2$Ph-*para*, $(CF_3)_2$Ph-*ortho*), -16.78 (s, 6H, Si($CH_3$)$_2$), -16.09 (s, 1H, $(CF_3)_2$Ph-*para*), -14.54 (s, 2H, $(CF_3)_2$Ph-*ortho*), -6.15 (s, 6H, Si($CH_3$)$_2$), 2.55 (s, 12H, ($CH_3$-O-$CH_2$)$_2$), DME), 2.83 (s, 2H, $(CF_3)_2$Ph-*ortho*), 3.12 (s, 8H, ($CH_3$-O-$CH_2$)$_2$), DME), 3.31 (s, 1H, $(CF_3)_2$Ph-*para*), 9.53 (s, 6H, Si($CH_3$)$_2$), 24.59 (s, 6H, Si($CH_3$)$_2$), 25.29 (s, 2H, $(CF_3)_2$Ph-*ortho*) ppm. $\mu_{eff}$ (293 K, toluene-$d_8$) = 2.69 $\mu_B$.

### 3.4.4. Attempted Alkylation of Fe[$^{(CF_3)_2Ph}$NON]Cl•LiCl•2DME

To a 15 mL solution of Fe[$^{(CF_3)_2Ph}$NON]Cl•LiCl•2DME (0.155 g, 0.172 mmol) was added a 5 mL solution of two molar equivalents of $LiCH_2SiMe_3$ (0.032 g, 0.344 mmol), dropwise while stirring. The reaction was left to stir over 36 hours, after which the solvent was removed under reduced pressure. The product was filtered through celite in toluene to remove any by-products, and after removal of the filtration solvent, a brown viscous oil was obtained (0.039 g). No X-ray quality crystals were able to be grown, and the product was unidentifiable via $^1$H NMR and $^{19}$F NMR analysis. Elemental analysis was not obtained due to preparation difficulties as a result of the oily state of the sample.

### 3.4.5. Attempted Alkylation of Li{$Co_2[^{(CF_3)_2Ph}NON]_2Cl$}•2DME

Li{$Co_2[^{(CF_3)_2Ph}NON]_2Cl$}•2DME (0.082 g, 0.054 mmol) was dissolved in a mixture of toluene and DME (15 mL total), as it was not entirely soluble in toluene. To this solution, one equivalent of $LiCH_2SiMe_3$ (0.005 g, 0.054 mmol) in 5 mL of DME was added, dropwise while stirring. The reaction was stirred overnight, whereupon the solvent was removed under reduced pressure. The now more-soluble product was dissolved in toluene and filtered through celite. Removal of the solvent yielded a green powder (0.050 g). No X-ray quality crystals were successfully grown, and the CHN

elemental analysis was not a match for the alkylation product. Anal. Calcd. for $C_{44}H_{47}N_4Co_2F_{24}O_2Si_5$: C, 38.35; H, 3.44; N, 4.07. Found: C, 42.16; H, 4.01; N, 4.00. $^1$H NMR (toluene-$d_8$, 500 MHz, 298 K): δ -37.67 (s, 1H, $(CF_3)_2$Ph-*para*), -33.21 (s, 3H, $(CF_3)_2$Ph-*para*, $(CF_3)_2$Ph-*ortho*), -16.70 (s, 6H, Si(C$H_3$)$_2$), -15.99 (s, 1H, $(CF_3)_2$Ph-*para*), -14.35 (s, 2H, $(CF_3)_2$Ph-*ortho*), -6.16 (s, 6H, Si(C$H_3$)$_2$), 1.66 (s, 9H, $CH_2$Si(C$H_3$)$_3$), 2.89 (s, 2H, $(CF_3)_2$Ph-*ortho*), 3.31 (s, 1H, $(CF_3)_2$Ph-*para*), 5.34 (s, 2H, C$H_2$Si$(CH_3)_3$), 9.48 (s, 6H, Si(C$H_3$)$_2$), 24.31 (s, 6H, Si(C$H_3$)$_2$), 25.45 (s, 2H, $(CF_3)_2$Ph-*ortho*) ppm.

### 3.4.6. Attempted Synthesis of Fe(II)-[$^{(CF_3)_2Ph}$NON]

[$^{(CF_3)_2Ph}$NON]$Li_2$ (0.474 g, 0.789 mmol) was dissolved in THF (10 mL), and added dropwise to a solution of $FeCl_2$ (0.100 g, 0.789 mmol) in THF (10 mL). The resulting solution was stirred at room temperature over 24 hours. The solvent was removed under reduced pressure, and then filtered through celite in toluene. Removal of the toluene yielded a dark brown solid of unknown yield. X-ray quality crystals were not able to be obtained through the slow evaporation method. $^1$H NMR (toluene-$d_8$, 500 MHz, 298 K): δ 0.06 (s, br), 1.06 (s, br), 3.31 (s), 6.77 (s), 7.24 (s), 10.29 (s, br). Anal. Calcd. for $C_{24}H_{26}N_2FeF_{12}O_2Si_2$ (equivalent to Fe[$^{(CF_3)_2Ph}$NON]•THF): C, 40.35; H, 3.67; N, 3.92. Found: C, 39.90; H, 3.63; N, 4.00.

### 3.4.7. Attempted Synthesis of Cr(II)-[$^{(CF_3)_2Ph}$NON]

[$^{(CF_3)_2Ph}$NON]$Li_2$ (0.100 g, 0.167 mmol) was dissolved in THF (10 mL), and added dropwise to a solution of $CrCl_2$ (0.021 g, 0.167 mmol) in THF (10 mL). The resulting solution was stirred at room temperature over 48 hours. The solvent was removed under reduced pressure, and then filtered through celite in toluene. Removal of the toluene yielded a dark solid of unknown yield. X-ray quality crystals were not able to be obtained through the slow evaporation method. $^1$H NMR (toluene-$d_8$, 500 MHz, 298 K): δ 0.08 (s, 4H), 0.43 (s, 1H), 3.05 (s, 7H), 3.20 (s, 5H) ppm. Anal. Calcd. for $C_{24}H_{26}N_2ClCrF_{12}LiO_2Si_2$ (equivalent to Cr[$^{(CF_3)_2Ph}$NON](LiCl)•2THF): C, 38.28; H, 3.48; N, 3.72. Found: C, 37.49; H, 3.92; N, 3.63.

### 3.4.8. X-Ray Crystallography

Parameters for collection of single crystal x-ray data as reported in Section 2.4.11. Both complexes **4** and **5** were found to have rotationally disordered $CF_3$ groups, and so were treated accordingly. In complex **4**, all other non-hydrogen atoms' coordinates and anisotropic displacement parameters were refined. In complex **5**, the two DME molecules were required to be rotationally and vibrationally restrained to allow the structure solution to be fully optimised and refined.

# Chapter 4.

# Conclusions

## 4.1. Research Summary

This research was divided into two major categories of study. In the first, the already well-examined [$^{t\text{Bu}}$NON]$^{2-}$ ligand was utilised in conjunction with the early 1$^{st}$ row transition metals with the goal of developing a structural and reactive trend along the 1$^{st}$ row, examining how the changing number of *d*-electrons on the metal affects the resulting complexes. The second category focused on altered electronics of the diamido ligand, as opposed to the more easily studied steric changes, in an examination of how a more electron-poor diamido ligand might affect the resulting coordination chemistry to 1$^{st}$ row transition metals, and their corresponding reactivity. Each of these categories yielded some amount of success, although as many questions were raised during the course of this research as were answered.

With regards to the utilisation of the [$^{t\text{Bu}}$NON]$^{2-}$ diamido ligand, the goal of developing the early 1$^{st}$ row transition metal complexes has been achieved. Coordination complexes of scandium ($d^0$), titanium ($d^1$), and vanadium ($d^2$), all in the +3 oxidation state, have successfully been synthesised and characterised with the [$^{t\text{Bu}}$NON]$^{2-}$ ligand. Each of these complexes forms a chloride-bridged dimer, {[$^{t\text{Bu}}$NON]MCl}$_2$, although the scandium centres are sufficiently electron-poor that they each retain a THF donor ligand. This correlates with the known yttrium complex, which behaves in the same manner.[43]

Reactivity of these complexes was a combination of successes and failures. Alkylation of each behaved differently. {[$^{t\text{Bu}}$NON]ScCl•THF}$_2$ (**1**) formed the monomeric complex, [$^{t\text{Bu}}$NON]ScCH$_2$SiMe$_3$•THF (**1a**), which still required the THF donor for electronic stability. {[$^{t\text{Bu}}$NON]TiCl}$_2$ (**2**) proved difficult to purify, and attempts to do so

through the alkylation reaction resulted in, at least partially, forming the hydroxide-bridged dimer, {[$^{t\text{Bu}}$NON]Ti(OH)}$_2$ (**2a**). These difficulties may be attributed to an impure commercial bottle of $TiCl_3$•3THF. Attempts to alkylate {[$^{t\text{Bu}}$NON]VCl}$_2$ (**3**) with $LiCH_2SiMe_3$ resulted in immediate activation of dinitrogen present in the atmosphere, and incorporation into the alkylated product, maintaining a dinuclear structure: {[$^{t\text{Bu}}$NON]V$CH_2SiMe_3$}$_2$($\mu$-$N_2$) (**3a**). To confirm that this was a repeatable reaction, the procedure was repeated with a different alkylating agent, $KCH_2Ph$, and again produced the related dinitrogen structure, {[$^{t\text{Bu}}$NON]V$CH_2Ph$}$_2$($\mu$-$N_2$) (**3b**). In each case, the dinitrogen species were found to be di-reduced, thereby requiring that each vanadium was oxidised to vanadium(IV). Preliminary attempts to further reduce these vanadium dinitrogen species were not met with success. Additionally, attempts to form the vanadium dinitrogen species without alkylation, *via* addition of the reducing agent $KC_8$, were also unsuccessful. Desiring to form hydrido complexes of the scandium and vanadium species, both alkylated and not, $KEt_3BH$ was the reagent of choice, and did not yield positive results. Attempts to polymerise ethylene with complex **1a** were largely inconclusive and require further attention. These preliminary reactivity studies may not have been fully successful, but the formation of interesting alkylated species is certainly encouraging, and fosters the desire to probe these complexes for further reactivity experiments.

The second half of this research focused on the [$^{(CF_3)_2Ph}$NON]$^{2-}$ ligand, and how the altered electronics around the amido groups affects the resulting bonding and structural properties of the metal complexes. Initial attempts to produce the early transition metal complexes to mirror those in the first section were unsuccessful, which by itself is a comment on how the amido groups are affected. However, formation of the iron(III) complex, [$^{(CF_3)_2Ph}$NON]FeCl•LiCl•2DME (**4**), and the cobalt(II) complex, Li{$Co_2Cl$[$^{(CF_3)_2Ph}$NON]$_2$}•2DME (**5**), show that this is a viable ligand for coordination, and produces intriguing structural motifs. Preliminary work to produce the alkylated complexes has suggested that it is possible, although concrete characterisation evidence was unable to be obtained. Additionally, initial attempts to oxidise complex **5** indicated a positive reaction, although concrete evidence was elusive. Therefore, this research has indicated that there is a substantial quantity of interesting chemistry waiting to be discovered, although it may be difficult to access.

## 4.2. Global Conclusions

An overall trend has certainly been discussed throughout this thesis as common structural motifs which best accomodate the charge of the diamido $[^{R}NON]^{2-}$ ligand and the postively charged metal. Halide-bridged dimers are typically observed for complexes where the metal exists in the +3 oxidation state, whereas amido-bridged dimers are formed when the metal is present in the +2 oxidation state. This motif remained largely true for the complexes developed within this research.

The target idea for developing the remaining $[^{t\text{Bu}}NON]^{2-}$ complexes pertained to the discovery of how the changing number of *d*-electrons affected the structure and reactivity of the resulting metal complexes. While some conclusions may be made, there are still many unknowns to be explored. The only other known M(III) $[^{t\text{Bu}}NON]$ complexes are of yttrium, chromium, and iron; the rest of the 1$^{st}$ row transition metal complexes are all in the M(II) state. Of the halide-bridged, M(III) complexes, two conclusions may be drawn with reasonable certainty. One: the exceptionally electron-poor metals, scandium and yttrium ($d^0$), require additional electron density than what the diamido ligands are able to offer, and so retain a THF donor ligand. Two: the silylether neutral donor displays a hemilabile nature, which only donates electron density to the electron-poor metals, and the resulting bond length appears to correlate with the ionic radii of the metal, which is a direct reflection of the number of *d*-electrons present. The bonding trend of the silylether backbone is somewhat extended into the M(II) complexes as well, as the silylether bond to the metal elongates as the number of *d*-electrons increases across the transition metals, with the exception of the manganese(II) congener, which contains the longest M-O interaction.

While the alkylation reactions were largely successful for these complexes, and even demonstrated vanadium's propensity towards dinitrogen activation directly, the various other small molecule activation reactions tested were unsuccessful on these preliminary trials. Further experimentation must seek to develop the proper conditions in which to perform these hydrido, reduction, and polymerisation reactions so that a positive result may be achieved.

Typical alterations of ligand structure involve changing sterics such that a desired result may be achieved in the final complex. In the Leznoff group, the alternative ligand $[^{(CF_3)_2Ph}NON]^{2-}$ was developed to illustrate how pulling electron density away from the coordinating amido groups affects the resultant structure of the metal complexes. Indeed, the non-standard structures achieved with both $[^{(CF_3)_2Ph}NON]FeCl•LiCl•2DME$ (**4**) and $Li\{Co_2Cl[^{(CF_3)_2Ph}NON]_2\}•2DME$ (**5**) are a testament to the fact that the changed electronics of the ligand results in a change in coordination. While the monomeric, bis(chloride)-containing iron(III) structure may be due to the interfering presence of two DME adducts forming an –"ate" complex, the cobalt(II) congener is not impeded by this. Although complex **5** is an amido-bridged dimer, as it was expected to be, its asymmetric nature is highly unusual and can only be attributed to the altered electronics of the ligand, as there don't appear to be any other altered variables. From these complexes, it is clear that a more electron-poor amido group does indeed change how the ligand coordinates to a metal. In particular, it is clear that specific conditions are required for the ligand to be able to bond to the metal to begin with; i.e., the metal must be appropriately electron-rich to coordinate under ambient (dry) conditions. As no further reactivity experiments can be confirmed at this time, despite some indication that the reactions were successful, further conclusions cannot be drawn from these two intriguing complexes.

## 4.3. Future Directions

Within this thesis, the questions asked were only partially answered. As is typical of scientific research, answers only tend to raise more questions with which to develop the field of study. Regarding the $[^{t\text{Bu}}NON]^{2-}$ complexes, although the target of synthesising the scandium, titanium, and vanadium complexes and probing their reactivity was completed, there is always more that could be done. For example, is the scandium complex (**1**) able to display the same ligand transfer ability that its yttrium counterpart exhibits, particularly since they are so similar in structure?[43] Is it possible to use this diamido scandium complex to follow the synthetic steps laid out by Evans' to target a dinitrogen scandium complex?[86] Under what catalytic conditions will complex **1** polymerise ethylene efficiently, if at all? Will it exhibit more success with alternate

catalytic monomers? Which hydrido transfer reagents will produce a scandium hydride complex? With the titanium diamido complex (**2**), were the purification problems directly related to the purity of the starting materials, or are these difficulties just inherent of this complex? If they can be resolved, how does the reactivity of this complex (alkylation, reduction, hydride addition, etc.) compare to both the scandium and the vanadium analogues? Which does it resemble more closely? The vanadium complexes **3**, **3a**, and **3b** clearly already exhibit intriguing behaviour, although the clear direction with these complexes is to completely reduce the dinitrogen species, until the bond is broken. While preliminary attempts were unsuccessful, a change in tactics may produce more positive results.

While progress has certainly been made regarding the electron-poor diamido ligand $[^{(CF_3)_2Ph}NON]^{2-}$, only the tip of the iceberg has been examined at this point. With the synthesis of the iron(III) and cobalt(II) complexes **4** and **5**, there is a clear way forward from here. Successful synthesis, isolation, and characterisation of the alkylated products represent the most direct step. From there, there are several questions to be answered which would provide further evidence as to how this electron-withdrawing ligand affects the overall complexes. First, is it still possible to oxidise the cobalt(II) centres in **5** to cobalt(III) with $I_2$, and in so doing transform the structure to that of the halide-bridged coordination usually encountered? Additionally, based on the failed reactions using this ligand, it seems that DME is the most successful solvent to use – but does that mean that it is the *only* solvent which will produce a successful reaction? And if so, is this the missing condition for the production of early transition metal complexes with this ligand? Next is the question of application. Due to complex **4**'s similarity to Kozak's iron(III) amine-bis(phenolate) complexes,[202] which are able to perform Grignard C-C cross coupling reactions, there may be a viable application for this electron-poor diamido iron(III) complex, even in other bond-activation type reactions.

This research has essentially focused on two sides of the same coin: in the first, we sought to determine how the changing metal affected the resulting coordination and reactivity of the overall complex; the second examined how an altered ligand affected the coordination and reactivity of the complex. These two aspects of diamido coordination chemistry are inherently related, and should be considered together when

designing a complex to fulfill a particular function. Diamido complexes typically follow a predictable coordination scheme, although this research has shown that a change in the electronics surrounding the binding of the ligand to the metal can have a strong impact on the resulting structure. This conclusion easily prompts additional investigation into what exactly these diamido coordination complexes are capable of.

# References


(1) Crabtree, R. H. *The Organometallic Chemistry of the Transition Metals*, 6th Ed.; John Wiley & Sons, Inc.: Hoboken, New Jersey, **2014**.

(2) Schrock, R. R.; Parshall, G. W. *Chem. Rev.* **1976**, *76*, 243–268.

(3) Davidson, P. J.; Lappert, M. F.; Pearce, R. *Acc. Chem. Res.* **1970**, *7*, 209–217.

(4) Wilkinson, G. *Science.* **1974**, *185*, 109–112.

(5) Bradley, D. C.; Chisholm, M. H. *Acc. Chem. Res.* **1976**, *9*, 273–280.

(6) Lappert, M. F.; Protchenko, A.; Power, P.; Seeber, A. In *Metal Amide Chemistry*; Wiley: U.K., **2009**; 149–204.

(7) Male, N. A. H.; Thornton-Pett, M.; Bochmann, M. *J. Chem. Soc., Dalton Trans.* **1997**, 2487–2494.

(8) MacLachlan, E. A.; Hess, F. M.; Patrick, B. O.; Fryzuk, M. D. *J. Am. Chem. Soc.* **2007**, *129*, 10895–10905.

(9) Schrock, R. R.; Baumann, R.; Reid, S. M.; Goodman, J. T.; Stumpf, R.; Davis, W. M. *Organometallics* **1999**, *18*, 3649–3670.

(10) Laplaza, C. E.; Cummins, C. C. *Science.* **1995**, *268*, 861–863.

(11) Cherry, J. P. F.; Johnson, A. R.; Baraldo, L. M.; Tsai, Y. C.; Cummins, C. C.; Kryatov, S. V.; Rybak-Akimova, E. V.; Capps, K. B.; Hoff, C. D.; Haar, C. M.; Nolan, S. P. *J. Am. Chem. Soc.* **2001**, *123*, 7271–7286.

(12) Yandulov, D. V.; Schrock, R. R.; Rheingold, A. L.; Ceccarelli, C.; Davis, W. M. *Inorg. Chem.* **2003**, *42*, 796–813.

(13) Ritleng, V.; Yandulov, D. V.; Weare, W. W.; Schrock, R. R.; Hock, A. S.; Davis, W. M. *J. Am. Chem. Soc.* **2004**, *126*, 6150–6163.

(14) Yandulov, D. V.; Schrock, R. R. *Science.* **2003**, *301*, 76–78.

(15) Hayes, C. E.; Leznoff, D. B. *Dalton Trans.* **2012**, *41*, 5743–5753.

(16) Moatazedi, Z.; Katz, M. J.; Leznoff, D. B. *Dalton Trans.* **2010**, *39*, 9889–9896.

(17) Dermer, V. O. C.; Fernelius, W. C. *Zeitschrift für Anorg. und Allg. Chemie* **1935**, *221*, 83–96.

(18) Bradley, D. C.; Copperthwaite, R. G. *Inorg. Synth.* **1978**, *18*, 112–120.

(19) Hursthouse, M. B.; Rodesiler, P. F. *J. Chem. Soc., Dalton Trans.* **1972**, 2100–2102.

(20) Ellison, J. J.; Power, P. P.; Shoner, S. C. *J. Am. Chem. Soc.* **1989**, *111*, 8044–8046.

(21) Kohn, R. D.; Kociok-Kohn, G.; Haufe, M. *Chem. Ber.* **1996**, *129*, 25–27.

(22) Olmstead, M. M.; Power, P. P.; Shoner, S. C. *Inorg. Chem.* **1991**, *30*, 2547–2551.

(23) Murray, B. D.; Power, P. P. *Inorg. Chem.* **1984**, *23*, 4584–4588.

(24) Bartlett, R. A.; Power, P. P. *J. Am. Chem. Soc.* **1987**, *109*, 7563–7564.

(25) Cloke, F. G. N.; Hitchcock, P. B.; Love, J. B. *J. Chem. Soc., Dalton Trans.* **1995**, 25–30.

(26) Scollard, J. D.; McConville, D. H. *J. Am. Chem. Soc.* **1996**, *118*, 10008–10009.

(27) Scollard, J. D.; McConville, D. H.; Vittal, J. J. *Organometallics* **1997**, *16*, 4415–4420.

(28) Aizenberg, M.; Turculet, L.; Davis, W. M.; Schattenmann, F.; Schrock, R. R. *Organometallics* **1998**, *17*, 4795–4812.

(29) Freundlich, J. S.; Schrock, R. R.; Davis, W. M. *J. Am. Chem. Soc.* **1996**, *118*, 3643–3655.

(30) Daniele, S.; Hitchcock, P. B.; Lappert, M. F. *Chem. Commun.* **1999**, 1909–1910.

(31) Müller, T. E.; Beller, M. *Chem. Rev.* **1998**, *98*, 675–704.

(32) Pohlki, F.; Doye, S. *Chem. Soc. Rev.* **2003**, *32*, 104–114.

(33) Keppert, D. L. *The Early Transition Metals*; Academic Press Inc.: New York, **1972**.

(34) Reid, S. M.; Neuner, B.; Schrock, R. R.; Davis, W. M. *Organometallics* **1998**, *17*, 4077–4089.

(35) Neuner, B.; Schrock, R. R. *Organometallics* **1996**, *15*, 5–6.

(36) Nomura, K.; Schrock, R. R.; Davis, W. M. *Inorg. Chem.* **1996**, *35*, 3695–3701.

(37) Piers, W. E.; Emslie, D. J. H. *Coord. Chem. Rev.* **2002**, *233-234*, 131–155.

(38) Kempe, R. *Angew. Chem. Int. Ed. Engl.* **2000**, *39*, 468–493.

(39) MacKay, B. A.; Fryzuk, M. D. *Chem. Rev.* **2004**, *104*, 385–401.

(40) Pool, J. A.; Lobkovsky, E.; Chirik, P. J. *Nature.* **2004**, *427*, 527–530.

(41) Piers, W. E.; Shapiro, P. J.; Bunel, E. E.; Bercaw, J. E. *Synth. Lett.* **1990**, 74–84.

(42) Fryzuk, M. D.; Yu, P.; Patrick, B. O. *Can. J. Chem.* **2001**, *79*, 1194–1200.

(43) Wong, E. W. Y.; Das, A. K.; Katz, M. J.; Nishimura, Y.; Batchelor, R. J.; Onishi, M.; Leznoff, D. B. *Inorg. Chim. Acta.* **2006**, *359*, 2826–2834.

(44) Mountford, P.; Ward, B. D. *Chem. Commun.* **2003**, 1797–1803.

(45) Love, J. B.; Clark, H. C. S.; Cloke, F. G. N.; Green, J. C.; Hitchcock, P. B. *J. Am. Chem. Soc.* **1999**, *121*, 6843–6849.

(46) Clancy, G. P.; Clark, H. C. S.; Clentsmith, G. K. B.; Cloke, F. G. N.; Hitchcock, P. B. *J. Chem. Soc., Dalton Trans.* **1999**, 3345–3347.

(47) Shaver, M. P.; Thomson, R. K.; Patrick, B. O.; Fryzuk, M. D. *Can. J. Chem.* **2003**, *81*, 1431–1437.

(48) Hao, S.; Berno, P.; Minhas, R. K.; Gambarotta, S. *Inorg. Chim. Acta.* **1996**, *244*, 37–49.

(49) Berno, P.; Moore, M.; Minhas, R.; Gambarotta, S. *Can. J. Chem.* **1996**, *74*, 1930–1935.

(50) Rosenberger, C.; Schrock, R. R.; Davis, W. M. *Inorg. Chem.* **1997**, *36*, 123–125.

(51) Shapiro, P. J.; Bunel, E.; Schaefer, W. P.; Bercaw, J. E. *Organometallics* **1990**, 867–869.

(52) Bochmann, M. *J. Chem. Soc., Dalton Trans.* **1996**, 255–270.

(53) Shapiro, P. J.; Schaefer, W. P.; Labinger, J. A.; Bercaw, J. E.; Cotter, W. D. *J. Am. Chem. Soc.* **1994**, *116*, 4623–4640.

(54) Okuda, J.; Schattenmann, F. J.; Wocadlo, S.; Massa, W. *Organometallics* **1995**, *14*, 789–795.

(55) Devore, D. D.; Timmers, F. J.; Hasha, D. L.; Rosen, R. K.; Marks, T. J.; Deck, P. A.; Stern, C. L. *Organometallics* **1995**, *14*, 3132–3134.

(56) Hughes, A. K.; Meetsma, A.; Teuben, J. H. *Organometallics* **1993**, 1936–1945.

(57) Hayes, P. G.; Piers, W. E.; McDonald, R. *J. Am. Chem. Soc.* **2002**, *124*, 2132–2133.

(58) Tinkler, S.; Deeth, R. J.; Duncalf, D. J.; Mccamley, A. *Chem. Commun.* **1996**, 2623–2624.

(59) Cloke, F. G. N.; Geldbach, T. J.; Hitchcock, P. B.; Love, J. B. *J. Organomet. Chem.* **1996**, *506*, 343–345.

(60) Horton, A. D.; de With, J.; Van Der Linden, A. J.; van de Weg, H.; de Jan, W.; van Arjan J., D. L.; van Henk., D. W. *Organometallics* **1996**, *15*, 2672–2674.

(61) Horton, A. D.; de With, J. *Chem. Commun.* **1996**, 1375–1376.

(62) Scollard, J. D.; McConville, D. H.; Vittal, J. J. *Organometallics* **1995**, *14*, 5478–5480.

(63) Scollard, J. D.; McConville, D. H.; Payne, N. C.; Vittal, J. J. *Macromolecules* **1996**, *29*, 5241–5243.

(64) Gade, L. H. *Chem. Commun.* **2000**, 173–181.

(65) Liang, L. C.; Schrock, R. R.; Davis, W. M.; McConville, D. H. *J. Am. Chem. Soc.* **1999**, *121*, 5797–5798.

(66) Graf, D. D.; Schrock, R. R.; Davis, W. M.; Stumpf, R. R. *Organometallics* **1999**, *18*, 843–852.

(67) Baumann, R.; Davis, W. M.; Schrock, R. R. *J. Am. Chem. Soc.* **1997**, *119*, 3830–3831.

(68) Liang, L.-C.; Schrock, R. R.; Davis, W. M. *Organometallics* **2000**, *19*, 2526–2531.

(69) Fryzuk, M. D.; Johnson, S. A. *Coord. Chem. Rev.* **2000**, *200-202*, 379–409.

(70) Eikey, R. A.; Abu-Omar, M. M. *Coord. Chem. Rev.* **2003**, *243*, 83–124.

(71) Fay, A. W.; Blank, M. A.; Lee, C. C.; Hu, Y.; Hodgson, K. O.; Hedman, B.; Ribbe, M. W. *J. Am. Chem. Soc.* **2010**, *132*, 12612–12618.

(72) Lee, C. C.; Hu, Y.; Ribbe, M. W. *Science* **2010**, *329*, 642.

(73) Hu, Y.; Lee, C. C.; Ribbe, M. W. *Science* **2011**, *333*, 753–755.

(74) Milsmann, C.; Semproni, S. P.; Chirik, P. J. *J. Am. Chem. Soc.* **2014**, *136*, 12099–12107.

(75) Groysman, S.; Villagrán, D.; Freedman, D. E.; Nocera, D. G. *Chem. Commun.* **2011**, *47*, 10242–10244.

(76) Liu, G.; Liang, X.; Meetsma, A.; Hessen, B. *Dalton Trans.* **2010**, *39*, 7891–7893.

(77) Milsmann, C.; Turner, Z. R.; Semproni, S. P.; Chirik, P. J. *Angew. Chemie Int. Ed.* **2012**, *51*, 5386–5390.

(78) Buijink, J.-K. F.; Meetsma, A.; Teuben, J. H. *Organometallics* **1993**, *12*, 2004–2005.

(79) Clentsmith, G. K. B.; Bates, V. M. E.; Hitchcock, P. B.; Cloke, F. G. N. *J. Am. Chem. Soc.* **1999**, *121*, 10444–10445.

(80) Vidyaratne, I.; Crewdson, P.; Lefebvre, E.; Gambarotta, S. *Inorg. Chem.* **2007**, *46*, 8836–8842.

(81) Hanna, T. E.; Lobkovsky, E.; Chirik, P. J. *Organometallics* **2009**, *28*, 4079–4088.

(82) Hanna, T. E.; Bernskoetter, W. H.; Bouwkamp, M. W.; Lobkovsky, E.; Chirik, P. J. *Organometallics* **2007**, *26*, 2431–2438.

(83) Hanna, T. E.; Keresztes, I.; Lobkovsky, E.; Bernskoetter, W. H.; Chirik, P. J. *Organometallics* **2004**, *23*, 3448–3458.

(84) Duchateau, R.; Gambarotta, S.; Beydoun, N.; Bensimon, C. *J . Am. Chem. Soc* **1991**, *113*, 8986–8988.

(85) Morello, L.; Yu, P.; Carmichael, C. D.; Patrick, B. O.; Fryzuk, M. D. *J. Am. Chem. Soc.* **2005**, *127*, 12796–12797.

(86) Demir, S.; Lorenz, S. E.; Fang, M.; Furche, F.; Meyer, G.; Ziller, J. W.; Evans, W. J. *J. Am. Chem. Soc.* **2010**, *132*, 11151–11158.

(87) Fryzuk, M. D.; Johnson, S. A.; Patrick, B. O.; Albinati, A.; Mason, S. A.; Koetzle, T. F. *J. Am. Chem. Soc.* **2001**, *123*, 3960–3973.

(88) Fontaine, P. P.; Yonke, B. L.; Zavalij, P. Y.; Sita, L. R. *J. Am. Chem. Soc.* **2010**, *132*, 12273–12285.

(89) Müller, T. E.; Hultzsch, K. C.; Yus, M.; Foubelo, F.; Tada, M. *Chem. Rev.* **2008**, *108*, 3795–3892.

(90) Gagne, M.; Marks, T. *J. Am. Chem. Soc.* **1989**, *111*, 4108–4109.

(91) O'Shaughnessy, P. N.; Scott, P. *Tetrahedron Asymmetry* **2003**, *14*, 1979–1983.

(92) Li, C.; Thomson, R. K.; Gillon, B.; Patrick, B. O.; Schafer, L. L. *Chem. Commun.* **2003**, 2462–2463.

(93) Ward, B. D.; Maisse-Francois, A.; Mountford, P.; Gade, L. H. *Chem. Commun.* **2004**, 704–705.

(94) Ong, T. G.; Yap, G. P. A.; Richeson, D. S. *J. Am. Chem. Soc.* **2003**, *125*, 8100–8101.

(95) Britovsek, G. J. P.; Gibson, V. C.; Kimberley, B. S.; Maddox, P. J.; McTavish, S. J.; Solan, G. A.; White, A. J. P.; Williams, D. J. *Chem. Commun.* **1998**, 849–850.

(96) Small, B. L.; Brookhart, M. *J . Am. Chem. Soc.* **1998**, *120*, 7143–7144.

(97) Small, B. L.; Brookhart, M.; Bennett, A. M. A. *J . Am. Chem. Soc.* **1998**, *120*, 4049–4050.

(98) Bradley, D. C.; Hursthouse, M. B.; Smallwood, R. J.; Welch, A. J. *J. Chem. Soc., Chem. Commun.* **1972**, 872–873.

(99) Olmstead, M.; Power, P.; Sigel, G. *Inorg. Chem.* **1986**, *25*, 1027–1033.

(100) Hope, H.; Olmstead, M. M.; Murray, B. D.; Power, P. P. *J. Am. Chem. Soc.* **1985**, *107*, 712–713.

(101) Power, P. P. *Chem. Rev.* **2012**, *112*, 3482–3507.

(102) Lin, C. Y.; Fettinger, J. C.; Grandjean, F.; Long, G. J.; Power, P. P. *Inorg. Chem.* **2014**, *53*, 9400–9406.

(103) Hartwig, J. F.; Andersen, R. A.; Bergman, R. G. *Organometallics* **1991**, *10*, 1875–1887.

(104) Rais, D.; Bergman, R. G. *Chem. Eur. J.* **2004**, *10*, 3970–3978.

(105) Kaplan, A. W.; Ritter, J. C. M.; Bergman, R. G. *J. Am. Chem. Soc.* **1998**, *120*, 6828–6829.

(106) Fox, D. J.; Bergman, R. G. *J. Am. Chem. Soc.* **2003**, *125*, 8984–8985.

(107) Holland, A. W.; Bergman, R. G. *J. Am. Chem. Soc.* **2002**, *124*, 14684–14695.

(108) Matsuzaka, H.; Kamura, T.; Ariga, K.; Watanabe, Y.; Okubo, T.; Ishii, T.; Yamashita, M.; Kondo, M. *Organometallics* **2000**, *19*, 216–218.

(109) Villanueva, L. A.; Abboud, K. A.; Boncella, J. M. *Organometallics* **1994**, *13*, 3921–3931.

(110) Hitchcock, P. B.; Lappert, M. F.; Pierssens, L. J. *Chem. Commun.* **1996**, 1189–1190.

(111) Bunge, S. D.; Just, O.; Rees, W. S. *Angew. Chemie Int. Ed.* **2000**, *39*, 3082–3084.

(112) Park, S.; Roundhill, D. M.; Rheingold, A. L. *Inorg. Chem.* **1987**, *26*, 3972–3974.

(113) Matsuzaka, H.; Ariga, K.; Kase, H.; Kamura, T.; Kondo, M.; Kitagawa, S.; Yamasaki, M. **1997**, *31*, 4514–4516.

(114) Blake Jr., R. E.; Heyn, R. H.; Tilley, T. D. *Polyhedron* **1992**, *11*, 709–710.

(115) O'Mahoney, C. A.; Parkin, I. P.; Williams, D. J.; Woollins, J. D. *Polyhedron* **1989**, *8*, 1979–1981.

(116) Kretschmer, V. M.; Heck, L. *Zeitschrift für Anorg. und Allg. Chemie* **1982**, *490*, 215–229.

(117) Fryzuk, M. D.; MacNeil, P. A. *J. Am. Chem. Soc.* **1981**, *103*, 3592–3593.

(118) Fryzuk, M. D.; MacNeil, P. A.; Rettig, S. J.; Secco, A. S.; Trotter, J. *Organometallics* **1982**, *1*, 918–930.

(119) Fryzuk, M. D.; MacNeil, P. A. *Organometallics* **1983**, *2*, 355–356.

(120) Fryzuk, M. D.; MacNeil, P. A.; Rettig, S. J. *Organometallics* **1986**, *5*, 2469–2476.

(121) Fryzuk, M. D. *J. Organomet. Chem.* **1987**, *332*, 345–360.

(122) Fryzuk, M. D.; Joshi, K. *Organometallics* **1989**, *8*, 722–726.

(123) Kempe, R. *Eur. J. Inorg. Chem.* **2003**, 791–803.

(124) Kempe, R.; Noss, H.; Irrgang, T. *J. Organomet. Chem.* **2002**, *647*, 12–20.

(125) Glatz, G.; Demeshko, S.; Motz, G.; Kempe, R. *Eur. J. Inorg. Chem.* **2009**, 1385–1392.

(126) Mund, G.; Gabert, A. J.; Batchelor, R. J.; Britten, J. F.; Leznoff, D. B. *Chem. Commun.* **2002**, 2990–2991.

(127) Das, A. K.; Moatazedi, Z.; Mund, G.; Bennet, A. J.; Batchelor, R. J.; Leznoff, D. B. *Inorg. Chem.* **2007**, *46*, 366–368.

(128) Haftbaradaran, F.; Mund, G.; Batchelor, R. J.; Britten, J. F.; Leznoff, D. B. *Dalton Trans.* **2005**, 2343–2345.

(129) Elias, A. J.; Roesky, H. W.; Robinson, W. T.; Sheldrick, G. M. *J. Chem. Soc., Dalton Trans.* **1993**, *1*, 495–500.

(130) Leznoff, D. B.; Mund, G.; Jantunen, K. C. *Journal of Nuclear Science and Technology*, **2002**, *Supplement*, 406–409.

(131) Cochran, F. V.; Bonitatebus, P. J.; Schrock, R. R. *Organometallics* **2000**, *19*, 2414–2416.

(132) Bryndza, H. E.; Fong, L. K.; Paciello, R. A.; Tam, W.; Bercaw, J. E. *J. Am. Chem. Soc.* **1987**, *109*, 1444–1456.

(133) Hasan, K.; Fowler, C.; Kwong, P.; Crane, A. K.; Collins, J. L.; Kozak, C. M. *Dalton Trans.* **2008**, 2991–2998.

(134) Chard, E. F.; Dawe, L. N.; Kozak, C. M. *J. Organomet. Chem.* **2013**, *737*, 32–39.

(135) Chowdhury, R. R.; Crane, A. K.; Fowler, C.; Kwong, P.; Kozak, C. M. *Chem. Commun.* **2008**, 94-96.

(136) Alcock, N. W.; O'Sullivan, R. D.; Parkins, A. W. *J. Chem. Soc., Chem. Commun.* **1980**, 1216–1218.

(137) O'Sullivan, R. D.; Parkins, A. W.; Alcock, N. W. *J. Chem. Soc., Dalton Trans.* **1986**, 571–575.

(138) Bryndza, H. E.; Fultz, W. C.; Tam, W. *Organometallics* **1985**, *4*, 939–940.

(139) Cowan, R.; Trogler, W. *Organometallics* **1987**, *6*, 2451–2453.

(140) Kempe, R. *Chem. Eur. J.* **2001**, *7*, 1630–1636.

(141) Jantunen, K. C.; Batchelor, R. J.; Leznoff, D. B. *Organometallics* **2004**, *23*, 2186–2193.

(142) Jantunen, K. C.; Haftbaradaran, F.; Katz, M. J.; Batchelor, R. J.; Schatte, G.; Leznoff, D. B. *Dalton Trans.* **2005**, *50*, 3083–3091.

(143) Mund, G.; Vidovic, D.; Batchelor, R. J.; Britten, J. F.; Sharma, R. D.; Jones, C. H. W.; Leznoff, D. B. *Chem. Eur. J.* **2003**, *9*, 4757–4763.

(144) Mund, G.; Batchelor, R. J.; Sharma, R. D.; Jones, C. H. W.; Leznoff, D. B. *J. Chem. Soc., Dalton Trans.* **2002**, 136–137.

(145) Ebsworth, E. A. V.; Rankin, D. W. H.; Cradock, S. *Structural Methods in Inorganic Chemistry*, 2nd Ed.; Blackwell Scientific Publications: Oxford, **1991**.

(146) Bertini, I.; Luchinat, C. In *Physical Methods for Chemists*; Drago, R. S., Ed.; Saunders College Publishing: Orlando, FL, **1992**; 500–558.

(147) La Mar, G. N.; Horrocks Jr., W. D.; Holm, R. H. *NMR of Paramagnetic Molecules: Principles and Applications*; Academic Press: New York, **1973**.

(148) Pavia, D. L.; Lampman, G. M.; Kriz, G. S. *Introduction to Spectroscopy*, 3rd Ed.; Thomson Learning, Inc.: Bellingham, Washington, **2001**.

(149) Evans, D. F. *J. Chem. Soc.* **1959**, 2003–2005.

(150) Piguet, C. *J. Chem. Ed.* **1997**, *74*, 815–816.

(151) Ziller, J. W.; Rheingold, A. L. In *Physical Methods for Chemists*; Drago, R. S., Ed.; Saunders College Publishing: Orlando, FL, **1992**; 689–712.

(152) Bain, G. A.; Berry, J. F. *J. Chem. Ed.* **2008**, *85*, 532.

(153) Housecroft, C. E.; Sharpe, A. G. *Inorganic Chemistry*, 4th Ed.; Pearson Education Limited: Harlow, England, **2012**.

(154) Drago, R. S. In *Physical Methods for Chemists*; Saunders College Publishing: Gainesville, FL, **1992**; 559–603.

(155) Drago, R. S. In *Physical Methods for Chemists*; Drago, R. S., Ed.; Saunders College Publishing: Orlando, FL, **1992**; 469–499.

(156) Drago, R. S. In *Physical Methods for Chemists*; Saunders College Publishing: Gainesville, FL, **1992**; 360–408.

(157) Krzystek, J.; Zvyagin, S. A.; Ozarowski, A.; Trofimenko, S.; Telser, J. *J. Magn. Reson.* **2006**, *178*, 174–183.

(158) Knight, L. K.; Piers, W. E.; Fleurat-Lessard, P.; Parvez, M.; McDonald, R. *Organometallics* **2004**, *23*, 2087–2094.

(159) Skinner, M. E. G.; Mountford, P. *J. Chem. Soc., Dalton Trans.* **2002**, 1694–1703.

(160) Luo, Y.; Feng, X.; Wang, Y.; Fan, S.; Chen, J.; Lei, Y.; Liang, H. *Organometallics* **2011**, *30*, 3270–3274.

(161) Chen, F.; Fan, S.; Wang, Y.; Chen, J.; Luo, Y. *Organometallics* **2012**, *31*, 3730–3735.

(162) Lei, Y.; Su, Q.; Chen, J.; Luo, Y. *J. Organomet. Chem.* **2014**, *769*, 119–123.

(163) Meermann, C.; Gerstberger, G.; Spiegler, M.; Törnroos, K. W.; Anwander, R. *Eur. J. Inorg. Chem.* **2008**, 2014–2023.

(164) Estler, F.; Eickerling, G.; Herdtweck, E.; Anwander, R. *Organometallics* **2003**, *22*, 1212–1222.

(165) Karl, M.; Seybert, G.; Massa, W.; Dehnicke, K. *Zeitschrift für Anorg. und Allg. Chemie* **1999**, *625*, 375–376.

(166) Britovsek, G. J. P.; Gibson, V. C.; Wass, D. F. *Angew. Chemie Int. Ed.* **1999**, *38*, 428–447.

(167) Shannon, R. D. *Acta Cryst.* **1976**, *A32*, 751–767.

(168) Slone, C. S.; Weinberger, D. M.; Mirkin, C. A. In *Progress in Inorganic Chemistry*; Karlin, K. D., Ed.; John Wiley & Sons, Inc.: New York, **1999**; 233–350.

(169) Addison, A. W.; Rao, T. N.; Reedijk, J.; van Rijn, J.; Verschoor, G. C. *J. Chem. Soc., Dalton Trans.* **1984**, 1349–1356.

(170) Bai, G.; Wei, P.; Stephan, D. W. *Organometallics* **2006**, *25*, 2649–2655.

(171) Kahn, O. *Molecular Magnetism*; VCH: New York, **1993**.

(172) Hayes, P. G.; Piers, W. E.; Lee, L. W. M.; Knight, L. K.; Parvez, M.; Elsegood, M. R. J.; Clegg, W. *Organometallics* **2001**, *20*, 2533–2544.

(173) Nishiura, M.; Hou, Z. *Nat. Chem.* **2010**, *2*, 257–268.

(174) Johnson, A. L.; Davidson, M. G.; Mahon, M. F. *Dalton Trans.* **2007**, 5405–5411.

(175) Nomura, K.; Liu, J. *Dalton Trans.* **2011**, *40*, 7666–7682.

(176) Li, J.-L.; Gao, Z.-W.; Sun, P.; Gao, L.-X.; Tikkanen, W. *Inorg. Chim. Acta* **2011**, *368*, 231–236.

(177) Desmangles, N.; Jenkins, H.; Ruppa, K. B.; Gambarotta, S. *Inorg. Chim. Acta* **1996**, *250*, 1–4.

(178) Song, J.; Berno, P.; Gambarotta, S. *J . Am. Chem. Soc.* **1994**, *116*, 6927–6928.

(179) Kilgore, U. J.; Sengelaub, C. A.; Fan, H.; Tomaszewski, J.; Karty, J. A.; Baik, M. H.; Mindiola, D. J. *Organometallics* **2009**, *28*, 843–852.

(180) Cohen, J. D.; Fryzuk, M. D.; Loehr, T. M.; Mylvaganam, M.; Rettig, S. J. *Inorg. Chem.* **1998**, *37*, 112–119.

(181) Fryzuk, M. D. *Science.* **1997**, *275*, 1445–1447.

(182) Pool, J. A.; Lobkovsky, E.; Chirik, P. J. *J. Am. Chem. Soc.* **2003**, *125*, 2241–2251.

(183) Fulmer, G. R.; Miller, A. J. M.; Sherden, N. H.; Gottlieb, H. E.; Nudelman, A.; Stoltz, B. M.; Bercaw, J. E.; Goldberg, K. I. *Organometallics* **2010**, *29*, 2176–2179.

(184) Arndt, S.; Voth, P.; Spaniol, T. P.; Okuda, J. *Organometallics* **2000**, *19*, 4690–4700.

(185) Nishiura, M.; Baldamus, J.; Shima, T.; Mori, K.; Hou, Z. *Chem. Eur. J.* **2011**, *17*, 5033–5044.

(186) Schumann, H.; Meese-Marktscheffel, J. A.; Esser, L. *Chem. Rev.* **1995**, *95*, 865–986.

(187) Schumann, B. H. *Angew. Chemie Int. Ed.* **1984**, *23*, 474–493.

(188) Halcovitch, N. R.; Fryzuk, M. D. *Organometallics* **2013**, *32*, 5705–5708.

(189) Piers, W. E.; Shapiro, P. J.; Bunel, E. E.; Bercaw, J. E. *Synlett.* **1990**, 74–84.

(190) Burger, B. J.; Thompson, M. E.; Cotter, W. D.; Bercaw, J. E. *J. Am. Chem. Soc.* **1990**, *112*, 1566–1577.

(191) Hajela, S.; Bercaw, J. E. *Organometallics* **1994**, *13*, 1147–1154.

(192) Fryzuk, M. D.; Giesbrecht, G.; Rettig, S. J. *Organometallics* **1996**, *15*, 3329–3336.

(193) Hajela, S.; Schaefer, W. P.; Bercaw, J. E. *J. Organomet. Chem.* **1997**, *532*, 45–53.

(194) Budzelaar, P. H. M.; van Oort, A. B.; Orpen, A. G. *Eur. J. Inorg. Chem.* **1998**, 1485–1494.

(195) Fergusson, J. E. In *Preparative Inorganic Reactions, Volume 7*; Jolly, W. L., Ed.; John Wiley & Sons, Inc.: New York, **1971**; 93–164.

(196) Betteridge, P. W.; Carruthers, J. R.; Cooper, R. I.; Prout, K.; Watkin, D. J. *J. Appl. Crystallogr.* **2003**, *36*, 1487–1487.

(197) Farrugia, L. J. *J. Appl. Crystallogr.* **1997**, *30*, 565–565.

(198) Persistence of Vision Raytracer. Version 3.6.1; Persistence of Vision Pty. Ltd. : Williamstown, Victoria, Australia, **2004**.

(199) Bryan, A. M.; Merrill, W. A.; Reiff, W. M.; Fettinger, J. C.; Power, P. P. *Inorg. Chem.* **2012**, *51*, 3366–3373.

(200) Carlin, R. L.; van Duyneveldt, A. J. *Magnetic Properties of Transition Metal Compounds*; Springer-Verlag: New York, **1977**.

(201) Moatazedi, Z. Coordination and Organometallic Diamido-Donor Iron and Cobalt Complexes, **2012**.

(202) Hasan, K.; Dawe, L. N.; Kozak, C. M. *Eur. J. Inorg. Chem.* **2011**, 4610–4621.

# Appendix A.

# Additional Spectroscopic Data

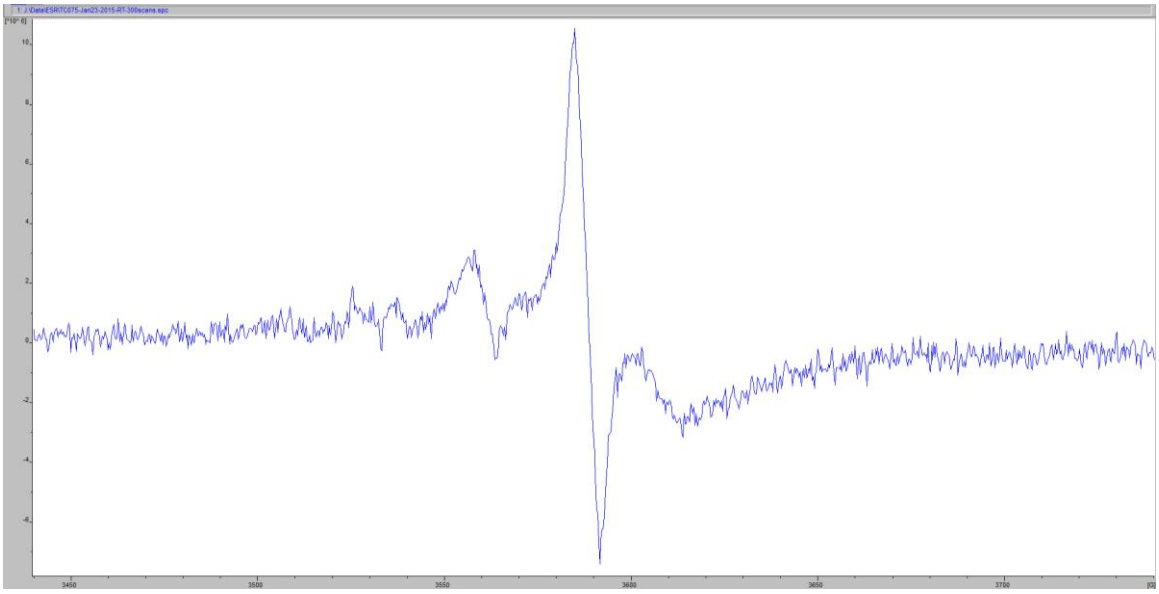

**Figure A1. ESR spectrum of {[$^{t\text{Bu}}$NON]TiCl}$_2$ (2); room temperature, 300 scans.**

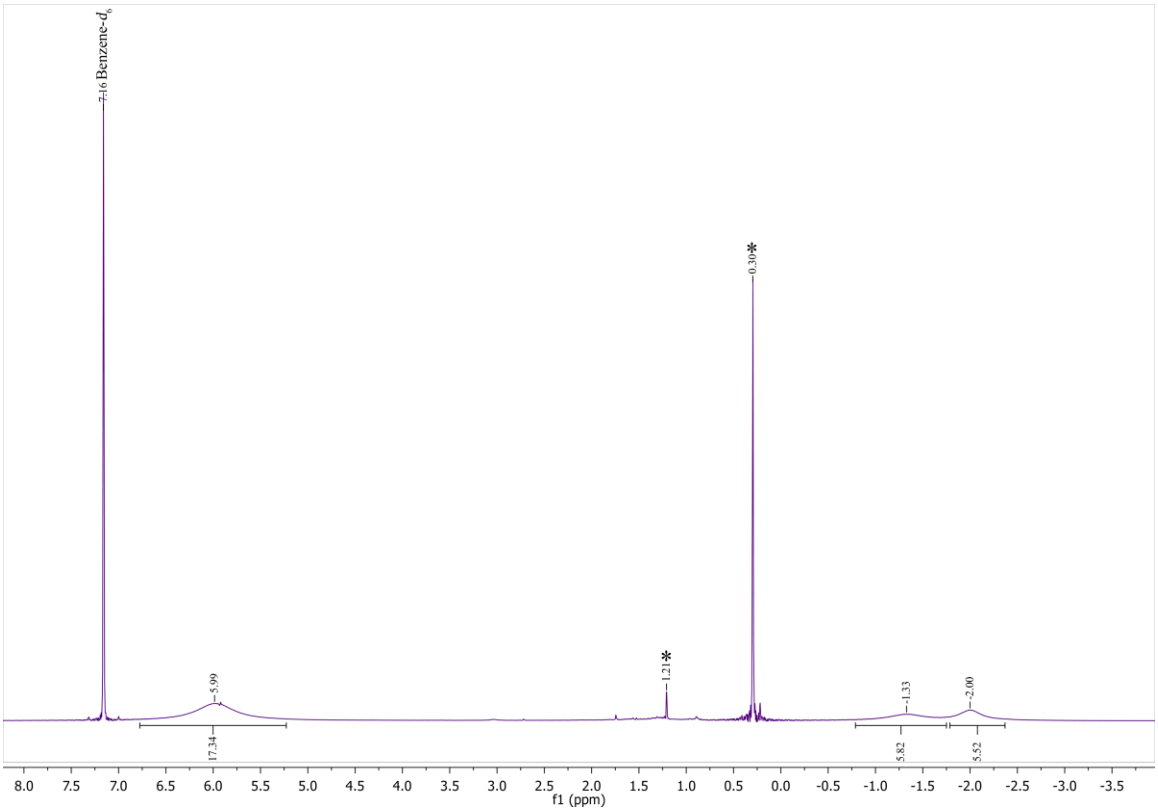


**Figure A2.** **$^1$H NMR spectrum of the reduction reaction of {[$^{tBu}$NON]VCl}$_2$ (3) with $KC_8$ in benzene-$d_6$.**

* = decomposition/impurity

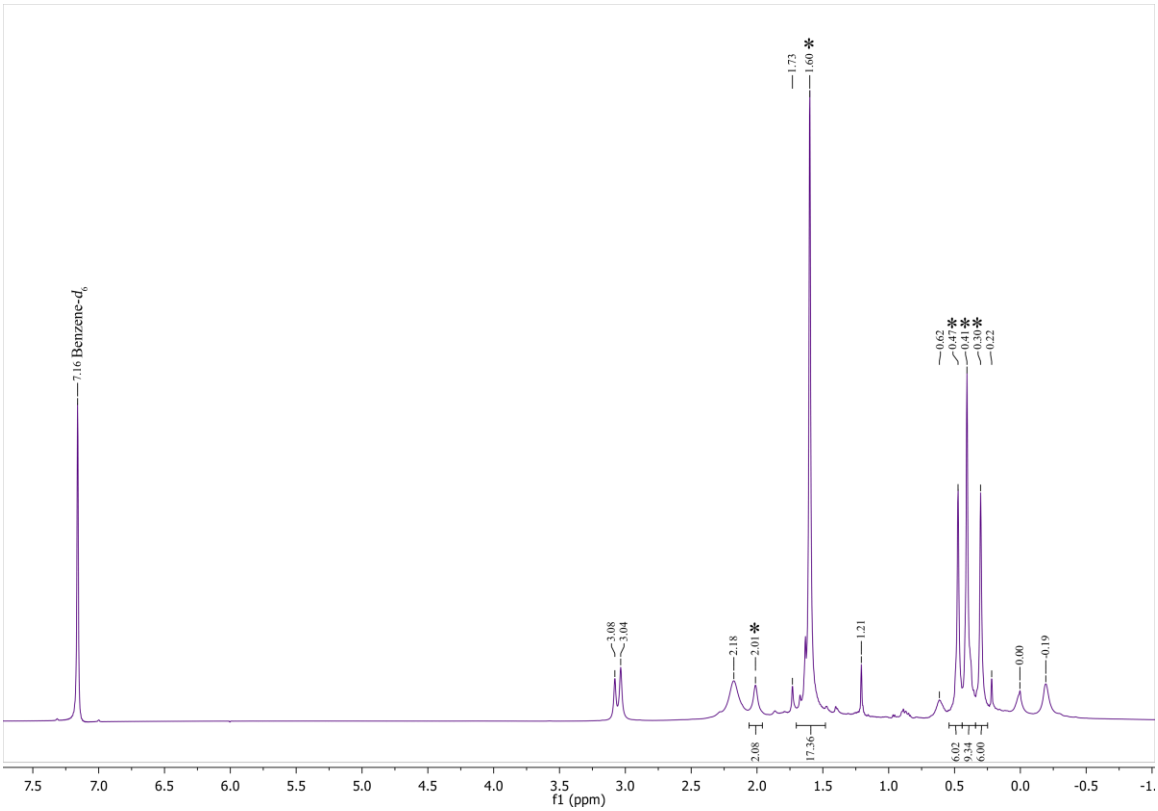


**Figure A3.** **$^1$H NMR spectrum of the reduction reaction of {[$^{t\text{Bu}}$NON]VCH$_2$SiMe$_3$}$_2$($\mu$-N$_2$) (3a) with KC$_8$ in benzene-$d_6$.**

* = remaining starting material

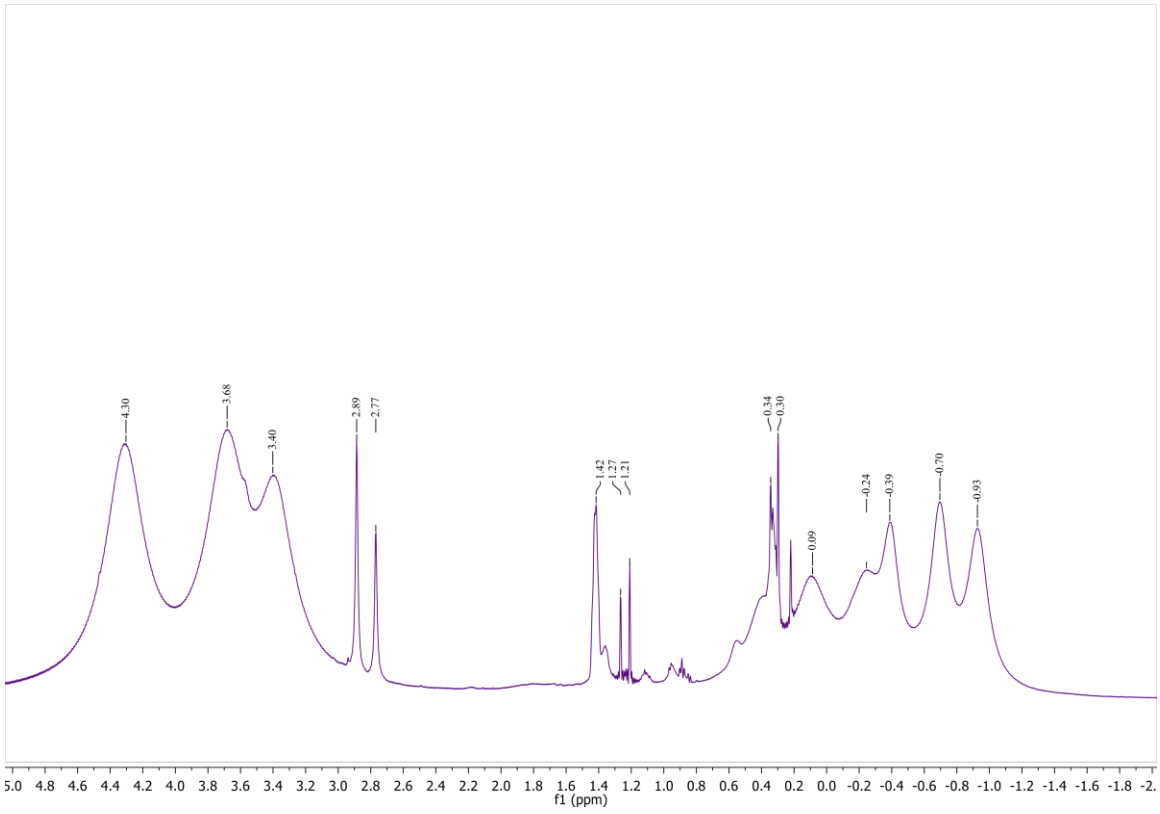


**Figure A4.** **$^{1}$H NMR spectrum of reaction of {[$^{t\text{Bu}}$NON]VCl}$_2$ (3) with KEt$_3$BH in benzene-$d_6$.**

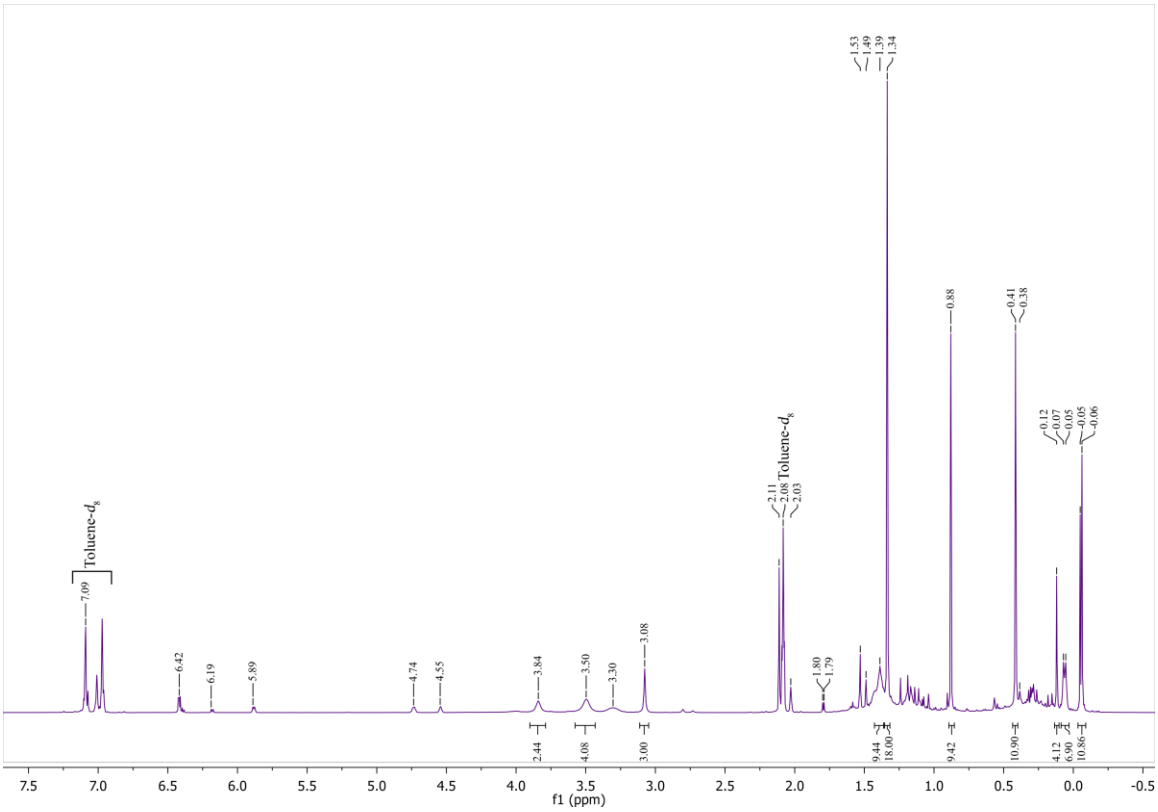


**Figure A5.** **$^1$H NMR spectrum of the reaction of [$^{t\text{Bu}}$NON]ScCH$_2$SiMe$_3$•THF (1a) with B(C$_6$F$_5$)$_3$ in toluene-$d_8$.**

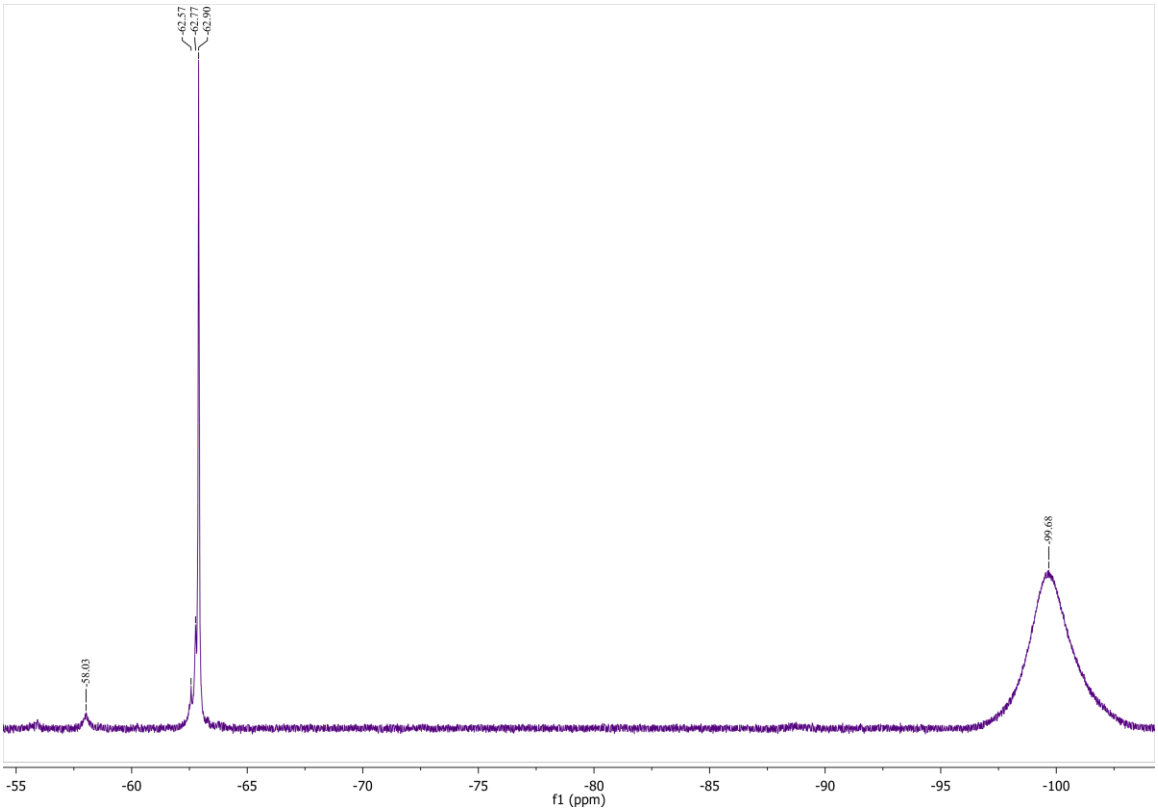


**Figure A6. $^{19}$F NMR spectrum of [$^{(CF_3)_2Ph}$NON]FeCl•LiCl•2DME (4) in toluene-$d_8$.**

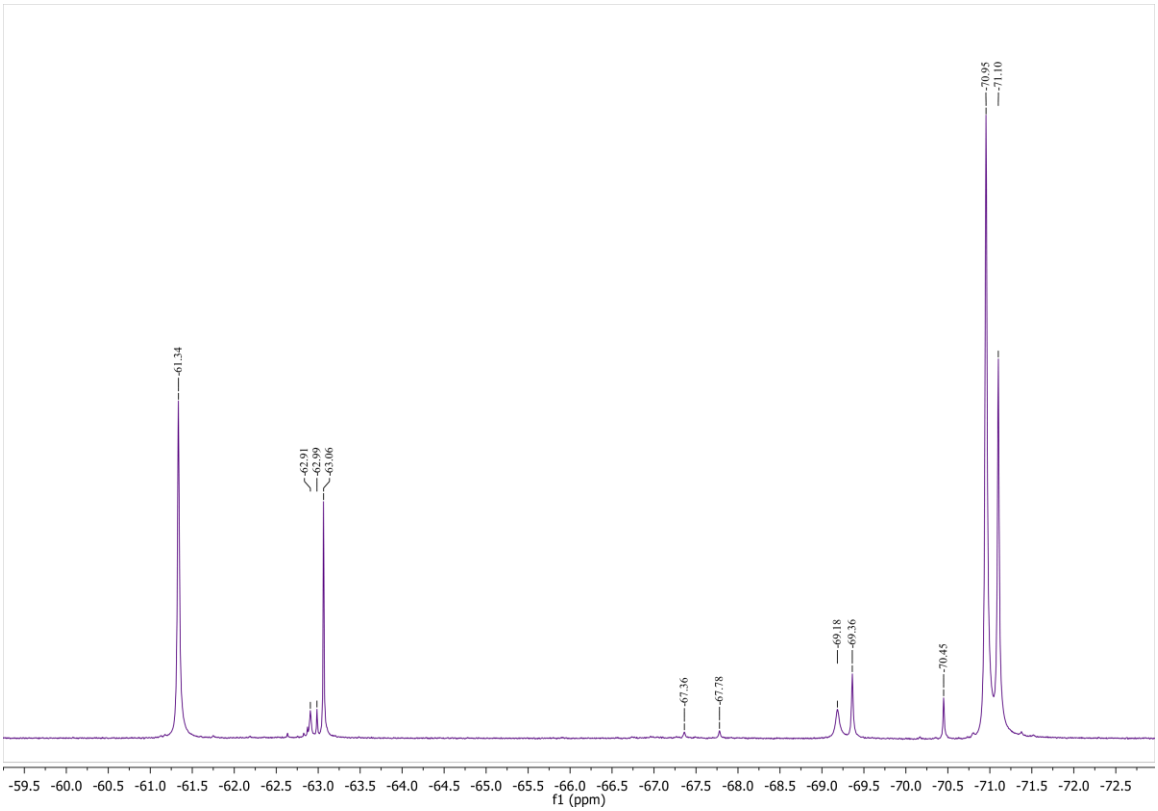


**Figure A7.** **$^{19}$F NMR spectrum of Li{$Co_2Cl[^{(CF_3)_2Ph}NON]_2$}•2DME (5) in toluene-$d_8$; reaction in DME.**

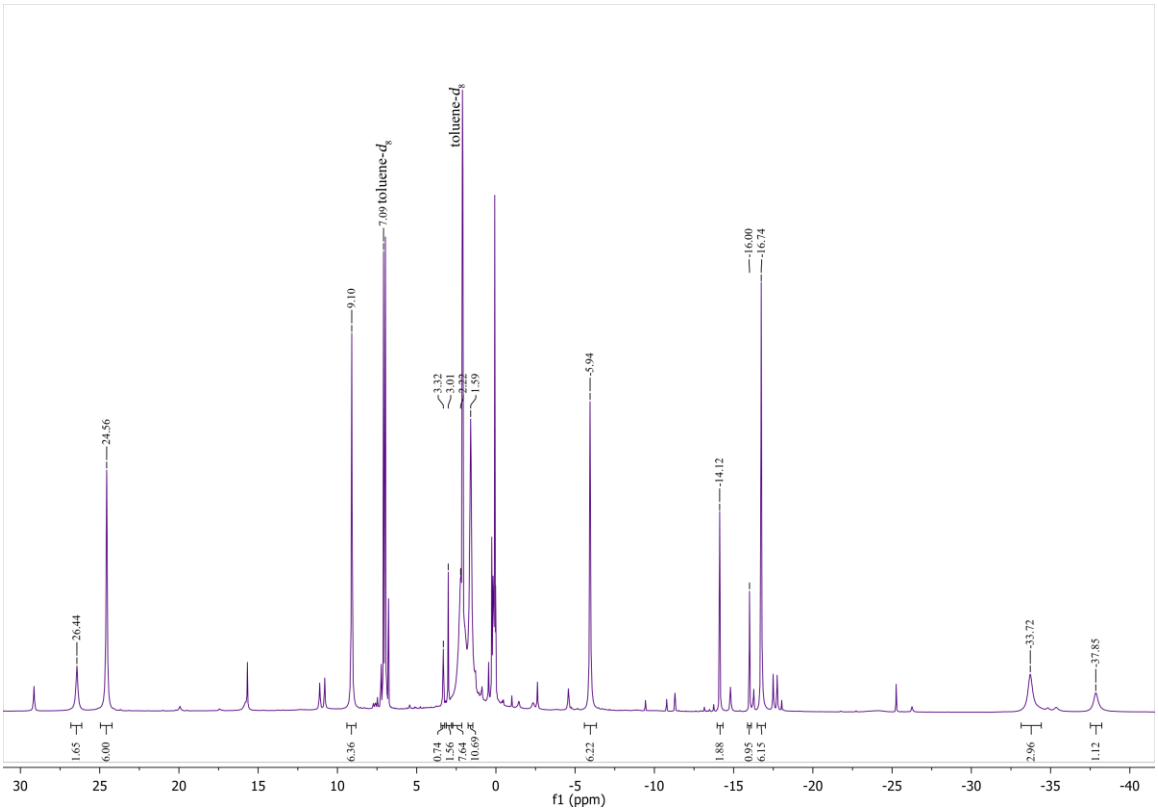


**Figure A8.** **$^{1}$H NMR spectrum of Li{$Co_2Cl[^{(CF_3)_2Ph}NON]_2$} (5) in toluene-$d_8$; reaction in THF.**

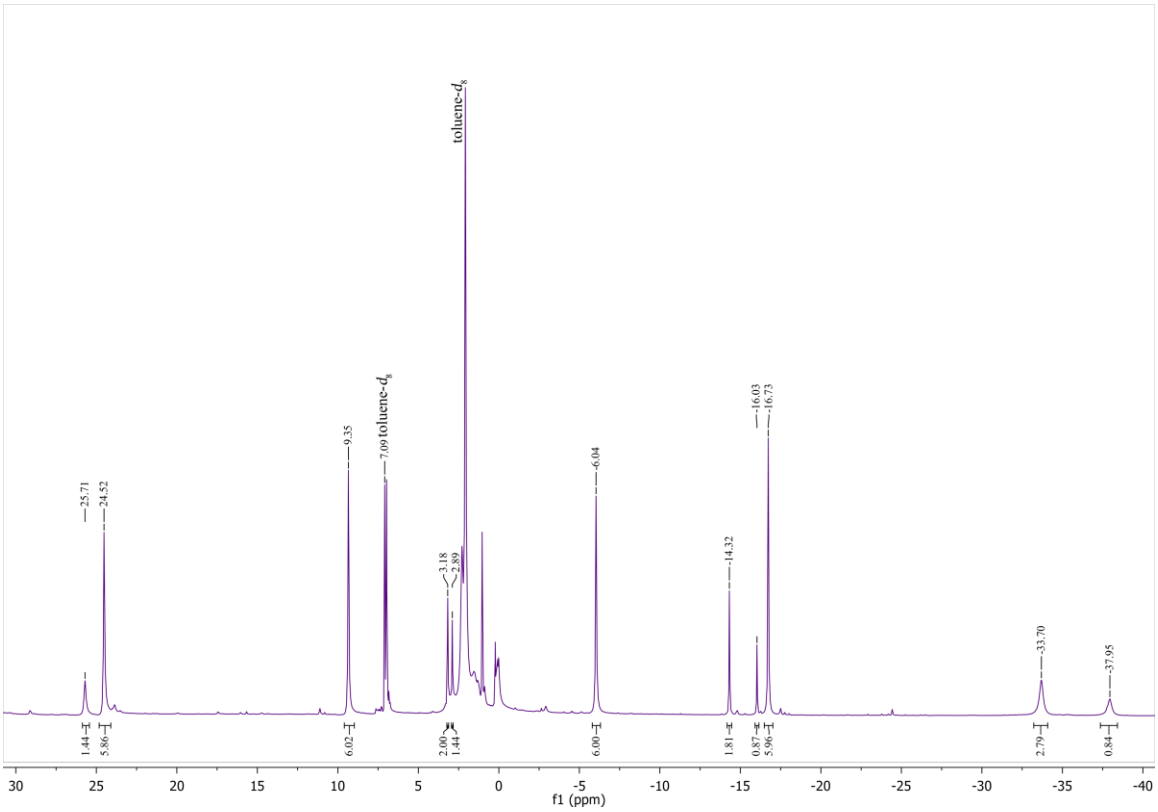


**Figure A9.** **$^1$H NMR spectrum of Li{$Co_2Cl[^{(CF_3)_2Ph}NON]_2$}•2DME (5) in toluene-$d_8$; reaction in $Et_2O$.**

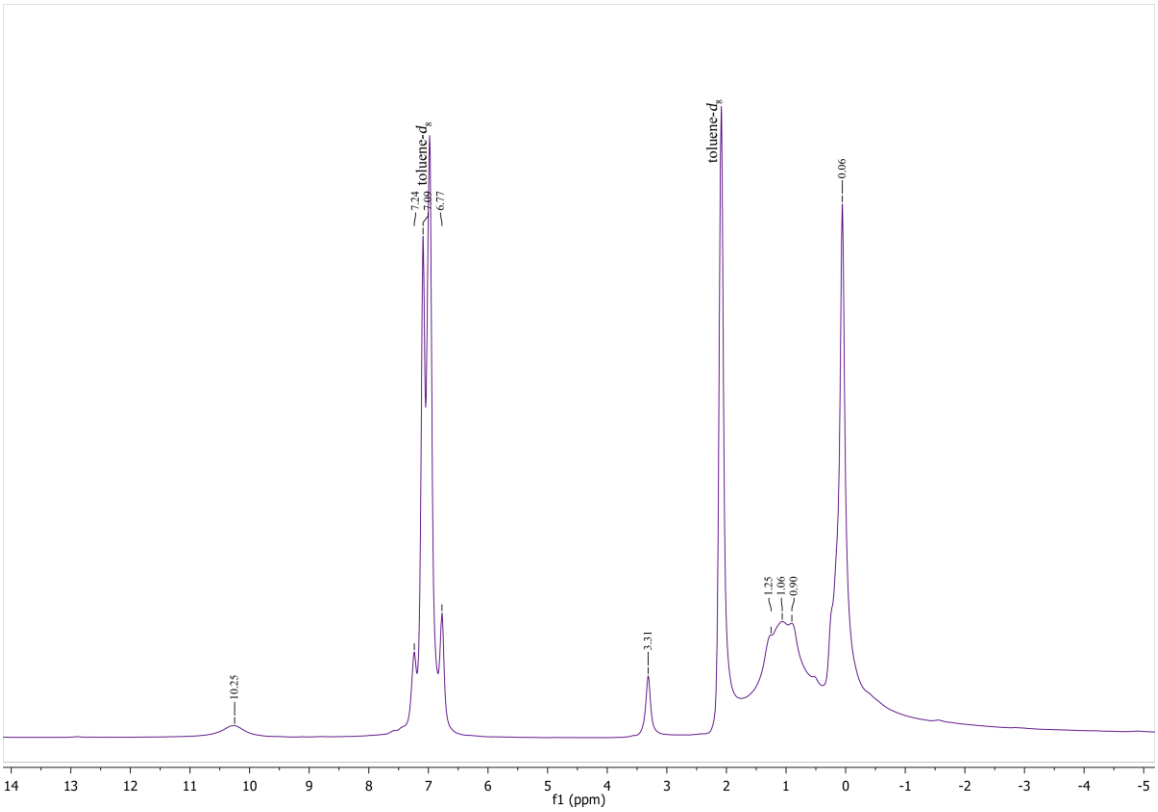


**Figure A10. $^1$H NMR spectrum of the reaction of [$^{(CF_3)_2Ph}$NON]$Li_2$ and $FeCl_2$ in toluene-$d_8$.**

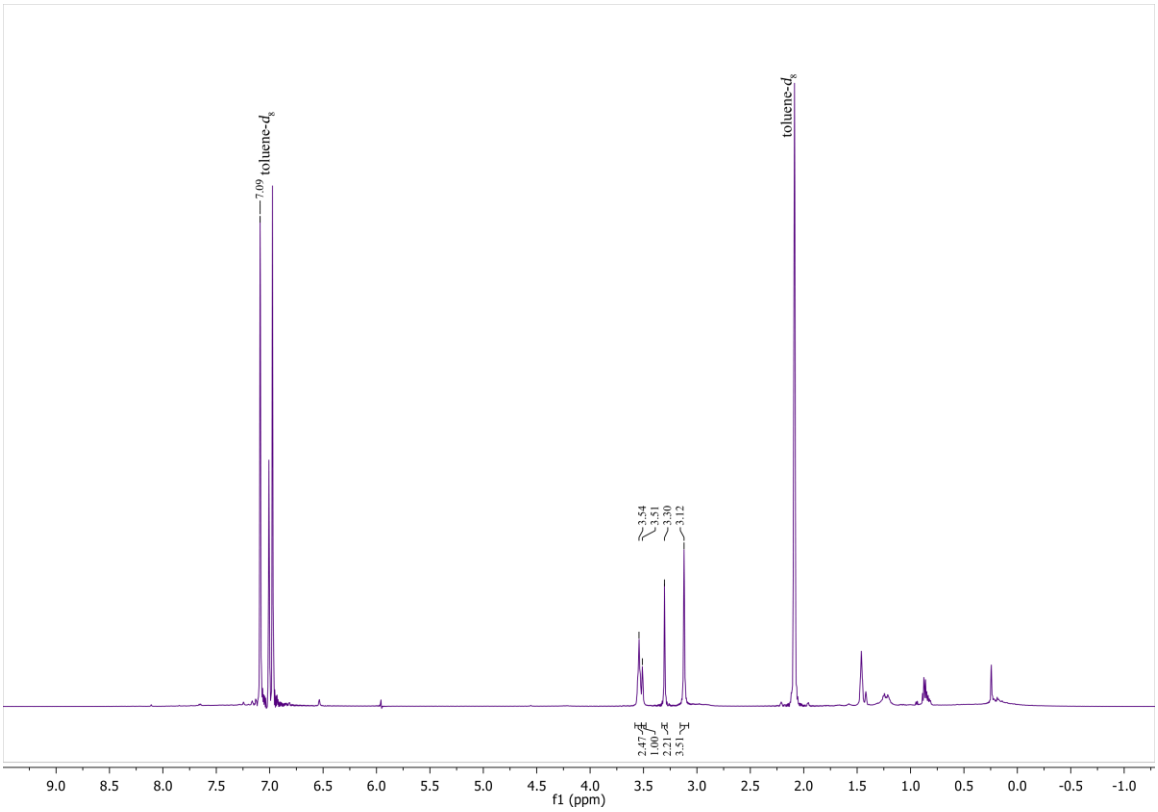


**Figure A11. $^1$H NMR spectrum of the reaction of [$^{(CF_3)_2Ph}$NON]$Li_2$ and $CrCl_2$ in toluene-$d_8$.**

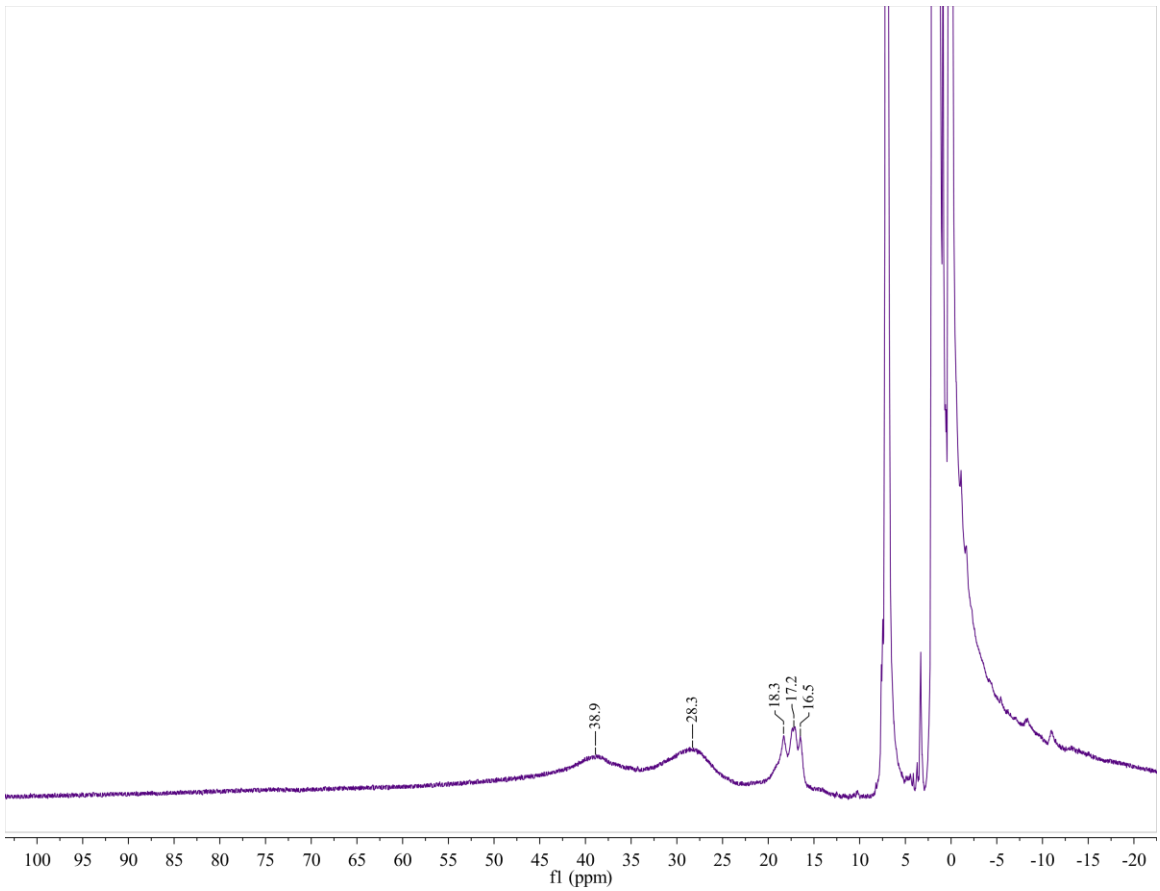


**Figure A12.** **$^{1}$H NMR spectrum of the alkylation reaction of [$^{(CF_3)_2Ph}$NON]FeCl•LiCl•2DME (4) in toluene-$d_8$.**

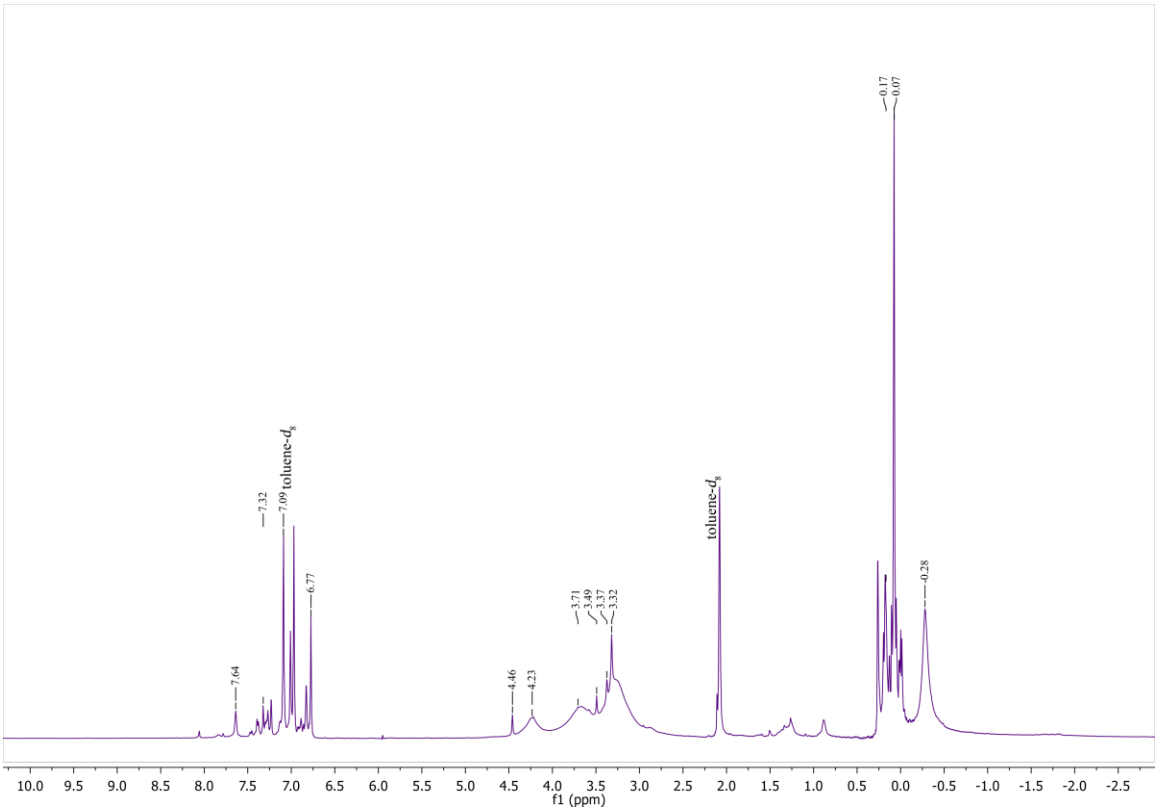


**Figure A13.** **$^1$H NMR spectrum of the oxidation reaction of Li{$Co_2Cl[^{(CF_3)_2Ph}NON]_2$}•2DME (5) with $I_2$ in toluene-$d_8$.**

# Appendix B.

# Supplementary Crystallographic Data

**Table B1. Summary of crystallographic data for complexes 1 and 1a.**

| | **1** | **1a** |
|---|---|---|
| Empirical Formula | $C_{32}H_{76}N_4Cl_2Sc_2O_4Si_4$ | $C_{20}H_{49}N_2O_2ScSi_3$ |
| MW (g mol$^{-1}$) | 854.13 | 478.83 |
| Crystal system | Monoclinic | Orthorhombic |
| Space Group | P $2_1/c$ | P $n$ $a$ $2_1$ |
| a (Å) | 13.6831(7) | 16.8406(5) |
| b (Å) | 15.4037(7) | 10.4944(3) |
| c (Å) | 23.2729(11) | 16.6330(5) |
| α (°) | 90 | 90 |
| β (°) | 105.2899(9) | 90 |
| γ (°) | 90 | 90 |
| Vol. (Å$^3$) | 4731.6(4) | 2939.58(15) |
| Z | 12 | 6 |
| T (K) | 150 | 150 |
| ρ (g cm$^{-3}$) | 1.199 | 1.082 |
| μ (mm$^{-1}$) | 0.536 | 0.388 |
| Total/Unique Reflections | 87500 / 14596 | 44909 / 11271 |
| Refined Reflections | 8369 | 8023 |
| R [$I_o \geq n\sigma(I_o)$] | 0.0461 | 0.0332 |
| Rw [$I_o \geq n\sigma(I_o)$] | 0.0506 | 0.0375 |
| Goodness of Fit | 0.9680 | 0.9773 |

Note: For R-values, n = 2 for **1**, n = 3 for **1a**.

**Table B2. Summary of crystallographic data for complexes 2 and 2a.**

| | **2** | **2a** |
|---|---|---|
| Empirical Formula | $C_{24}H_{60}N_4Cl_2O_2Si_4Ti_2$ | $C_{24}H_{62}N_4O_4Si_4Ti_2$ |
| $M_W$ (g mol$^{-1}$) | 715.74 | 678.85 |
| Crystal system | Monoclinic | Triclinic |
| Space Group | P $2_1/n$ | P $\bar{1}$ |
| a (Å) | 10.8952(2) | 8.3561(2) |
| b (Å) | 11.3011(2) | 10.5524(2) |
| c (Å) | 16.1530(3) | 11.6276(3) |
| α (°) | 90 | 68.2692(9) |
| β (°) | 104.0936(8) | 86.9529(10) |
| γ (°) | 90 | 71.9988(9) |
| Vol. (Å$^3$) | 1929.02(4) | 903.62(2) |
| Z | 4 | 1 |
| T (K) | 150 | 150 |
| ρ (g cm$^{-3}$) | 1.211 | 1.248 |
| μ (mm$^{-1}$) | 0.701 | 0.607 |
| Total/Unique Reflections | 37799 / 3554 | 125571 / 14265 |
| Refined Reflections | 3329 | 9998 |
| R [$I_o \geq 3\sigma(I_o)$] | 0.0491 | 0.0307 |
| $R_w$ [$I_o \geq 3\sigma(I_o)$] | 0.0816 | 0.0407 |
| Goodness of Fit | 1.0980 | 1.0563 |

**Table B3. Summary of crystallographic data for complexes 3, 3a, and 3b.**

| | **3** | **3a** | **3b** |
|---|---|---|---|
| Empirical Formula | $C_{24}H_{60}N_4Cl_2O_2Si_4V_2$ | $C_{32}H_{82}N_6O_2Si_6V_2$ | $C_{38}H_{74}N_6O_2Si_4V_2$ |
| $M_W$ (g mol$^{-1}$) | 721.89 | 853.43 | 861.26 |
| Crystal system | Triclinic | Triclinic | Triclinic |
| Space Group | P $\bar{1}$ | P $\bar{1}$ | P $\bar{1}$ |
| a (Å) | 10.5159(5) | 9.4236(2) | 9.2261(3) |
| b (Å) | 12.3566(6) | 14.4353(3) | 14.9339(6) |
| c (Å) | 16.5815(9) | 19.5632(3) | 18.6754(7) |
| α (°) | 79.5984(13) | 73.2482(8) | 73.3913(13) |
| β (°) | 72.7813(12) | 89.9215(9) | 89.7952(13) |
| γ (°) | 71.2715(12) | 72.3682(8) | 74.3371(13) |
| Vol. (Å$^3$) | 1940.35(11) | 2417.79(8) | 2366.65(9) |
| Z | 4 | 4 | 2 |
| T (K) | 150 | 150 | 150 |
| ρ (g cm$^{-3}$) | 1.236 | 1.172 | 1.209 |
| μ (mm$^{-1}$) | 0.768 | 4.913 | 0.533 |
| Total/Unique Reflections | 43344 / 8835 | 9394 / 9394 | 34703 / 9953 |
| Refined Reflections | 6523 | 7548 | 6775 |
| R [$I_o \geq n\sigma(I_o)$] | 0.0395 | 0.0395 | 0.0367 |
| $R_w$ [$I_o \geq n\sigma(I_o)$] | 0.0542 | 0.0402 | 0.0454 |
| Goodness of Fit | 1.0794 | 1.0767 | 1.0541 |

Note: For R-values, n = 3 for **3**, n = 2 for **3a**, and n = 3 for **3b**.

**Table B4. Summary of crystallographic data for complexes 4 and 5.**

| | **4** | **5** |
|---|---|---|
| Empirical Formula | $C_{28}H_{38}N_2Cl_2F_{12}FeLiO_5Si_2$ | $C_{48}H_{56}N_4ClCo_2F_{24}LiO_6Si_4$ |
| $M_W$ (g mol$^{-1}$) | 900.45 | 1513.54 |
| Crystal system | Triclinic | Monoclinic |
| Space Group | P $\bar{1}$ | Cc |
| a (Å) | 9.8564(3) | 10.9573(5) |
| b (Å) | 12.8273(3) | 24.0356(11) |
| c (Å) | 17.2463(4) | 25.3112(11) |
| α (°) | 81.1870(11) | 90 |
| β (°) | 86.2970(11) | 101.0540(10) |
| γ (°) | 68.3202(11) | 90 |
| Vol. (Å$^3$) | 2002.23(5) | 6542.4(5) |
| Z | 4 | 8 |
| T (K) | 150 | 150 |
| ρ (g cm$^{-3}$) | 1.493 | 1.529 |
| μ (mm$^{-1}$) | 0.663 | 0.735 |
| Total/Unique Reflections | 103879 / 23868 | 77716 / 12755 |
| Refined Reflections | 16664 | 10632 |
| R [$I_o \geq 3\sigma (I_o)$] | 0.0558 | 0.0585 |
| $R_w$ [$I_o \geq 3\sigma (I_o)$] | 0.0953 | 0.0772 |
| Goodness of Fit | 1.1911 | 0.9948 |

# Appendix C.

# Fractional Atomic Coordinates and Isotropic Thermal Parameters

**Table C1. {[$^{t\text{Bu}}$NON]ScCl•THF}$_2$ (1).**

| Atom | x | y | z | U(iso) (Å$^2$) | Occ | Type |
|---|---|---|---|---|---|---|
| Sc1 | 0.28306(3) | 0.25831(3) | 0.38482(2) | 0.0127 | 1.0000 | Uani |
| Sc2 | -0.01527(3) | 0.21775(3) | 0.342554(19) | 0.0114 | 1.0000 | Uani |
| Cl10 | 0.14904(4) | 0.13561(4) | 0.38250(3) | 0.0202 | 1.0000 | Uani |
| Cl20 | 0.12061(4) | 0.32767(3) | 0.32515(3) | 0.0163 | 1.0000 | Uani |
| Si10 | 0.43461(5) | 0.11952(4) | 0.39640(3) | 0.0195 | 1.0000 | Uani |
| Si11 | 0.39275(5) | 0.22271(4) | 0.50933(3) | 0.0194 | 1.0000 | Uani |
| Si20 | -0.15939(5) | 0.30143(4) | 0.24043(3) | 0.0149 | 1.0000 | Uani |
| Si21 | -0.13494(5) | 0.35790(4) | 0.37760(3) | 0.0157 | 1.0000 | Uani |
| N10 | 0.36827(14) | 0.18288(13) | 0.33995(9) | 0.0171 | 1.0000 | Uani |
| N11 | 0.31827(15) | 0.30449(12) | 0.47287(9) | 0.0167 | 1.0000 | Uani |
| N20 | -0.08859(14) | 0.20976(12) | 0.25204(8) | 0.0133 | 1.0000 | Uani |
| N21 | -0.06629(14) | 0.27168(12) | 0.41177(9) | 0.0154 | 1.0000 | Uani |
| O10 | 0.38893(12) | 0.16364(10) | 0.44900(8) | 0.019 | 1.0000 | Uani |
| O11 | 0.35195(12) | 0.37754(10) | 0.35615(7) | 0.0171 | 1.0000 | Uani |
| O20 | -0.12217(12) | 0.33774(10) | 0.31009(7) | 0.0167 | 1.0000 | Uani |
| O21 | -0.08795(12) | 0.09150(10) | 0.35602(7) | 0.0169 | 1.0000 | Uani |
| C11 | 0.4055(2) | 0.00172(16) | 0.39524(14) | 0.0339 | 1.0000 | Uani |
| C12 | 0.5753(2) | 0.1321(2) | 0.41921(15) | 0.0354 | 1.0000 | Uani |
| C13 | 0.3416(2) | 0.15142(19) | 0.55932(14) | 0.0354 | 1.0000 | Uani |
| C14 | 0.5269(2) | 0.24992(19) | 0.54769(14) | 0.0355 | 1.0000 | Uani |
| C21 | -0.1272(2) | 0.38604(16) | 0.19155(12) | 0.0249 | 1.0000 | Uani |
| C22 | -0.30028(19) | 0.28855(18) | 0.22002(13) | 0.0275 | 1.0000 | Uani |
| C23 | -0.27293(19) | 0.35997(19) | 0.37453(14) | 0.0302 | 1.0000 | Uani |
| C24 | -0.0836(2) | 0.46917(16) | 0.39694(12) | 0.0254 | 1.0000 | Uani |
| C100 | 0.3614(2) | 0.16995(17) | 0.27583(12) | 0.024 | 1.0000 | Uani |
| C101 | 0.3174(2) | 0.25083(18) | 0.24058(12) | 0.0292 | 1.0000 | Uani |
| C102 | 0.2921(2) | 0.09249(19) | 0.25155(14) | 0.0357 | 1.0000 | Uani |
| C103 | 0.4664(2) | 0.1528(2) | 0.26597(15) | 0.0406 | 1.0000 | Uani |
| C110 | 0.29694(19) | 0.38534(15) | 0.50185(11) | 0.0192 | 1.0000 | Uani |

| | | | | | | |
|---|---|---|---|---|---|---|
| C111 | 0.1965(2) | 0.42469(17) | 0.46623(12) | 0.0257 | 1.0000 | Uani |
| C112 | 0.2895(2) | 0.36870(19) | 0.56549(12) | 0.0284 | 1.0000 | Uani |
| C113 | 0.3811(2) | 0.45196(17) | 0.50465(13) | 0.029 | 1.0000 | Uani |
| C200 | -0.06538(19) | 0.15560(15) | 0.20462(10) | 0.017 | 1.0000 | Uani |
| C201 | -0.0344(2) | 0.06446(16) | 0.22910(12) | 0.0253 | 1.0000 | Uani |
| C202 | 0.0230(2) | 0.19543(17) | 0.18463(12) | 0.0249 | 1.0000 | Uani |
| C203 | -0.15785(19) | 0.14795(16) | 0.15063(11) | 0.0226 | 1.0000 | Uani |
| C210 | -0.0542(2) | 0.24804(17) | 0.47485(11) | 0.0216 | 1.0000 | Uani |
| C211 | -0.1414(2) | 0.1904(2) | 0.48122(14) | 0.0385 | 1.0000 | Uani |
| C212 | -0.0515(3) | 0.32856(19) | 0.51359(13) | 0.0351 | 1.0000 | Uani |
| C213 | 0.0451(2) | 0.1990(2) | 0.49850(13) | 0.0343 | 1.0000 | Uani |
| C300 | 0.46197(17) | 0.38340(16) | 0.36767(13) | 0.0224 | 1.0000 | Uani |
| C301 | 0.30574(18) | 0.45459(15) | 0.32418(12) | 0.0215 | 1.0000 | Uani |
| C302 | 0.48175(19) | 0.46167(17) | 0.33282(14) | 0.0284 | 1.0000 | Uani |
| C303 | 0.39120(19) | 0.51990(16) | 0.33135(14) | 0.0269 | 1.0000 | Uani |
| C304 | -0.19861(18) | 0.08871(16) | 0.33310(12) | 0.021 | 1.0000 | Uani |
| C305 | -0.0510(2) | 0.00621(15) | 0.37877(12) | 0.023 | 1.0000 | Uani |
| C306 | -0.2296(2) | 0.00055(17) | 0.35109(13) | 0.0277 | 1.0000 | Uani |
| C307 | -0.1373(2) | -0.05532(16) | 0.35211(13) | 0.0268 | 1.0000 | Uani |
| H111 | 0.4365 | -0.0239 | 0.4334 | 0.0472(10) | 1.0000 | Uiso |
| H113 | 0.3334 | -0.0063 | 0.3862 | 0.0474(10) | 1.0000 | Uiso |
| H112 | 0.4307 | -0.0265 | 0.3652 | 0.0473(10) | 1.0000 | Uiso |
| H122 | 0.6017 | 0.103 | 0.4561 | 0.0491(10) | 1.0000 | Uiso |
| H121 | 0.5938 | 0.1923 | 0.4232 | 0.0496(10) | 1.0000 | Uiso |
| H123 | 0.6039 | 0.1061 | 0.3897 | 0.0498(10) | 1.0000 | Uiso |
| H132 | 0.3803 | 0.0994 | 0.5663 | 0.0505(10) | 1.0000 | Uiso |
| H133 | 0.3459 | 0.18 | 0.5969 | 0.0506(10) | 1.0000 | Uiso |
| H131 | 0.2719 | 0.1376 | 0.5401 | 0.0511(10) | 1.0000 | Uiso |
| H141 | 0.566 | 0.1977 | 0.5573 | 0.0503(10) | 1.0000 | Uiso |
| H143 | 0.5292 | 0.2815 | 0.5836 | 0.0504(10) | 1.0000 | Uiso |
| H142 | 0.5566 | 0.2848 | 0.5226 | 0.0505(10) | 1.0000 | Uiso |
| H212 | -0.1614 | 0.4399 | 0.1946 | 0.0326(10) | 1.0000 | Uiso |
| H211 | -0.0553 | 0.3959 | 0.2044 | 0.0325(10) | 1.0000 | Uiso |
| H213 | -0.1449 | 0.3664 | 0.1506 | 0.0324(10) | 1.0000 | Uiso |
| H222 | -0.3302 | 0.3429 | 0.2262 | 0.0368(10) | 1.0000 | Uiso |
| H223 | -0.3197 | 0.2451 | 0.2448 | 0.0363(10) | 1.0000 | Uiso |
| H221 | -0.3248 | 0.272 | 0.1785 | 0.0367(10) | 1.0000 | Uiso |

| | | | | | | |
|---|---|---|---|---|---|---|
| H231 | -0.3075 | 0.4033 | 0.3464 | 0.0406(10) | 1.0000 | Uiso |
| H232 | -0.2822 | 0.3735 | 0.4133 | 0.0403(10) | 1.0000 | Uiso |
| H233 | -0.3029 | 0.3042 | 0.3622 | 0.0405(10) | 1.0000 | Uiso |
| H242 | -0.1196 | 0.5099 | 0.3679 | 0.0327(10) | 1.0000 | Uiso |
| H243 | -0.0891 | 0.4865 | 0.4357 | 0.0323(10) | 1.0000 | Uiso |
| H241 | -0.0133 | 0.4708 | 0.3975 | 0.0324(10) | 1.0000 | Uiso |
| H1013 | 0.3082 | 0.2404 | 0.1987 | 0.0392(10) | 1.0000 | Uiso |
| H1011 | 0.3638 | 0.299 | 0.2529 | 0.0392(10) | 1.0000 | Uiso |
| H1012 | 0.2529 | 0.266 | 0.2475 | 0.0394(10) | 1.0000 | Uiso |
| H1021 | 0.2848 | 0.0874 | 0.2094 | 0.0491(10) | 1.0000 | Uiso |
| H1022 | 0.3228 | 0.0393 | 0.2708 | 0.0491(10) | 1.0000 | Uiso |
| H1023 | 0.2261 | 0.1006 | 0.2588 | 0.0490(10) | 1.0000 | Uiso |
| H1032 | 0.46 | 0.1472 | 0.2238 | 0.0574(10) | 1.0000 | Uiso |
| H1033 | 0.5118 | 0.201 | 0.2817 | 0.0573(10) | 1.0000 | Uiso |
| H1031 | 0.4941 | 0.0993 | 0.2859 | 0.0574(10) | 1.0000 | Uiso |
| H1113 | 0.1829 | 0.4769 | 0.4865 | 0.0334(10) | 1.0000 | Uiso |
| H1111 | 0.1431 | 0.3831 | 0.4637 | 0.0337(10) | 1.0000 | Uiso |
| H1112 | 0.2004 | 0.4405 | 0.4266 | 0.0335(10) | 1.0000 | Uiso |
| H1121 | 0.2732 | 0.4226 | 0.583 | 0.0374(10) | 1.0000 | Uiso |
| H1122 | 0.3544 | 0.3481 | 0.5904 | 0.0371(10) | 1.0000 | Uiso |
| H1123 | 0.2375 | 0.3258 | 0.5658 | 0.0377(10) | 1.0000 | Uiso |
| H1133 | 0.3673 | 0.5052 | 0.5234 | 0.0391(10) | 1.0000 | Uiso |
| H1131 | 0.445 | 0.4288 | 0.5277 | 0.0390(10) | 1.0000 | Uiso |
| H1132 | 0.3849 | 0.4662 | 0.4648 | 0.0393(10) | 1.0000 | Uiso |
| H2011 | -0.0183 | 0.0293 | 0.1985 | 0.0330(10) | 1.0000 | Uiso |
| H2013 | 0.0255 | 0.0681 | 0.2631 | 0.0333(10) | 1.0000 | Uiso |
| H2012 | -0.0898 | 0.0382 | 0.2412 | 0.0329(10) | 1.0000 | Uiso |
| H2022 | 0.0431 | 0.1578 | 0.157 | 0.0324(10) | 1.0000 | Uiso |
| H2021 | 0.0796 | 0.2034 | 0.2186 | 0.0322(10) | 1.0000 | Uiso |
| H2023 | 0.0031 | 0.2515 | 0.1662 | 0.0327(10) | 1.0000 | Uiso |
| H2033 | -0.1438 | 0.1083 | 0.1215 | 0.0293(10) | 1.0000 | Uiso |
| H2031 | -0.2154 | 0.1269 | 0.1628 | 0.0292(10) | 1.0000 | Uiso |
| H2032 | -0.1753 | 0.204 | 0.1321 | 0.0296(10) | 1.0000 | Uiso |
| H2111 | -0.1339 | 0.1759 | 0.523 | 0.0525(10) | 1.0000 | Uiso |
| H2113 | -0.2057 | 0.2204 | 0.4666 | 0.0522(10) | 1.0000 | Uiso |
| H2112 | -0.1411 | 0.1362 | 0.459 | 0.0524(10) | 1.0000 | Uiso |
| H2122 | -0.0401 | 0.3117 | 0.5552 | 0.0474(10) | 1.0000 | Uiso |

| | | | | | | |
|---|---|---|---|---|---|---|
| H2121 | -0.1164 | 0.3599 | 0.5007 | 0.0477(10) | 1.0000 | Uiso |
| H2123 | 0.0039 | 0.3663 | 0.5102 | 0.0474(10) | 1.0000 | Uiso |
| H2131 | 0.0544 | 0.1865 | 0.5403 | 0.0475(10) | 1.0000 | Uiso |
| H2133 | 0.1021 | 0.2338 | 0.4942 | 0.0474(10) | 1.0000 | Uiso |
| H2132 | 0.0419 | 0.1436 | 0.4768 | 0.0475(10) | 1.0000 | Uiso |
| H3002 | 0.4929 | 0.3904 | 0.4103 | 0.0226(10) | 1.0000 | Uiso |
| H3001 | 0.4866 | 0.3299 | 0.3542 | 0.0228(10) | 1.0000 | Uiso |
| H3012 | 0.2517 | 0.4758 | 0.3404 | 0.0206(10) | 1.0000 | Uiso |
| H3011 | 0.2787 | 0.4396 | 0.2824 | 0.0208(10) | 1.0000 | Uiso |
| H3022 | 0.5456 | 0.4903 | 0.3519 | 0.0305(10) | 1.0000 | Uiso |
| H3021 | 0.4809 | 0.4437 | 0.2925 | 0.0307(10) | 1.0000 | Uiso |
| H3031 | 0.4013 | 0.5511 | 0.3694 | 0.0275(10) | 1.0000 | Uiso |
| H3032 | 0.3775 | 0.561 | 0.2985 | 0.0278(10) | 1.0000 | Uiso |
| H3041 | -0.2275 | 0.137 | 0.3512 | 0.0205(10) | 1.0000 | Uiso |
| H3042 | -0.2164 | 0.0946 | 0.2899 | 0.0202(10) | 1.0000 | Uiso |
| H3051 | -0.0357 | 0.0064 | 0.4223 | 0.0235(10) | 1.0000 | Uiso |
| H3052 | 0.0095 | -0.0078 | 0.3664 | 0.0236(10) | 1.0000 | Uiso |
| H3061 | -0.24 | 0.0028 | 0.3907 | 0.0287(10) | 1.0000 | Uiso |
| H3062 | -0.2899 | -0.0215 | 0.3224 | 0.0281(10) | 1.0000 | Uiso |
| H3071 | -0.1346 | -0.1073 | 0.3756 | 0.0288(10) | 1.0000 | Uiso |
| H3072 | -0.1359 | -0.071 | 0.3118 | 0.0287(10) | 1.0000 | Uiso |

**Table C2. [$^{tBu}$NON]ScCH$_2$SiMe$_3$•THF (1a).**

| Atom | x | y | z | U(iso) (Å$^2$) | Occ | Type |
|---|---|---|---|---|---|---|
| Sc1 | 0.736399(17) | 0.57815(3) | 0.27953(5) | 0.019 | 1.0000 | Uani |
| Si1 | 0.70336(4) | 0.47792(5) | 0.44031(6) | 0.0309 | 1.0000 | Uani |
| Si2 | 0.57019(3) | 0.50603(5) | 0.30256(6) | 0.0309 | 1.0000 | Uani |
| Si3 | 0.71475(3) | 0.92271(5) | 0.29435(6) | 0.0318 | 1.0000 | Uani |
| N1 | 0.78712(9) | 0.50766(15) | 0.38685(10) | 0.0252 | 1.0000 | Uani |
| N2 | 0.62926(9) | 0.53037(15) | 0.22130(11) | 0.0261 | 1.0000 | Uani |
| O1 | 0.63982(8) | 0.53346(13) | 0.37150(9) | 0.0281 | 1.0000 | Uani |
| O2 | 0.82285(8) | 0.50668(13) | 0.19371(9) | 0.0279 | 1.0000 | Uani |
| C1 | 0.68544(18) | 0.5709(3) | 0.53441(15) | 0.0594 | 1.0000 | Uani |
| C2 | 0.67774(16) | 0.3088(2) | 0.46290(17) | 0.0501 | 1.0000 | Uani |
| C3 | 0.49099(14) | 0.6239(3) | 0.32501(18) | 0.0572 | 1.0000 | Uani |
| C4 | 0.52633(15) | 0.3446(2) | 0.31649(17) | 0.0531 | 1.0000 | Uani |
| C5 | 0.76925(11) | 0.78119(17) | 0.26128(12) | 0.0305 | 1.0000 | Uani |
| C6 | 0.68007(19) | 0.9071(3) | 0.40096(16) | 0.0544 | 1.0000 | Uani |
| C7 | 0.62539(16) | 0.9483(3) | 0.22954(17) | 0.0565 | 1.0000 | Uani |
| C8 | 0.77626(16) | 1.0721(2) | 0.2886(2) | 0.0571 | 1.0000 | Uani |
| C10 | 0.86822(12) | 0.5048(2) | 0.42117(13) | 0.0317 | 1.0000 | Uani |
| C20 | 0.60400(13) | 0.5265(2) | 0.13670(14) | 0.0375 | 1.0000 | Uani |
| C21 | 0.83432(15) | 0.3709(2) | 0.17942(18) | 0.0479 | 1.0000 | Uani |
| C22 | 0.88126(14) | 0.5800(3) | 0.14762(15) | 0.0428 | 1.0000 | Uani |
| C23 | 0.91582(19) | 0.3632(3) | 0.1413(2) | 0.0667 | 1.0000 | Uani |
| C24 | 0.92927(17) | 0.4857(3) | 0.10257(18) | 0.0635 | 1.0000 | Uani |
| C100 | 0.88220(16) | 0.6221(2) | 0.47352(16) | 0.048 | 1.0000 | Uani |
| C101 | 0.88151(15) | 0.3827(2) | 0.47019(17) | 0.0472 | 1.0000 | Uani |
| C102 | 0.92974(13) | 0.5068(3) | 0.35352(15) | 0.0464 | 1.0000 | Uani |
| C200 | 0.5924(2) | 0.3873(3) | 0.11035(19) | 0.077 | 1.0000 | Uani |
| C201 | 0.52754(19) | 0.6013(4) | 0.1234(2) | 0.0811 | 1.0000 | Uani |
| C202 | 0.66691(17) | 0.5843(3) | 0.08344(15) | 0.0538 | 1.0000 | Uani |
| H11 | 0.6324 | 0.5556 | 0.5543 | 0.078(3) | 1.0000 | Uiso |
| H12 | 0.7207 | 0.5397 | 0.5756 | 0.077(3) | 1.0000 | Uiso |
| H13 | 0.6942 | 0.6622 | 0.5248 | 0.078(3) | 1.0000 | Uiso |
| H21 | 0.6807 | 0.2539 | 0.4157 | 0.065(3) | 1.0000 | Uiso |
| H22 | 0.6253 | 0.301 | 0.4821 | 0.065(3) | 1.0000 | Uiso |
| H23 | 0.7147 | 0.2721 | 0.5003 | 0.065(3) | 1.0000 | Uiso |
| H31 | 0.4706 | 0.6081 | 0.3789 | 0.077(3) | 1.0000 | Uiso |

| | | | | | | |
|---|---|---|---|---|---|---|
| H32 | 0.4494 | 0.615 | 0.2866 | 0.077(3) | 1.0000 | Uiso |
| H33 | 0.5107 | 0.7118 | 0.3205 | 0.076(3) | 1.0000 | Uiso |
| H41 | 0.5647 | 0.2811 | 0.3075 | 0.071(3) | 1.0000 | Uiso |
| H42 | 0.5054 | 0.3375 | 0.3711 | 0.071(3) | 1.0000 | Uiso |
| H43 | 0.4829 | 0.3323 | 0.2792 | 0.070(3) | 1.0000 | Uiso |
| H51 | 0.82 | 0.7892 | 0.2856 | 0.037(3) | 1.0000 | Uiso |
| H52 | 0.7742 | 0.7906 | 0.2047 | 0.037(3) | 1.0000 | Uiso |
| H61 | 0.6547 | 0.9864 | 0.4198 | 0.079(3) | 1.0000 | Uiso |
| H62 | 0.7244 | 0.8943 | 0.4366 | 0.078(3) | 1.0000 | Uiso |
| H63 | 0.6426 | 0.8359 | 0.4076 | 0.078(3) | 1.0000 | Uiso |
| H71 | 0.5914 | 0.8727 | 0.2309 | 0.089(3) | 1.0000 | Uiso |
| H72 | 0.5971 | 1.023 | 0.2479 | 0.088(3) | 1.0000 | Uiso |
| H73 | 0.644 | 0.9638 | 0.1756 | 0.088(3) | 1.0000 | Uiso |
| H81 | 0.7416 | 1.1391 | 0.2989 | 0.082(3) | 1.0000 | Uiso |
| H82 | 0.7968 | 1.0824 | 0.2354 | 0.081(3) | 1.0000 | Uiso |
| H83 | 0.8181 | 1.0701 | 0.3299 | 0.082(3) | 1.0000 | Uiso |
| H211 | 0.7926 | 0.3428 | 0.1431 | 0.079(4) | 1.0000 | Uiso |
| H212 | 0.833 | 0.3227 | 0.2298 | 0.080(4) | 1.0000 | Uiso |
| H221 | 0.915 | 0.6285 | 0.1865 | 0.070(4) | 1.0000 | Uiso |
| H222 | 0.8541 | 0.6356 | 0.1105 | 0.071(4) | 1.0000 | Uiso |
| H231 | 0.9558 | 0.3538 | 0.1855 | 0.100(4) | 1.0000 | Uiso |
| H232 | 0.9185 | 0.2929 | 0.1052 | 0.099(4) | 1.0000 | Uiso |
| H241 | 0.985 | 0.5063 | 0.0992 | 0.096(4) | 1.0000 | Uiso |
| H242 | 0.9066 | 0.482 | 0.047 | 0.097(4) | 1.0000 | Uiso |
| H1001 | 0.9376 | 0.6187 | 0.4925 | 0.054(2) | 1.0000 | Uiso |
| H1002 | 0.8461 | 0.6141 | 0.52 | 0.054(2) | 1.0000 | Uiso |
| H1003 | 0.8727 | 0.7023 | 0.4431 | 0.053(2) | 1.0000 | Uiso |
| H1011 | 0.8435 | 0.3893 | 0.5142 | 0.054(2) | 1.0000 | Uiso |
| H1012 | 0.9361 | 0.3845 | 0.4896 | 0.054(2) | 1.0000 | Uiso |
| H1013 | 0.8715 | 0.3067 | 0.4372 | 0.053(2) | 1.0000 | Uiso |
| H1021 | 0.9837 | 0.5051 | 0.3771 | 0.052(2) | 1.0000 | Uiso |
| H1022 | 0.9239 | 0.4295 | 0.3195 | 0.052(2) | 1.0000 | Uiso |
| H1023 | 0.9236 | 0.5847 | 0.3226 | 0.052(2) | 1.0000 | Uiso |
| H2001 | 0.6437 | 0.342 | 0.1197 | 0.100(2) | 1.0000 | Uiso |
| H2002 | 0.5773 | 0.3879 | 0.0543 | 0.100(2) | 1.0000 | Uiso |
| H2003 | 0.5487 | 0.3527 | 0.143 | 0.100(2) | 1.0000 | Uiso |
| H2011 | 0.5345 | 0.6903 | 0.1403 | 0.100(2) | 1.0000 | Uiso |

| | | | | | | |
|---|---|---|---|---|---|---|
| H2012 | 0.4866 | 0.5599 | 0.1546 | 0.101(2) | 1.0000 | Uiso |
| H2013 | 0.5134 | 0.5973 | 0.0663 | 0.100(2) | 1.0000 | Uiso |
| H2021 | 0.6477 | 0.5851 | 0.028 | 0.062(2) | 1.0000 | Uiso |
| H2022 | 0.6781 | 0.6732 | 0.0997 | 0.063(2) | 1.0000 | Uiso |
| H2023 | 0.7134 | 0.5322 | 0.0876 | 0.062(2) | 1.0000 | Uiso |

**Table C3. {[$^{t\text{Bu}}$NON]TiCl}$_2$ (2).**

| Atom | x | y | z | U(iso) (Å$^2$) | Occ | Type |
|---|---|---|---|---|---|---|
| Ti1 | -0.01141(4) | 0.62696(4) | 0.44803(3) | 0.027 | 1.0000 | Uani |
| Cl10 | 0.05344(15) | 0.57684(14) | 0.59733(9) | 0.0303 | 0.5000 | Uani |
| Cl11 | 0.11354(16) | 0.56703(15) | 0.58659(10) | 0.037 | 0.5000 | Uani |
| Si1 | -0.20407(7) | 0.76534(7) | 0.34647(5) | 0.0314 | 1.0000 | Uani |
| Si2 | 0.04690(8) | 0.69709(8) | 0.29602(5) | 0.0367 | 1.0000 | Uani |
| N1 | -0.1470(2) | 0.7370(2) | 0.45358(15) | 0.0321 | 1.0000 | Uani |
| N2 | 0.1287(2) | 0.6774(3) | 0.39958(17) | 0.0455 | 1.0000 | Uani |
| O1 | -0.09725(16) | 0.68353(15) | 0.31345(11) | 0.0252 | 1.0000 | Uani |
| C1 | -0.1974(4) | 0.9215(3) | 0.3118(3) | 0.062 | 1.0000 | Uani |
| C2 | -0.3612(3) | 0.7020(3) | 0.2935(3) | 0.0535 | 1.0000 | Uani |
| C3 | 0.0603(6) | 0.8414(4) | 0.2431(3) | 0.0822 | 1.0000 | Uani |
| C4 | 0.0608(3) | 0.5747(3) | 0.2215(2) | 0.0486 | 1.0000 | Uani |
| C10 | -0.1949(4) | 0.7948(3) | 0.5226(2) | 0.0492 | 1.0000 | Uani |
| C13 | -0.1035(4) | 0.8846(4) | 0.5657(3) | 0.0605 | 1.0000 | Uani |
| C20 | 0.2676(3) | 0.6941(5) | 0.4328(3) | 0.072 | 1.0000 | Uani |
| C23 | 0.2951(5) | 0.7910(5) | 0.4907(6) | 0.1503 | 1.0000 | Uani |
| C110 | -0.3207(6) | 0.8254(11) | 0.5039(5) | 0.07 | 0.513(5) | Uani |
| C111 | -0.3179(7) | 0.8869(7) | 0.4710(5) | 0.0507 | 0.487(5) | Uani |
| C120 | -0.2592(9) | 0.7072(7) | 0.5615(6) | 0.0603 | 0.487(5) | Uani |
| C121 | -0.1582(8) | 0.7022(7) | 0.6087(4) | 0.0554 | 0.513(5) | Uani |
| C210 | 0.3145(7) | 0.7883(9) | 0.3611(7) | 0.0802 | 0.523(5) | Uani |
| C211 | 0.3412(7) | 0.6285(9) | 0.3735(6) | 0.0661 | 0.477(5) | Uani |
| C220 | 0.3151(7) | 0.5936(11) | 0.5183(6) | 0.0718 | 0.477(5) | Uani |
| C221 | 0.3351(6) | 0.5960(7) | 0.4462(7) | 0.0754 | 0.523(5) | Uani |
| H11 | -0.2073 | 0.9224 | 0.2512 | 0.0945 | 1.0000 | Uiso |
| H13 | -0.2643 | 0.9655 | 0.3266 | 0.0941 | 1.0000 | Uiso |
| H12 | -0.1174 | 0.9572 | 0.3389 | 0.0935 | 1.0000 | Uiso |
| H21 | -0.3687 | 0.6927 | 0.2329 | 0.081 | 1.0000 | Uiso |
| H23 | -0.4288 | 0.7517 | 0.3017 | 0.0813 | 1.0000 | Uiso |
| H22 | -0.3669 | 0.6254 | 0.3181 | 0.0806 | 1.0000 | Uiso |
| H31 | -0.0065 | 0.8452 | 0.192 | 0.1192 | 1.0000 | Uiso |
| H32 | 0.054 | 0.9056 | 0.2809 | 0.1187 | 1.0000 | Uiso |
| H33 | 0.1397 | 0.8438 | 0.2298 | 0.1193 | 1.0000 | Uiso |
| H41 | 0.004 | 0.5887 | 0.167 | 0.0758 | 1.0000 | Uiso |
| H42 | 0.1459 | 0.5716 | 0.2154 | 0.0763 | 1.0000 | Uiso |

| | | | | | | |
|---|---|---|---|---|---|---|
| H43 | 0.0398 | 0.5013 | 0.2448 | 0.0755 | 1.0000 | Uiso |
| H131 | -0.131 | 0.9208 | 0.6122 | 0.0918 | 1.0000 | Uiso |
| H132 | -0.0946 | 0.9461 | 0.5248 | 0.0924 | 1.0000 | Uiso |
| H133 | -0.0215 | 0.848 | 0.5887 | 0.0923 | 1.0000 | Uiso |
| H232 | 0.3846 | 0.7934 | 0.5185 | 0.2018 | 1.0000 | Uiso |
| H231 | 0.2453 | 0.7835 | 0.5329 | 0.2025 | 1.0000 | Uiso |
| H233 | 0.2726 | 0.8627 | 0.4577 | 0.2022 | 1.0000 | Uiso |
| H1201 | -0.2877 | 0.7437 | 0.607 | 0.0909 | 0.487(5) | Uiso |
| H1202 | -0.2019 | 0.6437 | 0.5849 | 0.0908 | 0.487(5) | Uiso |
| H1203 | -0.3303 | 0.6767 | 0.5191 | 0.0911 | 0.487(5) | Uiso |
| H2111 | 0.4308 | 0.6336 | 0.3973 | 0.0969 | 0.477(5) | Uiso |
| H2112 | 0.3209 | 0.6674 | 0.3185 | 0.0969 | 0.477(5) | Uiso |
| H2113 | 0.3161 | 0.5468 | 0.3668 | 0.0967 | 0.477(5) | Uiso |
| H2211 | 0.4225 | 0.5992 | 0.4675 | 0.0902 | 0.523(5) | Uiso |
| H2212 | 0.2963 | 0.5228 | 0.4347 | 0.0903 | 0.523(5) | Uiso |
| H1101 | -0.3394 | 0.8614 | 0.5526 | 0.083 | 0.513(5) | Uiso |
| H1102 | -0.3417 | 0.8783 | 0.4569 | 0.083 | 0.513(5) | Uiso |
| H1103 | -0.3687 | 0.7547 | 0.4905 | 0.083 | 0.513(5) | Uiso |
| H2213 | 0.3452 | 0.6003 | 0.3895 | 0.0901 | 0.523(5) | Uiso |

**Table C4. {[$^{t\text{Bu}}$NON]Ti(OH)}$_2$ (2a).**

| Atom | x | y | z | U(iso) (Å$^2$) | Occ | Type |
|---|---|---|---|---|---|---|
| Ti1 | 0.442137(15) | 0.522531(13) | 0.383194(11) | 0.0127 | 1.0000 | Uani |
| Si1 | 0.33485(3) | 0.34799(2) | 0.286261(19) | 0.0159 | 1.0000 | Uani |
| Si2 | 0.11316(3) | 0.65728(2) | 0.26228(2) | 0.017 | 1.0000 | Uani |
| N1 | 0.51993(8) | 0.37471(7) | 0.31324(6) | 0.0159 | 1.0000 | Uani |
| N2 | 0.29199(8) | 0.70445(6) | 0.27013(6) | 0.0154 | 1.0000 | Uani |
| O3 | 0.61980(7) | 0.53929(6) | 0.44871(5) | 0.0176 | 1.0000 | Uani |
| O1 | 0.20407(7) | 0.47964(6) | 0.32394(5) | 0.0163 | 1.0000 | Uani |
| C1 | 0.30735(12) | 0.17704(9) | 0.39487(9) | 0.0257 | 1.0000 | Uani |
| C2 | 0.28203(13) | 0.37431(11) | 0.12367(9) | 0.0291 | 1.0000 | Uani |
| C3 | -0.04904(11) | 0.70131(10) | 0.36815(10) | 0.0283 | 1.0000 | Uani |
| C4 | 0.00958(13) | 0.71286(10) | 0.10592(9) | 0.0305 | 1.0000 | Uani |
| C10 | 0.69437(10) | 0.29254(8) | 0.30025(7) | 0.0198 | 1.0000 | Uani |
| C20 | 0.31168(10) | 0.84838(7) | 0.20429(7) | 0.0182 | 1.0000 | Uani |
| C101 | 0.77544(12) | 0.18336(10) | 0.42736(9) | 0.0282 | 1.0000 | Uani |
| C102 | 0.79792(12) | 0.39626(11) | 0.24658(9) | 0.0294 | 1.0000 | Uani |
| C103 | 0.69569(13) | 0.21505(13) | 0.21207(11) | 0.0364 | 1.0000 | Uani |
| C201 | 0.46525(12) | 0.86009(9) | 0.26030(9) | 0.0266 | 1.0000 | Uani |
| C202 | 0.15410(12) | 0.96616(8) | 0.21309(9) | 0.0258 | 1.0000 | Uani |
| C203 | 0.33738(14) | 0.87156(10) | 0.06745(8) | 0.0289 | 1.0000 | Uani |
| H11 | 0.1991 | 0.174 | 0.3826 | 0.0385(7) | 1.0000 | Uiso |
| H13 | 0.3216 | 0.1691 | 0.4781 | 0.0376(7) | 1.0000 | Uiso |
| H12 | 0.3902 | 0.0968 | 0.3845 | 0.0387(7) | 1.0000 | Uiso |
| H21 | 0.1638 | 0.3944 | 0.1099 | 0.0426(7) | 1.0000 | Uiso |
| H23 | 0.313 | 0.4528 | 0.0659 | 0.0429(7) | 1.0000 | Uiso |
| H22 | 0.3393 | 0.2918 | 0.1053 | 0.0432(7) | 1.0000 | Uiso |
| H31 | -0.1351 | 0.6576 | 0.3734 | 0.0423(7) | 1.0000 | Uiso |
| H32 | -0.0954 | 0.8015 | 0.3399 | 0.0420(7) | 1.0000 | Uiso |
| H33 | 0.0039 | 0.6712 | 0.448 | 0.0417(7) | 1.0000 | Uiso |
| H42 | -0.0719 | 0.6626 | 0.1152 | 0.0450(7) | 1.0000 | Uiso |
| H41 | -0.0473 | 0.8142 | 0.0773 | 0.0455(7) | 1.0000 | Uiso |
| H43 | 0.0943 | 0.6939 | 0.0497 | 0.0442(7) | 1.0000 | Uiso |
| H1012 | 0.8893 | 0.131 | 0.4194 | 0.0415(7) | 1.0000 | Uiso |
| H1011 | 0.7786 | 0.2295 | 0.4824 | 0.0405(7) | 1.0000 | Uiso |
| H1013 | 0.716 | 0.1141 | 0.4649 | 0.0409(7) | 1.0000 | Uiso |
| H1021 | 0.9111 | 0.3432 | 0.2317 | 0.0427(7) | 1.0000 | Uiso |

| | | | | | | |
|---|---|---|---|---|---|---|
| H1023 | 0.8088 | 0.4437 | 0.3027 | 0.0425(7) | 1.0000 | Uiso |
| H1022 | 0.7408 | 0.4651 | 0.1655 | 0.0429(7) | 1.0000 | Uiso |
| H1031 | 0.8109 | 0.1623 | 0.2073 | 0.0530(7) | 1.0000 | Uiso |
| H1033 | 0.6453 | 0.2847 | 0.1309 | 0.0531(7) | 1.0000 | Uiso |
| H1032 | 0.6356 | 0.1477 | 0.2455 | 0.0509(7) | 1.0000 | Uiso |
| H2011 | 0.4753 | 0.954 | 0.2154 | 0.0386(7) | 1.0000 | Uiso |
| H2012 | 0.4524 | 0.845 | 0.347 | 0.0388(7) | 1.0000 | Uiso |
| H2013 | 0.5644 | 0.7921 | 0.248 | 0.0390(7) | 1.0000 | Uiso |
| H2022 | 0.1698 | 1.0589 | 0.1711 | 0.0369(7) | 1.0000 | Uiso |
| H2021 | 0.1375 | 0.951 | 0.2991 | 0.0375(7) | 1.0000 | Uiso |
| H2023 | 0.0562 | 0.9639 | 0.1742 | 0.0364(7) | 1.0000 | Uiso |
| H2032 | 0.3546 | 0.9631 | 0.024 | 0.0415(7) | 1.0000 | Uiso |
| H2031 | 0.4335 | 0.7998 | 0.0594 | 0.0422(7) | 1.0000 | Uiso |
| H2033 | 0.2393 | 0.8701 | 0.0266 | 0.0420(7) | 1.0000 | Uiso |
| H1 | 0.6914 | 0.5466 | 0.4211 | 0.05 | 1.0000 | Uiso |

**Table C5. {[$^{t\text{Bu}}$NON]VCl}$_2$ (3).**

| Atom | x | y | z | U(iso) (Å$^2$) | Occ | Type |
|---|---|---|---|---|---|---|
| V1 | 0.03055(5) | 0.36503(4) | 0.46642(3) | 0.0189 | 1.0000 | Uani |
| V2 | 0.52633(4) | 0.13492(4) | -0.03188(3) | 0.0174 | 1.0000 | Uani |
| Cl1 | 0.13409(7) | 0.51899(6) | 0.42324(4) | 0.0261 | 1.0000 | Uani |
| Cl2 | 0.61797(8) | -0.04706(6) | -0.08574(5) | 0.0341 | 1.0000 | Uani |
| Si10 | 0.25476(9) | 0.17611(7) | 0.43729(6) | 0.0324 | 1.0000 | Uani |
| Si11 | 0.05903(9) | 0.29017(7) | 0.31509(5) | 0.0251 | 1.0000 | Uani |
| Si20 | 0.75523(8) | 0.21163(7) | -0.07244(5) | 0.026 | 1.0000 | Uani |
| Si21 | 0.53260(8) | 0.27735(7) | -0.17868(5) | 0.0265 | 1.0000 | Uani |
| N10 | 0.1267(3) | 0.2280(2) | 0.52415(16) | 0.028 | 1.0000 | Uani |
| N11 | -0.0764(2) | 0.34558(19) | 0.39813(14) | 0.0217 | 1.0000 | Uani |
| N20 | 0.6397(2) | 0.1807(2) | 0.01939(15) | 0.0247 | 1.0000 | Uani |
| N21 | 0.4066(2) | 0.2508(2) | -0.09005(14) | 0.0235 | 1.0000 | Uani |
| O10 | 0.1841(2) | 0.27074(16) | 0.36463(13) | 0.0253 | 1.0000 | Uani |
| O20 | 0.66755(19) | 0.20012(16) | -0.13892(12) | 0.0227 | 1.0000 | Uani |
| C1 | 0.4240(4) | 0.2006(4) | 0.4277(3) | 0.0578 | 1.0000 | Uani |
| C2 | 0.2845(5) | 0.0273(3) | 0.4138(3) | 0.0702 | 1.0000 | Uani |
| C3 | 0.0714(4) | 0.1538(3) | 0.2781(2) | 0.0444 | 1.0000 | Uani |
| C4 | 0.0913(4) | 0.3961(3) | 0.2233(2) | 0.0479 | 1.0000 | Uani |
| C5 | 0.9236(3) | 0.0994(3) | -0.0954(2) | 0.0399 | 1.0000 | Uani |
| C6 | 0.7841(4) | 0.3555(3) | -0.0937(3) | 0.0541 | 1.0000 | Uani |
| C7 | 0.5397(4) | 0.4269(3) | -0.2114(3) | 0.05 | 1.0000 | Uani |
| C8 | 0.5488(4) | 0.2088(4) | -0.2733(2) | 0.0448 | 1.0000 | Uani |
| C100 | 0.1034(4) | 0.1789(3) | 0.6130(2) | 0.0356 | 1.0000 | Uani |
| C101 | 0.1952(4) | 0.0553(4) | 0.6215(3) | 0.0605 | 1.0000 | Uani |
| C102 | 0.1322(5) | 0.2522(4) | 0.6659(2) | 0.0552 | 1.0000 | Uani |
| C103 | -0.0491(4) | 0.1761(3) | 0.6471(2) | 0.0416 | 1.0000 | Uani |
| C110 | -0.2279(3) | 0.3717(3) | 0.40671(18) | 0.0246 | 1.0000 | Uani |
| C111 | -0.2544(3) | 0.3246(3) | 0.3355(2) | 0.0374 | 1.0000 | Uani |
| C112 | -0.2935(3) | 0.5012(3) | 0.4016(2) | 0.0362 | 1.0000 | Uani |
| C113 | -0.2941(3) | 0.3158(3) | 0.4915(2) | 0.0352 | 1.0000 | Uani |
| C200 | 0.6358(3) | 0.1887(3) | 0.1078(2) | 0.0392 | 1.0000 | Uani |
| C201 | 0.7400(5) | 0.2487(5) | 0.1105(3) | 0.077 | 1.0000 | Uani |
| C202 | 0.6689(4) | 0.0692(4) | 0.1538(2) | 0.0631 | 1.0000 | Uani |
| C203 | 0.4894(4) | 0.2593(4) | 0.1523(2) | 0.0507 | 1.0000 | Uani |
| C210 | 0.2550(3) | 0.3059(3) | -0.07408(19) | 0.0275 | 1.0000 | Uani |

| | | | | | | |
|---|---|---|---|---|---|---|
| C211 | 0.1976(10) | 0.3439(8) | 0.0121(6) | 0.0541 | 0.448(3) | Uani |
| C212 | 0.2248(8) | 0.4246(6) | -0.0458(5) | 0.0541 | 0.552(3) | Uani |
| C213 | 0.1952(8) | 0.2153(7) | -0.0867(5) | 0.0416 | 0.448(3) | Uani |
| C214 | 0.1686(7) | 0.2406(5) | -0.0017(4) | 0.0416 | 0.552(3) | Uani |
| C215 | 0.2185(9) | 0.4095(7) | -0.1384(5) | 0.0471 | 0.448(3) | Uani |
| C216 | 0.2076(7) | 0.3144(6) | -0.1530(4) | 0.0471 | 0.552(3) | Uani |
| H11 | 0.4904 | 0.1692 | 0.3771 | 0.0899 | 1.0000 | Uiso |
| H12 | 0.4145 | 0.2825 | 0.4233 | 0.0901 | 1.0000 | Uiso |
| H13 | 0.4596 | 0.1631 | 0.4756 | 0.0901 | 1.0000 | Uiso |
| H21 | 0.3364 | -0.0271 | 0.4509 | 0.1063 | 1.0000 | Uiso |
| H22 | 0.337 | 0.018 | 0.3561 | 0.1059 | 1.0000 | Uiso |
| H23 | 0.1956 | 0.0094 | 0.4224 | 0.106 | 1.0000 | Uiso |
| H31 | 0.0134 | 0.1686 | 0.2387 | 0.069 | 1.0000 | Uiso |
| H32 | 0.1661 | 0.1192 | 0.2475 | 0.0686 | 1.0000 | Uiso |
| H33 | 0.0422 | 0.1017 | 0.3254 | 0.0687 | 1.0000 | Uiso |
| H41 | 0.0896 | 0.4654 | 0.2432 | 0.0732 | 1.0000 | Uiso |
| H42 | 0.0211 | 0.4147 | 0.1928 | 0.0732 | 1.0000 | Uiso |
| H43 | 0.1809 | 0.3663 | 0.1858 | 0.0728 | 1.0000 | Uiso |
| H51 | 0.9805 | 0.1173 | -0.1502 | 0.0611 | 1.0000 | Uiso |
| H52 | 0.9082 | 0.0257 | -0.095 | 0.0615 | 1.0000 | Uiso |
| H53 | 0.9709 | 0.0937 | -0.0533 | 0.0609 | 1.0000 | Uiso |
| H61 | 0.8491 | 0.3577 | -0.0646 | 0.0839 | 1.0000 | Uiso |
| H62 | 0.8205 | 0.3722 | -0.1525 | 0.084 | 1.0000 | Uiso |
| H63 | 0.6991 | 0.4146 | -0.0745 | 0.0836 | 1.0000 | Uiso |
| H71 | 0.5232 | 0.4673 | -0.1623 | 0.079 | 1.0000 | Uiso |
| H72 | 0.4706 | 0.4665 | -0.2422 | 0.0788 | 1.0000 | Uiso |
| H73 | 0.6307 | 0.4272 | -0.248 | 0.079 | 1.0000 | Uiso |
| H81 | 0.6365 | 0.2077 | -0.3128 | 0.069 | 1.0000 | Uiso |
| H82 | 0.4758 | 0.2505 | -0.2999 | 0.0692 | 1.0000 | Uiso |
| H83 | 0.5444 | 0.1296 | -0.2576 | 0.0693 | 1.0000 | Uiso |
| H1011 | 0.2931 | 0.0536 | 0.5986 | 0.0948 | 1.0000 | Uiso |
| H1012 | 0.1803 | 0.0268 | 0.6815 | 0.095 | 1.0000 | Uiso |
| H1013 | 0.1724 | 0.0059 | 0.5915 | 0.095 | 1.0000 | Uiso |
| H1021 | 0.0716 | 0.3307 | 0.6626 | 0.0848 | 1.0000 | Uiso |
| H1022 | 0.1144 | 0.2206 | 0.7245 | 0.0851 | 1.0000 | Uiso |
| H1023 | 0.2284 | 0.2526 | 0.644 | 0.0848 | 1.0000 | Uiso |
| H1031 | -0.1136 | 0.2554 | 0.6465 | 0.064 | 1.0000 | Uiso |

| | | | | | | |
|---|---|---|---|---|---|---|
| H1032 | -0.0693 | 0.1312 | 0.6109 | 0.0641 | 1.0000 | Uiso |
| H1033 | -0.0626 | 0.1395 | 0.7052 | 0.0642 | 1.0000 | Uiso |
| H1111 | -0.3522 | 0.3469 | 0.3403 | 0.0579 | 1.0000 | Uiso |
| H1112 | -0.209 | 0.3555 | 0.2807 | 0.0574 | 1.0000 | Uiso |
| H1113 | -0.2217 | 0.2408 | 0.339 | 0.0578 | 1.0000 | Uiso |
| H1121 | -0.2501 | 0.537 | 0.3474 | 0.0569 | 1.0000 | Uiso |
| H1122 | -0.3925 | 0.5194 | 0.4068 | 0.0569 | 1.0000 | Uiso |
| H1123 | -0.2798 | 0.533 | 0.4474 | 0.057 | 1.0000 | Uiso |
| H1131 | -0.2809 | 0.3463 | 0.5379 | 0.0534 | 1.0000 | Uiso |
| H1132 | -0.2521 | 0.2335 | 0.495 | 0.0541 | 1.0000 | Uiso |
| H1133 | -0.3922 | 0.3298 | 0.4981 | 0.0536 | 1.0000 | Uiso |
| H2011 | 0.739 | 0.2499 | 0.1677 | 0.1197 | 1.0000 | Uiso |
| H2012 | 0.7169 | 0.3272 | 0.0846 | 0.1199 | 1.0000 | Uiso |
| H2013 | 0.8328 | 0.2083 | 0.0801 | 0.1199 | 1.0000 | Uiso |
| H2021 | 0.7603 | 0.0235 | 0.1253 | 0.0948 | 1.0000 | Uiso |
| H2022 | 0.6674 | 0.0738 | 0.2112 | 0.0946 | 1.0000 | Uiso |
| H2023 | 0.6003 | 0.0307 | 0.1547 | 0.0948 | 1.0000 | Uiso |
| H2031 | 0.4225 | 0.2207 | 0.1546 | 0.0777 | 1.0000 | Uiso |
| H2032 | 0.4864 | 0.267 | 0.2097 | 0.0778 | 1.0000 | Uiso |
| H2033 | 0.4666 | 0.3348 | 0.1229 | 0.0781 | 1.0000 | Uiso |
| H2111 | 0.1005 | 0.379 | 0.021 | 0.0653 | 0.448(3) | Uiso |
| H2112 | 0.2408 | 0.3975 | 0.0183 | 0.0653 | 0.448(3) | Uiso |
| H2113 | 0.214 | 0.2792 | 0.0524 | 0.0653 | 0.448(3) | Uiso |
| H2121 | 0.128 | 0.462 | -0.0351 | 0.0653 | 0.552(3) | Uiso |
| H2122 | 0.2738 | 0.4689 | -0.0893 | 0.0653 | 0.552(3) | Uiso |
| H2123 | 0.254 | 0.4169 | 0.0045 | 0.0653 | 0.552(3) | Uiso |
| H2131 | 0.0973 | 0.2454 | -0.0773 | 0.0501 | 0.448(3) | Uiso |
| H2132 | 0.2347 | 0.1941 | -0.1431 | 0.0501 | 0.448(3) | Uiso |
| H2133 | 0.2163 | 0.1497 | -0.0478 | 0.0501 | 0.448(3) | Uiso |
| H2141 | 0.0726 | 0.2797 | 0.0057 | 0.0501 | 0.552(3) | Uiso |
| H2142 | 0.1939 | 0.2368 | 0.0494 | 0.0501 | 0.552(3) | Uiso |
| H2143 | 0.1863 | 0.165 | -0.0159 | 0.0501 | 0.552(3) | Uiso |
| H2151 | 0.1206 | 0.4422 | -0.1258 | 0.0563 | 0.448(3) | Uiso |
| H2152 | 0.2612 | 0.4653 | -0.1356 | 0.0563 | 0.448(3) | Uiso |
| H2153 | 0.2512 | 0.3848 | -0.1938 | 0.0563 | 0.448(3) | Uiso |
| H2161 | 0.1103 | 0.3499 | -0.1416 | 0.0563 | 0.552(3) | Uiso |
| H2162 | 0.2543 | 0.3587 | -0.1978 | 0.0563 | 0.552(3) | Uiso |

| | | | | | | |
|---|---|---|---|---|---|---|
| H2163 | 0.2278 | 0.2394 | -0.1691 | 0.0563 | 0.552(3) | Uiso |

**Table C6. {[$^{t\text{Bu}}$NON]VCH$_2$SiMe$_3$}$_2$($\mu$-N$_2$) (3a).**

| Atom | x | y | z | U(iso) (Å$^2$) | Occ | Type |
|---|---|---|---|---|---|---|
| V1 | 0.30643(4) | 0.15553(2) | 0.154435(18) | 0.0141 | 1.0000 | Uani |
| V2 | 0.44479(4) | -0.15184(2) | 0.344120(18) | 0.0149 | 1.0000 | Uani |
| Si1 | 0.06657(7) | 0.34015(4) | 0.22462(3) | 0.025 | 1.0000 | Uani |
| Si2 | 0.37253(7) | -0.33463(4) | 0.27259(3) | 0.0245 | 1.0000 | Uani |
| Si10 | 0.16021(6) | 0.22758(4) | 0.01381(3) | 0.019 | 1.0000 | Uani |
| Si11 | 0.38273(7) | 0.32131(4) | 0.06249(3) | 0.0212 | 1.0000 | Uani |
| Si20 | 0.36064(6) | -0.22245(4) | 0.48401(3) | 0.0196 | 1.0000 | Uani |
| Si21 | 0.67031(7) | -0.32006(4) | 0.43647(3) | 0.0222 | 1.0000 | Uani |
| N1 | 0.37719(18) | 0.04198(12) | 0.22415(9) | 0.0168 | 1.0000 | Uani |
| N2 | 0.41355(18) | -0.03847(13) | 0.27438(9) | 0.0176 | 1.0000 | Uani |
| N10 | 0.24605(18) | 0.11260(13) | 0.07863(9) | 0.0176 | 1.0000 | Uani |
| N11 | 0.45041(19) | 0.22622(13) | 0.14304(9) | 0.0197 | 1.0000 | Uani |
| N20 | 0.34517(19) | -0.10820(13) | 0.41973(9) | 0.019 | 1.0000 | Uani |
| N21 | 0.65351(19) | -0.22520(13) | 0.35640(9) | 0.021 | 1.0000 | Uani |
| O10 | 0.22259(16) | 0.29795(10) | 0.05270(8) | 0.0216 | 1.0000 | Uani |
| O20 | 0.48765(16) | -0.29491(11) | 0.44568(8) | 0.0223 | 1.0000 | Uani |
| C1 | 0.1170(2) | 0.21774(16) | 0.20282(11) | 0.0212 | 1.0000 | Uani |
| C2 | -0.0347(3) | 0.4481(2) | 0.14395(16) | 0.0441 | 1.0000 | Uani |
| C3 | -0.0630(3) | 0.3379(2) | 0.29825(16) | 0.041 | 1.0000 | Uani |
| C4 | 0.2297(3) | 0.3675(2) | 0.25906(15) | 0.0353 | 1.0000 | Uani |
| C5 | 0.3117(2) | -0.21213(16) | 0.29492(12) | 0.023 | 1.0000 | Uani |
| C6 | 0.2410(3) | -0.3290(2) | 0.19786(14) | 0.0379 | 1.0000 | Uani |
| C7 | 0.3653(3) | -0.44172(19) | 0.35238(15) | 0.0381 | 1.0000 | Uani |
| C8 | 0.5622(3) | -0.3646(2) | 0.23920(15) | 0.0365 | 1.0000 | Uani |
| C11 | -0.0477(2) | 0.27290(18) | 0.00780(13) | 0.0303 | 1.0000 | Uani |
| C12 | 0.2158(3) | 0.24376(18) | -0.07872(12) | 0.0286 | 1.0000 | Uani |
| C13 | 0.3337(3) | 0.45634(18) | 0.06170(15) | 0.0355 | 1.0000 | Uani |
| C14 | 0.4981(3) | 0.3056(2) | -0.01288(13) | 0.0328 | 1.0000 | Uani |
| C21 | 0.4295(3) | -0.24168(18) | 0.57750(12) | 0.0301 | 1.0000 | Uani |
| C22 | 0.1895(3) | -0.26273(17) | 0.48840(13) | 0.0293 | 1.0000 | Uani |
| C23 | 0.7434(3) | -0.45502(17) | 0.43691(14) | 0.0351 | 1.0000 | Uani |
| C24 | 0.7715(3) | -0.3072(2) | 0.51334(13) | 0.0352 | 1.0000 | Uani |
| C100 | 0.2357(2) | 0.01252(15) | 0.07765(11) | 0.0195 | 1.0000 | Uani |
| C101 | 0.1970(3) | 0.01379(18) | 0.00111(12) | 0.028 | 1.0000 | Uani |
| C102 | 0.1124(2) | -0.01116(17) | 0.12422(12) | 0.0251 | 1.0000 | Uani |

| | | | | | | |
|---|---|---|---|---|---|---|
| C103 | 0.3866(2) | -0.07061(16) | 0.10513(13) | 0.025 | 1.0000 | Uani |
| C110 | 0.6016(2) | 0.20070(17) | 0.17975(12) | 0.0235 | 1.0000 | Uani |
| C111 | 0.6508(3) | 0.2965(2) | 0.16502(15) | 0.0357 | 1.0000 | Uani |
| C112 | 0.7143(3) | 0.12222(19) | 0.15165(14) | 0.0331 | 1.0000 | Uani |
| C113 | 0.6006(3) | 0.1577(2) | 0.26033(13) | 0.0309 | 1.0000 | Uani |
| C200 | 0.2444(2) | -0.00724(15) | 0.42075(11) | 0.0201 | 1.0000 | Uani |
| C201 | 0.3202(2) | 0.07440(16) | 0.39295(12) | 0.0249 | 1.0000 | Uani |
| C202 | 0.0988(2) | 0.01818(17) | 0.37433(12) | 0.0251 | 1.0000 | Uani |
| C203 | 0.2077(3) | -0.00846(18) | 0.49741(12) | 0.0275 | 1.0000 | Uani |
| C210 | 0.7826(2) | -0.20079(17) | 0.32039(12) | 0.0242 | 1.0000 | Uani |
| C211 | 0.8238(3) | -0.1232(2) | 0.34894(15) | 0.0345 | 1.0000 | Uani |
| C212 | 0.7437(3) | -0.15726(19) | 0.23955(13) | 0.0308 | 1.0000 | Uani |
| C213 | 0.9191(3) | -0.29765(19) | 0.33554(15) | 0.0351 | 1.0000 | Uani |
| H11 | 0.1213 | 0.1667 | 0.2472 | 0.034(2) | 1.0000 | Uiso |
| H12 | 0.0337 | 0.2233 | 0.1722 | 0.034(2) | 1.0000 | Uiso |
| H21 | -0.0445 | 0.5117 | 0.1521 | 0.074(2) | 1.0000 | Uiso |
| H22 | 0.0199 | 0.4453 | 0.1014 | 0.074(2) | 1.0000 | Uiso |
| H23 | -0.1331 | 0.444 | 0.1336 | 0.073(2) | 1.0000 | Uiso |
| H31 | -0.0951 | 0.4047 | 0.3057 | 0.070(2) | 1.0000 | Uiso |
| H32 | -0.0119 | 0.2882 | 0.343 | 0.070(2) | 1.0000 | Uiso |
| H33 | -0.1507 | 0.3216 | 0.2864 | 0.070(2) | 1.0000 | Uiso |
| H41 | 0.3081 | 0.3661 | 0.2258 | 0.062(2) | 1.0000 | Uiso |
| H42 | 0.2727 | 0.3172 | 0.305 | 0.062(2) | 1.0000 | Uiso |
| H43 | 0.1962 | 0.4339 | 0.2664 | 0.063(2) | 1.0000 | Uiso |
| H51 | 0.2323 | -0.217 | 0.3253 | 0.036(2) | 1.0000 | Uiso |
| H52 | 0.2694 | -0.1606 | 0.2506 | 0.036(2) | 1.0000 | Uiso |
| H61 | 0.2715 | -0.3913 | 0.186 | 0.054(2) | 1.0000 | Uiso |
| H62 | 0.1415 | -0.3178 | 0.2121 | 0.054(2) | 1.0000 | Uiso |
| H63 | 0.24 | -0.2744 | 0.1561 | 0.054(2) | 1.0000 | Uiso |
| H71 | 0.4013 | -0.5057 | 0.3423 | 0.067(2) | 1.0000 | Uiso |
| H72 | 0.425 | -0.4465 | 0.3948 | 0.067(2) | 1.0000 | Uiso |
| H73 | 0.2615 | -0.4319 | 0.3643 | 0.067(2) | 1.0000 | Uiso |
| H81 | 0.5889 | -0.4309 | 0.2301 | 0.063(2) | 1.0000 | Uiso |
| H82 | 0.6384 | -0.3675 | 0.2738 | 0.063(2) | 1.0000 | Uiso |
| H83 | 0.5629 | -0.3127 | 0.1951 | 0.063(2) | 1.0000 | Uiso |
| H111 | -0.0854 | 0.228 | -0.0103 | 0.0519(19) | 1.0000 | Uiso |
| H112 | -0.0802 | 0.2701 | 0.0552 | 0.0510(19) | 1.0000 | Uiso |

| | | | | | | |
|---|---|---|---|---|---|---|
| H113 | -0.0849 | 0.3418 | -0.024 | 0.0516(19) | 1.0000 | Uiso |
| H121 | 0.1984 | 0.3146 | -0.1036 | 0.0482(19) | 1.0000 | Uiso |
| H122 | 0.3209 | 0.2082 | -0.0799 | 0.0477(19) | 1.0000 | Uiso |
| H123 | 0.1563 | 0.2186 | -0.1033 | 0.0484(19) | 1.0000 | Uiso |
| H131 | 0.2752 | 0.4979 | 0.0174 | 0.0593(19) | 1.0000 | Uiso |
| H132 | 0.4208 | 0.4764 | 0.0648 | 0.0591(19) | 1.0000 | Uiso |
| H133 | 0.2726 | 0.4678 | 0.0997 | 0.0592(19) | 1.0000 | Uiso |
| H141 | 0.5239 | 0.2353 | -0.0132 | 0.0521(19) | 1.0000 | Uiso |
| H142 | 0.588 | 0.3229 | -0.0071 | 0.0522(19) | 1.0000 | Uiso |
| H143 | 0.4423 | 0.3491 | -0.0582 | 0.0518(19) | 1.0000 | Uiso |
| H211 | 0.4785 | -0.3136 | 0.599 | 0.0516(19) | 1.0000 | Uiso |
| H212 | 0.5009 | -0.2049 | 0.5796 | 0.0512(19) | 1.0000 | Uiso |
| H213 | 0.3471 | -0.2203 | 0.6058 | 0.0509(19) | 1.0000 | Uiso |
| H221 | 0.2074 | -0.3283 | 0.5241 | 0.0495(19) | 1.0000 | Uiso |
| H222 | 0.1082 | -0.2143 | 0.5022 | 0.0495(19) | 1.0000 | Uiso |
| H223 | 0.1599 | -0.2685 | 0.4435 | 0.0498(19) | 1.0000 | Uiso |
| H231 | 0.7009 | -0.462 | 0.3947 | 0.0582(19) | 1.0000 | Uiso |
| H232 | 0.8498 | -0.4738 | 0.4366 | 0.0582(19) | 1.0000 | Uiso |
| H233 | 0.717 | -0.498 | 0.4787 | 0.0583(19) | 1.0000 | Uiso |
| H241 | 0.7565 | -0.3537 | 0.5579 | 0.0589(19) | 1.0000 | Uiso |
| H242 | 0.8775 | -0.3232 | 0.5083 | 0.0590(19) | 1.0000 | Uiso |
| H243 | 0.7345 | -0.2377 | 0.5164 | 0.0590(19) | 1.0000 | Uiso |
| H1011 | 0.1032 | 0.068 | -0.0179 | 0.0365(12) | 1.0000 | Uiso |
| H1012 | 0.2754 | 0.0266 | -0.0298 | 0.0362(12) | 1.0000 | Uiso |
| H1013 | 0.1842 | -0.0501 | 0.0002 | 0.0360(12) | 1.0000 | Uiso |
| H1021 | 0.1064 | -0.0776 | 0.1247 | 0.0291(12) | 1.0000 | Uiso |
| H1022 | 0.134 | -0.0106 | 0.1718 | 0.0291(12) | 1.0000 | Uiso |
| H1023 | 0.016 | 0.0412 | 0.1041 | 0.0287(12) | 1.0000 | Uiso |
| H1031 | 0.3813 | -0.1361 | 0.1026 | 0.0316(12) | 1.0000 | Uiso |
| H1032 | 0.4126 | -0.0756 | 0.1537 | 0.0316(12) | 1.0000 | Uiso |
| H1033 | 0.4624 | -0.051 | 0.0754 | 0.0313(12) | 1.0000 | Uiso |
| H1111 | 0.6565 | 0.3258 | 0.114 | 0.0470(12) | 1.0000 | Uiso |
| H1112 | 0.5785 | 0.3484 | 0.1816 | 0.0472(12) | 1.0000 | Uiso |
| H1113 | 0.7471 | 0.2795 | 0.1899 | 0.0472(12) | 1.0000 | Uiso |
| H1121 | 0.8122 | 0.103 | 0.1758 | 0.0433(12) | 1.0000 | Uiso |
| H1122 | 0.7188 | 0.1508 | 0.0995 | 0.0433(12) | 1.0000 | Uiso |
| H1123 | 0.6835 | 0.0621 | 0.1596 | 0.0433(12) | 1.0000 | Uiso |

| | | | | | | |
|---|---|---|---|---|---|---|
| H1131 | 0.7006 | 0.1395 | 0.2817 | 0.0392(12) | 1.0000 | Uiso |
| H1132 | 0.534 | 0.2089 | 0.2789 | 0.0397(12) | 1.0000 | Uiso |
| H1133 | 0.5682 | 0.0975 | 0.2707 | 0.0393(12) | 1.0000 | Uiso |
| H2011 | 0.3411 | 0.0827 | 0.343 | 0.0293(12) | 1.0000 | Uiso |
| H2012 | 0.4137 | 0.0565 | 0.4212 | 0.0293(12) | 1.0000 | Uiso |
| H2013 | 0.2576 | 0.1401 | 0.3965 | 0.0291(12) | 1.0000 | Uiso |
| H2021 | 0.0355 | 0.0853 | 0.3712 | 0.0308(12) | 1.0000 | Uiso |
| H2022 | 0.0454 | -0.0297 | 0.396 | 0.0300(12) | 1.0000 | Uiso |
| H2023 | 0.1196 | 0.0152 | 0.3268 | 0.0303(12) | 1.0000 | Uiso |
| H2031 | 0.1418 | 0.0586 | 0.4964 | 0.0339(12) | 1.0000 | Uiso |
| H2032 | 0.3009 | -0.0253 | 0.5268 | 0.0341(12) | 1.0000 | Uiso |
| H2033 | 0.1577 | -0.0593 | 0.5169 | 0.0337(12) | 1.0000 | Uiso |
| H2111 | 0.7375 | -0.0634 | 0.3418 | 0.0453(12) | 1.0000 | Uiso |
| H2112 | 0.8571 | -0.1523 | 0.3999 | 0.0452(12) | 1.0000 | Uiso |
| H2113 | 0.9046 | -0.1044 | 0.3236 | 0.0451(12) | 1.0000 | Uiso |
| H2121 | 0.8279 | -0.1423 | 0.2158 | 0.0401(12) | 1.0000 | Uiso |
| H2122 | 0.7149 | -0.2063 | 0.2211 | 0.0399(12) | 1.0000 | Uiso |
| H2123 | 0.6599 | -0.0939 | 0.228 | 0.0405(12) | 1.0000 | Uiso |
| H2131 | 1.0033 | -0.2807 | 0.3123 | 0.0458(12) | 1.0000 | Uiso |
| H2132 | 0.9458 | -0.3287 | 0.3862 | 0.0456(12) | 1.0000 | Uiso |
| H2133 | 0.8944 | -0.3465 | 0.3158 | 0.0457(12) | 1.0000 | Uiso |

**Table C7. {[$^{t\text{Bu}}$NON]VCH$_2$Ph}$_2$($\mu$-N$_2$) (3b).**

| Atom | x | y | z | U(iso) (Å$^2$) | Occ | Type |
|---|---|---|---|---|---|---|
| V1 | 0.26439(5) | 0.67212(3) | 0.18672(2) | 0.0178 | 1.0000 | Uani |
| V2 | 0.44425(5) | 0.33654(3) | 0.31355(2) | 0.0175 | 1.0000 | Uani |
| Si10 | 0.08053(9) | 0.84035(5) | 0.21702(4) | 0.0237 | 1.0000 | Uani |
| Si11 | 0.34117(9) | 0.84328(6) | 0.10761(4) | 0.0253 | 1.0000 | Uani |
| Si20 | 0.69240(8) | 0.18077(5) | 0.39314(4) | 0.023 | 1.0000 | Uani |
| Si21 | 0.44884(9) | 0.15879(6) | 0.28654(4) | 0.025 | 1.0000 | Uani |
| N1 | 0.3417(2) | 0.54855(16) | 0.23223(11) | 0.0163 | 1.0000 | Uani |
| N2 | 0.3889(2) | 0.46086(15) | 0.26647(11) | 0.0163 | 1.0000 | Uani |
| N10 | 0.1499(2) | 0.71734(15) | 0.26082(11) | 0.0196 | 1.0000 | Uani |
| N11 | 0.4208(2) | 0.71885(16) | 0.13590(11) | 0.0219 | 1.0000 | Uani |
| N20 | 0.6399(2) | 0.30624(15) | 0.36177(11) | 0.0194 | 1.0000 | Uani |
| N21 | 0.3864(2) | 0.28148(16) | 0.24165(12) | 0.0217 | 1.0000 | Uani |
| O10 | 0.1748(2) | 0.84008(13) | 0.14064(10) | 0.0235 | 1.0000 | Uani |
| O20 | 0.5318(2) | 0.16898(13) | 0.36152(10) | 0.0233 | 1.0000 | Uani |
| C1 | 0.1107(3) | 0.6565(2) | 0.10952(15) | 0.0271 | 1.0000 | Uani |
| C2 | 0.0990(3) | 0.7163(2) | 0.02978(15) | 0.0233 | 1.0000 | Uani |
| C3 | 0.0012(3) | 0.8099(2) | 0.00335(15) | 0.0269 | 1.0000 | Uani |
| C4 | 0.1856(3) | 0.6801(2) | -0.02283(16) | 0.0338 | 1.0000 | Uani |
| C5 | -0.0107(3) | 0.8649(2) | -0.07137(16) | 0.0296 | 1.0000 | Uani |
| C6 | 0.1734(4) | 0.7346(3) | -0.09737(17) | 0.04 | 1.0000 | Uani |
| C7 | 0.0761(3) | 0.8274(2) | -0.12169(16) | 0.0358 | 1.0000 | Uani |
| C11 | 0.1304(4) | 0.9222(2) | 0.26517(18) | 0.0392 | 1.0000 | Uani |
| C12 | -0.1234(3) | 0.8846(2) | 0.18476(17) | 0.0322 | 1.0000 | Uani |
| C13 | 0.4309(4) | 0.9129(2) | 0.15301(19) | 0.0405 | 1.0000 | Uani |
| C14 | 0.3099(4) | 0.9070(2) | 0.00557(16) | 0.035 | 1.0000 | Uani |
| C21 | 0.2773(3) | 0.3411(2) | 0.39279(15) | 0.0264 | 1.0000 | Uani |
| C22 | 0.3209(3) | 0.27980(19) | 0.47183(15) | 0.0229 | 1.0000 | Uani |
| C23 | 0.3732(3) | 0.3161(2) | 0.52492(16) | 0.0302 | 1.0000 | Uani |
| C24 | 0.3123(3) | 0.1837(2) | 0.49714(15) | 0.0261 | 1.0000 | Uani |
| C25 | 0.4127(3) | 0.2601(2) | 0.59904(16) | 0.033 | 1.0000 | Uani |
| C26 | 0.3518(3) | 0.1277(2) | 0.57104(16) | 0.0301 | 1.0000 | Uani |
| C27 | 0.4029(3) | 0.1656(2) | 0.62233(16) | 0.0327 | 1.0000 | Uani |
| C31 | 0.7193(3) | 0.1205(2) | 0.49528(16) | 0.0334 | 1.0000 | Uani |
| C32 | 0.8548(3) | 0.1185(2) | 0.34890(19) | 0.0392 | 1.0000 | Uani |
| C33 | 0.5874(4) | 0.0846(2) | 0.23864(18) | 0.0363 | 1.0000 | Uani |

| | | | | | | |
|---|---|---|---|---|---|---|
| C34 | 0.2999(4) | 0.0981(2) | 0.32063(18) | 0.0367 | 1.0000 | Uani |
| C100 | 0.1089(3) | 0.66497(19) | 0.33543(14) | 0.022 | 1.0000 | Uani |
| C101 | 0.0070(3) | 0.7365(2) | 0.37188(16) | 0.035 | 1.0000 | Uani |
| C102 | 0.0216(3) | 0.5950(2) | 0.32488(16) | 0.0326 | 1.0000 | Uani |
| C103 | 0.2519(3) | 0.6098(2) | 0.38743(14) | 0.0246 | 1.0000 | Uani |
| C110 | 0.5801(3) | 0.6703(2) | 0.12578(15) | 0.0276 | 1.0000 | Uani |
| C111 | 0.6385(4) | 0.7350(3) | 0.05960(18) | 0.0425 | 1.0000 | Uani |
| C112 | 0.5906(3) | 0.5751(2) | 0.10939(17) | 0.0328 | 1.0000 | Uani |
| C113 | 0.6780(3) | 0.6526(2) | 0.19712(16) | 0.0318 | 1.0000 | Uani |
| C200 | 0.7419(3) | 0.3666(2) | 0.36801(15) | 0.0226 | 1.0000 | Uani |
| C201 | 0.8642(3) | 0.3116(2) | 0.43232(18) | 0.0358 | 1.0000 | Uani |
| C202 | 0.6527(3) | 0.4600(2) | 0.38396(16) | 0.0283 | 1.0000 | Uani |
| C203 | 0.8162(3) | 0.3899(2) | 0.29432(17) | 0.0319 | 1.0000 | Uani |
| C210 | 0.2928(3) | 0.3267(2) | 0.16850(15) | 0.0266 | 1.0000 | Uani |
| C211 | 0.3710(3) | 0.3923(2) | 0.11366(15) | 0.0298 | 1.0000 | Uani |
| C212 | 0.1373(3) | 0.3849(2) | 0.18183(17) | 0.0358 | 1.0000 | Uani |
| C213 | 0.2725(4) | 0.2488(2) | 0.13451(18) | 0.0426 | 1.0000 | Uani |
| H11 | 0.0119 | 0.6734 | 0.1296 | 0.029(6) | 1.0000 | Uiso |
| H12 | 0.1393 | 0.5871 | 0.1121 | 0.028(6) | 1.0000 | Uiso |
| H31 | -0.0591 | 0.8371 | 0.0374 | 0.026(4) | 1.0000 | Uiso |
| H41 | 0.2551 | 0.6159 | -0.0065 | 0.036(4) | 1.0000 | Uiso |
| H51 | -0.0788 | 0.9303 | -0.0879 | 0.031(4) | 1.0000 | Uiso |
| H61 | 0.2317 | 0.7072 | -0.1328 | 0.043(4) | 1.0000 | Uiso |
| H71 | 0.0705 | 0.8658 | -0.1732 | 0.038(4) | 1.0000 | Uiso |
| H111 | 0.0549 | 0.9374 | 0.2991 | 0.064(3) | 1.0000 | Uiso |
| H112 | 0.1367 | 0.9815 | 0.2289 | 0.064(3) | 1.0000 | Uiso |
| H113 | 0.2271 | 0.8897 | 0.2939 | 0.064(3) | 1.0000 | Uiso |
| H121 | -0.1844 | 0.8889 | 0.2265 | 0.050(3) | 1.0000 | Uiso |
| H122 | -0.1491 | 0.84 | 0.1619 | 0.049(3) | 1.0000 | Uiso |
| H123 | -0.1447 | 0.9488 | 0.1478 | 0.049(3) | 1.0000 | Uiso |
| H131 | 0.3683 | 0.9805 | 0.1426 | 0.065(3) | 1.0000 | Uiso |
| H132 | 0.4458 | 0.8833 | 0.2064 | 0.065(3) | 1.0000 | Uiso |
| H133 | 0.5277 | 0.9139 | 0.1338 | 0.065(3) | 1.0000 | Uiso |
| H141 | 0.3989 | 0.9257 | -0.0123 | 0.057(3) | 1.0000 | Uiso |
| H142 | 0.227 | 0.9647 | -0.004 | 0.057(3) | 1.0000 | Uiso |
| H143 | 0.289 | 0.8642 | -0.0208 | 0.057(3) | 1.0000 | Uiso |
| H211 | 0.1968 | 0.3208 | 0.3716 | 0.025(5) | 1.0000 | Uiso |

| | | | | | | |
|---|---|---|---|---|---|---|
| H212 | 0.2376 | 0.4092 | 0.3923 | 0.025(5) | 1.0000 | Uiso |
| H231 | 0.3779 | 0.3825 | 0.5094 | 0.036(4) | 1.0000 | Uiso |
| H241 | 0.2779 | 0.1569 | 0.4618 | 0.032(4) | 1.0000 | Uiso |
| H251 | 0.4486 | 0.2874 | 0.6338 | 0.038(4) | 1.0000 | Uiso |
| H261 | 0.3443 | 0.0614 | 0.5864 | 0.036(4) | 1.0000 | Uiso |
| H271 | 0.4307 | 0.1258 | 0.6736 | 0.038(4) | 1.0000 | Uiso |
| H311 | 0.7088 | 0.0555 | 0.5052 | 0.051(3) | 1.0000 | Uiso |
| H312 | 0.8205 | 0.1166 | 0.5148 | 0.052(3) | 1.0000 | Uiso |
| H313 | 0.6449 | 0.1561 | 0.5205 | 0.051(3) | 1.0000 | Uiso |
| H321 | 0.8399 | 0.1481 | 0.2952 | 0.060(3) | 1.0000 | Uiso |
| H322 | 0.8606 | 0.0488 | 0.3594 | 0.060(3) | 1.0000 | Uiso |
| H323 | 0.9468 | 0.1249 | 0.3675 | 0.061(3) | 1.0000 | Uiso |
| H331 | 0.6491 | 0.1231 | 0.2097 | 0.057(3) | 1.0000 | Uiso |
| H332 | 0.5352 | 0.063 | 0.2058 | 0.056(3) | 1.0000 | Uiso |
| H333 | 0.6534 | 0.0272 | 0.2752 | 0.057(3) | 1.0000 | Uiso |
| H341 | 0.3391 | 0.0396 | 0.3612 | 0.058(3) | 1.0000 | Uiso |
| H342 | 0.2174 | 0.1417 | 0.3368 | 0.058(3) | 1.0000 | Uiso |
| H343 | 0.2599 | 0.0805 | 0.281 | 0.058(3) | 1.0000 | Uiso |
| H1011 | 0.063 | 0.7803 | 0.3815 | 0.0403(14) | 1.0000 | Uiso |
| H1012 | -0.0832 | 0.7743 | 0.3384 | 0.0402(14) | 1.0000 | Uiso |
| H1013 | -0.023 | 0.7001 | 0.4195 | 0.0400(14) | 1.0000 | Uiso |
| H1021 | -0.001 | 0.5571 | 0.3737 | 0.0352(14) | 1.0000 | Uiso |
| H1022 | 0.081 | 0.5496 | 0.2991 | 0.0349(14) | 1.0000 | Uiso |
| H1023 | -0.0736 | 0.6323 | 0.2952 | 0.0354(14) | 1.0000 | Uiso |
| H1031 | 0.3067 | 0.6553 | 0.3939 | 0.0260(14) | 1.0000 | Uiso |
| H1032 | 0.2243 | 0.5768 | 0.4365 | 0.0250(14) | 1.0000 | Uiso |
| H1033 | 0.3171 | 0.5611 | 0.368 | 0.0253(14) | 1.0000 | Uiso |
| H1111 | 0.6371 | 0.7972 | 0.0679 | 0.0531(14) | 1.0000 | Uiso |
| H1112 | 0.5775 | 0.7476 | 0.0134 | 0.0526(14) | 1.0000 | Uiso |
| H1113 | 0.7415 | 0.7017 | 0.0541 | 0.0532(14) | 1.0000 | Uiso |
| H1121 | 0.695 | 0.5446 | 0.1014 | 0.0353(14) | 1.0000 | Uiso |
| H1122 | 0.5251 | 0.5862 | 0.0644 | 0.0354(14) | 1.0000 | Uiso |
| H1123 | 0.5589 | 0.5315 | 0.1521 | 0.0355(14) | 1.0000 | Uiso |
| H1131 | 0.6745 | 0.7152 | 0.2055 | 0.0361(14) | 1.0000 | Uiso |
| H1132 | 0.7809 | 0.6189 | 0.1922 | 0.0366(14) | 1.0000 | Uiso |
| H1133 | 0.6419 | 0.6123 | 0.2401 | 0.0360(14) | 1.0000 | Uiso |
| H2011 | 0.8183 | 0.2947 | 0.4798 | 0.0423(14) | 1.0000 | Uiso |

| | | | | | | |
|---|---|---|---|---|---|---|
| H2012 | 0.9282 | 0.2517 | 0.4245 | 0.0424(14) | 1.0000 | Uiso |
| H2013 | 0.9289 | 0.3529 | 0.436 | 0.0424(14) | 1.0000 | Uiso |
| H2021 | 0.72 | 0.4988 | 0.3872 | 0.0293(14) | 1.0000 | Uiso |
| H2022 | 0.5735 | 0.498 | 0.3439 | 0.0293(14) | 1.0000 | Uiso |
| H2023 | 0.6058 | 0.4442 | 0.4316 | 0.0291(14) | 1.0000 | Uiso |
| H2031 | 0.8711 | 0.3294 | 0.2855 | 0.0363(14) | 1.0000 | Uiso |
| H2032 | 0.885 | 0.4282 | 0.2979 | 0.0363(14) | 1.0000 | Uiso |
| H2033 | 0.7385 | 0.4278 | 0.2526 | 0.0359(14) | 1.0000 | Uiso |
| H2111 | 0.3786 | 0.4462 | 0.1321 | 0.0313(14) | 1.0000 | Uiso |
| H2112 | 0.4713 | 0.3558 | 0.1077 | 0.0310(14) | 1.0000 | Uiso |
| H2113 | 0.3152 | 0.419 | 0.0641 | 0.0312(14) | 1.0000 | Uiso |
| H2121 | 0.0741 | 0.415 | 0.1351 | 0.0400(14) | 1.0000 | Uiso |
| H2122 | 0.0896 | 0.3402 | 0.216 | 0.0409(14) | 1.0000 | Uiso |
| H2123 | 0.1434 | 0.4352 | 0.2038 | 0.0398(14) | 1.0000 | Uiso |
| H2131 | 0.3732 | 0.2124 | 0.123 | 0.0524(14) | 1.0000 | Uiso |
| H2132 | 0.2069 | 0.28 | 0.0886 | 0.0521(14) | 1.0000 | Uiso |
| H2133 | 0.2277 | 0.2034 | 0.1693 | 0.0524(14) | 1.0000 | Uiso |

**Table C8.** **[$^{(CF_3)_2Ph}$NON]FeCl•LiCl•2DME (4).**

| Atom | x | y | z | U(iso) (Å$^2$) | Occ | Type |
|---|---|---|---|---|---|---|
| Fe1 | 0.21423(3) | 1.02210(2) | 0.254142(14) | 0.0159 | 1.0000 | Uani |
| Cl1 | 0.05000(6) | 0.99677(5) | 0.34104(3) | 0.0263 | 1.0000 | Uani |
| Cl2 | 0.39843(6) | 1.02035(5) | 0.32749(3) | 0.0268 | 1.0000 | Uani |
| Si1 | 0.38519(6) | 0.92411(4) | 0.10670(3) | 0.017 | 1.0000 | Uani |
| Si2 | 0.16701(6) | 1.16633(4) | 0.08831(3) | 0.019 | 1.0000 | Uani |
| N1 | 0.28224(17) | 0.90281(13) | 0.18918(9) | 0.0176 | 1.0000 | Uani |
| N2 | 0.12834(18) | 1.16510(13) | 0.18842(9) | 0.0201 | 1.0000 | Uani |
| O1 | 0.32490(16) | 1.06230(12) | 0.08337(9) | 0.0225 | 1.0000 | Uani |
| O2 | -0.21607(18) | 0.93575(17) | 0.25780(10) | 0.0321 | 1.0000 | Uani |
| O3 | -0.2770(2) | 0.87004(16) | 0.40541(11) | 0.0334 | 1.0000 | Uani |
| O4 | 0.5931(2) | 1.18054(15) | 0.26618(10) | 0.0302 | 1.0000 | Uani |
| O5 | 0.67902(19) | 1.11717(14) | 0.41547(9) | 0.0282 | 1.0000 | Uani |
| C1 | 0.5805(2) | 0.8771(2) | 0.13036(14) | 0.0283 | 1.0000 | Uani |
| C2 | 0.3657(3) | 0.8569(2) | 0.02191(12) | 0.0274 | 1.0000 | Uani |
| C3 | 0.1879(3) | 1.29993(19) | 0.04285(14) | 0.0307 | 1.0000 | Uani |
| C4 | 0.0303(3) | 1.1367(2) | 0.03400(14) | 0.0322 | 1.0000 | Uani |
| C10 | 0.27715(19) | 0.79573(14) | 0.21815(10) | 0.0172 | 1.0000 | Uani |
| C11 | 0.3268(2) | 0.74279(16) | 0.29357(11) | 0.0216 | 1.0000 | Uani |
| C12 | 0.2187(2) | 0.74012(15) | 0.17354(11) | 0.0193 | 1.0000 | Uani |
| C13 | 0.3183(2) | 0.63772(17) | 0.32221(12) | 0.025 | 1.0000 | Uani |
| C14 | 0.2127(2) | 0.63475(16) | 0.20357(12) | 0.0233 | 1.0000 | Uani |
| C15 | 0.2608(3) | 0.58202(17) | 0.27850(13) | 0.0261 | 1.0000 | Uani |
| C16 | 0.3779(3) | 0.5824(2) | 0.40229(14) | 0.0344 | 1.0000 | Uani |
| C17 | 0.1493(3) | 0.5790(2) | 0.15309(16) | 0.0365 | 1.0000 | Uani |
| C20 | 0.0276(2) | 1.25832(15) | 0.21905(12) | 0.0213 | 1.0000 | Uani |
| C21 | 0.0488(2) | 1.28022(17) | 0.29397(13) | 0.0255 | 1.0000 | Uani |
| C22 | -0.0963(2) | 1.33387(17) | 0.17815(14) | 0.0267 | 1.0000 | Uani |
| C23 | -0.0500(3) | 1.37375(19) | 0.32477(15) | 0.0313 | 1.0000 | Uani |
| C24 | -0.1930(3) | 1.42685(18) | 0.20978(16) | 0.0315 | 1.0000 | Uani |
| C25 | -0.1720(3) | 1.44831(19) | 0.28299(17) | 0.0353 | 1.0000 | Uani |
| C26 | -0.0182(4) | 1.3930(3) | 0.40476(18) | 0.0445 | 1.0000 | Uani |
| C27 | -0.3228(3) | 1.5040(2) | 0.1617(2) | 0.0439 | 1.0000 | Uani |
| C30 | -0.1408(3) | 0.8213(3) | 0.2896(2) | 0.0422 | 1.0000 | Uani |
| C31 | -0.2354(3) | 0.7876(2) | 0.3531(2) | 0.0413 | 1.0000 | Uani |
| C32 | -0.1460(3) | 0.9726(3) | 0.18992(15) | 0.0462 | 1.0000 | Uani |

| | | | | | | |
|---|---|---|---|---|---|---|
| C33 | -0.3584(4) | 0.8424(3) | 0.47101(19) | 0.0486 | 1.0000 | Uani |
| C40 | 0.5484(3) | 1.2648(2) | 0.31725(16) | 0.0353 | 1.0000 | Uani |
| C41 | 0.6642(3) | 1.2281(2) | 0.37994(16) | 0.0366 | 1.0000 | Uani |
| C42 | 0.4971(4) | 1.2116(3) | 0.20097(16) | 0.0424 | 1.0000 | Uani |
| C43 | 0.7731(3) | 1.0805(2) | 0.48250(13) | 0.0338 | 1.0000 | Uani |
| F161 | 0.3205(4) | 0.6443(2) | 0.45670(12) | 0.1019 | 1.0000 | Uani |
| F163 | 0.3578(4) | 0.4859(2) | 0.42574(14) | 0.0901 | 1.0000 | Uani |
| F171 | 0.1702(4) | 0.47305(18) | 0.18079(15) | 0.0789 | 1.0000 | Uani |
| F172 | 0.1991(4) | 0.5802(2) | 0.08092(13) | 0.077 | 1.0000 | Uani |
| F173 | 0.0060(3) | 0.6306(3) | 0.1456(2) | 0.0926 | 1.0000 | Uani |
| F261 | -0.0046(3) | 1.3058(2) | 0.45980(12) | 0.0677 | 1.0000 | Uani |
| F262 | 0.1082(3) | 1.4082(3) | 0.40548(15) | 0.0804 | 1.0000 | Uani |
| F263 | -0.1230(3) | 1.4824(2) | 0.42871(16) | 0.0835 | 1.0000 | Uani |
| F271 | -0.4195(3) | 1.4601(3) | 0.1580(3) | 0.1146 | 1.0000 | Uani |
| F273 | -0.3960(4) | 1.5967(3) | 0.1937(3) | 0.121 | 1.0000 | Uani |
| Li1 | -0.3363(6) | 1.0246(4) | 0.3364(3) | 0.034 | 1.0000 | Uani |
| H11 | 0.6342 | 0.8939 | 0.0859 | 0.052(3) | 1.0000 | Uiso |
| H13 | 0.5923 | 0.9144 | 0.1723 | 0.052(3) | 1.0000 | Uiso |
| H12 | 0.6201 | 0.7971 | 0.1471 | 0.051(3) | 1.0000 | Uiso |
| H22 | 0.4218 | 0.8767 | -0.0196 | 0.052(3) | 1.0000 | Uiso |
| H21 | 0.266 | 0.887 | 0.0051 | 0.052(3) | 1.0000 | Uiso |
| H23 | 0.3989 | 0.7747 | 0.0339 | 0.052(3) | 1.0000 | Uiso |
| H32 | 0.214 | 1.2975 | -0.0117 | 0.056(3) | 1.0000 | Uiso |
| H33 | 0.263 | 1.3106 | 0.0691 | 0.057(3) | 1.0000 | Uiso |
| H31 | 0.0995 | 1.3661 | 0.0466 | 0.056(3) | 1.0000 | Uiso |
| H41 | 0.0634 | 1.134 | -0.0199 | 0.057(3) | 1.0000 | Uiso |
| H43 | -0.0643 | 1.1953 | 0.0334 | 0.057(3) | 1.0000 | Uiso |
| H42 | 0.0221 | 1.0653 | 0.0565 | 0.0494 | 1.0000 | Uiso |
| H111 | 0.3683 | 0.7766 | 0.3245 | 0.032(3) | 1.0000 | Uiso |
| H121 | 0.1818 | 0.7752 | 0.1218 | 0.030(3) | 1.0000 | Uiso |
| H151 | 0.2544 | 0.5116 | 0.2994 | 0.037(3) | 1.0000 | Uiso |
| H211 | 0.132 | 1.2308 | 0.3222 | 0.037(3) | 1.0000 | Uiso |
| H221 | -0.1161 | 1.3207 | 0.1287 | 0.039(3) | 1.0000 | Uiso |
| H251 | -0.2375 | 1.5112 | 0.3037 | 0.048(3) | 1.0000 | Uiso |
| H301 | -0.0463 | 0.8067 | 0.3114 | 0.058(3) | 1.0000 | Uiso |
| H302 | -0.1281 | 0.7751 | 0.247 | 0.059(3) | 1.0000 | Uiso |
| H312 | -0.1796 | 0.7127 | 0.3806 | 0.058(3) | 1.0000 | Uiso |

| | | | | | | |
|---|---|---|---|---|---|---|
| H311 | -0.3207 | 0.785 | 0.3304 | 0.057(3) | 1.0000 | Uiso |
| H322 | -0.1998 | 1.0539 | 0.1716 | 0.078(3) | 1.0000 | Uiso |
| H321 | -0.0456 | 0.9595 | 0.2009 | 0.077(3) | 1.0000 | Uiso |
| H323 | -0.1526 | 0.9304 | 0.1492 | 0.077(3) | 1.0000 | Uiso |
| H332 | -0.376 | 0.8961 | 0.5057 | 0.085(3) | 1.0000 | Uiso |
| H333 | -0.3011 | 0.7683 | 0.4975 | 0.085(3) | 1.0000 | Uiso |
| H331 | -0.4483 | 0.844 | 0.4519 | 0.083(3) | 1.0000 | Uiso |
| H401 | 0.5408 | 1.3385 | 0.288 | 0.050(3) | 1.0000 | Uiso |
| H402 | 0.4523 | 1.2709 | 0.3408 | 0.051(3) | 1.0000 | Uiso |
| H411 | 0.6377 | 1.2753 | 0.4201 | 0.052(3) | 1.0000 | Uiso |
| H412 | 0.761 | 1.2225 | 0.3582 | 0.052(3) | 1.0000 | Uiso |
| H421 | 0.5255 | 1.1506 | 0.1699 | 0.072(3) | 1.0000 | Uiso |
| H423 | 0.5011 | 1.2782 | 0.169 | 0.072(3) | 1.0000 | Uiso |
| H422 | 0.3971 | 1.2267 | 0.219 | 0.072(3) | 1.0000 | Uiso |
| H432 | 0.7933 | 1.0026 | 0.5005 | 0.061(3) | 1.0000 | Uiso |
| H431 | 0.7279 | 1.1255 | 0.5228 | 0.060(3) | 1.0000 | Uiso |
| H433 | 0.8633 | 1.0908 | 0.4667 | 0.061(3) | 1.0000 | Uiso |
| F1620 | 0.5237(5) | 0.5307(5) | 0.3985(3) | 0.0629 | 0.521(4) | Uiso |
| F1621 | 0.5100(6) | 0.5878(5) | 0.4132(3) | 0.0629 | 0.479(4) | Uiso |
| F2720 | -0.2948(4) | 1.5217(4) | 0.0835(2) | 0.0477 | 0.521(4) | Uiso |
| F2721 | -0.2839(5) | 1.5592(4) | 0.1039(3) | 0.0477 | 0.479(4) | Uiso |

**Table C9. $Li\{Co_2Cl[^{(CF_3)_2Ph}NON]_2\}$•2DME (5).**

| Atom | x | y | z | U(iso) (Å$^2$) | Occ | Type |
|---|---|---|---|---|---|---|
| Co1 | 0.01389(14) | 0.61763(3) | 0.41280(6) | 0.0211 | 1.0000 | Uani |
| Co2 | 0.01891(14) | 0.59002(3) | 0.51211(6) | 0.0219 | 1.0000 | Uani |
| Li1 | -0.3376(17) | 0.9587(8) | 0.1970(6) | 0.0751 | 1.0000 | Uani |
| Cl1 | 0.1073(2) | 0.56965(8) | 0.59802(8) | 0.0416 | 1.0000 | Uani |
| Si1 | -0.19388(19) | 0.64639(8) | 0.33720(9) | 0.0355 | 1.0000 | Uani |
| Si2 | -0.2674(2) | 0.61472(9) | 0.44947(9) | 0.0418 | 1.0000 | Uani |
| Si10 | 0.23510(18) | 0.54643(6) | 0.44971(8) | 0.0231 | 1.0000 | Uani |
| Si20 | 0.2351(2) | 0.66908(7) | 0.48074(9) | 0.0311 | 1.0000 | Uani |
| N1 | -0.0367(5) | 0.6426(2) | 0.3393(2) | 0.0295 | 1.0000 | Uani |
| N2 | -0.1640(5) | 0.5877(2) | 0.5015(2) | 0.0293 | 1.0000 | Uani |
| N10 | 0.0749(4) | 0.54515(19) | 0.45021(19) | 0.0232 | 1.0000 | Uani |
| N20 | 0.0748(4) | 0.66270(18) | 0.4801(2) | 0.0236 | 1.0000 | Uani |
| O1 | -0.1865(4) | 0.62464(19) | 0.40040(18) | 0.0338 | 1.0000 | Uani |
| O2 | 0.2609(4) | 0.61356(17) | 0.44662(17) | 0.0264 | 1.0000 | Uani |
| O5 | -0.4699(10) | 0.9689(4) | 0.2376(5) | 0.1601 | 1.0000 | Uani |
| O6 | -0.3267(13) | 0.8851(4) | 0.2267(4) | 0.1636 | 1.0000 | Uani |
| O7 | -0.3922(11) | 1.0445(5) | 0.1794(4) | 0.1604 | 1.0000 | Uani |
| O8 | -0.1804(11) | 0.9868(6) | 0.2204(6) | 0.2152 | 1.0000 | Uani |
| C1 | -0.2620(7) | 0.7178(4) | 0.3288(4) | 0.0604 | 1.0000 | Uani |
| C2 | -0.2898(7) | 0.5980(4) | 0.2898(3) | 0.0548 | 1.0000 | Uani |
| C3 | -0.3329(9) | 0.6829(5) | 0.4644(4) | 0.081 | 1.0000 | Uani |
| C4 | -0.3988(9) | 0.5668(6) | 0.4230(4) | 0.0972 | 1.0000 | Uani |
| C5 | 0.2664(6) | 0.5136(3) | 0.3871(3) | 0.0335 | 1.0000 | Uani |
| C6 | 0.3366(6) | 0.5161(3) | 0.5096(3) | 0.0401 | 1.0000 | Uani |
| C7 | 0.2698(8) | 0.7319(3) | 0.4434(4) | 0.052 | 1.0000 | Uani |
| C8 | 0.3281(7) | 0.6684(4) | 0.5485(4) | 0.0609 | 1.0000 | Uani |
| C10 | 0.0289(5) | 0.6637(2) | 0.3022(2) | 0.0272 | 1.0000 | Uani |
| C11 | -0.0280(5) | 0.6858(3) | 0.2527(2) | 0.0299 | 1.0000 | Uani |
| C12 | 0.1594(6) | 0.6637(3) | 0.3134(2) | 0.0338 | 1.0000 | Uani |
| C13 | 0.0407(6) | 0.7084(3) | 0.2171(2) | 0.0356 | 1.0000 | Uani |
| C14 | 0.2260(6) | 0.6866(3) | 0.2777(3) | 0.04 | 1.0000 | Uani |
| C15 | 0.1685(6) | 0.7096(3) | 0.2294(3) | 0.038 | 1.0000 | Uani |
| C16 | -0.0286(7) | 0.7335(3) | 0.1663(3) | 0.0455 | 1.0000 | Uani |
| C17 | 0.3653(7) | 0.6893(5) | 0.2926(3) | 0.0635 | 1.0000 | Uani |
| C20 | -0.2144(6) | 0.5620(3) | 0.5419(3) | 0.0324 | 1.0000 | Uani |

| | | | | | | |
|---|---|---|---|---|---|---|
| C21 | -0.2398(9) | 0.5052(3) | 0.5408(4) | 0.0592 | 1.0000 | Uani |
| C22 | -0.2445(9) | 0.5919(4) | 0.5843(4) | 0.059 | 1.0000 | Uani |
| C23 | -0.2909(12) | 0.4804(4) | 0.5820(5) | 0.0877 | 1.0000 | Uani |
| C24 | -0.2963(9) | 0.5638(5) | 0.6238(4) | 0.0688 | 1.0000 | Uani |
| C25 | -0.3205(10) | 0.5092(5) | 0.6222(4) | 0.0803 | 1.0000 | Uani |
| C26 | -0.3275(14) | 0.4206(5) | 0.5797(6) | 0.2114 | 1.0000 | Uani |
| C27 | -0.334(3) | 0.5993(8) | 0.6684(8) | 0.1646 | 1.0000 | Uani |
| C55 | -0.5246(15) | 1.0158(6) | 0.2560(7) | 0.1828 | 1.0000 | Uani |
| C56 | -0.4862(19) | 0.9205(6) | 0.2686(6) | 0.1978 | 1.0000 | Uani |
| C57 | -0.4438(14) | 0.8710(5) | 0.2403(9) | 0.1982 | 1.0000 | Uani |
| C58 | -0.2754(18) | 0.8404(6) | 0.2044(7) | 0.2026 | 1.0000 | Uani |
| C60 | -0.4978(13) | 1.0570(8) | 0.1385(7) | 0.1772 | 1.0000 | Uani |
| C61 | -0.2775(12) | 1.0573(8) | 0.1620(5) | 0.2115 | 1.0000 | Uani |
| C62 | -0.1736(14) | 1.0449(7) | 0.2080(8) | 0.2515 | 1.0000 | Uani |
| C63 | -0.0839(15) | 0.9709(8) | 0.2641(7) | 0.2439 | 1.0000 | Uani |
| C100 | 0.0131(6) | 0.4936(2) | 0.4449(2) | 0.0265 | 1.0000 | Uani |
| C101 | -0.0908(9) | 0.4844(3) | 0.4053(3) | 0.0596 | 1.0000 | Uani |
| C102 | 0.0515(6) | 0.4503(3) | 0.4803(3) | 0.0382 | 1.0000 | Uani |
| C103 | -0.1536(10) | 0.4333(4) | 0.4005(3) | 0.0694 | 1.0000 | Uani |
| C104 | -0.0089(7) | 0.3983(3) | 0.4739(3) | 0.0454 | 1.0000 | Uani |
| C105 | -0.1068(9) | 0.3896(3) | 0.4341(3) | 0.0605 | 1.0000 | Uani |
| C106 | -0.2659(18) | 0.4232(7) | 0.3576(6) | 0.157 | 1.0000 | Uani |
| C107 | 0.0327(11) | 0.3520(4) | 0.5128(6) | 0.0943 | 1.0000 | Uani |
| C200 | 0.0168(6) | 0.7124(3) | 0.4941(3) | 0.0346 | 1.0000 | Uani |
| C201 | -0.0254(9) | 0.7533(3) | 0.4551(4) | 0.0564 | 1.0000 | Uani |
| C202 | 0.0032(7) | 0.7215(3) | 0.5471(3) | 0.0417 | 1.0000 | Uani |
| C203 | -0.0768(11) | 0.8014(4) | 0.4698(5) | 0.0822 | 1.0000 | Uani |
| C204 | -0.0509(10) | 0.7700(3) | 0.5610(4) | 0.0619 | 1.0000 | Uani |
| C205 | -0.0869(13) | 0.8107(4) | 0.5225(5) | 0.0916 | 1.0000 | Uani |
| C206 | -0.1244(19) | 0.8441(5) | 0.4270(7) | 0.1308 | 1.0000 | Uani |
| C207 | -0.0671(15) | 0.7783(4) | 0.6183(6) | 0.0923 | 1.0000 | Uani |
| F161 | 0.0393(5) | 0.7367(3) | 0.12826(19) | 0.0797 | 1.0000 | Uani |
| F162 | -0.0638(8) | 0.7849(2) | 0.1731(2) | 0.0992 | 1.0000 | Uani |
| F163 | -0.1313(6) | 0.7087(3) | 0.1457(2) | 0.0964 | 1.0000 | Uani |
| F171 | 0.4203(5) | 0.6861(5) | 0.2537(3) | 0.151 | 1.0000 | Uani |
| F172 | 0.4019(7) | 0.7383(5) | 0.3152(6) | 0.1878 | 1.0000 | Uani |
| F173 | 0.4141(5) | 0.6565(4) | 0.3296(3) | 0.1314 | 1.0000 | Uani |

| | | | | | | |
|---|---|---|---|---|---|---|
| F261 | -0.2689(18) | 0.3950(5) | 0.6225(7) | 0.2945 | 1.0000 | Uani |
| F262 | -0.4410(15) | 0.4096(5) | 0.5869(7) | 0.2387 | 1.0000 | Uani |
| F263 | -0.2918(16) | 0.3928(4) | 0.5417(7) | 0.2412 | 1.0000 | Uani |
| F271 | -0.3171(12) | 0.5748(7) | 0.7126(4) | 0.1962 | 1.0000 | Uani |
| F272 | -0.4582(13) | 0.6033(7) | 0.6606(6) | 0.1287 | 0.5961 | Uani |
| F273 | -0.291(2) | 0.6467(6) | 0.6736(7) | 0.3066 | 1.0000 | Uani |
| F1061 | -0.2940(8) | 0.4640(4) | 0.3241(3) | 0.1449 | 1.0000 | Uani |
| F1062 | -0.2771(11) | 0.3781(4) | 0.3372(4) | 0.1712 | 1.0000 | Uani |
| F1063 | -0.3750(9) | 0.4236(7) | 0.3860(5) | 0.2037 | 1.0000 | Uani |
| F1071 | 0.1353(7) | 0.3615(2) | 0.5456(3) | 0.103 | 1.0000 | Uani |
| F1072 | 0.0640(13) | 0.3074(3) | 0.4857(6) | 0.1987 | 1.0000 | Uani |
| F1073 | -0.0533(9) | 0.3272(4) | 0.5297(4) | 0.1426 | 1.0000 | Uani |
| F2061 | -0.0842(8) | 0.8394(3) | 0.3838(3) | 0.1129 | 1.0000 | Uani |
| F2062 | -0.104(2) | 0.8939(3) | 0.4449(5) | 0.2669 | 1.0000 | Uani |
| F2063 | -0.2474(12) | 0.8421(7) | 0.4097(6) | 0.2331 | 1.0000 | Uani |
| F2071 | -0.1307(11) | 0.7395(3) | 0.6351(3) | 0.1457 | 1.0000 | Uani |
| F2072 | 0.0442(9) | 0.7809(4) | 0.6507(3) | 0.1306 | 1.0000 | Uani |
| F2073 | -0.1182(8) | 0.8265(3) | 0.6258(3) | 0.1204 | 1.0000 | Uani |
| H11 | -0.337 | 0.7194 | 0.3426 | 0.0945 | 1.0000 | Uiso |
| H12 | -0.2811 | 0.7283 | 0.2919 | 0.094 | 1.0000 | Uiso |
| H13 | -0.2054 | 0.744 | 0.3481 | 0.0942 | 1.0000 | Uiso |
| H21 | -0.3737 | 0.5974 | 0.2959 | 0.079 | 1.0000 | Uiso |
| H22 | -0.2566 | 0.5612 | 0.2946 | 0.0798 | 1.0000 | Uiso |
| H23 | -0.2889 | 0.6099 | 0.2533 | 0.0792 | 1.0000 | Uiso |
| H31 | -0.3874 | 0.6966 | 0.4327 | 0.1271 | 1.0000 | Uiso |
| H32 | -0.2653 | 0.7089 | 0.4755 | 0.127 | 1.0000 | Uiso |
| H33 | -0.3785 | 0.6779 | 0.4929 | 0.1268 | 1.0000 | Uiso |
| H41 | -0.4462 | 0.5815 | 0.3894 | 0.1379 | 1.0000 | Uiso |
| H42 | -0.367 | 0.53 | 0.4169 | 0.1381 | 1.0000 | Uiso |
| H43 | -0.4505 | 0.5652 | 0.4498 | 0.1383 | 1.0000 | Uiso |
| H51 | 0.3553 | 0.5116 | 0.388 | 0.0541 | 1.0000 | Uiso |
| H52 | 0.2263 | 0.5344 | 0.3559 | 0.0543 | 1.0000 | Uiso |
| H53 | 0.2332 | 0.4767 | 0.3846 | 0.0539 | 1.0000 | Uiso |
| H61 | 0.3014 | 0.5244 | 0.541 | 0.061 | 1.0000 | Uiso |
| H62 | 0.4173 | 0.5326 | 0.5125 | 0.0615 | 1.0000 | Uiso |
| H63 | 0.3413 | 0.4766 | 0.504 | 0.061 | 1.0000 | Uiso |
| H71 | 0.2698 | 0.7637 | 0.4662 | 0.0822 | 1.0000 | Uiso |

| | | | | | | |
|---|---|---|---|---|---|---|
| H72 | 0.3504 | 0.7287 | 0.434 | 0.082 | 1.0000 | Uiso |
| H73 | 0.209 | 0.7381 | 0.4108 | 0.0821 | 1.0000 | Uiso |
| H81 | 0.3075 | 0.7009 | 0.5678 | 0.0951 | 1.0000 | Uiso |
| H82 | 0.4151 | 0.6696 | 0.5464 | 0.0953 | 1.0000 | Uiso |
| H83 | 0.3111 | 0.6358 | 0.5674 | 0.0953 | 1.0000 | Uiso |
| H111 | -0.1147 | 0.686 | 0.2437 | 0.0365 | 1.0000 | Uiso |
| H121 | 0.2028 | 0.6483 | 0.3451 | 0.0414 | 1.0000 | Uiso |
| H151 | 0.2145 | 0.7251 | 0.2055 | 0.0455 | 1.0000 | Uiso |
| H211 | -0.2254 | 0.4842 | 0.5115 | 0.0721 | 1.0000 | Uiso |
| H221 | -0.2279 | 0.6297 | 0.5872 | 0.0716 | 1.0000 | Uiso |
| H251 | -0.3563 | 0.4916 | 0.6487 | 0.091 | 1.0000 | Uiso |
| H551 | -0.5167 | 1.0461 | 0.2328 | 0.2302 | 1.0000 | Uiso |
| H552 | -0.4827 | 1.0244 | 0.2915 | 0.2302 | 1.0000 | Uiso |
| H553 | -0.6101 | 1.0093 | 0.2561 | 0.2302 | 1.0000 | Uiso |
| H561 | -0.433 | 0.9254 | 0.3026 | 0.2511 | 1.0000 | Uiso |
| H562 | -0.5696 | 0.9164 | 0.2734 | 0.2511 | 1.0000 | Uiso |
| H571 | -0.5062 | 0.8616 | 0.2101 | 0.2619 | 1.0000 | Uiso |
| H572 | -0.431 | 0.8405 | 0.2646 | 0.2619 | 1.0000 | Uiso |
| H581 | -0.2002 | 0.8506 | 0.1935 | 0.273 | 1.0000 | Uiso |
| H582 | -0.3348 | 0.8291 | 0.1738 | 0.273 | 1.0000 | Uiso |
| H583 | -0.2599 | 0.8105 | 0.2293 | 0.273 | 1.0000 | Uiso |
| H601 | -0.5725 | 1.0488 | 0.1508 | 0.2422 | 1.0000 | Uiso |
| H602 | -0.4963 | 1.0953 | 0.1295 | 0.2422 | 1.0000 | Uiso |
| H603 | -0.494 | 1.0352 | 0.1076 | 0.2422 | 1.0000 | Uiso |
| H611 | -0.2746 | 1.0953 | 0.1521 | 0.2753 | 1.0000 | Uiso |
| H612 | -0.2695 | 1.0344 | 0.1323 | 0.2753 | 1.0000 | Uiso |
| H621 | -0.1847 | 1.066 | 0.2385 | 0.332 | 1.0000 | Uiso |
| H622 | -0.0956 | 1.0539 | 0.1991 | 0.332 | 1.0000 | Uiso |
| H631 | -0.0897 | 0.9322 | 0.2705 | 0.3201 | 1.0000 | Uiso |
| H632 | -0.0961 | 0.991 | 0.295 | 0.3201 | 1.0000 | Uiso |
| H633 | -0.0039 | 0.9792 | 0.2568 | 0.3201 | 1.0000 | Uiso |
| H1011 | -0.1226 | 0.5139 | 0.3815 | 0.0657 | 1.0000 | Uiso |
| H1021 | 0.12 | 0.4554 | 0.5092 | 0.0483 | 1.0000 | Uiso |
| H1051 | -0.1448 | 0.3544 | 0.4296 | 0.0772 | 1.0000 | Uiso |
| H2011 | -0.0169 | 0.7478 | 0.42 | 0.0673 | 1.0000 | Uiso |
| H2021 | 0.031 | 0.6945 | 0.5724 | 0.0536 | 1.0000 | Uiso |
| H2051 | -0.1193 | 0.8439 | 0.5324 | 0.1012 | 1.0000 | Uiso |